

# **Influence of physico-chemical properties of biosorbents on heavy metal removal from industrial wastewater**

**Chaamila Dinusha Kumari Pathirana**

MPhil, BSc (Forestry and Environmental Science)

Submitted in Fulfilment of the Requirements for the Degree of  
Doctor of Philosophy



School of Civil and Environmental Engineering  
Science and Engineering Faculty  
Queensland University of Technology

2020



# Keywords

Sorption, sorption kinetics, pseudo second order, specific surface area, pore size, pore volume, sorption capacity, surface functional groups, total acidic groups, total basic groups, biosorbent, biosorption, heavy metals, breakthrough time, column

# Abstract

Heavy metals present in industrial wastewater play a major role in the degradation of surface water quality and can cause significant human and ecosystem health impacts. Chemical characteristics of heavy metals allow them to persist in the environment, in most instances only changing from one chemical state to another. This eventually leads to their accumulation in the food chain. Therefore, an efficient and cost effective treatment method is required for the removal of heavy metals from industrial wastewater before being discharged into the environment. Among the available treatment techniques, sorption, utilising agricultural waste is generally considered as an effective, economic and eco-friendly treatment option. Treatment efficiency of biosorbents primarily depends on the physico-chemical properties of the material.

Accurately predicting the performance of biosorbents is important for developing biosorbent based treatment methods. Sorption performance mainly depends on material physico-chemical properties and experimental conditions applied to the system. Although the influence of experimental conditions on sorption efficiency is generally understood, the influence of physico-chemical properties of biosorbents has neither been systematically investigated, nor quantitatively assessed. This limits the use of biomaterials for water treatment using sorption.

The innovative outcome of the present study is the approach developed to assess the sorption performance of biosorbents using sorbent physico-chemical properties in both, batch and continuous fixed bed columns. This enabled the quantification of sorption capacity, sorption kinetics and continuous fixed bed column breakthrough time using physico-chemical properties of the sorbent used. The study outcomes can also be used to assess the ability of different sorbents to remove heavy metals and provide the means to select sorbents with higher sorption efficiency in relation to a specific heavy metal species via the analysis of sorbent physico-chemical properties. Furthermore, the relative importance of each physico-chemical property in influencing the sorption performance can be identified.

In order to develop the data matrix for the analysis, two biosorbents with distinct physico-chemical properties were mixed in specific weight ratios to obtain several combinations of physiochemical properties. This method was used to manipulate the

inherent properties of the biosorbents using mixtures to obtain a series of samples with significant variations in their physico-chemical properties.  $\text{Pb}^{2+}$ ,  $\text{Cd}^{2+}$  and  $\text{Cu}^{2+}$  were selected for this study since these are commonly present in wastewater from textile and dye manufacturing industries. Physico-chemical properties were quantified while batch and column sorption experiments were used to generate data for the investigation of the influence of these physico-chemical properties on sorption capacity, rate of sorption and the performance of a continuous fixed bed sorption column. Mathematical models were developed to predict the influence of physico-chemical properties on sorption capacity and the sorption rate using Partial least square regression with  $k$  – fold cross validation. As the next step, an empirical equation was developed to estimate the breakthrough time of a continuous fixed bed sorbent column using parameters from the batch sorption studies.

Though a range of physico-chemical properties influence  $\text{Cu}^{2+}$ ,  $\text{Cd}^{2+}$  and  $\text{Pb}^{2+}$  sorption, their degree of importance was not equal. As identified in the current study, the key physico-chemical properties governing the sorption capacity of the selected biosorbents for all the three metal cations, are acidic surface functional groups followed by zeta potential. Among the acidic surface functional groups, Carboxylic plays a relatively prominent role in the sorption of  $\text{Cu}^{2+}$  and  $\text{Pb}^{2+}$  while lactonic are more important in providing binding sites to  $\text{Cd}^{2+}$ . Mathematical models developed to quantify the maximum sorption by biosorbents of  $\text{Cu}^{2+}$ ,  $\text{Cd}^{2+}$  and  $\text{Pb}^{2+}$  were found to be reliable as indicated by the high coefficient of determination values.

Influence of physico-chemical properties of sorbents on sorption kinetics was assessed using the pseudo second order kinetic constant. The present study developed predictive models to estimate pseudo second order kinetic rate constant values for the sorption of  $\text{Cu}^{2+}$ ,  $\text{Cd}^{2+}$  and  $\text{Pb}^{2+}$ . The models were found to be reliable with the capacity to estimate the kinetic constant using sorbent physico-chemical parameters and initial metal ion concentration. Acidic surface functional groups were found to exert the highest influence while a high specific surface area with micropore structures was seen to reduce sorption rates as metals need time to diffuse into intraparticle structures to find active sites.

It was found that breakthrough time for a sorbent in a column system can be predicted using the initial sorption rate in a batch system, with high predictability. Generally, a column is operated in an entirely different way when compared to a batch study.

Hence, predicting breakthrough time based on the initial sorption rate can be used for the preliminary estimation for the designing of a laboratory column. Mathematical simulations developed to understand sorption in a column systems gave higher values for breakthrough time for  $\text{Cu}^{2+}$  and  $\text{Cd}^{2+}$ , while the simulated value for  $\text{Pb}^{2+}$  was found to be lower than the experimental value. The simulation provided a relationship to correlate the results obtained from batch experiments to continuous fixed bed columns. The simulation needs further refinements to enhance the accuracy of the prediction of breakthrough time of a continuous fixed bed sorbent column using batch experiment equations and physico-chemical properties of the sorbent.

The outcomes of the study created new knowledge to enable the prediction of the performance of a sorbent in terms of heavy metal removal by using its physico-chemical properties. Such predictions would aid in creating treatment methods by modifying locally available biosorbents for enhancing the sorption performance.

# Table of Contents

Keywords.....	i
Abstract.....	ii
Table of Contents .....	v
List of Figures .....	x
List of Tables .....	xiv
List of Appendices.....	xvi
List of Abbreviations .....	xvii
Statement of Original Authorship .....	xix
Acknowledgements .....	xx
<i>Dedication</i> .....	xxi
<b>CHAPTER 1: INTRODUCTION .....</b>	<b>1</b>
1.1 BACKGROUND .....	1
1.2 RESEARCH PROBLEM.....	2
1.3 RESEARCH HYPOTHESES.....	3
1.4 AIMS AND OBJECTIVES.....	3
1.5 RESEARCH SCOPE.....	4
1.6 SIGNIFICANCE AND CONTRIBUTION TO THE KNOWLEDGE .....	4
1.7 THESIS OUTLINE .....	5
<b>CHAPTER 2: HEAVY METALS IN AQUEOUS SOLUTIONS AND REMOVAL .....</b>	<b>7</b>
2.1 INTRODUCTION .....	7
2.2 IMPACT OF HEAVY METALS ON HUMAN HEALTH.....	8
2.3 HEAVY METALS IN INDUSTRIAL WASTEWATER .....	10
2.4 CHEMISTRY OF METALS IN AQUEOUS SOLUTIONS .....	12
2.5 TREATMENT OPTIONS FOR HEAVY METAL CONTAMINATED WASTEWATER.....	14
2.5.1 Physico-chemical methods .....	14
2.5.2 Chemical Precipitation .....	15
2.5.3 Electrochemical Treatments.....	15
2.5.4 Ion Exchange.....	16
2.5.5 Membrane Filtration.....	16
2.5.6 Electrodialysis.....	17
2.5.7 Photocatalysis.....	17
2.5.8 Sorption .....	18
2.6 ADSORPTION AND ION EXCHANGE .....	20
2.6.1 Adsorption .....	20
2.6.2 Ion exchange .....	29
2.7 SUMMARY OF KEY FINDINGS .....	31

<b>CHAPTER 3: ROLE OF SORBENTS IN HEAVY METAL REMOVAL.....</b>	<b>33</b>
3.1 BACKGROUND.....	33
3.2 LOW-COST SORBENTS FOR HEAVY METAL REMOVAL.....	33
3.2.1 Clay and minerals.....	34
3.2.2. Industrial waste and sludge .....	34
3.2.3. Polymers and Resins.....	35
3.2.4 Biomaterials.....	35
3.3 AGRICULTURAL WASTE IN HEAVY METAL SORPTION.....	36
3.4 INFLUENTIAL PARAMETERS .....	43
3.4.1 Experimental conditions .....	44
3.4.2 Properties of biosorbent.....	46
3.5 SORPTION MODELLING .....	50
3.5.1 Isothermal modelling.....	50
3.5.2. Kinetic Modelling .....	52
3.6 BATCH SORPTION AND COLUMN SORPTION SYSTEMS .....	56
3.6.1 Batch sorption systems .....	56
3.6.2 Column sorption systems .....	57
3.7 USE OF FIXED BED COLUMNS IN SORPTION.....	58
3.7.1. Properties of fixed bed column sorption systems.....	59
3.7.2 Influence of the process parameters on breakthrough and exhaust points .....	62
3.7.3. Sorption models for column study .....	64
3.7.4. Fixed-bed systems in heavy metal removal.....	65
3.9 SUMMARY OF KEY FINDINGS.....	70
<b>CHAPTER 4: RESEARCH DESIGN AND METHODS.....</b>	<b>73</b>
4.1 BACKGROUND.....	73
4.2 RESEARCH DESIGN .....	73
4.2.1 Critical review of research literature .....	74
4.2.2 Selection of metal cations for sorption .....	74
4.2.3 Data generation .....	75
4.2.4 Biosorbent selection .....	75
4.2.5 Data analysis.....	76
4.3 RESEARCH METHODS.....	79
4.3.1 Selection of heavy metal ions .....	79
4.3.2 Preparation of metal solutions for sorption studies .....	79
4.3.3 Generation of biosorbent samples .....	79
4.3.4 Laboratory investigations of samples .....	81
4.4 DATA ANALYSIS TECHNIQUES .....	84
4.4.1. Descriptive statistical operations.....	84
4.4.2 Pearson correlation analysis .....	85
4.4.3 Variance inflation factors .....	86
4.4.4 Mahalanobis distance.....	86
4.4.5 Multivariate analysis techniques .....	87
4.5 SUMMARY.....	93
<b>CHAPTER 5: PRELIMINARY EXPERIMENTS.....</b>	<b>95</b>
5.1 INTRODUCTION.....	95
5.2 SELECTION OF HEAVY METALS FOR THE ANALYSIS.....	96



5.3 OVERVIEW OF PAST STUDIES ON SORBENT SELECTION .....	97
5.4 INITIAL SELECTION OF BIOSORBENTS .....	98
5.5 SECONDARY SELECTION OF BIOSORBENTS .....	101
5.5.1 Sorption capacity .....	101
5.5.2 Material characterisation .....	105
5.5 PROMETHEE .....	106
5.5.1 Preferred ranking order .....	106
5.5.2 Criteria Weighting .....	106
5.5.3 Preference function and Threshold .....	107
5.5.4 Q, P and S thresholds .....	107
5.5.5 PROMETHEE analysis .....	109
5.6 SUMMARY .....	110
<b>CHAPTER 6: LABORATORY TEST METHODS AND CALIBRATIONS..</b>	<b>111</b>
6.1 BACKGROUND .....	111
6.2 MATERIAL SURFACE AREA .....	112
6.3 ZETA POTENTIAL.....	113
6.4 SURFACE FUNCTIONAL GROUPS .....	116
6.5 SCANNING ELECTRON MICROSCOPIC ANALYSIS .....	117
6.6 FOURIER TRANSFORM INFRARED SPECTROSCOPY (FTIR) ANALYSIS.....	118
6.7 pH.....	120
6.8 ATOMIC ABSORPTION SPECTROMETRY .....	121
6.8.1 Principles of the instrument .....	122
6.8.2 Calibration .....	122
6.8.3 Analysis .....	123
6.9 BATCH SORPTION EXPERIMENTS.....	123
6.9.1 Determination of sorption capacity.....	123
6.9.2 Kinetic studies.....	124
6.10 CONTINUOUS FIXED BED COLUMN EXPERIMENTS .....	124
6.10.1 Preparation of the experimental set up.....	125
6.10.2 Determining the breakthrough time .....	127
6.11 QUALITY CONTROL AND QUALITY ASSURANCE .....	128
6.12 SUMMARY .....	129
<b>CHAPTER 7: INFLUENCE OF PHYSICO- CHEMICAL PROPERTIES ON</b>	<b>131</b>
<b>SORPTION CAPACITY.....</b>	<b>131</b>
7.1 INTRODUCTION .....	131
7.2 INVESTIGATION OF PHYSICO-CHEMICAL PROPERTIES .....	132
7.2.1 Specific surface area .....	133
7.2.2 Pore volume .....	134
7.2.3 Pore size .....	134
7.2.4 Surface functional groups .....	135
7.2.5 Zeta potential.....	137
7.2.6 SEM Analysis.....	138
7.2.7 FT-IR analysis.....	139
7.3 DETERMINATION OF MAXIMUM SORPTION CAPACITY .....	142

7.4 QUALITATIVE RELATIONSHIPS BETWEEN PHYSICO-CHEMICAL PROPERTIES OF BIOSORBENTS AND MAXIMUM SORPTION CAPACITY .....	144
7.5 QUANTITATIVE ANALYSIS OF THE INFLUENCE OF PHYSICO-CHEMICAL PROPERTIES ON MAXIMUM SORPTION CAPACITY .....	151
7.5.1 Relative importance of physico-chemical properties on sorption .....	152
7.5.2 Individual influence of acidic functional groups on sorption .....	154
7.6 PREDICTING THE EQUILIBRIUM SORPTION CAPACITY .....	155
7.7 SUMMARY OF KEY FINDINGS .....	157
<b>CHAPTER 8: INFLUENCE OF PHYSICO-CHEMICAL PROPERTIES ON SORPTION KINETICS.....</b>	<b>159</b>
8.1 INTRODUCTION .....	159
8.2 DETERMINING RATE CONSTANTS .....	160
8.3. QUALITATIVE RELATIONSHIPS BETWEEN PHYSICO-CHEMICAL PROPERTIES OF BIOSORBENTS AND PSEUDO SECOND ORDER KINETIC CONSTANTS ( $k_2$ ).....	167
8.4 MATHEMATICAL REPLICATION OF SORPTION KINETICS .....	171
8.4.1. Initial and subsequent model development .....	172
8.4.2. Uncertainty quantification and final model development .....	177
8.5. SUMMARY OF KEY FINDINGS.....	185
<b>CHAPTER 9: TRANSFERABILITY OF DATA BETWEEN BATCH AND COLUMN STUDIES.....</b>	<b>187</b>
9.1 INTRODUCTION .....	187
9.2 DETERMINING BREAKTHROUGH TIME .....	188
9.3 PREDICTING THE BREAKTHROUGH TIME USING BATCH PARAMETERS. .	190
9.3.1 Identifying relevant parameters generated through batch experiments .....	190
9.3.2 Development of a mathematical model for the prediction of experimental BT .....	192
9.4 SIMULATION OF SORPTION IN COLUMNS USING MODELS FROM BATCH EXPERIMENT .....	199
9.4.1 Design of the simulation .....	199
9.4.2 Comparison of outputs.....	202
9.5 SUMMARY OF KEY FINDINGS.....	205
<b>CHAPTER 10: CONCLUSIONS AND RECOMMENDATIONS FOR FUTURE RESEARCH .....</b>	<b>207</b>
10.1 CONCLUSIONS .....	207
10.1.1 Influence of physico-chemical properties on sorption capacity.....	207
10.1.2 Influence of physico-chemical properties on sorption kinetics .....	208
10.1.3 Transferability of research data between batch and column studies .....	209
10.2 PRACTICAL APPLICATION OF RESEARCH OUTCOMES.....	210
10.3 RECOMMENDATIONS FOR FUTURE RESEARCH .....	212
<b>REFERENCES .....</b>	<b>213</b>
<b>APPENDIX A1.....</b>	<b>249</b>
Background data analysis .....	249

<b>APPENDIX A2</b> .....	<b>253</b>
Data generated from laboratory analysis of the twenty one biosorbent samples used in the batch and column studies .....	253
<b>APPENDIX A3</b> .....	<b>261</b>
Packages, libraries and R studio codes used for the data analysis .....	261
<b>APPENDIX A4</b> .....	<b>271</b>
Statistical analysis outputs.....	271

# List of Figures

<b>Figure 2.1</b> Polarised water molecule .....	12
<b>Figure 2.2</b> Inner sphere and outer sphere aqua metal complex; M is a metal ion (Adapted from Marcus 1988) .....	13
<b>Figure 2.3</b> Dicarboxylic-metal ion chelate; R can be a hydrocarbon chain (Adapted from Marcus 1988) .....	14
<b>Figure 2.4</b> Basic terminology used in sorption theories (Adapted from Worch 2012) .....	20
<b>Figure 2.5</b> Schematic representation of adsorption: (a) Typical adsorption process; (b) Monolayer adsorption; (c) Multilayer adsorption.....	21
<b>Figure 2.6</b> Schematic diagram of a multilayer formation in the external surface of an adsorbent (+ denotes metal cations).....	24
<b>Figure 2.7</b> Chemisorption of metal ions with hydroxyl functional groups on the external surface (+ denotes metal cations) .....	24
<b>Figure 2.8</b> Schematic diagram of a monolayer formation on the external surface of adsorbent (+ denotes metal cations).....	25
<b>Figure 3.1</b> Schematic diagram illustrating the external diffusion, internal diffusion and mass action (red and blue circles denote the metal ion and the arrows indicate the diffusion directions).....	53
<b>Figure 3.2</b> Concentration profile during single-solute sorption in a fixed bed adsorber system of height $h$ .....	59
<b>Figure 3.3</b> Diagrammatic representation of the fixed-bed sorption process. MTZ mass transfer zone, FC fresh column, SC saturated column adopted from Worch 2012.....	61
<b>Figure 4.1</b> Design of data analysis methodology .....	77
<b>Figure 4.2</b> Summary of the data analysis methods used in the study.....	91
<b>Figure 5.1</b> Biosorbents: (a) Coconut shell biochar; (b) Coir pith; (c) Rice husk; (d) Rice straw; (e) Tea factory waste.....	100
<b>Figure 5.2</b> Sorption capacity of the biosorbents (a) sorption capacity of $Pb^{2+}$ (b) sorption capacity of $Cu^{2+}$ (c) sorption capacity of $Cd^{2+}$ in high metal concentrations (d) sorption capacity of $Pb^{2+}$ (e) sorption capacity of $Cu^{2+}$ (f) sorption capacity of $Cd^{2+}$ in low metal concentrations.....	103
<b>Figure 6.1</b> BET specific surface area analysis (a) glass sampling tube (b) glass rod (c) seal frit (d) ASAP 2020 instrument .....	113
<b>Figure 6.2</b> Electrical double layer around a nanoparticle and the concept of Zeta potential (Marchese et al. 2008).....	114

<b>Figure 6.3</b> Zeta potential analysis (a) capillary cell (b) Malvern Zetasizer Nano ZS.....	115
<b>Figure 6.4</b> Quantification of active sites: titration setup .....	117
<b>Figure 6.5</b> Scanning electron microscopic analysis (a) SEM specimen mounts and carbon (b) Tescan mira3 FEG-SEM (c) Inside of the sampling chamber.....	118
<b>Figure 6.6</b> Thermo Scientific Nicolet S10 FTIR spectrometer .....	120
<b>Figure 6.7</b> pH probe and pH/EC meter .....	121
<b>Figure 6.8</b> Atomic absorption spectrometer.....	122
<b>Figure 6.9</b> (a) Calibration curve with known concentration (b) determine concentration of the sample using calibration curve .....	123
<b>Figure 6.10</b> Batch experimental set up (shaking samples at 150 rpm) .....	124
<b>Figure 6.11</b> Schematic of a column design.....	125
<b>Figure 6.12</b> Wet packing of a column.....	126
<b>Figure 6.13</b> Schematic of the column setup for breakthrough curve determination.....	127
<b>Figure 6.14</b> Experimental setup for determination of breakthrough curve.....	128
<b>Figure 7.1</b> Statistical approach adopted in the analysis.....	132
<b>Figure 7.2</b> Specific surface area variation of samples.....	133
<b>Figure 7.3</b> Variation of pore volume.....	134
<b>Figure 7.4</b> Pore size variation of the samples.....	135
<b>Figure 7.5</b> Variation of acidic surface functional groups .....	136
<b>Figure 7.6</b> Variation of basic surface functional groups .....	137
<b>Figure 7.7</b> Variation of zeta potential.....	138
<b>Figure 7.8</b> SEM images of (a) CSB (b) Pores of CSB (c) TFW (d) Surface of TFW .....	139
<b>Figure 7.9</b> FT-IR spectra for: (a) sample 1 (100% CSB); (b) sample 6 (25%TFW:75%CSB); (c) sample 11 (50%:TFW:50%:CSB); (d) sample 16 (75%:TFW :25%:CSB) and (e) sample 21 (100% TFW) .....	141
<b>Figure 7.10</b> Variation of sorption capacity determined for Pb <sup>2+</sup> at six different initial concentrations: 2 mg/L, 10 mg/L, 50 mg/L, 100 mg/L, 200 mg/L and 300 mg/L .....	143
<b>Figure 7.11</b> Variation of maximum metal sorption capacities for the samples.....	144
<b>Figure 7.12</b> PCA biplot consisting of physico-chemical properties and sorption capacities of biosorbent mixtures (a) three acidic functional groups together as TAG (b) Carboxylic, Lactonic and Phenolic separately.....	146
<b>Figure 8.1</b> Calculated k <sub>2</sub> for the twenty one samples with initial metal ion concentration of: (a) 25 mg/L (b) 50 mg/L (c) 100 mg/L (d) 200 mg/L.....	162
<b>Figure 8.2</b> k <sub>2</sub> for the 21 samples with initial metal ion concentration of (a) Pb <sup>2+</sup> (b) Cu <sup>2+</sup> and (c) Cd <sup>2+</sup> .....	166

<b>Figure 8.3</b> PCA biplots for initial metal ion concentrations: (a) 25 mg/L (b) 50 mg/L (c) 100 mg/L and (d) 200 mg/L .....	169
<b>Figure 8.4</b> Mahalanobis distance values scored by individual objects. Threshold value (straight horizontal line) at 0.95 .....	172
<b>Figure 8.5</b> Main steps of the statistical analysis.....	174
<b>Figure 8.6</b> Biplot of PCA with individual objects grouped into high (200 mg/L and 100 mg/L) and low (50 mg/L and 25 mg/L) initial concentrations. ....	176
<b>Figure 8.7</b> 95% Confidence intervals for standardised regression coefficients of the models built for $Pb^{2+}$ in high initial concentrations; when all variables were used for modelling (continuous line) and when PV and TBG were removed (dotted line) .....	179
<b>Figure 8.8</b> 95% Confidence intervals for standardised regression coefficients of the models built for $Cd^{2+}$ in high initial concentrations; when all variables were used for modelling (continuous line) and when PV and TBG were removed (dotted line) .....	179
<b>Figure 8.9</b> 95% Confidence intervals for standardised regression coefficients of the models built for $Cu^{2+}$ in high initial concentrations; when all variables were used for modelling (continuous line) and when PV and TBG were removed (dotted line) .....	180
<b>Figure 8.10</b> 95% Confidence intervals for standardised regression coefficients of the models built for $Pb^{2+}$ in low initial concentrations; when all variables were used for modelling (continuous line) and when PV and TBG were removed (dotted line) .....	180
<b>Figure 8.11</b> 95% Confidence intervals for standardised regression coefficients of the models built for $Cd^{2+}$ in low initial concentrations; when all variables were used for modelling (continuous line) and when PV and TBG were removed (dotted line) .....	181
<b>Figure 8.12</b> 95% Confidence intervals for standardised regression coefficients of the models built for $Cu^{2+}$ in low initial concentrations; when all variables were used for modelling (continuous line) and when PV and TBG were removed (dotted line) .....	181
<b>Figure 9.1</b> Determination of breakthrough point for $Pb^{2+}$ at 200 mg/L for sample 1.....	189
<b>Figure 9.2</b> (a) Prediction interval and (b) 95% confidence interval of the linear regression model developed for the relationship between BT and $q_e$ for $Pb^{2+}$ at 200 mg/L initial concentration .....	194
<b>Figure 9.3</b> (a) Prediction interval and (b) 95% confidence interval of the linear regression model developed for the relationship between BT and $k_2$ for $Pb^{2+}$ .....	195

<b>Figure 9.4</b> (a) Prediction interval and (b) 95% confidence interval of the linear regression model developed for the relationship between BT and h for Pb <sup>2+</sup> .....	195
<b>Figure 9.5</b> (a) Prediction interval and (b) 95% confidence interval of the linear regression model developed for the relationship between BT and q <sub>e</sub> for Cd <sup>2+</sup> at 200 mg/L initial concentration .....	196
<b>Figure 9.6</b> (a) Prediction interval and (b) 95% confidence interval of the linear regression model developed for the relationship between BT and k <sub>2</sub> for Cd <sup>2+</sup> .....	196
<b>Figure 9.7</b> (a) Prediction interval and (b) 95% confidence interval of the linear regression model developed for the relationship between BT and h for Cd <sup>2+</sup> .....	197
<b>Figure 9.8</b> (a) Prediction interval and (b) 95% confidence interval of the linear regression model developed for the relationship between BT and q <sub>e</sub> for Cu <sup>2+</sup> at 200 mg/L initial concentration .....	197
<b>Figure 9.9</b> (a) Prediction interval and (b) 95% confidence interval of the linear regression model developed for the relationship between BT and k <sub>2</sub> for Cu <sup>2+</sup> .....	198
<b>Figure 9.10</b> (a) Prediction interval and (b) 95% confidence interval of the linear regression model developed for the relationship between BT and h for Cu <sup>2+</sup> .....	198
<b>Figure 9.11</b> Design of the column simulation using elements .....	201
<b>Figure 9.12</b> Simulation of sorption process .....	202
<b>Figure 9.13</b> Comparison of breakthrough curves obtained from the simulation and the laboratory experiment (a) Pb <sup>2+</sup> (b) Cu <sup>2+</sup> (c) Cd <sup>2+</sup> for sample 1 (100% CSB) .....	204
<b>Figure 10.1</b> Schematic representation of the potential application of research outcomes .....	211

# List of Tables

<b>Table 2.1</b> Heavy metals found in major industries (CEA 2015).....	11
<b>Table 2.2</b> Characteristics of Physisorption and Chemisorption (Ruthven 1984) .....	22
<b>Table 2.3</b> Charge densities of common metal ions (Basso et al. 2002) .....	23
<b>Table 2.4</b> Classification of acids and bases into hard, intermediate and soft categories (Adapted from Pearson 1968) .....	26
<b>Table 2.5</b> Characteristics of hard, intermediate and soft categories of ions and ligands .....	27
<b>Table 2.6</b> Hydration energy of common metal ions .....	30
<b>Table 3.1</b> Summary of sorption capacities of selected metal ions .....	38
<b>Table 3.2</b> Various fixed-bed column type sorption studies on heavy metal removal found in literature.....	67
<b>Table 4.1</b> Weight percentage of selected biosorbents used to generate mixtures .....	80
<b>Table 4.2</b> Significance of p values obtained by ANOVA for each variable in the material mixtures .....	81
<b>Table 4.3</b> Physico-chemical parameters for the characterisation of biosorbents .....	82
<b>Table 4.4</b> Parameters used for material surface interpretation .....	82
<b>Table 4.5</b> Parameters for column setup.....	84
<b>Table 5.1</b> Comparison of heavy metals present in industrial wastewater in Sri Lanka with industrial effluent discharging standards .....	96
<b>Table 5.2</b> Biosorbents and their sorption capacities .....	99
<b>Table 5.3</b> Source of biosorbents.....	99
<b>Table 5.4</b> Preparation of the biosorbents.....	101
<b>Table 5.5</b> Quantification of the physico-chemical properties of selected sorbents .....	105
<b>Table 5.6</b> Preference functions for PROMETHEE analysis (Brans et al. 1986).....	108
<b>Table 5.7</b> Ranking sense and preference function assigned for each criterion .....	109
<b>Table 5.8</b> PROMTHERE II complete ranking results for the three materials .....	110
<b>Table 7.1</b> Highest and lowest adoption capacities derived from the analysis.....	144
<b>Table 7.2</b> Pearson correlation matrix.....	148
<b>Table 7.3</b> cos2 values for PC1 and PC2.....	150
<b>Table 7.4</b> Variance inflation factors (VIFs) of the independent variables. ....	152
<b>Table 7.5</b> Regression coefficients and model parameters .....	153
<b>Table 7.6</b> Regression coefficients of acidic functional groups .....	155
<b>Table 7.7</b> Regression parameters and coefficients for prediction of $q_e$ using physico- chemical properties and initial metal ion concentration .....	157



<b>Table 8.1</b> Comparison of $k_2$ for $Pb^{2+}$ , $Cu^{2+}$ and $Cd^{2+}$ for different initial metal ion concentrations .....	163
<b>Table 8.2</b> PLS regression parameters for the initial models to predict $k_2$ .....	175
<b>Table 8.3</b> PLS regression parameters for the subsequent models of $k_2$ .....	177
<b>Table 8.4</b> PLS regression parameters of the final models to predict $k_2$ .....	182
<b>Table 8.5</b> PLS regression coefficients for the predictor variable ( $k_2$ ).....	183
<b>Table 8.6</b> Akaike's Information Criterion (AIC) of the models developed to predict $k_2$ using physico-chemical properties and metal ion concentration .....	184
<b>Table 9.1</b> Breakthrough time obtained from column experiments for $Pb^{2+}$ , $Cu^{2+}$ and $Cd^{2+}$ at 200 mg/L initial metal ion concentration.....	189
<b>Table 9.2</b> Parameters of the models developed for the prediction of BT .....	193

# List of Appendices

- Appendix A1** Background data analysis
- Appendix A2** Data generated from laboratory analysis of the twenty one biosorbent samples used in the batch and column studies
- Appendix A3** Packages, libraries and R Studio codes for the data analysis
- Appendix A4** Statistical analysis outputs

# List of Abbreviations

AAS	Atomic absorption spectrometry
ANOVA	Analysis of variance
BCa	Bias-corrected and accelerated
BDT	Beam Deceleration Technology
BET	Brunauer–Emmett–Teller
BJH	Barrett, Joyner, and Halenda
BOI	Board of Investment
BT	Breakthrough time
BTC	Breakthrough curve
Ca	Calcium
Cd	Cadmium
Cr	Chromium
CSB	Coconut shell biochar
Cu	Copper
DSC	Differential scanning calorimetry
Enet	Elastic Net
Fe	Iron
FT-IR	Fourier transform infrared spectroscopy
GAIA	Graphical Analysis for Interactive Assistance
GLR	Generalized Linear Regression
Hg	Mercury
IAR	International Agency for Research on Cancer
K	Potassium
MAE	Mean absolute error
MCDM	Multi-Criteria Decision Making
MTZ	Mass Transfer zone

Na	Sodium
Ni	Nickel
Pb	Led
PC	Principal Components
PCA	Principal Component Analysis
PLS	Partial Least Square Regression
PPMCC	Pearson product moment correlation coefficient
PROMETHEE	Preference Ranking Organisation Method for Enrichment Evaluations
PS	Pore size
PV	Pore volume
QA	Quality assurance
QC	Quality control
RMSE	Root mean square error
SEM	Scanning Electron Microscopy
SSA	Specific surface area
TAG	Total acidic group
TBG	Total basic group
TFW	Tea Factory waste
VIF	variance inflation factor
Zn	Zinc
ZP	Zeta potential

# Statement of Original Authorship

The work contained in this joint thesis undertaken between QUT and University of Peradeniya has not been previously submitted to meet the requirements for an award at this or any other higher education institution. To the best of my knowledge and belief, the thesis contains no material previously published or written by another person except where due reference is made.

Signature : [QUT Verified Signature](#)

Date : 20/04/2020

# Acknowledgements

I would like to express my deepest appreciation and gratitude to my principal supervisor, Prof. Ashantha Goonetilleke for giving me this great opportunity, as well as for his guidance, motivation and encouragement throughout my PhD study. Without his precious support, it would not have been possible to conduct this research study. I also wish to extend my sincere thanks to Dr. Prasanna Egodawatta for the advice and support at the crucial points of this research project. My appreciation is extended to Dr. Shameen Jinadasa for his insightful comments. I also wish to express my sincere gratitude to Dr. Abdul M. Ziyath for his valuable contributions and suggestions which aided me in planning and designing this research.

I am grateful to the University Grants Commission of Sri Lanka and the Queensland University of Technology, Brisbane for providing me financial aid throughout the Split/Joint-PhD program for pursuing this doctoral study. My gratitude also extends to the Department of Forestry and Environmental Science, University of Sri Jayewardenepura and the Department of Civil Engineering and Post graduate Institute of Agriculture, University of Peradeniya, Sri Lanka for the resources and the co-ordination provided. My sincere thanks also go to the technical staff in the Central Analytical Research facility (CARF) at QUT, especially to Ms. Elizabeth Graham, Dr. Sanjaleena Singh and Dr. Christopher East for their valuable support for my laboratory analysis.

My sincere thanks also goes to the technical officers of both, the Department of Civil Engineering, University of Peradeniya and the Department of Forestry and Environmental Science, University of Sri Jayewardenepura for the valuable technical support provided. I would also like to express my appreciation to Dr. Ayomi Jayarathne and Mr. Kannan Nadarajah for their enormous support during my laboratory investigations. Further, I wish to thank all other fellow research colleagues for their friendship and support given throughout this journey. Finally, my sincere appreciation goes to my beloved family and friends for providing the spiritual support during this doctoral study.

## *Dedication*

To my beloved parents, Palitha Pathirana and Karuna Pathirana, husband Yasas and my son Vidula who have always been my strength, love, encouragement and support throughout the course of this doctoral study.





# CHAPTER 1: INTRODUCTION

---

## 1.1 BACKGROUND

With the onset of industrialisation, mankind has witnessed development and prosperity as well as numerous environmental issues. One of such impacts is visible in the form of water pollution. Water quality refers to the physical, chemical, biological and aesthetic characteristics of water. It is a measure of the condition of water relative to the requirements of one or more biotic species or to any human need or purpose. Contaminants generated from industrial wastewater have the capacity to alter receiving water quality with respect to its suitability for human use. Heavy metals present in wastewater play a major role in the degradation of surface water quality and can cause significant health impacts (Terry and Stone 2002; Satarug and Moore 2004; Ziyath et al. 2011).

Chemical characteristics of heavy metals allow them to persist in the environment, in most instances only changing from one chemical state to another. This eventually leads to their accumulation in the food chain (Wang and Chen 2009). Their resistance to degradation and ensuing persistence in various water bodies ensures that even when present in dilute, almost untraceable quantities, their concentrations may eventually rise to significant levels through natural processes such as bioaccumulation and biomagnification, allowing them to exert relevant toxic effects on organisms (Wang and Chen 2009).

In light of these facts, an efficient treatment method is required for removal of heavy metals in industrial wastewater before being discharged into the environment. Among the available treatment techniques, sorption is generally considered as an effective, economic and eco-friendly treatment technique but these properties would depend on the sorbent used (Fu and Wang 2011). Low-cost sorbents with metal-binding capacities are increasingly being utilised for this purpose. Utilisation of low-cost biosorbents with high metal-binding capacities has been studied widely (Babel and Kurniawan 2004; Gautam et al. 2014). These include a variety of biomaterials such as microalgae (Pereira et al. 2013), bacteria species (Xu et al. 2017), fungal species (Iqbal and Edyvean 2005), sawdust (Ofomaja 2010) and plant materials (Dubey and Shiwani 2012). Use of different biosorbents from agricultural waste such as walnut shells

(Najam and Andrabi 2016), potato peel (Guechi and Hamdaoui 2016), rice straw (Amer et al. 2017), sesame (Cheraghi et al. 2015) and tea waste (Wan et al. 2014) in both, original and modified forms, is an important research focus (Hansen et al. 2010). Such studies have commonly emphasized the possibility of overcoming disposal issues associated with these agricultural waste materials by utilising them as biosorbents.

## **1.2 RESEARCH PROBLEM**

It is commonly known that the effectiveness of heavy metal removal using biosorbents strongly depends on the physico-chemical properties of the material (Anastopoulos et al. 2013b; Han et al. 2013; Gupta and Sen 2017). Even though the influence of biosorbent properties on heavy metal removal is noted, the relationship between these properties and the sorption behaviour is not clearly known. Understanding these properties and the manner in which they influence sorption behaviour is important in selecting biomaterials and in designing biosorption based treatment systems for heavy metal removal from industrial wastewater.

Predicting the capacities and rates of heavy metal removal by various biosorbents are the decisive factors which determine the effectiveness of the sorption process. A large quantum of research has been conducted using different biosorbents to assess their heavy metal removal capacity. In many cases, sorption capacities of different biosorbents in their original forms or treated forms have been investigated for heavy metal removal efficacy. However, quantitative investigations have not been undertaken to any great depth for describing how the physico-chemical properties such as specific surface area, pore size, surface charges and functional groups of the material affect its sorption efficiency. Such studies would guide as to which of the parameters exert significant influence on the sorption capacity and rate, in order to improve sorption efficiency. Therefore, understanding the relationships between material properties, sorption capacity and kinetics and incorporating those into existing fundamental concepts is important to enhance performance of biosorbents. This knowledge can be further developed to remove heavy metals in industrial wastewater. Current research addressed this knowledge gap by investigating the research question: ‘How to predict the sorption performance of biosorbents in terms of heavy metal removal, based on physico-chemical properties of a biosorbent?’

### **1.3 RESEARCH HYPOTHESES**

In order to respond to the above research question, the research study was undertaken based on the following hypotheses:

- Performance of biosorbents can be predicted using sorption capacity and sorption kinetics.
- Physico-chemical properties of sorbents exert a significant influence on sorption capacity and kinetics.

### **1.4 AIMS AND OBJECTIVES**

Aims

- To investigate the influence of physico-chemical properties of biosorbents on heavy metal sorption capacity.
- To define the sorption kinetics of biosorbents based on the identified influential physico-chemical properties.
- Investigating the approach for transferring research data between batch and column studies.

The primary objective was to predict the sorption performance to replicate sorption mechanisms with respect to the physico-chemical properties of biosorbents, in order to guide effective heavy metal removal from polluted water.

## **1.5 RESEARCH SCOPE**

The scope of this research study was as follows.

- This research focused on three heavy metals that are commonly found in industrial wastewater. Other metals and pollutants such as hydrocarbons, nutrients and microbial substances were not investigated.
- The research was confined to laboratory studies using metal solutions prepared by dissolving the metal nitrates in deionised water. The study did not use actual industrial wastewater.
- The study focused on the influence of physico-chemical properties of the sorbents on heavy metal sorption. Influence of different experimental conditions of the systems was not considered.
- Only two biomaterials were selected for the research. Their physico-chemical properties were manipulated by mixing them in different weight ratios to suit the research requirements. However, the knowledge created by this research study is generic and applicable to other biomaterials.
- The study focus was on developing predictive models to investigate the sorption mechanism and to assist the real world application of sorbents in terms of physico-chemical properties of the material. Recovery of heavy metals or life cycle analysis of the technology was not investigated.

## **1.6 SIGNIFICANCE AND CONTRIBUTION TO THE KNOWLEDGE**

This research study created new knowledge based on the quantitative analysis of metal sorption performance of biosorbents in heavy metal removal. The study outcomes provide an in-depth understanding of the influence of sorbent physico-chemical properties on metal sorption capacity and kinetics and hence, offers insights to the role of individual physico-chemical properties on sorption performance. Moreover, the relationship between individual physico-chemical properties of a sorbent and its sorption performance could be clearly defined. The knowledge created can be utilised to enhance the use of biosorbents for the removal of heavy metals by modifying their physico-chemical properties in order to enhance sorption performance.

The innovative outcome of the research study is the approach developed to assess the sorption performance using sorbent physico-chemical properties. The study identified

the relative importance of each physico-chemical property for determining the capacity and kinetics of metal sorption by a biosorbent. This knowledge can be utilised to predict and quantify the sorption performance based on the physico-chemical properties of the sorbent. This would enable assessment of the ability of different sorbents to remove heavy metals and would provide the means to select sorbents with relatively high sorption performance in relation to a specific heavy metal species via the analysis of sorbent physico-chemical properties. Suitability of a sorbent for pollutant removal is usually assessed via sorption equilibrium and sorption kinetics using batch studies. Then, fixed bed column studies are undertaken to evaluate the suitability of the sorbent by analysing the breakthrough and exhaustion points. This study provides a relationship between these two systems which could serve as an initial estimation of the breakthrough time of a continuous fixed bed column system using sorption parameters obtained in batch studies. These findings will provide guidance for the design of sorbent systems using biosorbents for the removal of heavy metals in wastewater.

## **1.7 THESIS OUTLINE**

This thesis contains ten chapters. Chapter 1 introduces the study providing details of the research problem, hypothesis, aims and objectives, scope of the study and the significance of the research. Chapter 2 and 3 discuss the outcomes of the critical review of literature. Chapter 2 includes the chemistry of metal cations in aqueous solutions and the available treatment methods including sorption. Chapter 3 discusses sorbents, use of agricultural waste as sorbents and the use of batch and column sorption experiments for analysing sorbent performance.

The design of the research study including the experimental procedures and data analysis is discussed in Chapter 4. Chapter 5 discusses the procedure adopted for selecting two agricultural waste materials for preparing the samples for the study. Chapter 6 describes the laboratory test methods used to analyse physico-chemical properties of the biosorbents. Laboratory analysis conducted to generate sorption capacities and kinetic constant values are discussed along with column sorption experiments, quality control and quality assurance procedures adopted.

Chapter 7-9 discusses the key findings of this study. Chapter 7 discusses the influence of physico-chemical properties on sorption capacity. Chapter 8 explains the influence

of physico-chemical properties on sorption kinetics using the kinetic constant. Chapter 9 presents relationships to transfer experiment data between batch and column studies. Finally, the conclusions derived from the study, practical applications of the research and recommendations for future research are presented in Chapter 10.

## **CHAPTER 2: HEAVY METALS IN AQUEOUS SOLUTIONS AND REMOVAL**

---

### **2.1 INTRODUCTION**

The discovery of heavy metals underneath the surface of the earth along with their excavation, extraction and utilization as resources to fulfil human needs was a pivotal step in the development of human technology and culture. The term ‘heavy metal’ is generally reserved for metals whose density exceeds  $5 \text{ gcm}^{-3}$ . Human exposure to heavy metals has also risen dramatically due to an exponential increase of their usage in several industrial, agricultural, domestic and technological applications (Bradl 2002).

Considering their impact on human health and the ecosystem, the removal of heavy metals from water and particularly industrial wastewater is imperative. Various treatment methods have been developed and used for removing heavy metals from wastewater including coagulation-flocculation (Semerjian and Ayoub 2003; Ayoub et al. 2001), chemical precipitation (Fu and Wang 2011), floatation and electrochemical processes (Kurniawan et al. 2006; Belkacem et al. 2008), adsorption (Ajmal et al. 1998; Minceva, Taparcevska, et al. 2008), ion exchange (Sapari et al. 1996) and membrane filtration (Mavrov et al. 2003). Use of advanced technologies for wastewater treatment however, appears to be limited, especially in developing countries owing to their high cost and low feasibility for smaller-scale applications. Treatment methods based on adsorption on the other hand, have assumed the role of alternative treatment techniques for wastewater laden with heavy metals (Ziyath et al. 2011; Barakat and Kumar 2015). Detailed investigations into feasible treatment methods to remove heavy metals from industrial wastewater requires a fundamental knowledge of the chemistry of metals in aqueous solutions. The critical review of literature below discusses the health effects of heavy metals, their chemistry and significance in aqueous solutions along with the treatment options for heavy metals in industrial wastewater.

## 2.2 IMPACT OF HEAVY METALS ON HUMAN HEALTH

Heavy metals exert detrimental effects on human health in several ways and carcinogenicity is one of them. Carcinogens are classified by various scientific committees and also by regulatory agencies. The latter classifications usually depend on national policies (Beyersmann and Hartwig 2008). The International Agency for Research on Cancer (IARC) categorises carcinogens into several groups. Their classification is based on carcinogenic hazard and Group 1 includes metals/metal compounds which are described as “carcinogenic to humans”. Group 2A includes those that are “probably carcinogenic to humans” while Group 2B and Group 3 are mentioned as “possibly carcinogenic to humans” and “not classifiable as to its carcinogenicity to humans” respectively.

Apart from carcinomas, heavy metals are known to cause other health issues as well. Studies on large populations who have been exposed to high concentrations of arsenic in their drinking water have shown that these people display various clinical conditions including diseases in heart and blood vessels, developmental anomalies, neurological disorders, diabetes mellitus, loss of hearing, liver diseases and blood disorders (Tchounwou et al. 2004; Year 2013; Centeno et al. 2002). Research has also shown significantly high mortality rates for carcinomas of the skin, liver, bladder and kidney with arsenic pollution in many regions around the world (Tchounwou et al. 2004).

Heavy metals also exhibit multiple oxidation-reduction products depending on the number of electrons removed or added to the valence shell, and the resulting oxidation-reduction products are either in cationic or anionic forms (Sparks 2003). Oxidation-reduction reactions have been identified as a crucial factor which determines the bioavailability of heavy metals in the environment

Many researchers have published studies where the adverse effects of lead on human population, both, paediatric and adult, are described. For the paediatric population, these include relationships between lead levels in blood and reduced hearing acuity, handicap in speech and language, retardation of growth, anti-social and/or delinquent behaviour, reduced attention span, delayed or compromised neurobehavioral development, lower IQ levels and diminished intelligence (Kaul et al. 1999; Factor-Litvak et al. 1998; Amodio-Cocchieri 1996). As for adults, decreased sperm count in



men and spontaneous abortions in women have been linked to high levels of lead exposure (Hertz-Picciotto 2000; Apostoli et al. 1998). In addition, Cadmium acts as a human carcinogen and is linked to kidney damage and renal disorders. Copper causes liver damage, Wilson disease and insomnia. Nickel is linked to dermatitis, nausea and chronic asthma while being a human carcinogen. Zinc can cause depression, lethargy and certain neurological signs (Babel and Kurniawan 2003). Various industries generate and discharge wastewater containing a range of heavy metals into the environment. Hence, industrial wastewater acts as a key source of heavy metal contamination of the environment. Therefore, significant attention should be given to treating heavy metals in industrial wastewater (Sörme and Lagerkvist 2002; Wang et al. 2016).

### 2.3 HEAVY METALS IN INDUSTRIAL WASTEWATER

A number of industries produce and release wastewater containing a variety of different heavy metals into the environment. For example, industries such as textile, dye manufacturing, mining, tanning and electroplating are identified as sources of heavy metals (CEA 2015). Another industrial example is electroplating and metal surface treatment works which generate significant amounts of wastewater containing metal ions such as cadmium, zinc, lead, chromium, nickel, copper, vanadium, platinum, silver and titanium. Activities that yield these contaminants include electroplating work, electroless deposition works, conversion coating techniques, anodizing cleaning methods, milling and etching. Printed circuit board production is also identified as a major source of heavy metal contaminants. Sn, Pb and Ni solder plates are the most widely used resistant overplates. Another example is wood processing industry where chromated copper-arsenate wood treatment produces waste materials containing arsenic. Types of heavy metals generated by major industrial settings are summarized in Table 2.1. Section 2.4 describes the chemical behaviour of metals in solutions and Section 2.5 outlines various treatment options for heavy metal contaminated wastewater.

**Table 2.1** Heavy metals found in major industries (CEA 2015)

<b>Industry</b>	<b>Cd</b>	<b>Cr</b>	<b>Cu</b>	<b>Fe</b>	<b>Hg</b>	<b>Mn</b>	<b>Pb</b>	<b>Ni</b>	<b>Sn</b>	<b>Zn</b>
Pulp, papermills, paperboard, building paper, board mills		X	X		X		X	X		X
Organic chemicals, petrochemicals	X	X		X	X		X		X	X
Alkalis, chlorine, inorganic chemicals	X	X		X	X		X		X	X
Fertilizers	X	X	X	X	X	X	X	X		
Petroleum refining	X	X	X	X			X	X		X
Basic steel works foundries	X	X	X	X	X		X	X	X	X
Basic non-ferrous metals works, foundries	X	X	X		X		X			X
Motor vehicles, aircraft plating, finishing	X	X	X		X			X		
Flat glass, cement, asbestos products, etc.		X								
Textile mill products		X								
Leather tanning, finishing		X								
Steam generation power plants		X								X
Dye manufacturing							X			
Metal plating		X	X					X		X

## 2.4 CHEMISTRY OF METALS IN AQUEOUS SOLUTIONS

Detailed investigation into feasible treatment methods to remove heavy metals from industrial wastewater requires a fundamental knowledge of the chemistry of metals in aqueous solutions. Thus, it is imperative to understand how the water molecules interact with metal cations. Water molecules are negatively polarised due to the difference in electronegativity between hydrogen and oxygen atoms in the molecule as shown in Figure 2.1. When dissolved in water, metal cations are attracted to water molecules due to this polarity. Apart from that, industrial wastewater contains numerous other ions and molecules which can contribute in various competitive interactions between themselves or with water molecules (Tunell and Lim 2006).

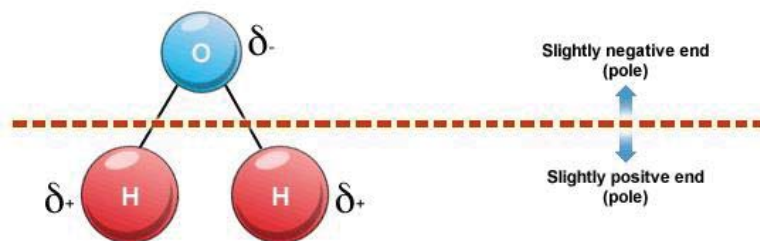


**Figure 2.1** Polarised water molecule

The interaction of water molecules with metal cations leads to the formation of inner and outer sphere complexes. Negatively polarised oxygen atoms in water molecules can attract metal cations and form an inner sphere aqua complex as illustrated in Figure 2.2. Six water molecules are often found bound to metals forming  $[M(H_2O)_6]^{2+}$ , where M is a metal cation (Marcus 1988). The number of water molecules found in the metal complex is determined by the solution concentration and ionic size (Ruthven 1984; Tunell and Lim 2006).

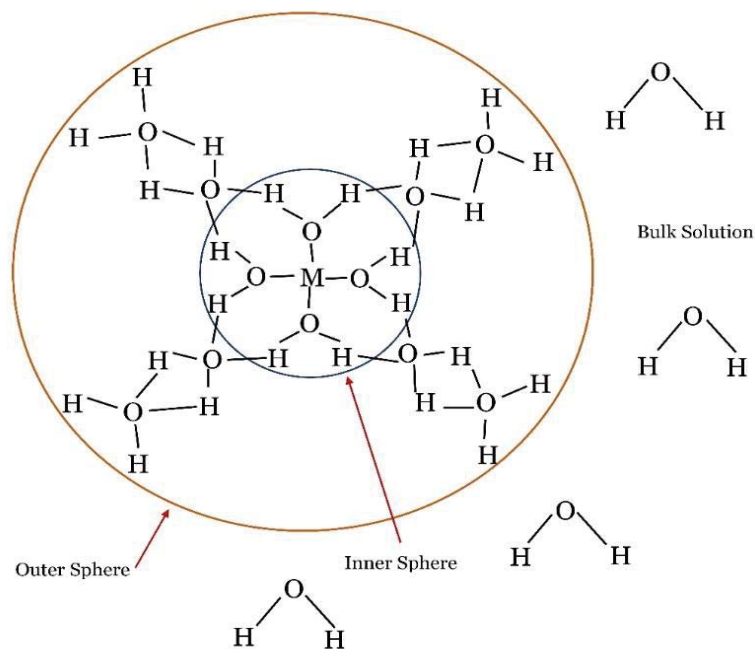


**Figure 2.2** Inner sphere and outer sphere aqua metal complex; M is a metal ion (Adapted from Marcus 1988)

However, depending on the chemical composition of the solution, thermodynamically preferred alternative anions such as chlorides ( $\text{Cl}^-$ ) and iodides ( $\text{I}^-$ ) may replace one or more of these water molecules. More complex ligands such as dicarboxylic acids could also replace water molecules in the same way. Such replacements can change the chemical structure of the complex for example, to  $[\text{M}(\text{H}_2\text{O})_5\text{Cl}]^{1+}$  from  $[\text{M}(\text{H}_2\text{O})_6]^{2+}$  (Ahmadi et al. 2009). Whilst anions such as  $\text{Cl}^-$  and  $\text{I}^-$  can bind directly to metal ions in proportion to their respective charges, more complex molecules such as dicarboxylic acids have several potential binding sites in a single molecule and form rings around the metal ion. This is illustrated in Figure 2.3 and the process is called ‘chelation’ (Norkus et al. 2003). The capacity for such interactions with metal ions is influenced by factors such as the ionic radius of the metal ions and the chemical composition of the solution (Ahmadi et al. 2009).

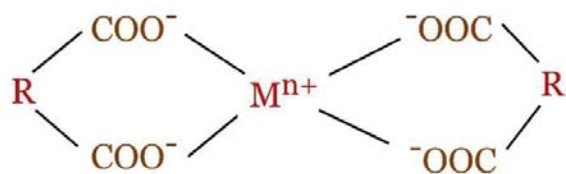


**Figure 2.3** Dicarboxylic-metal ion chelate; R can be a hydrocarbon chain (Adapted from Marcus 1988)

A metal cation can be present in different ionic forms depending on solution pH (Bradl 2004). For example, chromium cation ( $\text{Cr}^{3+}$ ) changes from predominantly free  $\text{Cr}^{3+}$  ion at pH 1 to  $[\text{CrOH}]^{2+}$ ,  $[\text{Cr}(\text{OH})_2]^+$  and  $[\text{Cr}(\text{OH})_3]^0$  as pH increases and reaches anionic  $[\text{Cr}(\text{OH})_4]^-$  at pH 11. Similarly, lead cation ( $\text{Pb}^{2+}$ ) changes to anionic  $[\text{Pb}(\text{OH})_3]^-$  at pH 11. Changes in the chemical form of metal cations have a significant influence on their interaction with other molecules and binding sites. Furthermore, water molecules in the inner sphere complex develop hydrogen bonds with water molecules in the bulk solution. This leads to the formation of the outer sphere complex as illustrated in Figure 2.2 (Hancock and Martell 1996). Consequently, the behaviour of metals in aqueous medium exerts considerable influence on the metal removal techniques, especially when chemical treatment techniques are considered.

## 2.5 TREATMENT OPTIONS FOR HEAVY METAL CONTAMINATED WASTEWATER

As explained in the Section 2.1, many treatment options have been developed for the treatment of wastewater containing heavy metals. The following discussion outlines various treatment techniques, which have been investigated for the removal of dissolved metals, primarily from industrial wastewater. The applicability of these methods along with their advantages and disadvantages are also discussed.

### 2.5.1 Physico-chemical methods

Physical separation techniques are mainly applicable to particulate forms of various metals or discrete particles. Physical separation usually includes mechanical screening, hydrodynamic clarification, gravity concentration, flotation, magnetic separation, electrostatic separation and attrition scrubbing (Dermont et al. 2008). Conventional chemical methods for removing heavy metals from water bodies include processes

such as chemical precipitation, flotation, adsorption, ion exchange and electrochemical deposition. There are several factors that can limit the applicability and reduce the effectiveness of such chemical processes. These include higher content of clay, calcite, iron, calcium, anions and higher buffering capacity (Fu and Wang 2011).

### **2.5.2 Chemical Precipitation**

Chemical precipitation is a popular method for heavy metal removal from inorganic effluent in various industries, mainly due to its simple operation and low capital cost. The conventional chemical precipitation processes employed usually end up producing insoluble precipitates of heavy metals as hydroxides, sulfides, carbonates and phosphates. The precipitation process generates very fine particles and methods such as chemical precipitation, coagulation and flocculation processes are used to increase their particle size in order to remove them as sludge. This however, leads to extra operational cost for sludge disposal. The most commonly used precipitation technique is hydroxide treatment due to its relative simplicity and low cost (Fu and Wang 2011; Ku and Jung 2001).

### **2.5.3 Electrochemical Treatments**

Electrolytic recovery is one of the technologies used to remove metals from wastewater. This process employs electricity to pass a current through an aqueous solution using a cathode plate and an insoluble anode. The purpose is to precipitate the heavy metals in a weak acidic or neutralized catholyte as hydroxides. Electrochemical treatment of wastewater involves electro-deposition, electrocoagulation, electro-flotation and electro-oxidation (Shim et al. 2014). Electrocoagulation is the most commonly employed method and it aims to achieve precipitation of metal ions by hydroxide formation to facilitate removal (Mollah et al. 2001). The coagulant is generated by electrolytic oxidation of a suitable anode material. Metal ions are removed from wastewater by allowing them to react with anions in the effluent. Chemical precipitation requires a considerable amount of chemicals in order to convert metals to an acceptable form for removal. Other disadvantages include higher volumes of sludge formation, slower processing, poor settling, aggregation of metal precipitates and certain long-term environmental impacts caused by sludge disposal (Aziz et al. 2008).

#### **2.5.4 Ion Exchange**

Ion exchange works by attracting soluble metal ions from the liquid phase to the solid phase. This method is commonly employed in water treatment as it is cost-effective. Ion exchange process normally involves low-cost materials and efficient operations. It is known to be very effective for removing heavy metals from aqueous solutions, especially when the concentration of heavy metals remains low. Cations or anions containing ion exchangers are employed to remove metal ions in the solution. Water insoluble, solid, synthetic ion exchange resins are an example. These have the capacity to replace positively or negatively charged ions from an electrolyte solution by releasing other ions with the same charges into the solution in equivalent amounts. This way, positively charged ions in cationic resins such as hydrogen and sodium ions are exchanged with positively charged ions in solutions such as nickel, copper and zinc. Similarly, the negative ions in the resins such as hydroxyl and chloride ions can be replaced by similar ions such as chromate, sulfate, nitrate, cyanide and dissolved organic carbon (Dizge et al. 2009; Hamdaoui 2009).

#### **2.5.5 Membrane Filtration**

Membrane filtration is an area of interest in the treatment of inorganic effluent. However, high operational cost due to membrane fouling is a notable disadvantage. This method has the capacity to remove various suspended solids, organic compounds and inorganic contaminants like heavy metals. Depending on the size of the particle/particles to be retained, numerous membrane filtration methods such as ultrafiltration, nanofiltration and reverse osmosis can be employed for heavy metal removal from wastewater. Ultrafiltration employs permeable membranes to separate heavy metals, macromolecules and various suspended solids from inorganic solutions on the basis of the pore size and molecular weight of the compounds (Shon et al. 2004). Depending on the membrane characteristics and operating conditions, ultrafiltration can be highly effective. It requires a lower driving force and a smaller space owing to its higher packing density. Polymer-supported ultrafiltration technique is a relatively newer technique with advantages like low-energy requirements, fast reaction kinetics and higher selectivity. Another technique referred to as complexation-ultrafiltration is considered to be an alternative to methods based on precipitation and ion exchange. It has a higher separation selectivity (Petrov and Nenov 2004; Trivunac et al. 2012). Reverse osmosis is a separation process involving diffuse mechanisms. It uses pressure



to force a solution through a semipermeable membrane which ends up retaining the solute on one side and allows the solvent to pass to the other side. This technique can remove a variety of molecules, ions and bacteria from various solutions and has industrial applications (Chen et al. 2007).

### **2.5.6 Electrodialysis**

In electrodialysis, ionized metal species in a solution are passed through an ion exchange membrane by applying an electric potential. The membranes are thin sheets with either anionic or cationic characteristics. When a solution containing ionic species passes through the cell compartments, the anions migrate toward the anode and the cations toward the cathode, thereby, crossing the anion exchange and cation-exchange membranes (Chen et al. 2007). This method has high separation selectivity and can produce a highly concentrated stream for the recovery process. Valuable metals such as Cr and Cu can be recovered this way. Significant disadvantages are the higher energy requirement, need for membranes replacement, careful operation, a clean feed and periodic maintenance. The corrosion process also leads to higher cost (Kurniawan et al. 2006).

### **2.5.7 Photocatalysis**

The photocatalysis method has received attention in recent years. Photocatalytic process is conducted by the aqueous suspension of semiconductors. When the semiconductor-electrolyte interface is illuminated, electron-hole pairs ( $e^-/h^+$ ) are formed in the conduction and the valence band of the semiconductor, respectively, provided that the energy of light used is higher than the semiconductor band gap (Herrmann 1999). These charge carriers migrate to the semiconductor surface and are capable of reducing or oxidizing certain species in the solution having suitable redox potential. The common semiconductors used are,  $TiO_2$ , ZnO,  $CeO_2$ , CdS and ZnS, whereas  $TiO_2$  is established as the most efficient (Zhang and Itoh 2006). This method requires effective trapping of  $e^-/h^+$  to avoid recombination.  $OH^-$  are commonly used for trapping  $h^+$  while adsorbed oxygen species are used for the trapping of  $e^-$ . These processes generate hydroxyl radicals and superoxide species, respectively. Removal of these becomes a problem and is a disadvantage of the method. Photocatalysis has been studied for the removal of Cu(II),  $CN^-$ , Cr(III) and Cr(VI). This method has the capacity to remove metals and organic pollutants simultaneously and the by-products

are considered to be less harmful when compared with other methods. However, the application of this method is limited and the process takes a longer duration of time (Barakat et al. 2004; Kajitvichyanukul et al. 2005).

### **2.5.8 Sorption**

Sorption is a general term used to encompass any physical or chemical process that retains the 'sorbates' on the surface of a 'sorbent' (Del Campillo et al. 1999). It is one of the popular methods for treating wastewater that has received much attention in research literature. The most general definition describes sorption as an enrichment of chemical species from a fluid phase on the surface of a liquid or a solid. Various materials ranging from agricultural wastes (Ajmal et al. 1998; Garg et al. 2008) to commercial sorbents (Genç-Fuhrman et al. 2007; Minceva, Fajgar, et al. 2008) have been investigated for the removal of metals from water.

The main advantages of the sorption technique include its effectiveness over a wide range of metal concentrations and the simplicity of its application (Minceva, Taparcevska, et al. 2008). However, capital cost and regeneration cost can limit the use of some of the sorbents for water treatment in instances where large quantities of sorbents are required to treat large volumes of water (Kesraoui-Ouki et al. 1994). For example, use of activated carbon may not be economically viable for the removal of metals in drinking water due to its high capital and regeneration cost (Minceva, Taparcevska, et al. 2008). However, many low-cost natural sorbents such as zeolite, clay and biomass generally known as biosorbents (Wang and Chen 2009) can be used for the sorption of metals (Bailey et al. 1999; Kurniawan et al. 2006). Several reviews published on the usage of low-cost sorbents for the removal of metal ions in water have highlighted the significant potential that low cost sorbent materials have in water treatment (Bailey et al. 1999; Babel and Kurniawan 2003; Dąbrowski et al. 2004; Demirbas 2008; Kurniawan et al. 2006; Wang and Chen 2009; Ngah and Hanafiah 2008).

The disposal of sorbents after treatment is also of concern as the sorbents will contain metal ions in high concentrations. Some studies have noted that successful regeneration is feasible, during which the metal ions are released back to a chemical reagent such as ammonium acetate (Baran et al. 2007; Yu et al. 2001). The quantity of chemical reagent required for such a process is noted to be significantly low.

Consequently, if the metal is economically valuable, they can be recovered from the chemical reagent that contains the concentrated metals using chemical precipitation.

However, the major drawback in the sorption technique is the preferential removal of certain metal ions over the others, resulting in poor removal of less preferred metal ions. For example, Holan and Volesky (1995) reported that fungal biomass show high affinity to adsorb Pb over Cd and Ni. This results in moderate sorption of Cd and poor sorption of Ni since the most active sites are occupied by Pb (Holan and Volesky 1995). Wang and Chen (2009) produced the following affinity series for metal sorption by biosorbents based on a number of research studies:  $Cd > Co > Cr > Fe > Ni > Pb > Hg > Zn$ . This highlights that sorption of Cd is most preferred by biosorbents, whilst poor removal of Hg and Zn can be expected (Wang and Chen 2009). When the water source is a multi-component system consisting of various pollutants including diverse species of metal ions, the preferential sorption of sorbents can result in inadequate removal of certain metal ions. Consequently, the treated water will require additional treatment for the removal of these metal ions, which will incur additional cost.

Special attention should be given to the usage of the term 'sorption'. This term comprises both, absorption and adsorption. The more common term, absorption is defined as the transfer of a substance from one bulk phase into another bulk phase. In this case, the substance is enriched within the receiving phase and not only on its surface. The dissolution of various gases in liquids is a typical example of absorption. The term adsorption describes the enrichment of adsorbates on the surface of an adsorbent. In theories related to adsorption, basic terms depicted in Figure 2.4 are used. The solid material that provides the surface for the adsorption process is referred to as the adsorbent while the species that will be subjected to the process of sorption are called sorbate. It should be noted that adsorbed species can also be released from the surface and transferred back into the liquid phase. This reverse process is known as desorption.

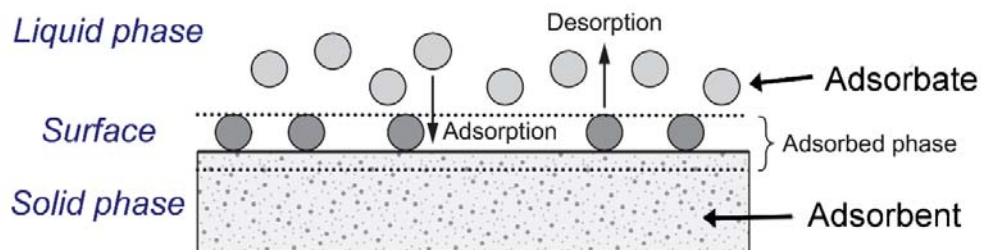


**Figure 2.4** Basic terminology used in sorption theories (Adapted from worch 2012)

In certain natural systems, some materials with a complex structure can bind substances from the aqueous phase to their surfaces (adsorption), but also into the interior of the material (absorption). A typical example of such complex binding mechanisms would be the uptake of organic solutes by certain soils and sediments. In cases like these, it is difficult to distinguish between adsorption and absorption. Hence, the more general term, ‘sorption’ is preferred. The mechanisms employed by sorbent materials are complex and are often found operating in combination in the removal of metals in water (Panayotova 2001; Erdem et al. 2004). There are two main types of surface retention mechanisms reported in the literature and the most common processes are adsorption and ion exchange.

## 2.6 ADSORPTION AND ION EXCHANGE

### 2.6.1 Adsorption

As indicated in Section 2.5, adsorption describes the enrichment of adsorbates on the surface of an adsorbent. The primary difference between ion exchange and adsorption mechanisms is that there is no exchange of ions involved in the adsorption mechanism (Kammerer et al. 2010). Depending on the manner adsorbates are bound to a surface, two types of mechanisms are identified; monolayer adsorption and multilayer adsorption. In monolayer adsorption, all the adsorbate molecules are adsorbed to the surface. In multilayer type, adsorption can accommodate more than one layer of adsorbate molecules although not all adsorbate molecules are in contact with the adsorbent surface (Figure 2.5b and 2.5c). The adsorption capacity of a material is denoted as the measure of the quantity of adsorbate adsorbed per unit mass of the adsorbent (Inglezakis and Pouloupoulos 2006).

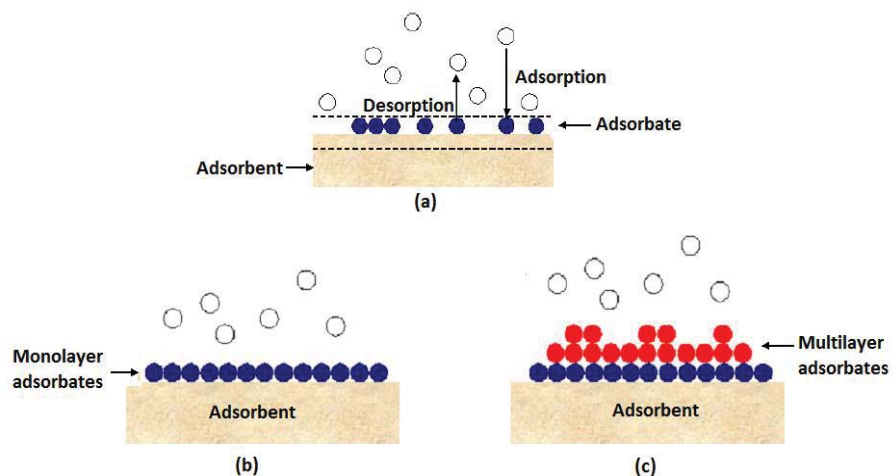


**Figure 2.5** Schematic representation of adsorption: (a) Typical adsorption process; (b) Monolayer adsorption; (c) Multilayer adsorption

Adsorption can generally be classified as physisorption or chemisorption depending on the characteristics of the bonding between metal cations and the adsorbent active sites (Inglezakis and Pouloupoulos 2006). Although this distinction is conceptually useful, many intermediate cases exist and classifying a particular system unequivocally is not always possible (Ruthven 1984). Characteristics of these two types of adsorption are listed in Table 2.2. Accordingly, sorbents which have high capability for performing chemisorption are more favourable to metal removal as the sorption is more stable. However, the process takes a long time to establish.

**Table 2.2** Characteristics of Physisorption and Chemisorption (Ruthven 1984)

<b>Physisorption</b>	<b>Chemisorption</b>
Lower heat of adsorption (less than 2 or 3 times latent heat of evaporation)	Higher heat of adsorption (more than 2 or 3 times latent heat of evaporation)
Monolayer or multilayer adsorption	Monolayer adsorption
No dissociation of adsorbed species	Dissociation can happen
Significant at relatively low temperatures	Possible over a wide range of temperature
Rapid, non-activated and reversible	Activated, may be slow and irreversible
No electron transfer although polarization of sorbate can happen	Electron transfer happens leading to formation of bonds between sorbate and surface

*a. Physisorption*

During physisorption, dipole interaction is developed when metal cations approach the negative sites of adsorbents. This causes a relatively weak van der Waals attractive force to be developed between outer sphere of metal cations and the adsorbent framework (Inglezakis and Pouloupoulos 2006). Therefore, physisorption is an outer sphere complexation process and strong chemical bonds are not formed since electron transfer does not occur between molecules. As such, physisorption causes only a very small change in enthalpy during the adsorption of metals. Hence, heat of adsorption for the physisorption mechanism is typically 20 - 40 kJ/mol (Inglezakis and Pouloupoulos 2006). The adsorption activation energy (E) for the physisorption mechanism is typically less than 8 kJ/mol (Uluozlu et al. 2008).

The attraction is not fixed to a specific site and the adsorbate is relatively free to move on the surface. The strength of physisorption largely depends on the strength of dipole interaction. Though dipole interaction is stable at low temperatures, increase in the temperature weakens the interaction, which causes desorption of metal ions (Murzin and Salmi 2005). The interaction is stronger when the molecules are closer to each

other. Physisorption of metal ions by adsorbent materials depends on the charge densities of the metal ions (Erdem et al. 2004).

Charge density of an ion is given as follows:

$$\text{Charge density} = \frac{Q}{r^3} \quad \text{Equation 2.1}$$

where Q is the amount of electric charge of the cation and r is the ionic radius (Basso et al. 2002). Charge densities of selected metal ions are given in Table 2.3.

**Table 2.3** Charge densities of common metal ions (Basso et al. 2002)

<b>Metal</b>	<b>Charge density / (<math>10^{-19}\text{C/m}</math>)</b>
Pb	8.6
Cd	9.8
Zn	3.4
Ni	2.2
Cu	10.1
Cr	14.8

Cations with high charge densities have a strong cationic field. Therefore, their interaction with an anionic field of adsorbents is stronger than those of cations with low charge densities (Eisenman 1962). Consequently, the physisorption force is stronger for cations with high charge densities. Multilayer formation (Figure 2.6) is possible during physisorption since physisorbed cations can form hydrogen bonding with water molecules in bulk solution (Nagao 1971).

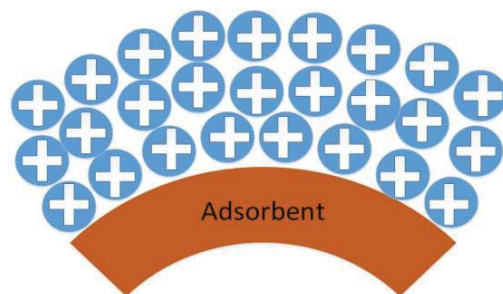


**Figure 2.6** Schematic diagram of a multilayer formation in the external surface of an adsorbent (+ denotes metal cations)

*b. Chemisorption*

Chemisorption is an inner sphere complexation phenomenon, in which metal ions participate in the exchange of electrons with the active sites that are present on the external surface or inside the pores of the adsorbent. This results in the formation of a strong metal-ligand complex. As an example, the metal-hydroxide complexation is illustrated in Figure 2.7.

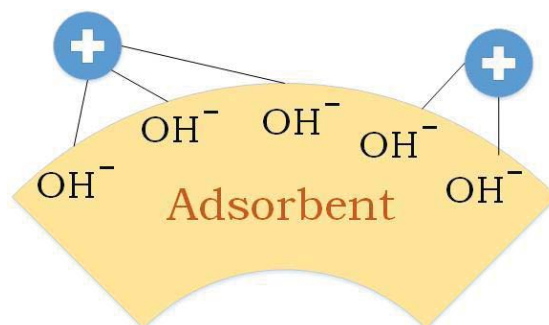


**Figure 2.7** Chemisorption of metal ions with hydroxyl functional groups on the external surface (+ denotes metal cations)

Unlike physisorption, the chemisorption mechanism has to overcome an activation energy barrier. Therefore, significant enthalpy change is observed during the chemisorption process. Heat of adsorption in the case of chemisorption is high, typically in the range of 40-800 kJ/mol (Haque and Sexton 1968; Inglezakis and Pouloupoulos 2006).



In the case of physisorption, the distance between metal cations and the surface of sorbents is longer. In contrast, chemisorption bonds are formed close to the surface of the sorbent (Murzin and Salmi 2005). Metal ions strongly interact with the surface of the sorbent, which prevents hydrogen bond formation with other molecules in the bulk solution. Therefore, a monolayer can be formed during chemisorption as illustrated in Figure 2.8.

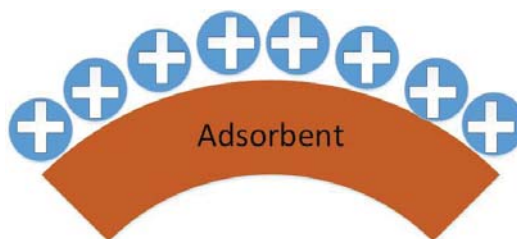


**Figure 2.8** Schematic diagram of a monolayer formation on the external surface of adsorbent (+ denotes metal cations)

Desorption of chemisorbed metal ions from the sorbent framework is difficult due to the strong bond that is formed. In contrast, metal cations adsorbed via physisorption can be easily desorbed by means of chemical agents such as ammonium acetate. Therefore, desorption studies with ammonium acetate have been used effectively to distinguish the contribution of chemisorption to the overall removal of metals (Mozgawa and Bajda 2005).

The chemisorption process is commonly explained using the Lewis Hard Soft Acid Base (HSAB) theory which is a concept introduced by Pearson (1968), to explain the stability of metal complexes and the mechanisms of their reactions. This theory is widely used to understand the chemical reaction between cations and anions in a qualitative context. Any molecule that has the ability to accept electrons is called a 'Lewis acid' while the molecule that donates the electrons is called 'Lewis base'. According to these definitions, metal cations act as Lewis acids whereas ligands are Lewis bases. HSAB theory classifies metal ions and ligands into hard, intermediate and soft categories as listed in Table 2.4.

**Table 2.4** Classification of acids and bases into hard, intermediate and soft categories (Adapted from Pearson 1968)

	Hard	Intermediate	Soft
<b>Acid</b>	$H^+$ , $Li^+$ , $Na^+$ , $K^+$ $Be^{2+}$ , $Mg^{2+}$ , $Ca^{2+}$ , $Sr^{2+}$ $BF_3$ , $BCl_3$ , $B(OR)_3$ $Al^{3+}$ , $Al(CH_3)_3$ , $AlCl_3$ , $AlH_3$ $Cr^{3+}$ , $Mn^{2+}$ , $Fe^{3+}$ , $Co^{3+}$	$B(CH_3)_3$ $Fe^{2+}$ , $Co^{2+}$ , $Ni^{2+}$ , $Cu^{2+}$ , $Zn^{2+}$ , $Rh^{3+}$ , $Ir^{3+}$ , $Ru^{3+}$ , $Os^{2+}$	$BH_3$ , $Tl^+$ , $Tl(CH_3)_3$ $Cu^+$ , $Ag^+$ , $Au^+$ , $Cd^{2+}$ , $Hg_2^{2+}$ , $Hg_2^+$ , $CH_3Hg^+$ , $[CO(CN)_5]^{2-}$ , $Pd^{2+}$ , $Pt^{2+}$ , $Pt^+$ , $Br_2$ , $I_2$
<b>Base</b>	$F^-$ , $Cl^-$ , $H_2O$ , $OH^-$ , $O_2^-$ $ROH$ , $RO^-$ , $R_2O$ , $CH_3COO^-$ $NO_3^-$ , $ClO_4^-$ , $CO_3^{2-}$ , $SO_4^{2-}$ , $PO_4^{3-}$ $NH_3$ , $RNH_2$ , $N_2H_4$	Ions with formal oxidation states of 4 or higher $HX$ (hydrogen-bonding molecules)	Metals with zero oxidation state $\pi$ acceptors: e.g., trinitrobenzene, quinines, Tetracyanoethylene
		$Br^-$	$H^-$ $I^-$ $H_2S$ , $SH^-$ , $S_2^{2-}$ , $SCN^-$ , $CN^-$ , $RNC$ , $CO$ $S_2O_3^{2-}$
		$NO_2^-$ , $N_3^-$ , $SO_3^{2-}$ $C_6H_5NH_2$ , $C_5H_5N$ , $N_2$	$PR_3$ , $P(OR)_3$ , $AsR_3$ , $C_2H_4$ , $C_6H_6$

**Note:** 'R' stands for an alkyl or aryl group

‘Hard’ and ‘soft’ are relative terms and the corresponding acids or bases are distinguished based on their properties including electronegativity, polarizability and ionic size (Pearson 1968). For example, a base with low electronegativity is regarded as a ‘soft’ species, which prefers to bond with a soft cation. The characteristics of hard, intermediate and soft categories of ions and ligands are listed in Table 2.5 (Miessler et al. 2013). According to HSAB theory, hard acids generally prefer to bind to hard bases, and soft acids prefer to bind to soft bases.

**Table 2.5** Characteristics of hard, intermediate and soft categories of ions and ligands

Type of Acid/Base	Characteristics
Hard acids	<ul style="list-style-type: none"> <li>* Atomic centres with small ionic radii (&lt;90 pm).</li> <li>* High positive charge.</li> <li>* Empty orbitals in their valence shells.</li> <li>* Low electronegativity (0.7-1.6) and low electron affinity.</li> <li>* Likely to be strongly solvated.</li> </ul>
Soft acids	<ul style="list-style-type: none"> <li>* Large radii (&gt;90 pm).</li> <li>* Low or partial positive charge.</li> <li>* Completely filled orbitals in their valence shells.</li> <li>* Intermediate electronegativity (1.9-2.5)</li> </ul>
Hard bases	<ul style="list-style-type: none"> <li>* Small radii (around 120pm) &amp; highly solvated.</li> <li>* Electronegative atomic centres (3.0-4.0).</li> <li>* Weakly polarizable.</li> <li>* Difficult to be oxidized.</li> </ul>
Soft bases	<ul style="list-style-type: none"> <li>* Large atoms (&gt;170 pm) with intermediate electronegativity (2.5-3.0).</li> <li>* High polarizability</li> <li>* Easily undergoes oxidation.</li> </ul>

However, the main limitation of HSAB theory is that it is qualitative and the comparison of the ‘hardness’ or ‘softness’ of two acids or bases is not possible. For example, though Na<sup>+</sup> and K<sup>+</sup> are hard acids, the relative hardness of one over the other

is not readily discernible. For this purpose, Parr and Pearson (1983) proposed a property called ‘absolute hardness ( $\eta$ )’ based on the ionisation potential (I) and electron affinity (A) of a species‘s’ as shown below.

$$\eta_s = \frac{1}{2}(I_s - A_s) \quad \text{Equation 2.2}$$

Where:

$\eta$  -absolute hardness

I -ionisation potential

A -electron affinity

The absolute hardness ( $\eta$ ) can be used to compare the hardness of two metals where the metal ion with a higher  $\eta$  value is relatively harder (Parr and Pearson 1983). Klopman (1968) observed that ‘softness’ is correlated to the tendency of an acid or base to form covalent bonding, while ‘hardness’ is associated with the tendency of an acid or base to participate in ionic bonding (Klopman 1968). Based on this concept, Hancock and Marsicano (1978) proposed equation 2.3 for predicting the chemical hardness of acids and bases (H) based on the tendency of a metal ion or a ligand to form ionic (E) or covalent bonds (C).

$$H = \frac{E}{C} \quad \text{Equation 2.3}$$

Where:

H- Chemical hardness of acids and bases

E -Tendency of a metal ion or ligand to form ionic bonds

C- Tendency of a metal ion or ligand to form covalent bonds

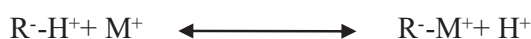
The above parameter (H) provides a reasonable estimation of hardness for metal acids (Hancock and Marsicano 1978). Thus, parameter ‘H’ can be used for comparing the relative hardness or softness of different metal ions. The affinity for metal ions when physisorption mechanism is in operation is primarily influenced by the charge densities, whilst chemical hardness of metals governs the affinity for the chemisorption mechanism.

Chemisorption and ion-exchange are two primary processes in relation to outer sphere and inner-sphere surface complexation (Chorover and Brusseau 2008). Past

researchers have pointed out that ion-exchange is neither a bond nor an adsorption process (Farquhar et al. 1997). However, in most research literature, ion-exchange is referred to as non-specific adsorption or an electrostatic sorption process, which involves weak electrostatic bonds associated with the outer-sphere complexation (Bradl 2004; Inglezakis and Pouloupoulos 2006; McBride 1994; Sparks 2003; Polcaro et al. 2003). Therefore, in this research study, ion-exchange was considered as an outer-sphere complexation process and was considered for sorption.

### 2.6.2 Ion exchange

Ion exchange is not considered as a strict chemical reaction. It is a re-distribution of ions between solid and liquid phases (Inglezakis and Pouloupoulos 2006). Several synthetic cation exchange resins that contain  $H^+$  ions that can be exchanged for metal cations have been investigated for their efficiencies in removing dissolved metal cations (Sapari et al. 1996; Rengaraj et al. 2003). Cation exchange resins exchange  $H^+$  with metal ions in the solution as follows:



Where  $R-H^+$  is an ion exchange resin and  $M^+$  is a metal ion.

The ion exchange process is driven by the Le Chatelier's principle and depends on the physical and chemical conditions prevailing in the system. Le Chatelier's principle states that if an equilibrium system is disturbed by a change in conditions such as concentration, the equilibrium will shift to counteract the effect of such a disturbance. Introduction of a sorbent into a metal solution divides the system into solid and liquid phases. The solid phase contains exchangeable cations such as  $H_3O^+$ ,  $Na^+$ ,  $Ca^{2+}$  and  $K^+$  at higher concentrations whilst metal ions are found in higher concentrations in the liquid phase. This uneven distribution of ions between solid and liquid phases disturbs the equilibrium of the system (De Villiers et al. 1997). Therefore, according to the Le Chatelier's principle, some exchangeable cations will move into the solution, whilst some metal ions will be transferred to the sorbent to restore the system back to equilibrium. The amount of exchangeable cations and metal ions which engage in the exchange process is influenced by a temperature dependent equilibrium constant. Furthermore, metals subjected to ion exchange can be desorbed back to the bulk solution depending on the physical and chemical conditions of the system such as pH and temperature (Murzin and Salmi 2005). Consequently, sorbents can be regenerated

in a controlled environment by providing favourable physico-chemical conditions for the desorption of metals, which can eventually be safely disposed.

The tendency of a metal ion in a multi metal system for participating in exchange depends on the strength of interaction between the specific metal ion and water molecules (Colella 1996). The strength of interaction is dependent on the hydration energy, which is defined as the energy released when one mole of a substance is dissolved into solution (Dimitriu et al. 2007). In other words, it is the energy released due to the formation of aqua metal complexes during the dissolution of a metal ion in water. Some metals release more energy during the formation of aqua complexes. Hence, they have high hydration energy. As a result, more energy is required to detach water molecules from the metal cations in order to facilitate bonding with the active sites in sorbents. As such, metals with high hydration energy will stay in solution instead of detaching the water molecules and being exchanged for cations in sorbents (Eisenbud et al. 1962). Consequently, metals with low hydration energy are preferred for participation in the ion exchange process. Hydration energy values of selected metal ions are given in Table 2.6 (Marcus 1991).

**Table 2.6** Hydration energy of common metal ions

<b>Metal</b>	<b>Hydration energy/ (kJ/mol)</b>
Pb	-1425
Cd	-1755
Zn	-1955
Ni	-1980
Cu	-2010
Cr	-4010

Based on the hydration energy, it can be concluded that the affinity of metals for ion exchange should ideally follow the order  $Pb > Cd > Zn > Ni > Cu > Cr$ . Hence, poor preference of sorbents in relation to some metals such as Cu and Cr is a major problem encountered when using ion exchange mechanism for the removal of metals from a multi metal system.

A major drawback in using biosorbents for wastewater treatment is the selectivity of certain metal ions over others, which results in poor removal of less preferred metals.

Industrial wastewater is a multi-component system consisting of different metal ions and organic pollutants. Therefore, the selectivity of biosorbents needs to be taken into consideration in order to enhance the treatment efficacy. This has been investigated by using a mixture of sorbents to ensure similar affinity for the sorption of all metals (Ziyath et al. 2011) or by using a sequence of adsorbents with different affinities. Hence, a fundamental understanding of sorption science is essential for achieving improved treatment efficiencies. The next chapter focuses on further details on sorption, various sorbents, parameters influencing the process and sorption modelling.

## **2.7 SUMMARY OF KEY FINDINGS**

Heavy metals exert detrimental effects on human health and the environment. Dissolved forms of heavy metals are more hazardous than their particulate forms due to their ready bioavailability to organisms. The interaction of water molecules with metal cations leads to the formation of inner and outer sphere complexes. Negatively polarised oxygen atoms in water molecules can attract metal cations and form an inner sphere aqua complex. This behaviour of metals in aqueous medium exerts a considerable influence on treatment techniques, especially when chemical treatment techniques are considered. Among the different available treatment techniques, sorption is generally considered as an effective technique over a wide range of metal ions. Regarding metal ion removal by a specific material, it is difficult to distinguish the contribution of adsorption, absorption and ion exchange.

Sorption performance of biosorbents depends on the physico-chemical properties. Even though the influence of biosorbent physico-chemical properties on sorption performance is noted, the possibility of developing a quantitative relationship between material physico-chemical properties and their sorption performance was not explored in past studies. The present study aims at bridging this knowledge gap by developing a quantitative model of the relationship between physico-chemical properties of biosorbents and their sorption performance. The knowledge created can be utilised to enhance the use of biosorbents for the removal of heavy metals by modifying their physico-chemical properties in order to enhance sorption performance.

This page intentionally left blank.



# CHAPTER 3: ROLE OF SORBENTS IN HEAVY METAL REMOVAL

---

## 3.1 BACKGROUND

As discussed in the Section 2.6, the term ‘sorption’ comprises three different processes (adsorption, absorption and ion exchange) and distinguishing between these three or quantifying the contribution of each process to the overall process of sorption is difficult. There is no consensus in research literature regarding how these three processes can be distinguished in a practical setting. It is also evident that most researchers use the term ‘sorption’ even for studies where only the adsorption process is under investigation. Hence, the term ‘sorption’ is used in the present study.

In Chapter 2, it was concluded that sorption is a preferred technique for the removal of dissolved metal ions from industrial wastewater, due to better cost and environmental benefits, when other commonly available techniques (such as chemical precipitation and membrane filtration) are considered. However, the efficiency of the sorption system depends on the sorbent material/materials used and the selective sorption of metal ions was identified as the key issue to be addressed in order to utilise the sorption process for the treatment of metals in industrial wastewater. Hence, selection of an appropriate sorbent is crucial for the removal of metal ions using sorption. For these reasons, a fundamental knowledge regarding the different sorption processes, sorption capacities of various sorbents and the factors influencing the efficiency of sorption is essential to develop approaches for enhancing the sorption of dissolved metal ions.

This chapter aims to discuss different types of sorbents and sorption systems available, their applicability, sorption modelling and the influential parameters in the sorption process. Special emphasis is given to the use of biosorbents for heavy metal removal.

## 3.2 LOW-COST SORBENTS FOR HEAVY METAL REMOVAL

Identification and assessment of low-cost sorbents with metal-binding capacities has attracted much attention in recent years (Ziyath et al. 2011; Leung et al. 2000). A variety of sorbents including those of biological, organic or mineral origins, feedstock, polymeric materials (synthetic polymers) and industrial by-products have been

investigated for this purpose (Kurniawan et al. 2006). While various low-cost sorbents derived from above sources are being developed and applied for the removal of heavy metals from contaminated wastewater, the efficiency of such treatments depends mainly on the characteristics of sorbent/sorbents (Stoica et al. 2012). Commonly investigated low- cost sorbents and their applications as found in literature, are briefly discussed below.

### **3.2.1 Clay and minerals**

Clay, a fine, natural, raw material, is found abundantly on the terrestrial surface and is composed mainly of silica, alumina, water and weathered rock. Clay also has a number of physical properties such as plasticity, ability to shrink under fire or under air-drying, fineness of grain, rigidity and cohesion (Kennedy 1990; Das and Sobhan 2013; McConnell et al. 2013). Based on multiple properties, clays are extensively divided into groups. Accordingly, kaolinite, montmorillonite and illite are the primary clay materials and almost all clays are composed of one or more of these three types (Grim 1962; Murray 2006). Most of the clay minerals are negatively charged and possess higher cation exchange capacities, small particle sizes with complex porous structures yielding high surface area and pore volume, allowing them to effectively adsorb various metal cations from solutions. This metal sorption involves a number of complex mechanisms such as direct bonding with the surface of clay minerals, surface complexation and ion exchange (Churchman et al. 2006). Utilization of both, natural and treated/modified clay types as potential biosorbents in the removal of various heavy metal ions from aqueous solutions have been studied extensively. Natural clay was assessed for the removal of  $\text{Cu}^{2+}$  from Cachaça where the calculations of sorption kinetics displayed pseudo-second-order behaviour (Zacaroni et al. 2015). Similar studies for arsenic (Bentahar et al. 2016),  $\text{Cd}^{2+}$ ,  $\text{Pb}^{2+}$  and  $\text{Cr}^{6+}$  (Khan and Singh 2010) are available. Thermally treated clay samples have also been investigated for the removal of  $\text{Cd}^{2+}$  (Rao and Kashifuddin 2016).

### **3.2.2. Industrial waste and sludge**

Industrial wastes investigated for their sorption properties include fly ash, steel and aluminium industry wastes, fertilizer industry wastes, leather and paper industry wastes. Blast furnace slag, sludge and dust are the commonly utilised steel industry wastes for sorption studies (Worch 2012; Hegazi 2013). Aluminium industry generates

red mud as a waste material which is formed during production and is a popular subject for sorption studies. Fertilizer industry also produces a variety of by-products and some have been subjected to sorption studies such as carbonaceous sorbent prepared from carbon slurry (De Gisi et al. 2016). For heavy metal removal via sorption, basic oxygen furnace slag, black liquor, blast furnace slag, brick powder, fly ash in raw form as well as in chemically treated forms, hydrated cements, iron complexed leather industry waste materials, marble powder, red mud and certain solid waste from leather industry have been mentioned in research literature. The heavy metals whose removal investigated include  $\text{Cu}^{2+}$ ,  $\text{Pb}^{2+}$ ,  $\text{Zn}^{2+}$ ,  $\text{As}^{3+}$ ,  $\text{Cd}^{2+}$ ,  $\text{Cr}^{3+}$ ,  $\text{As}^{5+}$ ,  $\text{Fe}^{2+}$ ,  $\text{Ni}^{2+}$  and  $\text{Cr}^{6+}$  (De Gisi et al. 2016).

### **3.2.3. Polymers and Resins**

Selective sorption techniques with the utilization of chelating resins has received considerable interest from the scientific community over the past decade. The advantages of such methods include simplicity, high efficiency and low cost. Processes employed include ion exchange, physical sorption and chelation (Deepatana and Valix 2006; Shukla et al. 2006; Pramanik et al. 2004). Researchers have utilised various methods for the production of such chelating resins. The polymerization of conventional chelating monomers is one such method. Such monomers include acrylic acid, methacrylic acid and vinylpyridine (Li et al. 2002; Dakova et al. 2007; Liu et al. 2005). Another method is grafting low-molecular weight ligands one after the other onto prepared synthetic polymers using techniques such as functionalization reactions (Atia et al. 2005; Donia et al. 2006; Navarro et al. 2001). However, the high cost of production of polymeric materials (compared to the cost of activated carbons) and the necessity for extractive regeneration by solvents make polymeric sorbents less suitable for treatment of large amounts of water with complex compositions such as wastewater. For this reason, polymeric sorbents are used for the recycling of valuable chemicals from process wastewater.

### **3.2.4 Biomaterials**

The number of low-cost biomaterials investigated for their sorption abilities remains very high. They can be classified as; agricultural and household by-products, industrial by-products, sludge, soil and ore materials and novel low-cost sorbents (Ali et al. 2012). Some of these by-products are known to pose a number of disposal problems

due to their high volumes, various toxicities and physical properties (i.e. petroleum industrial waste materials, scrap tyres, rice husk). Using these waste as low-cost sorbents provides certain means to mitigate such problems. In general, biomaterials in their raw form can be subjected to various modifications to yield desirable physico-chemical properties. These properties include specific surface area, pore-size distribution, pore volume and the presence of surface functional groups. Such techniques of modification involve modification of chemical, physical and biological characteristics, whereas modification with chemical compounds has been used more frequently. Such chemical compounds include organic and mineral acids (HCl, HNO<sub>3</sub>, H<sub>2</sub>SO<sub>4</sub>, acetic acid, citric acid and formic acid), bases and basic solutions (NaOH, Na<sub>2</sub>CO<sub>3</sub>, Ca(OH)<sub>2</sub> and CaCl<sub>2</sub>), oxidizing agents (H<sub>2</sub>O<sub>2</sub> and K<sub>2</sub>MnO<sub>4</sub>) and several other mineral and organic chemical compounds such as formaldehyde, glutaraldehyde, CH<sub>3</sub>OH, polyethyleneimine and epichlorohydrin (De Gisi et al. 2016).

As for agricultural solid waste materials, they are mostly derived from low-cost and readily available sources. It should also be noted that agricultural and household waste materials have been investigated by many researchers for their abilities to remove various pollutant forms via sorption. A wide variety of agricultural solid waste materials have been investigated for the sorption of various dyes and heavy metals from solutions. The main components of these agricultural waste materials were hemicellulose, lignin, lipids, proteins, sugars, water, hydrocarbons and starch. They typically have numerous functional groups with potential sorption capacities for various pollutants (De Gisi et al. 2016). Agricultural waste materials are employed for sorption in both, the natural and modified forms. When used in the natural form, the material is commonly washed, ground and sieved until it reaches the desired particle size, before being used in sorption studies. Section 3.4 describes the usage of agricultural waste in heavy metal removal. Such studies have commonly emphasised the possibility of overcoming disposal issues associated with the specific agricultural waste materials by utilising them as biosorbents.

### **3.3 AGRICULTURAL WASTE IN HEAVY METAL SORPTION**

Researchers have highlighted the significant potential in the use of agricultural waste for the removal of metal ions from wastewater (Gupta et al. 2009; Wang and Chen 2009). Those studies have investigated the sorption capacities of biosorbents from

agricultural wastes. Some of these studies have used biosorbents in their natural form while others have used them after modifications using physical and/or chemical treatments designed to increase their sorption capabilities. It has been noted that the efficiency of the sorbent in question depends on the sorption capacity, affinity and physico-chemical nature of the material used. A great number of such studies have focused on the removal of Cadmium, Lead and Copper using agricultural waste.

For Lead removal, black gram husk, flowers of *Humulus lupulus*, tea waste, coffee waste and water hyacinth have been investigated. Efficiency values ranging from 70% to 98% have been reported (Ahluwalia and Goyal 2005; Iqbal et al. 2002; Wan et al. 2014; Gardea-Torresdey et al. 2002). Other studies have investigated *Pinus sylvestries* (Taty-Costodes et al. 2003) and rubber wood saw dust (Raji et al. 1997) for this purpose and demonstrated efficiency values ranging from 85% to 90%. Modifying these materials aiming to increase their performance have failed to yield satisfactory results. All of these studies generally reported an optimum pH range of 5-6.

As for Cadmium removal, hazelnut shells, peanut hulls, walnut shells and green coconut shells have managed to yield significant results (Johns et al. 1998; Kurniawan et al. 2006). Experimenting on activated carbon from bagasse pith, coir pith, peanut shells and dates has given removal efficiency values ranging from 50% to 98% (Gupta et al. 2001; Kadirvelu et al. 2001; Kannan and Rengasamy 2005; Krishnan and Anirudhan 2003; Mohan and Singh 2002). Chemically treating agricultural waste materials have interested researchers. Biosorbents such as base treated rice husk, treated juniper fibres, modified peanut shells, succinic anhydride treated sugarcane and corncob modified with citric acid have been investigated in various studies (Karnitz Jr et al. 2007; Min et al. 2004). Most of these studies have demonstrated that agricultural waste either in natural form or modified form is highly efficient in removing cadmium ions.

Studies focused on Copper ion removal using saw dust (Ajmal et al. 1998; Larous et al. 2005) have reported high efficiency rates. Basci et al. (2003) concluded that wheat shells and carbonized coir pith have high efficiency values for sequestering copper (Basci et al. 2004). Ajmal et al. (2005) and Palma et al. (2003) used Mustard oil cakes and modified bark of *Pinus radiata* which yielded similar results (Ajmal et al. 2005; Palma et al. 2003; Ajmal et al. 1998). Table 3.1 summarises the heavy metal sorption capacities reported for different biosorbents by a range of studies.

**Table 3.1** Summary of sorption capacities of selected metal ions

Sorbent	Sorption capacity				Initial Metal concentration	Reference
	Cr <sup>3+</sup>	Cu <sup>2+</sup>	Pb <sup>2+</sup>	Zn <sup>2+</sup>		
Agave bagasse (HCl)					60 mg/l	Velazquez-Jimenez et al. 2013
Agave bagasse (HCl)			42.31 mg/g		60 mg/l	Velazquez-Jimenez et al. 2013
Agave bagasse (HNO <sub>3</sub> )					60 mg/l	Velazquez-Jimenez et al. 2013
Banana peel					30–80 mg/l	Anwar et al. 2010
Banana peel			2.18 mg/g		30–80 mg/l	Anwar et al. 2010
Barley straw (raw)		4.64 mg/g			0.0001–0.001 mol/l	Pehlivan et al. 2012
Chemically modified orange peel		289.0 mg/g			50–500 mg/l	Feng et al. 2009

*Continued on next page.*

Sorbent	Sorption capacity					Initial Metal concentration	Reference
	Cr <sup>3+</sup>	Cu <sup>2+</sup>	Pb <sup>2+</sup>	Zn <sup>2+</sup>	Cd <sup>2+</sup>		
Garden grass (raw)			58.34 mg/g			1-500 mg/l	Hossain et al. 2012
Mango peel waste		46.09 mg/g				10-500 mg/l	Iqbal et al. 2009
Mango peel waste				28.21 mg/g		10-500 mg/l	Iqbal et al. 2009
Olive stone (raw)	3.19	×				3.0 × 10 <sup>-4</sup> to 0.15 mol/l	Fiol et al. 2006
Olive stone (raw)		10-5 mol/g	4.47 × 10 <sup>-5</sup> mol/g			3.0 × 10 <sup>-4</sup> to 0.15 mol/l	Fiol et al. 2006
Olive stone (raw)						3.0 × 10 <sup>-5</sup> to 0.15 mol/l	Fiol et al. 2006
Potato peels	0.3877 mg/g					150-400 mg/l	Aman et al. 2008
Rice shell	2.95 mg/g					25-500 mg/l	Aydin et al. 2008
Rice straw						25-350 mg/ml	Ding et al. 2012

*Continued on next page.*

Sorbent	Sorption capacity					Initial Metal concentration	Reference
	Cr <sup>3+</sup>	Cu <sup>2+</sup>	Pb <sup>2+</sup>	Zn <sup>2+</sup>	Cd <sup>2+</sup>		
Sulfured orange peel			164.0 mg/g			25–800 mg/l	Liang et al. 2011
Sulfured orange peel				80.0 mg/g		25–800 mg/l	Liang et al. 2011
Sunflower hull (raw)		57.14 mg/g				25–200 mg/l	Witek-Krowiak, 2012
Wheat shell (raw)		17.42 mg/g				25–500 mg/l	Aydin et al. 2008
Wheat stem (raw)					0.1032 mmol/g	0.1–1.2 mmol/l	Tan and Xiao 2009
Tea waste		21.02 mg/g	33.49 mg/g		16.87 mg/g		Wan 2014; Cay et al. 2004
Rice husk	2.1 mg/g	3.89 mg/g	4.2 mg/g			1.0 g/l	Sobhanardakani et al. 2013
Coir pith	1.26 mg/g					1.0 g/l	Amarasinghe 2011; Kulkarni 2014

*Continued on next page.*



Sorbent	Sorption capacity				Initial Metal concentration	Reference
	Cr <sup>3+</sup>	Cu <sup>2+</sup>	Pb <sup>2+</sup>	Zn <sup>2+</sup>		
Coir pith			2.2 mg/g		1.0 g/l	Amarasinghe 2011; Kulkarni 2014
Coir pith					4.04 mg/g	Amarasinghe 2011; Kulkarni 2014
Coconut shell charcoal	3.7 mg/g					Huang et al 2006; Kulkarni 2014
Coconut shell charcoal			7.2 mg/g			Huang et al 2014; Kulkarni 2014
Coconut shell charcoal					4.7 mg/g	Huang et al 2014; Kulkarni 2014
Rice straw	3.9 mg/g					Rocha et al 2009; Amuda 2011
Rice straw		8.9 mg/g				Jiang et al 2012; Amuda 2011
Rice straw			1.2 mg/g			Jiang et al 2012

*Continued on next page.*

<b>Sorbent</b>	<b>Sorption capacity</b>				<b>Initial Metal concentration</b>	<b>Reference</b>
	<b>Cr<sup>3+</sup></b>	<b>Cu<sup>2+</sup></b>	<b>Pb<sup>2+</sup></b>	<b>Zn<sup>2+</sup></b>		
Saw dust	2.25 mg/g					Sahmoune et al. 2016; Kulkarni 2014
Saw dust			1.2 mg/g			Sahmoune et al. 2016; Kulkarni 2014
Saw dust					4.04 mg/g	Sahmoune et al. 2011; Kulkarni 2013
*Biochar (Minimum)	3.0 mg/g	3.0 mg/g	4.0 mg/g	8.0 mg/g	5.0 mg/g	Liu et al. 2010; Mohan et al. 2007; Inyang et al. 2012; Mubarak et al. 2013
*Biochar (Maximum)	20.0 mg/g	18.0 mg/g	100.0 mg/g	120.0 mg/g	40.0 mg/g	Kołodźńska et al. 2012; Tong et al. 2011; Cao et al. 2009; Han et al. 2013

\*Sorption capacity of biochar has a wide range of variations based on the type of biomass used for its preparation.

Table 3.1 highlights the variation in sorption capacities obtained by different studies even for the same material at different experimental conditions. This is mainly due to the influence of experiential conditions such as pH, temperature and initial metal ion concentration on the sorption capacity of a sorbent. High variability in sorption capacity is evident when different biosorbents are used under the same experimental conditions (Hansen et al. 2010; Dai et al. 2018). Similar observations have been made when the same biosorbent from different batches were used under the same experimental conditions (Amarasinghe and Williams 2007; Wan et al. 2014). This variation is attributed to the high variability of the physical and chemical configurations within the material. However, similar sorption capacity values can be obtained if the studies were conducted under similar experimental conditions and for the same batch of a biosorbent (Wang and Chen 2009). This is a limitation in the use of biosorption as a potential wastewater treatment technique as the ultimate removal efficiency relies on the properties of the material. Hence, it is important to understand the influence of physico-chemical properties of the biosorbent on sorption capacity. Relationships between the sorption capacity of a sorbent and the experimental conditions has been extensively studied (Chuah et al. 2005; Hansen et al. 2010; Wang and Chen 2009) by varying the experiential conditions using a single batch of biosorbent. However, studies that adequately explain the relationship between physico-chemical properties of the biosorbent and the sorption capacity are limited as it is a challenge to investigate the influence of each parameter separately. Understanding the influence of physico-chemical properties on sorption is imperative as that knowledge can be used to enhance the sorption capacity of a material by changing the material properties. Furthermore, it is important to gain an in-depth understanding of the significant properties that contribute to sorption.

### **3.4 INFLUENTIAL PARAMETERS**

In reviewing available information from literature, probable influential parameters of biosorbents for heavy metal sorption can be discussed under two categories; experimental conditions and properties of biosorbents. pH of the solution, sorbent dose, agitation rate, contact time of the sorbent are the significant experimental conditions that influence heavy metal sorption (Wan et al. 2014; Xue et al. 2012). Influential properties of a biosorbent include particle size, specific surface area (SSA),

pore size (Dong et al. 1984; Jain and Ram 1997; Johnston and Johnston 1996) and surface functional groups (Fan et al. 2018).

### 3.4.1 Experimental conditions

#### *a. Solution pH*

The proton activity in an aqueous solution is commonly expressed as pH which serves as a measure of the acidity or alkalinity of the solution. Both, solids and heavy metals have chemical characteristics that are affected by the concentration of hydrogen ions ( $H^+$ ) in the solution. As an example, surface functional groups in solids are directly influenced by the  $H^+$  or  $OH^-$  ions (solution pH) in the surrounding solution (Bernardin Jr 1985). At low pH values, these sites develop positive charges due to the sorption of protons. As the pH value increases, these sites develop a neutral charge and ultimately reach a negative charge. Therefore, the extent of sorption at a given pH varies among the metal elements. Furthermore, pH influences the sorption mechanism (van der Linden et al. 2009).

For example, oxidic and carbonaceous sorbents possess functional groups on their surface that can be protonated or deprotonated. As a consequence, the surface of such sorbents is typically positively charged at low pH values and negatively charged at high pH values. The pH value at which the sum of positive charges equals the sum of negative charges is referred to as point of zero charge (Worch 2012). Although it is assumed that the surface charge has no influence on the sorption of neutral adsorbates, charged species can be influenced by additional attraction or repulsion forces. In pH ranges where the adsorbate species have the same charge as the surface, the sorption is relatively weak, not only as a result of the higher polarity of the charged adsorbate species, but also due to additional repulsion forces. Under certain conditions, pH ranges exist where the adsorbate species and the sorbent surface show opposite charges and consequently, attraction forces occur. Since these attraction forces act in addition to the van der Waals forces, a sorption maximum can often be observed in these pH ranges (van der Linden et al. 2009; Gupta and Sen 2017).

Metal precipitation is most sensitive to the pH of the solution (Bradl 2004). Precipitation is mainly a function of the pH and relative quantities of metal ions present in the solution. Metals may precipitate on the surface of solids particles as oxides, hydroxides, carbonates, sulphides or phosphates. Different metal elements have

different threshold pH values for initiating precipitation (Adriano 2001). In their studies using tea waste, Amarasinghe and Willams (2007) and Wang et al. (2014) noted that  $Pb^{2+}$ ,  $Cd^{2+}$  and  $Cu^{2+}$  sorption increases with the pH and a pH value of 4-5 range is most favourable. These observations emphasize that at low pH, the surface of the sorbent is surrounded by hydrogen ions ( $H^+$ ) which prevent the metal ions from approaching the binding sites on the sorbent. As such, pH of the solution is a significant parameter influencing its metal removal properties and should be controlled.

#### ***b. Sorbent dose***

Increasing sorbent dose increases the amount of available sorption sites. Therefore, in theory, metal sorption must increase with increasing sorption dose. Furthermore, it was proven in previous studies that metal sorption rate increases at high sorption doses. This is attributed to the reduction in competition between metal ions due to the availability of more sorption sites (Apiratikul and Pavasant 2008; Ismail et al. 2010; Jamil et al. 2010).

#### ***c. Initial metal concentration of the solution***

The initial concentration of metal ions is responsible for the important driving force working to overcome the mass transfer resistance of metal ions between the aqueous and solid phases (Malkoc and Nuhoglu 2005). Research studies report conflicting observations regarding the effects of initial concentration on the removal of metals. When the initial metal concentration of the solution is increased at a constant sorbent dose, documented observations include;

1. Decrease in the percentage uptake of metal ions (Hui et al. 2005; Ibrahim et al. 2010; Wang et al. 2006).
2. Increase in sorption capacity for up to a certain initial metal concentration, above which there is only a slight increase in sorption or no sorption (Kocaoba et al. 2007; Ören and Kaya 2006).

In experimental studies to evaluate the influence of initial metal concentration on sorption, the number of available sorption sites is fixed by keeping the sorbent dose constant. When the initial metal concentration is raised, the active sites available for the sorption of metal ions can become insufficient. This is the reason for the first category of observations mentioned above. In the case of the second type of observations given above, sorbent could have been exhausted since the active sites

were occupied by ions. Therefore, a significant increase in metal removal was not observed beyond a certain initial metal concentration.

### **3.4.2 Properties of biosorbent**

#### *a. Particle size*

Researchers have identified particle size as an important physical property of biosorbents, which can influence sorption efficiency. Past researchers have noted the increase in heavy metal sorption with the decrease in particle size of biosorbents (Chuah et al. 2005; Serencam et al. 2008; Wan et al. 2014). As an example, in a study carried out by Wan et al. (2014) using tea waste, it was found that the efficiency in the removal of Pb(II), Cd(II) and Cu(II) increased with the decrease in the material particle size. Similar results were obtained in a research study carried out by Amarasinghe et al. (2007) using tea waste which was compatible with those of similar studies conducted using different biosorbents such as tea waste and rice husk (Amarasinghe and Williams 2007; Chuah et al. 2005; Serencam et al. 2008; Wan et al. 2014).

However, the effect of material particle size on sorption is better described using clay and soil particles than by the use of biosorbents. Herngren et al. (2006) carried out a study on heavy metal concentrations in five different particle size ranges in urban stormwater runoff. They found that most of the heavy metals were adsorbed to particles below 150 $\mu$ m and the maximum concentration was found in the size range of 0.45 - 75 $\mu$ m (Herngren et al. 2006). A similar behaviour was reported by Birch and Scollen (2003), who demonstrated that the highest metals concentration is in the fraction smaller than 62 $\mu$ m (Birch and Scollen 2003). Most importantly, the particle size was shown to determine the mobility of associated pollutants (Deletic and Orr 2005). Li et al. (2006) summarised the data in the literature on metal concentrations as a function of different particle sizes and showed that the concentration increases with decreasing particle size (Li et al. 2006). Similarly, based on a detailed study of the sorption of metal ions in sediments, Jain and Ram (1997) and Gunawardana et al. (2011) found that there is a decrease in sorption with the increase in particle size (Gunawardana et al. 2011; Jain and Ram 1997). The above findings confirm that the particle size has a significant influence on sorption capacity.

### *b. Specific Surface Area*

Specific surface area (SSA) is measured as the surface area per unit mass, assuming a constant particle density and is expressed as  $\text{m}^2/\text{g}$  (Filep 1999; White 2006). Increase in SSA increases the sorption ability of particles by providing a large interface for the metal elements to interact with the particle surface (White 2006). Researchers have noted that SSA increases with decreasing particle size (Amarasinghe and Williams 2007). For a given material, higher surface area can provide more binding sites for metal removal and thereby, increase the sorption capacity.

SSA of a given biomaterial varies with the particle size. However, SSA varies among different soil constituents depending on the differences in the mineralogy and particle size distribution (Cerato and Lutenecker 2002). It has been proven in past research studies that soil mineralogy has a significant effect on specific surface area (Sparks 2003). In literature, the influence of specific surface area on sorption is mostly explored in studies on soil and clay. The number of studies that have investigated the influence of specific surface area on sorption using biosorbents is very limited.

Fine clay particles have the highest SSA values among other mineral constituents of solids, where different pollutants physically and chemically bind to clay particles. Depending on the clay type, such as swelling or non-swelling, SSA values can also change. As an example, swelling clays such as montmorillonite have the highest SSA values while kaolinite which is a type of non-swelling clay, has low SSA values (Sparks 2003). Many sorbents found to have high surface areas are known to be porous. With such materials, it is often useful to differentiate the external and internal surfaces. The external surface is generally regarded as the envelope surrounding the discrete particles or agglomerates. It is accepted that the external surface area should be defined to include all the prominences plus the surface areas of any cracks which are wider than they are deep. Consequently, the internal surface includes the walls of all cracks, pores and cavities which are deeper than they are wide and are accessible (Sing 1985). Porous sorbents typically have internal surface areas that exceed the external surface areas many times over. Specially, engineered sorbents are known to have extremely large internal surface areas where nearly the whole sorption capacity is provided by the internal surface area.

In the past, two common approaches have primarily been used to determine specific surface areas of clays and soil. The first is the measurement of external surface area

by the sorption of nitrogen at low temperatures (77K). In this method, the surface area is calculated from sorption isotherm data aided by the application of BET theory (Brunauer et al. 1938). This method is referred to as the BET method and the internal surface area determined is frequently referred to as the BET surface area. The BET model is based on the assumption of a multilayer sorption to a nonporous sorbent with energetically homogeneous surface without lateral interactions between the adsorbed molecules. However, the equations derived under these observations are often used to determine the internal surface of porous sorbents as well.

The second method is the measurement of total surface area of expanding clays by the sorption of polar liquids whose inner surfaces are inaccessible to nitrogen. The porosity in a biosorbent is considered negligible and biosorbents that have not undergone any treatment or activation are not defined as porous material (Tran et al. 2016). Hence, the specific surface area of biosorbents can be explained and analysed from gas sorption-desorption isotherms measured using a sorptometer. This method has been widely used by past researchers to obtain the specific surface area of biosorbents.

### *c. Surface Functional groups*

Sorption behaviour of carbon materials is decisively influenced by surface oxides bound in the form of various functional groups. The most common surface functional groups in organic matter are; -COOH (carboxyl), -OH (hydroxyl), -C<sub>6</sub>H<sub>4</sub>-OH (phenolic), -NH<sub>2</sub> (amino) and -NH (imino) compounds which are capable of binding cations (Filep 1999; Stevenson 1976). Among these, metals are mainly bound to the -COOH and -OH groups due to ionization of these groups. Thus, these groups can form stable complexes with positively charged heavy metal cations. Furthermore, the main functional groups facilitating metal uptake to algal biomass have been identified as sulfonates, carboxyl, and hydroxyl. These are mainly from polysaccharidic materials which happens to form most of the algal biomass surface wall (Davis et al. 2003; Naja et al. 2010; Schiewer and Volesky 1996). Surface oxides on a carbon surface can be acidic or basic. Hence, the functional groups can be quantified using titration methods (Boehm 1994). However, the acidity between each functional group should be sufficiently large to differentiate them by titration. FTIR spectroscopy is another method used to identify the functional groups which assigns sorption bands based on



the experience of molecular organic compounds (Fanning and Vannice 1993; Sellitti et al. 1990). This method can only be used for identification and not for quantification.

#### *d. Pore size*

Most of the engineered sorbents with large internal surface areas possess a large number of different pores with different shapes and sizes. The definitions by the International Union of Pure and Applied Chemistry (IUPAC) identifies three different types of pores: macropores (sizes above 25 nm), mesopores (sizes within 1 nm-25 nm) and micropores (sizes below 1 nm). The macropores and the mesopores are mainly relevant to mass transfer into the interior of the sorbent particles, whereas the micropore volume primarily determines the size of the internal surface and therefore, the sorbent capacity. Generally, the internal surface area increases with increasing micropore volume (Sing 1985). In principle, the higher the micropore volume, the larger the amount of adsorbate that can be adsorbed. However, it has to be considered that in the case of very fine pores and large adsorbate molecules, there may be a limitation in the extent of sorption by size exclusion. Such size exclusion can be found for instance, in the case of sorption of high-molecular-weight natural organic matter to microporous sorbents (Wu et al. 2009).

Although pore size analysis is important for both sorption kinetics studies and sorption equilibrium studies, it is not a simple matter and involves several key issues. All pore-size analyses are based on models that are subject to certain simplifications and restricted validations. Additionally, there is no single method that can be used for all ranges of pore sizes while the measurement procedures and the data analysis involved are considered complex and tedious. Since the shapes of the pores are typically irregular, simplifying assumptions in view of the pore geometry are commonly made. Finally, the results of different methods are often not comparable (Sing 1985).

The removal of metals using sorbents is a complex chemical process which is influenced by the experimental conditions and properties of the sorbent. Influence of all these properties has to be understood in order to design a proper treatment system for industrial wastewater. Apart from that, knowledge in relation to the isotherm and kinetics of the mechanisms employed by sorbents for the removal of metal ions is useful for understanding the sorption system and in controlling the sorption process. Consequently, it is essential to model the isotherm, kinetics and thermodynamics of

the sorption processes and, for this purpose, fundamental knowledge on various modelling approaches available is imperative.

### **3.5 SORPTION MODELLING**

Sorption modelling is important to understand performance and mechanisms of sorption. Two approaches are generally used for modelling a sorption system (Pagnanelli et al. 2002):

- i. Mechanistic approach.
- ii. Empirical approach.

In the mechanistic approach, models are derived to represent the system behaviour based purely on scientific theories while in the empirical approach, models are derived from systems based on experimental data (Volesky 2003). However, real world systems are generally too complex to be represented by theoretical models alone. Though empirical models can provide real time information about a system, the details barely provide any physical meaning unless interpreted using established theories (Wang and Chen 2009). Hence, modelling a system requires a combination of both, mechanistic and empirical approaches, to complement each other (Nestorov et al. 1999).

#### **3.5.1 Isothermal modelling**

Isotherm models are used to describe the equilibrium of ions between solid and solution phases. In this regard, sorption isotherm models can be used to calculate the maximum sorption capacity of a sorbent and to establish the affinity series. Isotherm models are widely used in sorption studies and are derived based on the assumption that the equilibrium sorption behaviour depends only on the temperature of the system. Consequently, the temperature of the system is maintained constant. In contrast, in most experimental studies, pH of the system is not controlled (Erdem et al. 2004; Ho and McKay 2002), even though the equilibrium behaviour depends on the pH of the system (Bosma and Wesselingh 1998). Hence, it is important to consider controlling the pH of the systems in sorption experiments.

Various isotherm models have been developed for different sorption scenarios. Among them, Langmuir and Freundlich models are widely used to determine whether the

sorption is of monolayer or multilayer nature. This is useful to predict the type of sorption mechanisms involved.

***a. Langmuir isotherm model***

Langmuir isotherm model is developed for an ideal homogeneous sorption scenario. Homogeneous sorption occurs if sorption sites of a sorbent are identical and equivalent. Thus, every sorption site in the sorbent has an equal affinity to adsorb metal ions (Kundu and Gupta 2006). Langmuir isotherm model also assumes that there is no further interaction or migration between adsorbed metal ions (Vijayaraghavan et al. 2006). Therefore, a rigid layer having the thickness of only one molecule (a monolayer) is formed during ideal Langmuir sorption. Additionally, no further sorption or desorption occurs once all sorption sites are occupied by metal ions. Langmuir isotherm equation is given as (Langmuir 1916):

$$Q_e = \frac{q_m K_a C_e}{1 + K_a C_e} \quad \text{Equation 3.1}$$

Where  $C_e$  and  $Q_e$  are equilibrium metal concentration in the solution (mg/L) and equilibrium sorption capacity (mg/g) respectively.  $q_m$  (mg/g) and  $K_a$  (L/mg) are Langmuir constants related to maximum sorption capacity and energy of sorption (or affinity term) respectively.

The following linearised form of Langmuir isotherm is often used in sorption studies:

$$\frac{C_e}{Q_e} = \frac{1}{q_m K_a} + \frac{C_e}{q_m} \quad \text{Equation 3.2}$$

***b. Freundlich isotherm model***

Freundlich isotherm characterises a more complex scenario than the Langmuir isotherm. The scenario is that sorption sites are heterogeneous, which means they are not identical and equivalent. Thus, the sorption sites have different degrees of affinity for the sorption of metal ions in such a way that stronger sorption sites are occupied first by metal ions and sorption continues until the weakest site is occupied. In Freundlich sorption scenario, formation of multilayer sorption is possible since adsorbed metal ions can attract other molecules from the bulk solution. Freundlich isotherm model is governed by the following Equation 3.3 (Freundlich 1906):

$$\log Q_e = \log K_F + \frac{1}{n} \log C_e \quad \text{Equation 3.3}$$

Where  $K_F$  is Freundlich constant (mg/g) and  $n$  is Freundlich exponent.

The  $K_F$  constant is an indicator of sorption capacity, while  $n$  is the indicator of intensity of the reaction. The  $n$  value can be used to predict the nature of the interaction between the metal ion and the sorbent (Foo and Hameed 2010). When the 'n' value is greater than 1, it implies that the sorption of metal ions is modified in a way that the metal sorption capacity of sorbents is increased such as by revealing previously inaccessible active sites (Jiang et al. 2002). In contrast, an  $n$  value of less than 1 indicates that the bonds between active sites and metal ions are weak. Consequently, metal ions prefer to form hydrogen bonds with already adsorbed metals instead of bonding with the active sites of sorbents. Therefore, an  $n$  value less than 1 corresponds to physisorption or ion exchange (Rengaraj et al. 2001).

### **3.5.2. Kinetic Modelling**

Sorption kinetics describes the mobility of a metal ion in the bulk solution until it is immobilised by the active sites of the sorbent material. Several mathematical models have been proposed to describe data obtained from sorption experiments. They are generally classified as sorption reaction models and sorption diffusion models (Qiu et al. 2009). While both, sorption diffusion models and sorption reaction models are applied for the purpose of describing the kinetic process of sorption, they are fundamentally different. Sorption diffusion models are developed based on three consecutive steps as explained by Lazaridis and Asouhidou (2003). These three steps are illustrated in Figure 3.1 (Lazaridis and Asouhidou 2003).

1. External diffusion - diffusion across the liquid film
2. Internal diffusion or intra-particle diffusion- diffusion along the pore walls of the sorbent
3. Mass action -sorption and desorption between the adsorbate and active sites of the sorbent.

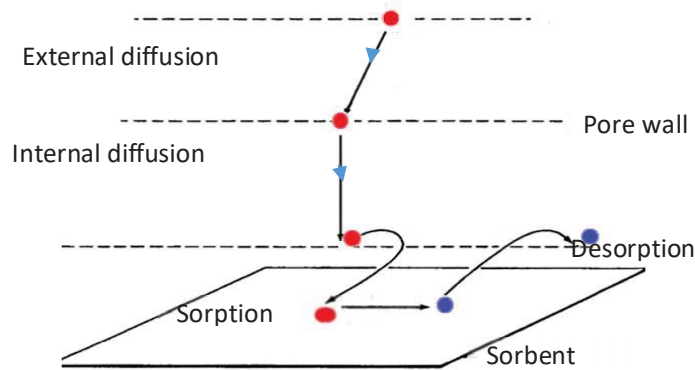


**Figure 3.1** Schematic diagram illustrating the external diffusion, internal diffusion and mass action (red and blue circles denote the metal ion and the arrows indicate the diffusion directions)

Considering the use of sorption diffusion models in kinetic modelling, Weber-Morris model (Weber 1963) is the method widely used to describe the intraparticle diffusion. It has been found that in many sorption studies, solute uptake varies proportionally with  $t^{1/2}$  rather than with contact time  $t$  (Alkan et al. 2007). Internal diffusion can be accelerated by changing the physico-chemical properties of biosorbents. This will enhance the sorption process and reduce the time taken for the process to occur.

Sorption reaction models are derived from chemical reaction kinetics and are based on the complete process of sorption without considering the intermediate steps mentioned above (Qiu et al. 2009). Pseudo first order model proposed by Lagergren (1898) and pseudo second order model proposed by Ho and McKay (1998) are the commonly used sorption reaction models to simulate sorption kinetics data (Ho and McKay 1999; Lagergren 1898). These sorption reaction models are widely used in the field of sorption using biosorbents (Largitte and Pasquier 2016). These two models were assessed for their suitability for experimental data and one was selected as the best fit model based on the difference in the correlation coefficient.

### *a. Pseudo first order model*

The generic form of Pseudo first order model is illustrated in Equation 3.4.

$$\frac{dq_t}{dt} = k_1(q_e - q_t) \quad \text{Equation 3.4}$$

Where  $k_1$  ( $\text{min}^{-1}$ ) is the pseudo first order rate constant for the model,  $q_e$  and  $q_t$  ( $\text{mg/g}$ ) are the sorption capacities at equilibrium and time  $t$ , respectively.

Integrating Equation 3.4 with the boundary layer conditions ( $t = 0, q_t = 0$ ) and ( $t = t, q_t = q_t$ ) gives:

$$\ln(q_e - q_t) = \ln q_e - k_1 t \quad \text{Equation. 3.5}$$

The metal binding rate can be found from the slope of the plot of  $\ln(q_e - q_t)$  vs.  $t$ . Pseudo first order model has been widely used to describe metal sorption to biosorbents, such as: removal of Cu(II), Ni(II) and Cd(II) using biochar (Xue et al. 2012); and removal of Zn using tea waste (Wasewar et al. 2008). Ho et al. (1998) pointed out that the equilibrium sorption capacity must be known to fit the pseudo first order model to experimental data. Ho et al. (1998) described the model as complex since it is difficult to find the accurate equilibrium sorption capacity if chemisorption, which is generally slow, is involved in metal sorption. In such cases, complex trial and error analysis is required (Ho and McKay 1998).

### *b. Pseudo second order model*

Therefore, Ho et al. (1998) proposed pseudo second order model given by Equation 3.6:

$$\frac{dq_t}{dt} = k_2(q_e - q_t)^2 \quad \text{Equation. 3.6}$$

Where  $k_2$  ( $\text{gmg}^{-1}\text{min}^{-1}$ ) is the pseudo second order reaction rate constant.  $q_e$  and  $q_t$  ( $\text{mg/g}$ ) are the sorption capacities at equilibrium and time  $t$ , respectively.

Integrating Equation 3.6 with the boundary conditions ( $t = 0, q_t = 0$ ) and ( $t = t, q_t = q_t$ ) gives:

$$\frac{1}{(q_e - q_t)} = \frac{1}{q_e} + k_2 t \quad \text{Equation 3.7}$$

The linearised form of the equation is:

$$\frac{t}{q_t} = \frac{1}{k_2 q_e^2} + \frac{1}{q_e} t \quad \text{Equation 3.8}$$

From the slope and intercept of  $t/q_t$  vs.  $t$  plot, the pseudo second order metal binding rate can be calculated and the equilibrium sorption capacity is not required to fit the experiment data. In addition, Ho et al. (1998) concluded that the pseudo second order model describes the metal binding process better than the pseudo first order model after testing both models using data available in research literature. However it should be noted that the necessity for equilibrium sorption capacity to fit the experimental data with the pseudo first order model can be avoided by rearranging Equation 3.5 as shown in Equation 3.9 and undertaking non-linear regression.

$$q_t = q_e(1 - e^{-k_1 t}) \quad \text{Equation 3.9}$$

Wan et al. (2014) used the pseudo second order model to simulate the kinetic process of sorption of  $\text{Cu}^{2+}$ ,  $\text{Pb}^{2+}$  and  $\text{Cd}^{2+}$  to tea waste. Furthermore, kinetic data on  $\text{Cu}^{2+}$  and  $\text{Pb}^{2+}$  sorption to tea waste, untreated rice straw and sodium hydroxide treated rice straw was best described by pseudo second order equations (Amarasinghe and Williams 2007; Brahmaiah et al. 2015; Wan et al. 2014). According to past research conducted on biochar and biomaterials, pseudo second order kinetic model was considered as the best suited model to describe the sorption kinetics of biosorbents (Kwak et al. 2019; Cherdchoo et al. 2019).

Many experiential studies have revealed that  $k_1$  and  $k_2$  is dependent on experimental conditions of the system.  $k_2$  is usually dependent on the initial solution concentration, pH and agitation rate of the system (Khamizov et al. 2018). Since  $k_1$  and  $k_2$  are interpreted as time scaling factors,  $k_1$  and  $k_2$  decrease with increasing initial metal ion concentration. At higher initial ion concentrations, a longer time is taken to reach equilibrium (Plazinski et al. 2009). It is necessary to fit both models with the experimental data and the model that best fits the experimental data can be used to determine the metal binding rate. According to published literature, pseudo first order model does not describe the kinetic data equally well as the pseudo second order model for many sorbents, confirming the superiority of the latter model over the former one

(Plazinski et al. 2009). However, Simonin (2016) suggested that using data close to or at equilibrium to test the suitability of pseudo first and second order models, can cause methodical bias. This methodical bias unfairly promotes the pseudo second order kinetic model as the best model. Hence, it was recommended to use sufficiently large amount of data including data far from the equilibrium to assess the suitability of these two models for different sorbents.

According to the past studies,  $k_1$  and  $k_2$  varies with experimental conditions such as pH, agitation rate and initial metal ion concentrations (Neris et al. 2019; Gupta and Sen 2017). Similarly,  $k_1$  and  $k_2$  varies from sorbent to sorbent due to the influence of material physico-chemical properties. The influence of material physico-chemical properties on internal diffusion and on the speed of the reactions has not been investigated widely and quantifications of such influence have not been analysed. This understanding is important as it can be used to enhance the sorption process. Sorption is usually analysed by batch systems and column systems. Batch systems are known as static systems while column systems are considered to be dynamic systems capable of offering real world simulations.

### **3.6 BATCH SORPTION AND COLUMN SORPTION SYSTEMS**

In sorption, the interface could be liquid–liquid, liquid–solid, gas–liquid or gas–solid. Among these, liquid–solid sorption is the most common interface when the process of sorption is applied to treatment of solutions such as water or wastewater. Additionally, there are various techniques by which, the contact between the adsorbate and the sorbent is maintained. These can be broadly classified as batch sorption systems and column sorption systems (Kafshgari et al. 2013; Miralles et al. 2010).

#### **3.6.1 Batch sorption systems**

In batch sorption systems, both the sorbent and adsorbate are thoroughly mixed in diluted solutions at constant volumes. It is easy to setup and maintain such a system in addition to being economical. This method is commonly used in sorption studies. However, it is not commonly found in industrial applications. Batch experiments are known as static systems. They are conducted by mixing a certain amount of solid material into solutions having specific concentrations of contaminants with a specific solid/liquid ratio. These mixtures are commonly stirred or shaken during the whole



reaction time (Wang and Chen 2009). This approach has the advantage that it does not require much laboratory space while all the variables under investigation could easily be obtained. Additionally, batch sorption tests easily provide information on sorption equilibrium characteristics and sorption kinetics. However, the batch approach is under criticism due to the fact that results obtained from a batch study do not correlate well with those observed in the field or at industrial scale. This discrepancy is caused by the fact that the operational conditions of the batch system are different from those at field scale (Amarasinghe and Williams 2007). Therefore, the results obtained from batch studies are not usually applied to situations at field scale. Instead, researchers usually rely on data obtained from column operations for designing industrial sorption systems.

### **3.6.2 Column sorption systems**

There are several types of column sorption systems available and these are, continuous moving bed sorption, continuous fixed bed sorption (which can be upflow or downflow), continuous fluidised bed sorption and pulsed bed sorption (Worch 2012). Each of these techniques possesses certain advantages and disadvantages. A brief description of each system is given below with pros and cons.

#### ***a. Continuous fixed-bed sorption***

In fixed-bed systems, the adsorbate is allowed to flow through a bed of sorbent (or sorbents) continuously at a constant rate. Similar to batch systems, this method is also economical and relatively easy to maintain (Miralles et al. 2010). It can be used for a relatively high quantity of wastewater having a high concentration of contaminants. One of the main advantages of this system is that the adsorbate is continuously in contact with a given quantity of fresh sorbents (Monash and Pugazhenthii 2010). Known problems associated with this system include sorbent attrition, feed channelling and non-uniform flow of sorbent particles (Patel 2019; Atar et al. 2012).

#### ***b. Continuous moving bed sorption***

Continuous moving bed sorption system is considered as a steady-state system where both the sorbent and the adsorbate are in continuous motion. This method is complex and costly when compared with other systems. This is due to the fact that the sorbent is continuously replaced while the fresh sorbent is constantly in contact with the adsorbate. Additionally, a large volume of sorbent is required to maintain such a

system and to achieve adequate sorption. It is essential to maintain a continuous regeneration of sorbent and a large sorbent storage (Patel 2019; Worch 2012).

*c. Continuous fluidised bed sorption*

In this method, the adsorbate is in contact with a fluidized bed of sorbent. The flow could either be sufficient or insufficient. As in the previous method, this technique is also complex and costly. It is applicable for a large quantity of wastewater having a higher pollution load. This method is applicable for industrial purposes as it allows rapid mixing of the sorbent and the adsorbate. The flow of adsorbate can be maintained continuously with proper control mechanisms. Among the disadvantages associated are the inability to measure the flow of adsorbate, leading to high deviations from the intended outcome with plug flow, bubbling or feed channelling. These can cause insufficient contact between the sorbent and the adsorbate. Additionally, the rapid mixing associated with this method leads to non-uniform residence time (Cavalcante Jr 2000; EPA 1983).

*d. Pulsed bed sorption*

In pulsed bed sorption, a portion of the exhausted sorbent is periodically withdrawn from one end of the column, usually from the bottom while adding fresh sorbent at the other end. Hence, a column is operated in a semi-continuous counter current way. Such a system could also be designed as a multi-column system with two or more columns placed in a series. Each time an exhausted bed is removed for regeneration, a fresh bed can be introduced at the downstream end of the multicolumn system. This method is not very costly and easy to setup. An automatic control system can also be designed for such a system. An additional advantage is the low volume of sorbent needed. The utilization of sorbent is considered efficient as it can be sent for regeneration as soon as the sorbent is exhausted. This method is used for handling a relatively small quantity of wastewater having a low pollution load (Worch 2012; Patel 2019) .

### **3.7 USE OF FIXED BED COLUMNS IN SORPTION**

As explained in Section 3.6.1, although batch systems are very useful in a laboratory setup, they do not provide an adequate understanding on the practical application in real world conditions. Additionally, since these systems are not capable of handling a large wastewater volume, they are not employed in industrial applications. The column setup however, is capable of handling a large volume of wastewater and is commonly

used in industrial applications (Patel 2019; Miralles et al. 2010). The column system also offers a better simulation of the real world and the data obtained from these systems is essential for designing industrial type sorption systems.

### 3.7.1. Properties of fixed bed column sorption systems

Sorption in a fixed bed system is considered to be a process depending mainly on time and distance (Patel and Vashi 2015). During the sorption process, each sorbent particle in the bed accumulates adsorbate from the solution until equilibrium is reached (Patel 2019). This equilibration process continues sequentially, layer by layer, from the column inlet to the column outlet. However, due to the slow sorption kinetics, no sharp boundary is observed between the loaded and the unloaded sorbent layers. Instead of such a sharp boundary, the equilibration takes place in a more or less broader zone of the sorbent bed, named as the mass transfer zone (MTZ) (Marsh and Rodríguez-Reinoso 2006). When single-solute sorption is considered, three different zones within the sorbent bed can be identified at a given time. These are illustrated in Figure 3.2.

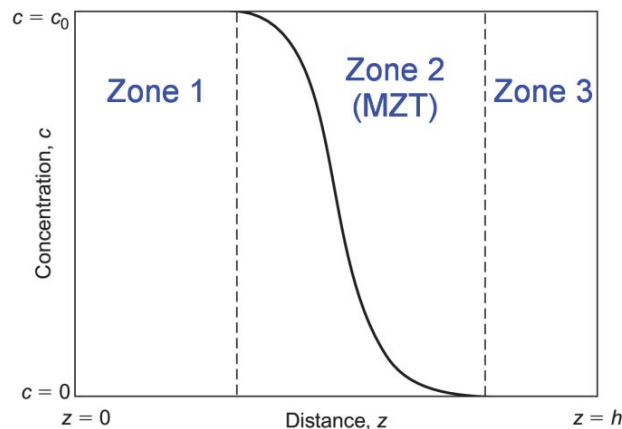


**Figure 3.2** Concentration profile during single-solute sorption in a fixed bed adsorber system of height  $h$ .

In the first zone between the adsorber inlet and the MTZ, the sorbent is already loaded with the adsorbate, which is in equilibrium with the inlet concentration ( $c_0$ ). The available sorption capacity in this zone is zero and no more transfer takes place from the liquid phase to the sorbent particles. Hence, the concentration in the liquid phase is constant and equals  $c_0$ . In the second zone (MTZ), the transfer from the liquid phase to the solid phase continues to take place. Due to the mass transfer from the liquid to

the solid phase, the concentration in this zone decreases from  $c = c_0$  to  $c = 0$ , and the adsorbed amount increases. The shape and the length of the MTZ depend on the sorption rate and the shape of the equilibrium curve. The sorbent in the third zone is maintained free of adsorbate. The fluid-phase concentration in this zone is  $c=0$  (Worch 2012; Chen et al. 2012).

During the sorption process, the MTZ travels through the adsorber with a velocity that is considerably slower than the water velocity. The stronger the sorption of the adsorbate, the greater the difference between the MTZ velocity and the water velocity. As long as the MTZ has not reached the adsorber outlet, the outlet concentration is maintained at  $c=0$ . The adsorbate appears in the adsorber outlet for the first time when the MTZ reaches the end of the adsorber bed. This time is referred to as breakthrough time. Once the breakthrough time is reached, the concentration in the adsorber outlet increases due to the progress of sorption in the MTZ and the related decrease in the remaining sorbent capacity. If the entire MTZ has left the adsorber, the outlet concentration equals  $c_0$ . At this point, all sorbent particles in the fixed bed are saturated to the equilibrium loading and no more adsorbate uptake takes place. The related time is referred to as the saturation time (Worch 2012; Patel 2019).

The concentration versus time curve, which is measurable at the adsorber outlet, is referred to as the breakthrough curve (BTC). The properties and the performance of a fixed-bed column system is commonly assessed via breakthrough curves. The BTC is considered to be a mirror of the MTZ and is therefore affected by the same factors such as sorption rate and the shape of the equilibrium curve (Aziz et al. 2014). The mechanism of this sorption is described based on different phenomena such as axial dispersion, film diffusion resistance, intraparticle diffusion resistance (in both pore and surface diffusion) and sorption equilibrium with the sorbent (Kafshgari et al. 2013; Miralles et al. 2010). The position of the BTC on the time axis depends on the traveling velocity of the MTZ, which in turn depends on the flow velocity and on the strength of sorption. For a given flow velocity, how late the breakthrough occurs depends on how adsorbable the solute is. The relationship between the movement of the MTZ and the development of the BTC is schematically shown in Figure 3.3. The spreading of the MTZ is mainly determined by the mass transfer resistance. In principle, dispersion also leads to a spreading of the MTZ, but this effect is usually negligible under the typical conditions of engineered fixed bed systems (Worch 2012; Chen et al. 2012).

In the limiting case of infinitely fast mass transfer processes and the absence of dispersion, the length of the MTZ reduces to zero and the sigmoid shaped BTC becomes a concentration step. The concentration step is referred to as ideal BTC, and the time after that the concentration step occurs is termed ideal breakthrough time (Aziz et al. 2014). Each real BTC can be approximated by a related ideal BTC (Worch 2012; Marsh and Rodríguez-Reinoso 2006).

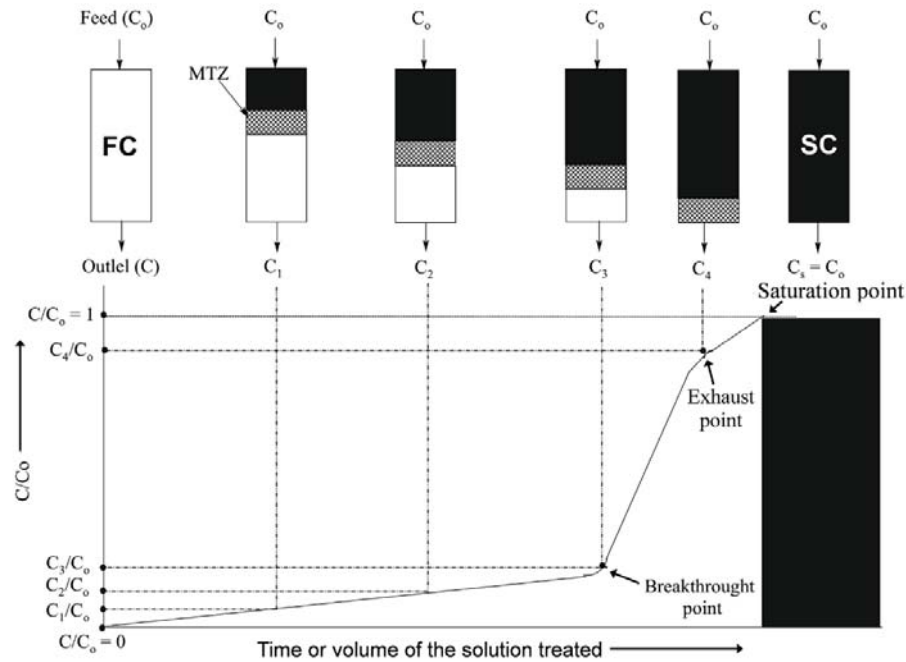


**Figure 3.3** Diagrammatic representation of the fixed-bed sorption process. MTZ mass transfer zone, FC fresh column, SC saturated column adopted from Worch 2012.

In Figure 3.3, the concentration of the adsorbate at the outlet is depicted as  $C$ .  $C_0$  is the initial concentration and  $C_1$ ,  $C_2$ ,  $C_3$  and  $C_4$  are adsorbate concentrations at different stages. At the initial stage,  $C$  is zero and therefore, the ratio of effluent to initial concentration ( $C/C_0$ ) is zero. As the sorption process progresses, the upper layers of sorbent become increasingly saturated with the continuous influx of the aqueous solution into the column and the sorption process becomes less efficient (Worch 2012). The primary sorption zone is progressively shifted down into the area with fresh sorbent in the column. Meanwhile, increasing amounts of adsorbate is seen to be escaping as effluent and is indicated in Figure 3.3 as points  $C_1/C_0$ ,  $C_2/C_0$ ,  $C_3/C_0$  and  $C_4/C_0$ . The downward displacement of the primary sorption zone depends on the initial concentration as well as the influx of the influent (Abdolali et al. 2017). However, the

influence of the former is seen to be more prominent than that of the latter. When the point  $C_s$  is reached, the column is completely saturated and the sorbent is exhausted after which, sorption ceases. At this point, the ratio of  $C/C_0$  is 1 (Chen et al. 2012). Process parameters related to fixed bed sorption systems influence breakthrough and exhaust points in a fixed-bed column system (Abdolali et al. 2017).

The important process parameters related to fixed-bed sorption systems include the initial adsorbate concentration, the flow rate of adsorbate in the column, bed height of the column, pH of the adsorbate, particle size of the sorbent and temperature of the column system. All these parameters play a vital role in the evaluation of the efficiency of the system and influence the breakthrough and exhaust points (Mohan and Sreelakshmi 2008). Breakthrough and exhaust points play an important role in analysing the performance of individual sorbents in fixed bed columns. Hence, the influence of these parameters has to be minimised or controlled by keeping them equal for all the sorbents under investigation, when designing fixed bed columns to evaluate the performance of sorbents.

### **3.7.2 Influence of the process parameters on breakthrough and exhaust points**

A brief description is provided how the process parameters influence breakthrough and exhaust points in a fixed-bed column system. From these process parameters, initial adsorbate concentration, flow rate and bed height are the most commonly investigated parameters in the literature.

#### ***a. Initial sorbate concentration***

Both, the breakthrough and exhaustion points are seen to appear early when the influent concentration is increased. The breakpoint time decreases with increased inlet concentration. The initial sorption is rapid due to the availability of a higher number of vacant sites for the process to occur. Thereafter, increasing the initial adsorbate concentration results in creating a greater driving force to overcome mass-transfer resistance in the liquid phase. This results in the quicker exhaustion of sites. The volume of effluent that can be processed also decreases (Moyo et al. 2017; Saravanan et al. 2018).

#### ***b. Flow rate of sorbate***

The time taken for saturation to occur is increased significantly when the flow rate is decreased. Conversely, breakthrough points generally appear early when the flow rate is high. This happens because an increase in the flow rate increases the amount of adsorbate adsorbed into a unit of bed height in the MTZ. This leads to an increase in the rate of mass transfer and causes quicker saturation (López-Cervantes et al. 2018). Additionally, when the flow rate is low, the adsorbate has more time to be in contact with the sorbent, leading to higher removal of adsorbate in the columns (Ahmed and Hameed 2018; Sheng et al. 2018).

#### ***c. Bed height of column***

Breakthrough time and exhaustion time decreases when the bed depth is increased. The volume of effluent that can be subjected to treatment can be improved by increasing the bed depth. These observations are explained by the increase in surface area and the number of binding sites available for the process of sorption. The time available for the interaction to take place also increases when BTC is increased (Fat'hi et al. 2014; Teutscherova et al. 2018).

#### ***d. pH of sorbate***

There are instances in literature where the optimal sorption was detected under an acidic pH and vice versa. The relationship between pH and the sorbent properties depends on the nature of the sorbent and the adsorbate (Ahmed and Hameed 2018; Banerjee and Chattopadhyaya 2017).

#### ***e. Particle size of sorbent***

When the particle size of the sorbent is increased, breakthrough and exhaustion times are delayed. While higher particle sizes are favourable to achieve better sorption capacities, a moderate flow rate is preferable for a better sorption. Since sorption is a surface phenomenon, the sorption capacity is expected to be proportionate to the specific surface area. However, literature indicates that smaller particles tend to develop high-pressure drops in fixed-bed column systems. Furthermore, a very small particle size seems to cause more problems associated with solid–liquid separation with the sorbent (Unger et al. 2008; Zou et al. 2013).

### *f. Temperature (T)*

When the temperature of the column system is elevated, breakthrough and exhaustion times are reduced. However, sorption capacity also decreases with higher temperatures. This is attributed to higher operating temperatures favouring the diffusion of the adsorbate into the sorbent causing low breakthrough and exhaustion times. Additionally, less amounts of adsorbate are needed to achieve the maximum sorption capacities at higher sorption temperatures. This observation indicates an exothermic process in action. For industrial applications, room temperature is considered to be the preferred temperature considering the cost of heating the system (Girish and Ramachandra Murty 2014; Ye et al. 2018).

#### **3.7.3. Sorption models for column study**

Mathematical models developed for the analysis of fixed-bed column systems make use of parameters such as sorbent capacity, operating life span and regeneration time for making predictions. These models serve to provide insight into the mechanisms behind the process. Axial dispersion, external film resistance and intraparticle diffusion resistance are the key factors influencing the process. Hence, the mathematical correlations developed for sorption in fixed-bed column systems are based on various assumptions regarding axial dispersion, external mass transfer, intraparticle diffusion and nonlinear isotherms.

A number of mathematical models have been developed in the past for the evaluation of efficiency and applicability of the fixed-bed column models for practical application. The Thomas model, bed depth service time model, the Adams and Bohart model, the Yoon–Nelson model, the Clark model, the Wolborska model and the modified dose response model are the most commonly used mathematical models employed to assess the column behaviour of fixed-bed column systems (Abdolali et al. 2017; Patel 2019). Among these, the Thomas model has gained much popularity and commonly found in literature. This model is constructed on the assumption of Langmuir kinetics of sorption–desorption that driving forces follow second-order reversible reaction kinetics with no axial dispersion. The model determines maximum solid-phase concentration of adsorbate on sorbent and the rate constant.

The bed depth service time model is developed based on Bohart and Adams quasi-chemical rate law. It describes the relationship between bed depth and service time in



terms of process concentrations and sorption parameters. The model is based on the hypothesis that the sorption rate is maintained by the surface reaction between adsorbate and the unused capacity of the sorbent. The rationale for this model is that since it takes time to achieve equilibrium in the column, the rate of the sorption process is directly proportional to the fraction of sorption capacity remaining in the system (Ngah et al. 2012).

The Adam–Bohart model was developed by investigating the relationship between  $C/C_0$  and time in a gas–charcoal sorption system. The equation is observed to be useful in analysing other continuous sorption systems. It proposes that the rate of sorption depends on the concentration of the sorbent and residual capacity of sorption (Dorado et al. 2014). Yoon–Nelson model is a relatively simple model which does not depend on the properties of adsorbate, type of the sorbent and any physical features of the sorption bed. The Clark model is based on two assumptions: (1) column sorption is a mass-transfer process with combination of Freundlich isotherm; and (2) behaviour of flow in a column is of piston type. Wolborska model investigated the relationship that describes the concentration distribution in a fixed-bed system for the low-concentration range of the breakthrough curve. Another relatively simple mathematical model used to describe the fixed-bed column sorption data is the modified dose response model. This model can reduce the error resulting from the use of the Thomas model predominantly at lower or higher time periods of the breakthrough curve (Biswas and Mishra 2015; Lee et al. 2015).

#### **3.7.4. Fixed-bed systems in heavy metal removal**

Various studies have attempted heavy metal removal using sorption via fixed-bed systems. Du et al. (2014) used synthetic sorbents, namely, polyacrylonitrile–potassium cobalt hexacyanoferrates and polyacrylonitrile–potassium nickel hexacyanoferrates for the sorption of cesium. The bed depth service time model and the Thomas model were employed to analyse the experimental data and the model parameters were evaluated (Du et al. 2014). Tomas and Adam Bohart models were used to analyse sorption data in relation to arsenite and arsenate. The synthesized sorbents were Ni and MgO metal oxides while carbon nanotube were used as the column system with microwave-assistance (Ali 2018). He et al. (2018) employed a new 3D yttrium-based graphene oxide–sodium alginate hydrogel for the removal of fluoride via a fixed-bed system where the Thomas model was used for the analysis.

Zaini et al. (2018) used vertical column experiments utilizing sugarcane bagasse for the removal of manganese (II). Receptoğlu et al. (2018) synthesised a new chelating sorbent and used it for the removal of boron. Yoon–Nelson model, Thomas model and modified dose response model were employed for the data analysis.

Studies that focus on the comparison of batch and column treatment systems are available. The study by Khan and Rao (2017) focused on the sorption of nickel(II) and copper(II) using chemically modified *Cucurbita moschata* and it was found that column treatment is more feasible than the batch process. In the study by Abdolali et al. (2017), chemically modified multi-metal-binding biosorbent was packed in fixed-bed columns and were used for the sorption of cadmium(II), copper(II), lead(II) and zinc(II) from aqueous solutions. Thomas, Yoon–Nelson and modified dose response models were utilized for the analysis. Vilvanathan and Shanthakumar (2018) performed column sorption tests for nickel and cobalt removal from aqueous solutions using the raw and biochar forms of *tectona grandis*. Applied models were Adam–Bohart, Thomas and Yoon–Nelson. Table 3.2 lists various fixed-bed column studies on heavy metal removal found in research literature along with the maximum sorption capacities obtained using the Thomas model.

Even though there are studies which have investigated the metal sorption capacities in batch and column systems separately as two systems, linkage between the parameters of the two systems for a particular biosorbent has not been investigated. Predicting the sorption parameters of a sorbent in a fixed bed column (which replicates the actual industrial application), using batch sorption parameters would be useful for designing a fixed column sorption system.

**Table 3.2** Various fixed-bed column type sorption studies on heavy metal removal found in literature.

<b>Heavy metal</b>	<b>Sorbent used</b>	<b>Maximum sorption capacity obtained (Thomas Model)</b>	<b>Reference</b>
Cd <sup>2+</sup>	Syzygium cumini L leaf powder	29.08 mg/g	Rao et al. (2011)
Cr <sup>2+</sup>	Pistachio shell	27.95 mg/g	Banerjee et al. (2018)
Cr <sup>6+</sup>	Modified corn stalk	323.70 mg/g	Chen et al. (2012)
Cr <sup>6+</sup>	Orthophosphoric acid-activated lignin	0.889 mmol/g	Albadarin et al. (2012)
Cr <sup>6+</sup>	Leonardite	127.53 mg/l	Dorado et al. (2014)
Cr <sup>6+</sup>	Alkaline anion exchange fiber	210.2 mg/g	Wang et al. (2015)
Cr <sup>6+</sup>	Ionic liquid functionalized cellulose (ILFC)	181.8 mg/g	Dong and Zhao (2018)
Cr <sup>6+</sup>	Co-immobilized activated carbon and Bacillus subtilis	11.7 mg/g	Sukumar et al. (2017)
Cr <sup>6+</sup>	Polypyrrole/Fe <sub>3</sub> O <sub>4</sub> nanocomposite	258.36 mg/g	Bhaumik et al. (2013)
Cr <sup>6+</sup> , Cu <sup>2+</sup> , Zn <sup>2+</sup>	Activated Neem bark	53.95, 12.45 and 23.54 mg/g	Maheshwari and Gupta (2016)

*Continued next page.*

<b>Heavy metal</b>	<b>Sorbent used</b>	<b>Maximum sorption capacity obtained (Thomas Model)</b>	<b>Reference</b>
Cs <sup>+</sup> , Sr <sup>2+</sup>	Montmorillonite–iron oxide composite	4.42 and 15.28 mg/g	Ararem et al. (2013)
Cu <sup>2+</sup>	Chitosan–zeolite	41.14 g/L	Ngah et al. (2012)
Cu <sup>2+</sup>	kenaf (Hibiscus cannabinus) fibers	47.27 mg/g	Hasfalina et al. (2012)
Cu <sup>2+</sup>	Polyaniline-coated sawdust	58.23 mg/g	Liu and Sun (2012)
Cu <sup>2+</sup>	Surface-modified eucalyptus globulus seeds	300.5 mg/g	Kumar et al. (2015)
Cu <sup>2+</sup>	Amino-functionalized ramie stalk	0.528 mmol/g	Wang et al. (2018)
Cu <sup>2+</sup>	Tetraethylenepentamine-modified sugarcane bagasse	0.26 mmol/g	Chen et al. (2017)
Cu <sup>2+</sup> , Mg <sup>2+</sup> , Ni <sup>2+</sup>	Yersiniabactin, immobilized to XAD16 resin	0.12, 0.2 and 0.1 mg/g	Moscattello et al. (2018)
Cu <sup>2+</sup> , Ni <sup>2+</sup>	Magnetized sawdust	43.45 and 33.08 mg/g	Kapur and Mondal (2016)
Cu <sup>2+</sup> , Ni <sup>2+</sup>	Magnetized sawdust (Fe <sub>3</sub> O <sub>4</sub> –SD)	31.89 and 23.59 mg/g	Kapur and Mondal (2016)

*Continued next page.*

<b>Heavy metal</b>	<b>Sorbent used</b>	<b>Maximum sorption capacity obtained (Thomas Model)</b>	<b>Reference</b>
Cu <sup>2+</sup> , Ni <sup>2+</sup>	Natural and immobilized marine algae Sargassum sp.	2.06 and 1.69 mmol/g	Barquilha et al. (2017)
Cu <sup>2+</sup> , Pb <sup>2+</sup> , Cd <sup>2+</sup>	Functionalized SBA-1 mesoporous silica with polyamidoamine	1.6, 1.3 and 1.0 mmol/g	Shahbazi et al. (2013)
Mn <sup>2+</sup>	Granular-activated carbon from agrowaste of mangostene fruit peel	7257.32 mg/g	Chowdhury et al. (2012)
Ni <sup>2+</sup> , Co <sup>2+</sup>	Sugarcane bagasse	1.060, 0.800, 1.029 mmol/g	Xavier et al. (2018)
Ni <sup>2+</sup> , Cr <sup>+6</sup>	TiO <sub>2</sub> agglomerated nanoparticles	33.18 and 12.94 mg/g	Debnath et al. (2010)
Pb <sup>2+</sup> , Cd <sup>2+</sup>	Dead calcareous skeletons	66.16 and 75.18 mg/g	Lim and Aris (2014)
Pb <sup>2+</sup> , Cd <sup>2+</sup>	Grape stalk wastes	31.53 and 49.40 mg/g	Miralles et al. (2010)
Pb <sup>2+</sup> , Cd <sup>2+</sup>	PAAC nanocomposite	36.20 and 37.25 mg/g	Zendejdel and Mohammadi (2018)
U <sup>6+</sup>	Grapefruit peel (GFP)	104.1 mg/g	Zou et al. (2013)

### 3.9 SUMMARY OF KEY FINDINGS

Agricultural waste has drawn much attention as potential biosorbents for the removal of heavy metals from aqueous solutions such as industrial wastewater. However, the efficiency of such treatment depends primarily on the sorbent/sorbents used. Due to the heterogeneity of the material, a range of sorption capacities have been reported in different studies even for the same material. This acts as an impediment for the use of biosorbents as a potential wastewater treatment technique as the ultimate removal efficiency relies on the properties of the material.

There are several influential parameters related to the sorption process. These include, experimental conditions such as solution pH, sorbent dose and initial metal concentration of the solution. Properties of biosorbents such as particle size, specific surface area and surface functional groups also affect sorption. An appreciable number of studies are available to describe the influence of experimental conditions on sorption. However, investigations on the influence of physico-chemical properties of biosorbents on the process of sorption are limited.

Sorption of metal ions is a complex process involving various mechanisms operating in parallel. Where sorption is concerned, sorption modelling is essential to understand the performance and the mechanisms involved. Both, the mechanistic approach and the empirical approach are used for modelling a sorption system and generally, a combination of the two is used. Isotherm models are used to describe the equilibrium of ions between solid and solution phases and various such models have been developed for different sorption scenarios. Among them, Langmuir and Freundlich models are widely used to assess whether the sorption is of monolayer or multilayer nature.

Sorption reaction models and sorption diffusion models are mathematical models proposed to describe the data obtained from the sorption experiments. Pseudo first order model and pseudo second order model are the two commonly used sorption reaction models for the simulation of sorption kinetics data. Weber-Morris model is the commonly used sorption diffusion model. The knowledge of metal sorption kinetics is important to enhance the overall metal removal process. Hence, comprehensive investigations are needed to understand the influence of the material

physico-chemical properties on metal removal rate so that this knowledge could be incorporated in a sorption kinetic model.

Sorption analyses are widely carried out using batch and fixed bed column systems. Batch systems are widely used to investigate the sorption capacities of different materials. However, fixed bed columns offer better simulation of the real world application of sorbents. Operating a column is not always feasible in order to study the sorption process due to space and time constraints. Hence, it is necessary to establish a robust relationship using batch sorption systems in order to predict the performance of the same materials in a fixed bed sorption system.

This page intentionally left blank.



# CHAPTER 4: RESEARCH DESIGN AND METHODS

---

## 4.1 BACKGROUND

Heavy metals entrained in various water bodies in the environment can adversely affect the quality of water and can impose significant risks to human health. Therefore, the need of effective and environmentally friendly treatment methods is imperative. Sorption using agricultural waste has been identified as one such method and as discussed in Chapter 3, surface physico-chemical properties of biosorbents play an important role in determining their sorption capacities and sorption kinetics. Therefore, new knowledge needs to be created to understand the relative influence of individual physico-chemical properties on the performance of sorbents. Quantification of such influence is imperative for creating specific biosorbents in order to enhance the sorption performance. Accordingly, a robust methodology was formulated to generate data sets on metal sorption capacity, kinetics, continuous fixed bed column breakthrough time and influential biosorbent physico-chemical properties.

This chapter describes the research design and methods adopted to accomplish the aims and objectives of the research study. The research design includes the overall strategy that was implemented in order to effectively address the research problem. Research methods describe the procedures used for the implementation of the research design and for the quantification of the various parameters needed for the envisaged analysis undertaken.

## 4.2 RESEARCH DESIGN

The key steps of the research design were:

- a. Critical review of research literature
- b. Selection of metal cations for sorption experiments
- c. Data generation
- d. Biosorbent selection
- e. Data analyses

#### **4.2.1 Critical review of research literature**

The critical review of research literature primarily focused on the following key areas:

- Sources of heavy metals and how they pollute water bodies;
- Health hazards associated with heavy metals;
- Methods employed for the removal of heavy metals from water along with their advantages and disadvantages;
- Different types of low-cost biosorbents described in research literature and their metal sorption abilities;
- Physico-chemical properties and other factors that influence the sorption ability of biosorbents;
- Usage of different models to describe the sorption kinetics of biosorbents;
- Usage of batch sorption systems and fixed bed column systems for heavy metal sorption, their advantages and disadvantages;
- Using batch and column analysis to understand metal sorption mechanisms;
- Laboratory test methods used for the determination of physico-chemical properties of biosorbents and metals;
- Data analyses techniques.

One of the key objectives of the literature review was to explore the existing knowledge gaps in relation to the above areas and their significance.

#### **4.2.2 Selection of metal cations for sorption**

The research study focused on a developing country as a case study where currently, the treatment of industrial wastewater is a challenge. A case study permits confirmation of new knowledge based on experimental results. Hence, a pilot study was conducted to assess the species of heavy metals commonly released from industrial wastewater. Furthermore, previous studies on wastewater characterisation in the country were also taken into consideration.

### 4.2.3 Data generation

Data generation was designed to:

- Understand how the physico-chemical properties of biosorbents affect sorption capacities and sorption kinetics of common metal ions in industrial wastewater.
- Investigate the relationship between batch and column sorption of sorbents.

As explained in Section 4.2.1, the selection of key physico-chemical properties for the study was based on a critical review of research literature. Specific surface area, average pore size, pore volume, surface functional groups and material zeta potential are the inherent properties of biosorbents that can be quantified and are recognised as varying from material to material (Naja et al. 2010; Schiewer and Volesky 1996). Hence, these parameters were chosen to be analysed and to be quantified in order to understand their influence on heavy metal sorption capacity and sorption kinetics of biomaterials. Generally, to determine the influence of a particular parameter, researchers had varied that particular parameter while the other parameters were kept constant. However, it was difficult to design the experiment as such in order to understand the impact of individual physico-chemical parameters on sorption as these parameters are inherent properties of the material and therefore, cannot be altered individually. Hence, it was necessary to manipulate the inherent properties of the material so that the variation in physico-chemical properties among the samples was significant. It was decided to generate samples with distinct physico-chemical properties using this approach.

Once the samples with distinct physico-chemical properties were generated, material characterisation was undertaken in order to quantify the physico-chemical properties of the biosorbents. Batch sorption experiments and column sorption experiments were conducted as the next steps in data generation. Accordingly, data generation consisted of three steps; material characterisation, batch sorption experiments and column sorption experiments.

### 4.2.4 Biosorbent selection

Based on the review of literature, five low-cost and locally available biosorbents from agricultural waste with metal removal capabilities were initially selected. Since the metal removal performance of a biosorbent depends highly on experimental

conditions, calculation and comparison of metal removal performance of the five biosorbents was needed to be done under similar experimental conditions. Accordingly, preliminary sorption experiments were set up under similar experimental conditions (pH, temperature, biosorbent dose and initial metal concentration) to obtain the sorption capacities for the selected metal ions. Sorption capacity (or loading) is defined as the amount of adsorbate taken up by the sorbent per unit mass (or volume) of the sorbent (Saeid Mokhatab et al. 2015). Out of these five biosorbents, two biosorbents were selected for sample generation based on these preliminary sorption experiments. Further details regarding this selection of biosorbents are given in Chapter 5.

#### **4.2.5 Data analysis**

Results derived from the laboratory experiments were analysed in three different steps to achieve the aims and objectives of the study. A schematic representation of the data analysis is shown in Figure 4.1. Firstly, the influence of different physico-chemical properties was analysed to identify the importance of each property for determining the sorption capacity of a biosorbent. Secondly, the influence of physico-chemical properties on sorption kinetics was analysed. This was further extended to predict the sorption kinetics of biosorbents using their physico-chemical properties. In the third stage, relationships between batch and column sorption systems were analysed to understand the correlation between these systems and to develop a relationship in order to predict column performance using batch sorption parameters for a particular biosorbent.

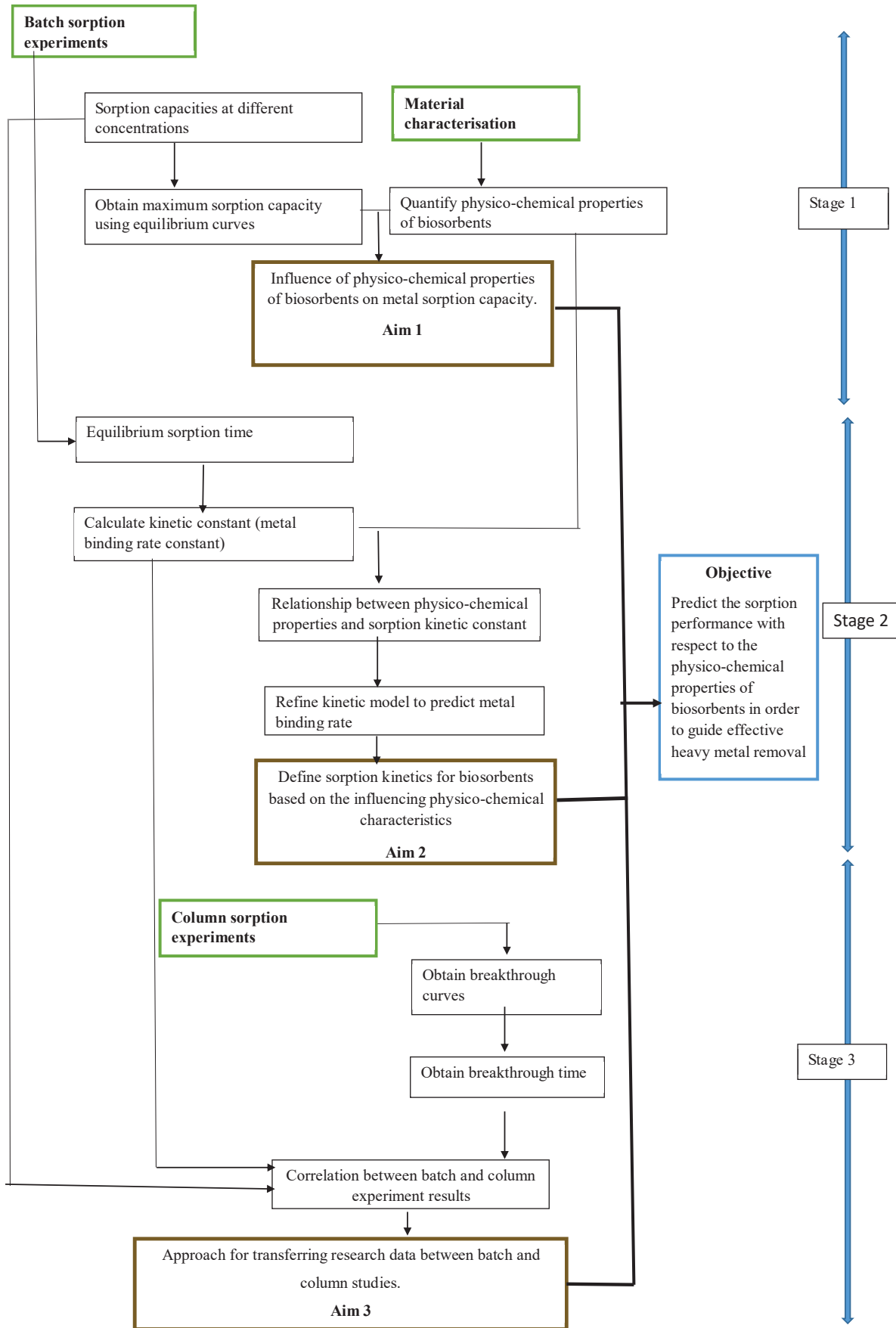


Figure 4.1 Design of data analysis methodology

## **4.3 RESEARCH METHODS**

### **4.3.1 Selection of heavy metal ions**

Sri Lanka was selected as the case study as it is a developing country where industrial wastewater treatment is a high priority and a challenge. Wastewater samples from five industrial outlets including discharges from an industrial zone were collected and tested for heavy metals that are commonly present in wastewater. Accordingly,  $\text{Pb}^{2+}$ ,  $\text{Cu}^{2+}$  and  $\text{Cd}^{2+}$  were the selected heavy metals for the study as their concentrations in wastewater exceeded the stipulated discharge limits. Details of the analysis and the results are given in Section 5.2.

### **4.3.2 Preparation of metal solutions for sorption studies**

Metal solutions containing the selected metal ions were prepared by dissolving the corresponding metal nitrate in deionised water. These solutions were used for the sorption studies. Metal nitrates were used as nitrate anions do not hydrolyse metals nor form metal-anion complexes (Perić et al. 2004; Ziyath et al. 2011). As such, nitrate anions do not interfere with the metal sorption processes of biomaterials.

### **4.3.3 Generation of biosorbent samples**

Out of the five biosorbents selected from the preliminary experiments, two materials with distinct physico-chemical properties were selected to prepare material mixtures via a multi criteria analytical protocol developed using the decision making method; PROMETHEE (Preference Ranking Organisation Method for Enrichment Evaluations). Accordingly, the two selected biosorbents were tea factory waste (TFW) and coconut shell biochar (CSB). Further details of this selection process is given in Chapter 5. The two selected biosorbents were mixed in specific weight ratios to obtain several combinations of mixtures with diverse physiochemical properties as given in Table 4.1. The objective of this exercise was to manipulate the inherent properties of biosorbents as mentioned in Section 4.2.4 and to obtain a series of samples with significant variations in physico-chemical properties. Accordingly, 21 biosorbent samples were obtained. An ANOVA was performed to investigate if there was a statistically significant difference in terms of physiochemical properties among the samples. The results indicated that the variations of different physico-chemical properties among the 21 mixtures were significant ( $p < 0.05$ ) except for zeta potential.

The ANOVA results are provided in Table 4.2. Hence, these samples were considered as twenty one separate biosorbents (henceforth referred as biosorbent samples).

**Table 4.1** Weight percentage of selected biosorbents used to generate mixtures

Sample	Weight % of CSB*	Weight % of TFW*
1	100	0
2	95	5
3	90	10
4	85	15
5	80	20
6	75	25
7	70	30
8	65	35
9	60	40
10	55	45
11	50	50
12	45	55
13	40	60
14	35	65
15	30	70
16	25	75
17	20	80
18	15	85
19	10	90
20	5	95
21	0	100

\* Biosorbents selected from preliminary experiments (Details of selection is given in Chapter 5)

**Table 4.2** Significance of p values obtained by ANOVA for each variable in the material mixtures

<b>Variable</b>	<b>Significance of P value obtained by ANOVA</b>
SSA	< 0.001
PS	< 0.005
PV	< 0.001
ZP	> 0.5
TAG	< 0.001
TBG	< 0.005

#### **4.3.4 Laboratory investigations of samples**

Laboratory experiments were conducted for the prepared mixtures (biosorbent samples) to quantify their physico-chemical properties, sorption capacities and kinetic constants. Fixed bed column systems were also prepared from these samples and the basic readings of such systems such as breakthrough times (the time taken for the adsorbate to appear in the adsorber outlet for the first time in a column system, as explained in details in Section 3.7) and sorption capacities were assessed.

##### ***a. Physico-chemical properties***

Samples were quantified using the physico-chemical properties mentioned in Section 4.2.4. Parameters used for the characterisation along with the test methods employed are given in Table 4.3. Detailed descriptions of the analysis undertaken and laboratory instruments used are given in Chapter 6.



**Table 4.3** Physico-chemical parameters for the characterisation of biosorbents

Parameter	Test method
Specific surface area	Brunauer–Emmett–Teller (BET) method
Pore size	BJH adsorption (Barrett, Joyner, and Halenda, 1951)
Pore Volume	Halenda, 1951)
Zeta potential	Zetasizer of Malvern Instruments
Concentrations of surface functional groups	Boehm titration (Boehm,1994)

### *b. Surface Morphology*

Surface characteristics and morphology of biosorbents are important parameters (Gundogdu et al. 2013) that can be used to interpret the sorption behaviour of biosorbents. Hence, the parameters given in Table 4.3 were used for further assessment of the material surface and the sorption behaviour. The respective test methods used are also included in Table 4.4. Detailed descriptions of the analysis undertaken and laboratory instruments used are given in Chapter 6.

**Table 4.4** Parameters used for material surface interpretation

Parameter	Test method
Surface Morphology	Scanning Electron Microscopy (SEM)
Surface functional groups	Fourier transform infrared spectroscopy (FT-IR)
Background Metal Concentration	Atomic Absorption Spectrometry

### *c. Batch sorption experiments*

Batch sorption experiments were conducted to determine the sorption capacities of TFW, CSB and the mixtures (biosorbent samples) for each metal ion ( $\text{Cu}^{2+}$ ,  $\text{Pb}^{2+}$  and  $\text{Cd}^{2+}$ ) by adding a known quantity of the biosorbent to a known volume of solution containing heavy metal ions. Details of the batch sorption experiments are given in Section 6.10. The quantity adsorbed and the percentage removal (sorption capacity) of metal ions was calculated using equation 4.1 and 4.2, respectively:

$$q_e = V(C_e - C_o)/m \quad \text{Equation 4.1}$$

$$\text{Sorption capacity} = 100\{(C_e - C_o)/C_o\} \quad \text{Equation 4.2}$$

Where  $q_e$  (mg/g) is the quantity of metal ions adsorbed per unit mass of sorbent,  $C_o$  (mg/L) is the initial metal ion concentration,  $C_e$  (mg/L) is the equilibrium metal ion concentration in the solution,  $V$  (L) is the volume of solution used and  $m$  (g) is the mass of the sorbent.

According to past research, metal binding process of the majority of biosorbents are well described by pseudo second order kinetic model (Dudu et al. 2015). Furthermore, previous research on the two selected biosorbents (TFW and CSB) also confirms that their reaction rate is best explained by pseudo second order kinetics (Wan et al. 2014; Amarasinghe and Williams 2007). Ho et al. (1998) concluded that pseudo second order model describes the metal binding process better than the pseudo first order model after testing both models using data available in research literature. Hence, pseudo second order model given by equation 4.3 was used for the analysis. Linearised form of the models is given in equation 4.4. From the slope and intercept of  $t/Q_t$  vs.  $t$  plot, the pseudo second order metal binding rate was calculated.

$$\frac{dQ_t}{dt} = k_2(Q_e - Q_t)^2 \quad \text{Equation 4.3}$$

Where  $k_2$  ( $\text{g} \cdot \text{mg}^{-1} \cdot \text{min}^{-1}$ ) is the pseudo second order reaction rate.  $Q_e$  and  $Q_t$  (mg/g) are the sorption capacities at equilibrium and time  $t$  respectively.

$$\frac{t}{Q_t} = \frac{1}{K_2 Q_e^2} + \frac{1}{Q_e} t \quad \text{Equation 4.4}$$

#### ***d. Column experiments***

The industrial application of the relationships were tested using fixed bed columns setup established in the laboratory. Columns with an internal diameter of 5.6 cm were filled up to 30 cm using a biosorbent sample, maintaining a constant porosity. Wet filling was undertaken in order to avoid air trapping during the filling process. Metal ion solutions containing 200 mg/L of  $\text{Cu}^{2+}$ ,  $\text{Cd}^{2+}$ , and  $\text{Pb}^{2+}$  were fed to the column at a constant flow rate from the bottom of the column. Solution leaving the system from the top was collected at frequent time intervals and analysed for the breakthrough time. Parameters of the fixed bed columns are described in Table 4.5. Detailed description of column systems is given in Section 6.11.

**Table 4.5** Parameters for column setup

<b>Parameter</b>	<b>Value</b>
Flow rate	10 mL/min
Porosity	50%
Height of the total column	35 cm
Height of the packing (biosorbent)	30 cm
Inner diameter	5.6 cm

#### **4.4 DATA ANALYSIS TECHNIQUES**

In order to achieve the aims and objectives of the study, it was necessary to use robust data analysis techniques and tools. The selected data analysis methods needed to have the capacity to handle large databases and to assess relationships between variables and objects. Therefore, the selection of appropriate data analyses techniques was imperative. The discussion below describes the various descriptive and multivariate statistical methods and statistical principles employed in this study to meet the stipulated requirements. Data analysis methods used in the study are illustrated in Figure 4.1.

##### **4.4.1. Descriptive statistical operations**

Basic statistical operations, such as mean (Equation 4.5) and standard deviation (Equation 4.6) are frequently used to assess the correlations between variables. They are considered to be univariate statistical methods that depicts the general distribution of a dataset made of a single variable. Mean is the mathematical average of the data set having a single variable, whereas standard deviation is a statistic that measures the dispersion of a dataset relative to its mean. It is calculated as the square root of the variance and provides an indication of the error margin in the measurement.

$$\bar{y} = \frac{\sum y_i}{N} \quad \text{Equation 4.5}$$

$$SD = \sqrt{\frac{(y_i - \bar{y})^2}{N-1}}$$

Equation 4.6

Where  $\bar{y}$  is the mean of the data,  $y_i$  is the  $i^{\text{th}}$  data point,  $N$  is the number of samples and  $SD$  is the standard deviation.

Using graphs to present data variation is very useful in distinguishing different trends and patterns. They can also help in identifying the nature and degree of correlation between different variables. Graphs were used in the study to represent the key physico-chemical properties of different material mixtures.

#### 4.4.2 Pearson correlation analysis

The Pearson product moment correlation coefficient (PPMCC) is a measure of the strength and direction of a linear association between two variables. PPMCC can take a range of values from +1 to -1 while a value of 0 indicates that there is no association between the two variables. A value greater than 0 indicates a positive association and a value less than 0 indicates a negative association.

PPMCC was used in the present study in the form of correlation matrices, for quantifying the linear relationships of variables. For example, it was helpful in identifying the associations between physico-chemical properties of the samples. A correlation matrix is a table showing correlation coefficient values between sets of variables. Each random variable in the table is correlated with each of the other variables in the table. The diagonal of the table is always a set of ones, as the correlation between a variable and itself is always one. Research literature recommends using a correlation matrix to confirm the correlations visually evident in a Principal Component Analysis (PCA) biplot (Miguntanna, Goonetilleke, et al. 2010). Therefore, correlation matrices were used to achieve Aim 1 of the study as illustrated in Figure 4.1.

PPMCC is an indicator of the strength of the relationship. The significance of this relationship is expressed in probability levels:  $p$  (e.g., significant at  $p=0.05$ ). This indicates how unlikely a given correlation coefficient,  $r$ , will occur given there is no relationship. It should be noted that in theory, calculation of PPMCC involves several assumptions. The variables should be measured at the interval or ratio level (i.e., they should be continuous variables) and there should be a linear relationship between the

variables. It is also assumed that there are no significant outliers. The variables should also be approximately normally distributed. In practice however, some of the assumptions may not be met by certain datasets (Puth et al. 2014).

In order to increase the accuracy of Pearson correlation analysis, it is recommended to perform a permutation test. In the present study, for each significantly correlating pair, correlation coefficient value and p value were reassessed by running a permutation test for Pearson's product-moment correlation (10000 permutations for each test). A permutation test builds sampling distribution by resampling the observed data which is highly useful in increasing the accuracy of correlation analysis when the number of samples is relatively small (Önder et al. 2003).

#### **4.4.3 Variance inflation factors**

Standard errors, and hence the variances of the estimated coefficients are inflated when multicollinearity exists. A variance inflation factor (VIF) quantifies how much the variance is inflated due to multicollinearity. In order to do this, VIF uses the variables in the least squares regression analysis. Variables having VIF values above 10 could have an adverse impact on statistical modelling outcomes (O'brien 2007) and therefore, such variables were identified and removed in the present study before creating mathematical models.

#### **4.4.4 Mahalanobis distance**

As a pre-treatment of data, detection of outliers was carried out using a multivariate model approach with calculation of Mahalanobis distance (Mahalanobis 1936). The Mahalanobis distance measures the distance between a specific data point and the mean of a multidimensional data distribution in units of standard deviations. It is a unitless and scale-invariant measurement, frequently used to detect outliers in the development of linear regression models. 0.95 was considered as the cut-off value for the present study. Those objects scoring higher values were excluded from the subsequent regression modelling. For example, Mahalanobis distance was employed to remove outliers when building mathematical models to depict the relationship between material physico-chemical properties and pseudo second order kinetic constant.

#### 4.4.5 Multivariate analysis techniques

Commonly used multivariate statistical methods were utilized for the study. These were, Principal Component Analysis (PCA), Generalized Linear Regression (GLR) and Partial Least Square Regression (PLS). These methods are advantageous in identifying correlations between variables and objects in large datasets. A brief description of each of these methods is given below.

##### *a. Principal component Analysis (PCA)*

Principal Component Analysis (PCA) is one of the most frequently used multivariate statistical technique and an established method of pattern recognition in large datasets. PCA was used in many past studies related to biosorption. For example, Milojković et al. (2016) investigated sorption characteristics of lead, copper, cadmium, nickel and zinc ions with the compost of '*Myriophyllum spicatum*'. PCA was applied for the analysis and differentiation of samples. Pine bark was used for biosorbent treatment of five different landfill leachates (Ribé et al. 2012) and PCA was used as a multivariate analysis technique for the recognition of patterns. Activated carbon derived from *Pistacia khinjuk* was investigated for the sorption of methylene blue and PCA was used for the initial analysis of data (Ghaedi et al. 2013).

PCA is a data analysis technique commonly employed to reduce the dimensionality of large sets of data and to streamline the representation of the data field in question. It produces a set of hypothetical, orthogonal variables known as principal components (PCs), of which the first few are capable of representing most of the variation denoted in the original data matrix. This simplifies the data analysis process, makes the interpretation of data more meaningful and allows easy visualisation of multidimensional data sets (Raychaudhuri et al. 1999).

In a typical PCA, the first principal component carries the highest variance in the respective data matrix. The second PC has the second highest variance and the other PCs have decreasing order of variance, while all PCs amount to the total variance. In other words, the first few PCs carry most of the variance found in the original data matrix and the analysis of the first few PCs can be used to interpret most of the useful information available in the original dataset.

In order to determine how many principal components should be retained, a number of different approaches are discussed in literature (Jolliffe 2011). One method is to

select a desired cumulative percentage of total variation that the selected PCs contribute. For example, if the desired cumulative percentage of total variation is 80%, the smallest number of PCs for which this chosen percentage is exceeded should be selected. The Scree plot method is more common and it involves plotting the eigenvalues in descending order and visually examining for a “big gap” or an “elbow” in such a graph. The component number defining an ‘elbow’ in the graph is then taken to be the number of components to be retained. For PCA, eigenvectors and eigenvalues exist in pairs where each eigenvector has a corresponding eigenvalue. An eigenvector defines a direction in the multidimensional data space and an eigenvalue is a number representing how much variance of data there is in that direction. While these two methods are commonly used, there are other statistical calculations used for determining as to how many PCs should be retained. These include various sequential tests and resample methods (Zhu and Ghodsi 2006).

One important advantage of PCA is the ability to present the outcomes graphically. PCA biplots are frequently used for this purpose. They represent the relationships between variables, relationships between objects and relationships between objects and variables. In PCA biplots, the loading of each variable is graphically represented as a vector while objects are depicted as data points. Vectors with acute angles and those close to each other are strongly correlated while the vectors with obtuse angles are weakly correlated. Vectors which are at right angles to each other represent variables which are not correlated, whereas clustering of objects indicates that they are of similar characteristics.

Pre-treatment of data is a common technique used prior to PCA. Different variables could be of different scales and this could affect the outcome of PCA. Pre-treatment of data is designed to eliminate this occurrence. Mean centring and standardising are the commonly used methods for data pre-treatment (Abdi and Williams 2010a). The combination of both these methods is commonly referred to as ‘auto scaling’ and this method is carried out by default by many software solutions available for PCA (Bro and Smilde 2003). In the present study, principal component analysis was performed to identify relationships between material physico-chemical properties, heavy metal sorption capacities and kinetic constants of biosorbent samples (biosorbent samples) as illustrated in Figure 4.1

### ***b. Generalized Linear Regression (GLR)***

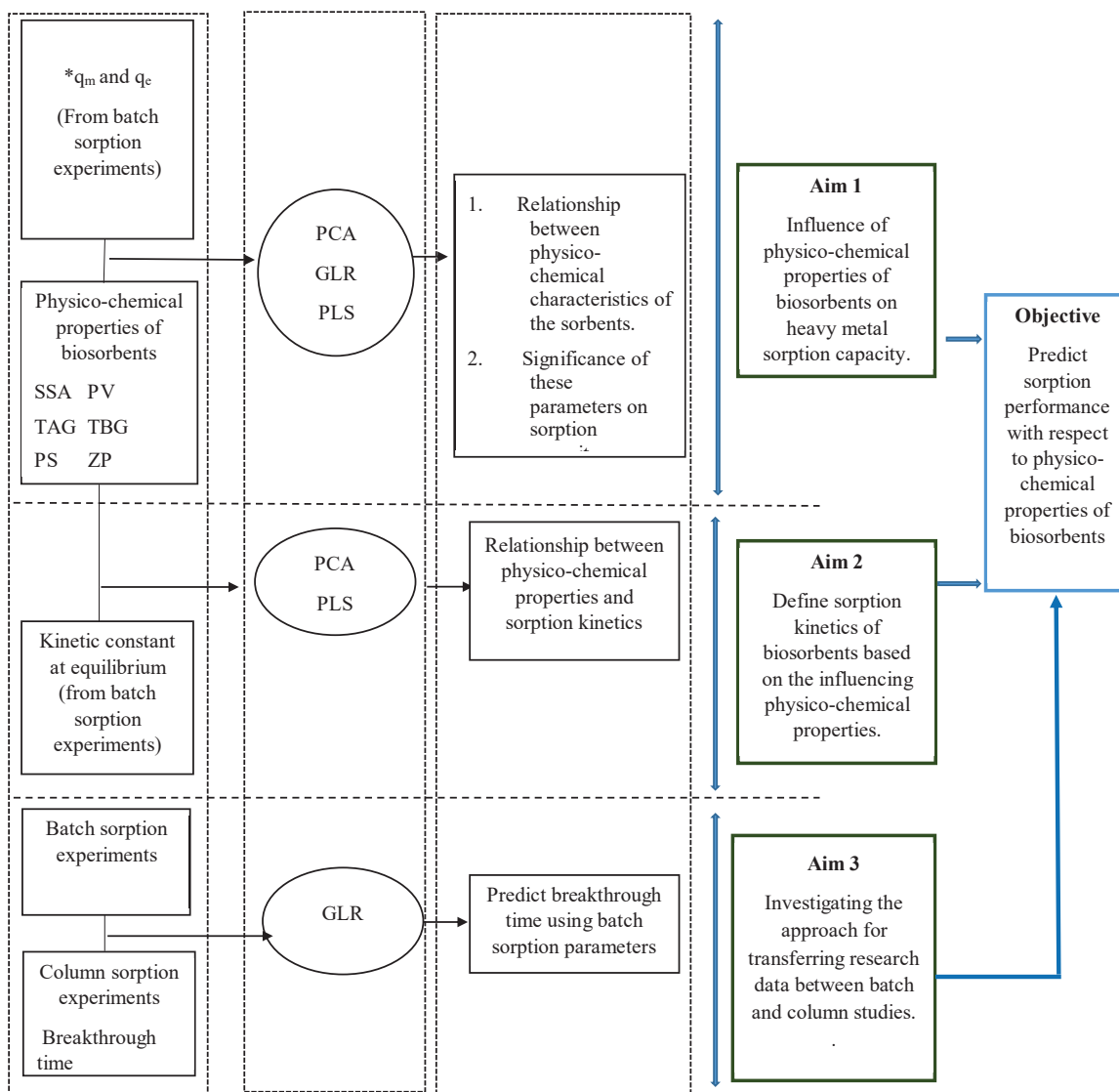
Generalized Linear Regression (GLR), is a multivariate technique for analysing correlation between one or more dependent variables (responses) and independent variables (predictors). It models the relationship between the responses and predictors by fitting a linear equation to the observed data. Depending on the algorithm employed, the choice of predictive variables is undertaken using an automatic procedure. Variable selection methods such as Stepwise Regression and Elastic Net (Enet) are commonly used to select a subset of the original set of variables in order to build the model. Enet is a ‘penalized regression method’ or ‘shrinkage method’ (Wang, Park, Carriere, et al. 2010) that can shrink the coefficients of redundant variables exactly to zero (Zou and Hastie 2005b), thereby employing a selection of variables as an integral feature. It has the ability to overcome the limitations of the other popular methods such as Ridge regression and Lasso regression (Ter Braak 2009). GLR with Enet was employed in the present study in order to construct mathematical models for the prediction of sorption capacities of biosorbents using their physico-chemical parameters (Aim 1 Figure 4.3). In the analysis for understanding the relationship between column performance and batch sorption parameters (Aim 3), GLR was used again. Since Enet has the ability to select variables, it was also used for the identification of the most important variables in the models.

### ***c. Partial least squares regression (PLS)***

Partial least squares regression (PLS) was employed to formulate mathematical models in order to understand the relationships between the independent variables and kinetic constant for  $\text{Pb}^{2+}$ ,  $\text{Cd}^{2+}$  and  $\text{Cu}^{2+}$ . PLS is a popular multivariate data analytical technique with a combination of features from PCA and multiple linear regression. It aims to predict dependent variables (responses) from independent variables (predictors) by the extraction of a set of orthogonal factors called latent variables having the best predictive power (Abdi and Williams 2010b). The efficiency and accuracy of the predictions obtained is commonly evaluated with cross-validation techniques such as bootstrapping and repeated k-fold cross validation. The latter was employed for the current study. PLS was used for building mathematical models in order to predict sorption capacities and kinetic constants of biosorbent samples using physico-chemical parameters to achieve Aims 1 and 2 (Figure 4.3). R software (Ver. 3.5.1) with R Studio was employed as the statistical tool for the data analysis.



This page intentionally left blank.



\*Maximum sorption capacity of a biosorbent (mg/g) is considered as the Maximum amount of heavy metals adsorbed per unit mass of the biosorbent at equilibrium in a batch system (Worch 2012).

$q_m$  – Maximum sorption capacity  $q_e$  - Equilibrium sorption capacity

**Figure 4.2** Summary of the data analysis methods used in the study

## 4.5 SUMMARY

This chapter has explained the research design, methods and data analysis techniques used to achieve the aims and objectives of the study. Research design of the study primarily focused on critical review of literature, selection of heavy metals, data generation, biosorbents selection and data analysis.

$Pb^{2+}$ ,  $Cu^{2+}$  and  $Cd^{2+}$  were selected for the analysis and metal solutions were prepared. From the five biosorbents initially selected via the preliminary experiments, two materials with distinct physico-chemical properties were selected to prepare material mixtures. The two selected biosorbents were mixed in specific weight ratios to obtain several combinations of mixtures with diverse physiochemical properties creating twenty one different mixtures. Laboratory experiments were conducted to quantify the physico-chemical properties and surface morphology. Sorption capacity and kinetics data was obtained using batch sorption experiments. Fixed bed columns were used to analyse the breakthrough values.

Finally, the various descriptive and multivariate statistical methods along with statistical principles employed in this study were described. Multivariate statistical methods used in this study were Principal Component Analysis, Generalized Linear Regression and Partial Least Square Regression.

This page intentionally left blank.

## **CHAPTER 5: PRELIMINARY EXPERIMENTS**

---

### **5.1 INTRODUCTION**

This chapter describes the procedure undertaken for the selection of heavy metals and biosorbents. As described in Section 2.3, industrial wastewater contains high amounts of heavy metals. Hence, it is necessary to identify the metals that are present in industrial wastewater which exceed the specified discharge limits.

Biosorbents were selected in order to prepare the biosorbent samples used for building the data matrix with different physico-chemical properties as independent variables. As explained in Section 4.2.5, two biosorbents with distinct physico-chemical properties needed to be selected for the preparation of the samples by mixing them in different weight ratios. Various low-cost agricultural wastes (Ajmal et al. 1998; Garg et al. 2008) have been investigated for the removal of metals from industrial wastewater. Most of these sorbent materials generally exhibit high metal sorption capacities indicating that they can be utilized for the removal of metal ions from polluted waters, such as industrial wastewater and stormwater runoff (Wan et al. 2014; Cherdchoo et al. 2019). However, the effectiveness of a sorbent in removing metals is dependent on the physical and chemical properties of the solution (Section 3.5). For an example, a material that is efficient in high pH solutions may not be equally effective in removing metals from a low pH system. Therefore, it is important to identify the materials that are effective for a particular system. This is generally achieved using batch sorption experiments in which, the sorbent is introduced to a solution that has similar properties as the polluted water. Furthermore, to compare the sorption capacities of different materials, it is important to maintain the same experimental conditions such as pH, agitation rate, sorbent dose and the sorbate concentration.

Several past studies have compared the performance of various sorbent materials in removing metal ions from water with varying degrees of success. This chapter initially provides a critical overview of such studies and evaluation methods adopted. Then, it explains the initial selection of biosorbents based on the existing knowledge followed by a secondary selection based on metal sorption capacities and physico-chemical properties, using a multi criteria decision making tool. As a result of the secondary

selection, two biosorbents with distinct physico-chemical properties having the ability to remove heavy metals were selected to prepare the samples for generating the data base.

## 5.2 SELECTION OF HEAVY METALS FOR THE ANALYSIS

A pilot study was conducted in Sri Lanka to identify the heavy metals commonly found in industrial wastewater discharge which exceed the specified limits. As a significant number of industries in Sri Lanka are dye and textile-based industries (CEA 2017), five such outlets were selected for the pilot study. Samples 1 and 2 were taken from textile industry outlets, Samples 3 and 4 were from wastewater discharging points of dye manufacturing industries and Sample 5 was taken from the outlet of the treatment plant at Katunayake Industrial Zone. Water samples were analysed for heavy metals and pH. Results obtained from the analysis are given in Table 5.1

**Table 5.1** Comparison of heavy metals present in industrial wastewater in Sri Lanka with industrial effluent discharging standards

Parameter	Sample	Sample	Sample	Sample	Sample	Discharge
	1	2	3	4	5	Limits BOI, Sri Lanka/ppm
Cu <sup>2+</sup>	3.70	3.50	0.70	0.84	4.52	3.0
Cd <sup>2+</sup>	0.26	0.21	0.25	0.56	0.37	0.1
Pb <sup>2+</sup>	1.68	2.10	1.10	1.80	0.90	0.1
Cr <sup>3+</sup>	0.20	0.40	0.20	0.10	0.30	0.5
Zn <sup>2+</sup>	<0.20	<0.20	<0.20	0.21	2.10	2.0
Ni <sup>2+</sup>	0.50	0.5	<0.50	0.50	<0.50	3.0
pH	6.0	6.5	5.9	5.5	5.4	6.0-8.5

According to the outcomes of the analysis, Cu<sup>2+</sup>, Pb<sup>2+</sup> and Cd<sup>2+</sup> concentrations in the effluent from the industrial wastewater was higher than the discharge limits specified by the Board of investment (BOI), Sri Lanka. Accordingly, these three metal cations were selected for the study.

### 5.3 OVERVIEW OF PAST STUDIES ON SORBENT SELECTION

Metal removal performance of sorbent materials is generally evaluated in a single sorbent-single metal solution system using sorption capacity at high and low concentrations (Chuah et al. 2005; Joseph et al. 2019). Comparative studies with the aim of evaluating the performance of various sorbents in removing metals from single and multi-metal solutions are limited. Amarasinghe and Williams (2007) used Pb and Cu sorption capacities of tea waste and activated carbon under similar experimental conditions in order to investigate the sorption performance of tea waste. A study was undertaken by Genç-Fuhrman et al. (2007) in which, the performance of eleven different sorbents were assessed for the simultaneous removal of As, Cd, Cr, Cu, Ni and Zn from stormwater. Then the sorbents were ranked based on the value of the distribution coefficient ( $K_d$ ) as given in Equation 5.1:

$$K_d = \frac{Q_e}{C_e} \quad \text{Equation 5.1}$$

In this study, both  $Q_e$  and  $C_e$  were determined from sorption experiments conducted under similar experimental conditions. Sorbents having high average  $K_d$  values were considered as efficient for the removal of metals. Accordingly, sorption capacities under similar experimental conditions, at low and high concentrations of initial metal ion solutions and distribution coefficients, were used to evaluate and compare the sorption performance of different sorbents.

Multi-Criteria Decision Making (MCDM) methods have been applied in research studies in order to assist decision making when dealing with multivariate problems. These methods involve the ranking of objects from best to worst, based on the preference of variables (Behzadian et al. 2010). Different MCDM methods are reported in research literature such as ELECTRE, SMART, PROMETHEE and GAIA, which have different decision-making abilities (Behzadian et al. 2010; Keller et al. 1991; Khalil et al. 2004). Among them, PROMETHEE (Preference Ranking Organization Method for Enrichment Evaluation) and GAIA (Graphical Analysis for Interactive Assistance) are recognised as the most effective decision making methods compared to other MCDM methods (Keller et al. 1991; Khalil et al. 2004).

Kokot et al. (1992) used PROMETHEE for selecting suitable microwave digestion methods for solids, whilst Khalil et al. (2004) applied the technique for selecting

appropriate sites for sewage effluent renovation. The latter is one of the earliest use of PROMETHEE in the field of environmental engineering (Behzadian et al. 2010). Furthermore, Carmody et al. (2007) used PROMETHEE to compare various potential sorbent materials for cleaning oil spills. It is interesting to note that in the study by Carmody et al. (2007), non-technical qualitative criteria, such as ease of use and biodegradability were introduced into the analysis along with conventional technical criteria, such as sorption and retention capacities. Importantly, in the approach by Carmody et al. (2007), the data matrix was expanded stepwise, i.e. by adding one criterion at a time, which was helpful in extracting information on the influence of each criterion in ranking the sorbents. Such an approach could be particularly useful in multi-disciplinary forums, where an immediate response regarding the influence of a particular criterion in decision making is of interest.

#### **5.4 INITIAL SELECTION OF BIOSORBENTS**

Based on the review of literature (Section 3.4), considering their sorption affinity for the selected metals ( $\text{Cu}^{2+}$ ,  $\text{Pb}^{2+}$ ,  $\text{Cd}^{2+}$ ), five low-cost and locally available biosorbents originating from agricultural waste were initially selected (Table 5.1). Special consideration was given to the possibility of mitigating any disposal problems associated with these materials by using them as biosorbents. The selected five biosorbents and their sorption capacities are given in Table 5.2. The sources of these biosorbents are listed in Table 5.3. Physical appearances of these biosorbents are illustrated in Figure 5.1.



**Table 5.2** Biosorbents and their sorption capacities

Sorbent	Sorption capacity			Initial metal ion concentration	Reference
	Cu <sup>2+</sup> mg/g	Pb <sup>2+</sup> mg/g	Cd <sup>2+</sup> mg/g		
Coconut shell biochar		7.2	4.7		Kulunivan 2014;
		13.26	3.36		Paranavithana et al. (2016
Coir pith		2.2	4.04		Kulkarni 2013
Rice husk	3.89	4.2		1.0 g/L	Sobhawardali et al. 2013
Rice straw			13.84	25–350 mg/mL	Ding et al. 2012
Tea Factory waste	21.02 48.0	33.49 65.0	16.87	1.0 g/L	Wan 2014; Amarasinghe and Williams 2007

**Table 5.3** Source of biosorbents

Biosorbent	Source
Coconut shell biochar	Haycarb PLC , Sri Lanka
Coir pith	Local market, Sri Lanka
Rice husk	Rice mill, Sri Lanka
Rice straw	Harvested from paddy fields, Sri Lanka
Tea factory waste	Mid country tea, Sri Lanka



(a)



(b)



(c)



(d)



(e)

**Figure 5.1** Biosorbents: (a) Coconut shell biochar; (b) Coir pith; (c) Rice husk; (d) Rice straw; (e) Tea factory waste

The five biosorbents selected (Table 5.3) were prepared for preliminary experiments according to the methods given in Table 5.4. After preparation, samples were used for analysing the sorption capacities of these biosorbents.

**Table 5.4** Preparation of the biosorbents

<b>Biosorbent</b>	<b>Preparation for the experiment</b>
Rice straw	Cut to small pieces, washed with distilled water, oven dried for 24 hours and ground to small particle using a ball mill and sieved.
Rice husk	Washed with distilled water, oven dried for 24 hours and ground into small particle using a ball mill and sieved.
Tea factory waste	Cut to small pieces, washed with distilled water, oven dried for 24 hours and ground into smaller particles using a ball mill and sieved.
Coir pith	Washed with distilled water, oven dried for 24 hours and ground into small particles using a ball mill and sieved.
Coconut shell biochar	Washed with distilled water, oven dried for 24 hours and ground into small particle using ball mill and sieved.

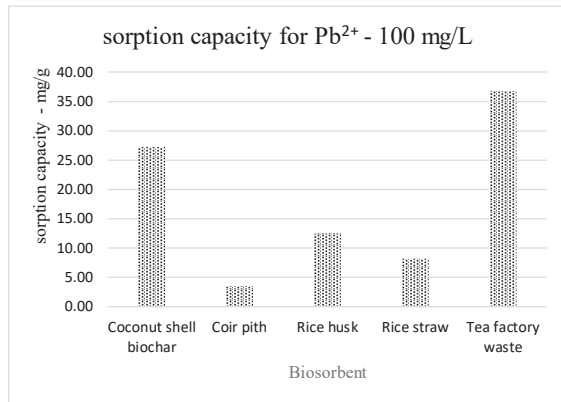
## 5.5 SECONDARY SELECTION OF BIOSORBENTS

Biosorbents selected initially were subjected to batch experiments with high (100 mg/L) and low concentrations (10 mg/L) of each metal ion separately. At lower concentrations of sorbate, most of the sorbents indicate high sorption capacities as there are sufficient amounts of binding sites on their surfaces. Sorbent saturation occurs at high initial sorbate concentrations. Hence, most of the past studies have analysed the sorption capacities of sorbents at both high and low concentrations (Wan et al. 2014; Najam and Andrabi 2016). Biosorbents with the highest sorption capacities for each metal were selected from batch screening and were subjected to further selection based on their physico-chemical properties.

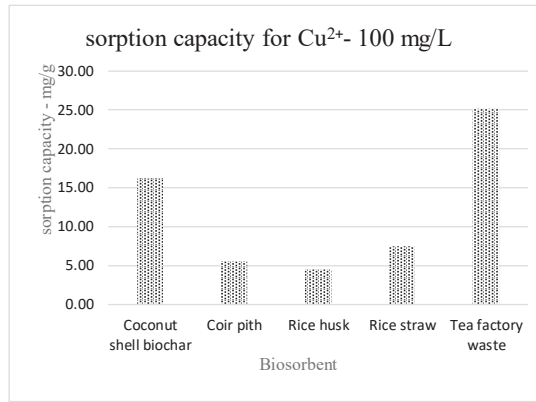
### 5.5.1 Sorption capacity

A metal stock solution (with a concentration of 1 g/L) of  $\text{Pb}^{2+}$  was prepared and diluted to 100 mg/L and 10 mg/L. Exactly 5 g of biosorbents were used for the experiments. Solution pH was kept at  $5.5 \pm 0.5$  and the system was agitated at 150 rpm. Volume of the solution was kept at 1000 mL. The same experiment was repeated for both  $\text{Cu}^{2+}$  and  $\text{Cd}^{2+}$ . Details of batch experiments are given in Section 6.8. Particle size used for the experiments was 125 $\mu\text{m}$ -150  $\mu\text{m}$ . Results obtained for the two concentrations for different biosorbents are given in Figure 5.2.

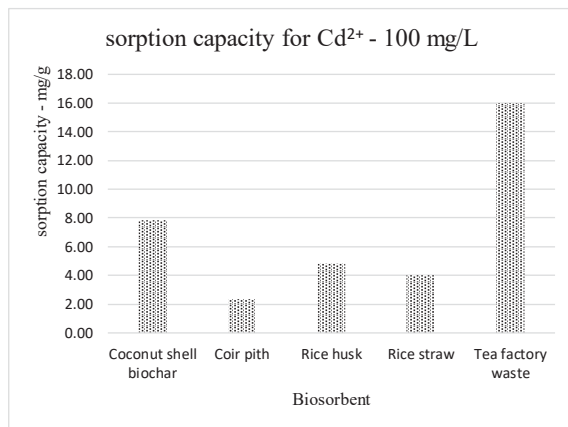
Accordingly, tea factory waste, coconut shell biochar and rice husk yielded the highest sorption capacities for  $\text{Pb}^{2+}$ ,  $\text{Cu}^{2+}$  and  $\text{Cd}^{2+}$  in single metal solutions. Results show similar variations in both, high and low concentrations. Hence, these three biosorbents were selected for further investigations conducted by quantifying their physico-chemical properties.



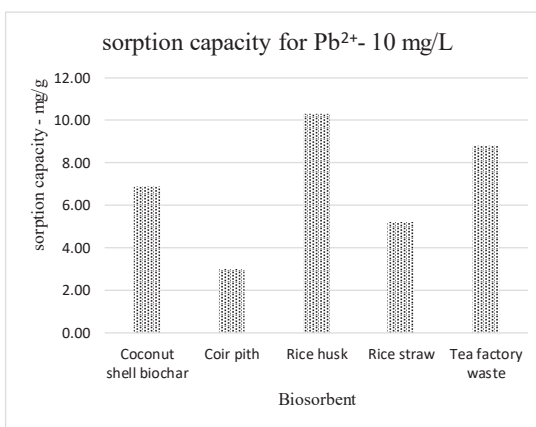
(a)



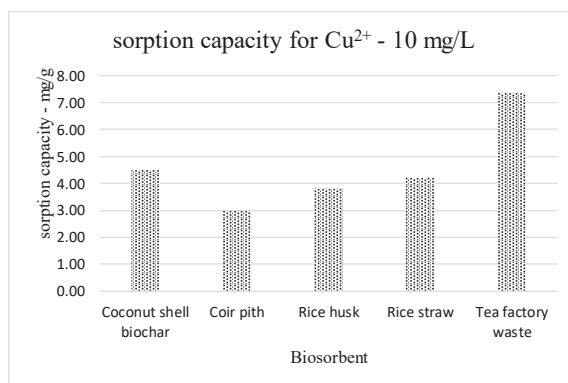
(b)



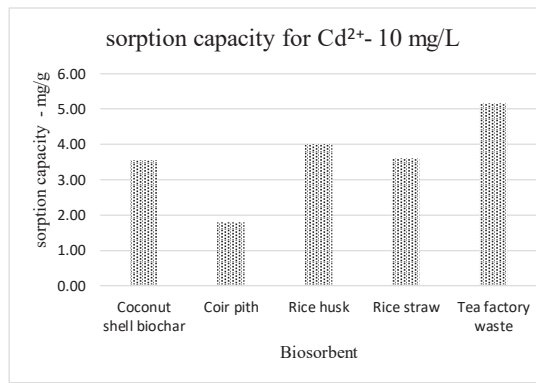
(c)



(d)



(e)



(f)

**Figure 5.2** Sorption capacity of the biosorbents (a) sorption capacity of  $Pb^{2+}$  (b) sorption capacity of  $Cu^{2+}$  (c) sorption capacity of  $Cd^{2+}$  in high metal concentrations (d) sorption capacity of  $Pb^{2+}$  (e) sorption capacity of  $Cu^{2+}$  (f) sorption capacity of  $Cd^{2+}$  in low metal concentrations

### 5.5.2 Material characterisation

The three selected biosorbents (coconut shell biochar, tea factory waste and rice husk) were investigated for their physico-chemical properties that were measured quantitatively. Several studies have reported that physico-chemical characteristics such as specific surface area (SSA), pore size (PS), pore volume (PV), zeta potential (ZP) and surface functional groups play a critical role in the metal sorption capacity of a biosorbent (Anastopoulos et al. 2013a; Albadarin et al. 2014). Accordingly, SSA, PS, PV and ZP were investigated. As for surface functional groups, total acidic groups (TAG) and total basic groups (TBG) were included as they are considered the most commonly found surface functional groups in biosorbents (Fan et al. 2018). Details on quantification experiments are given in Chapter 6. Results obtained from the experiments are given in the Table 5.5.

**Table 5.5** Quantification of the physico-chemical properties of selected sorbents

<b>Material</b>	<b>SSA</b> m <sup>3</sup> /g	<b>PS</b> A <sup>0</sup>	<b>PV</b> m <sup>3</sup> /g	<b>Zeta potential</b> mV	<b>TAG</b> mmol/g	<b>TBG</b> mmol/g
Tea factory waste	1	42.98	0.0009	-48.54	2.91	0.65
Rice husk	1.72	48.32	0.0093	-21.00	1.48	0.92
Coconut shell biochar	202	31.80	0.0096	-40.21	0.65	2.09

The two materials demonstrating the highest degree of variability in terms of physico-chemical properties were selected for preparing material mixtures as explained in Section 4.3. A multi criteria analytical protocol developed using the decision making method PROMETHEE was used for this purpose. Multi criteria decision making (MCDM) methods are employed to aid the decision making process when multi variable problems are involved. Among the various MCDM methods, PROMETHEE was used for this study as it is regarded as a more sophisticated technique (Brans et al. 1986; Keller et al. 1991). Selecting only two materials to prepare material mixtures with different weight ratios was considered to be adequate to achieve the envisaged study aims and objectives.

## **5.5 PROMETHEE**

PROMETHEE is a non-parametric data analysis method (i.e. mean and standard deviation are not used) that quantifies the degree of preference of one object to another for each variable in a data matrix (Behzadian et al. 2010; Macharis et al. 2004). Therefore, it can provide useful information related to ranking and pattern recognition. It is also known as an outranking method. Outranking methods are based on a familiar way of thinking where, instead of trying to define what solution is good and what solution is bad, comparison of one solution to another is undertaken. Outranking methods do not require the decision-maker to define what is good or what is bad. Instead, they use the results of the pairwise comparison of the actions to build a relative ranking of the actions from the best to the worst.

There are two different PROMETHEE rankings. PROMETHEE I is a partial ranking. Therefore, all the actions are not necessarily compared and the ranking can include incomparability. PROMETHEE II is a complete ranking where all the actions are compared and no incomparability is seen in the ranking. In order to implement PROMETHEE analysis, several additional parameters such as preferred ranking order, weighting, preference function and threshold need to be preselected by the decision-maker (Mareschal 2013).

### **5.5.1 Preferred ranking order**

Two ranking orders, maximised and minimised can be specified depending on the preference criterion (variable or parameter). Accordingly, objects are either top-down or bottom-up in ranking order.

### **5.5.2 Criteria Weighting**

The weights of the criteria are essential parameters to reflect the priorities of the decision-maker. The importance of one criterion over another criterion is measured so that the decision-maker is able to weigh each criterion as equally important or most important to least important. The weights are non-negative numbers representing the relative importance of the criteria. In PROMETHEE they are defined independently from the scale of measurement of the criteria. More important criteria have larger weights while less important ones have smaller weights. It should be noted that

assigning weights to the criteria is not straightforward. It involves the priorities and perceptions of the decision-maker (Mareschal 2013).

### **5.5.3 Preference function and Threshold**

PROMETHEE makes no assumption as to what is good or what is bad. It is based on the pairwise comparison of the actions. Therefore, the deviation between the evaluations of two actions on a particular criterion has to be modelled. For small deviations, either a weak preference or no preference at all is expected. For larger deviations, larger preference levels are expected.

With PROMETHEE, preference levels are measured on a scale from 0 to 1 where 0 stands for no preference at all while 1 means a full preference. The deviation has to be translated to such a preference degree between 0 and 1. That is the purpose of the preference function. It mathematically determines the selectivity of an object relative to others. PROMETHEE requires to associate a preference function to each criterion in order to model the way the decision-maker perceives the measurement scale of the criterion. There are six different types of preference functions available in Visual PROMETHEE software and these are given in Table 5.6.

The Usual preference function is a simple function with no threshold. It can be the right choice for a criterion with few very different evaluations. The U-shape preference function introduces the notion of an indifference threshold (called Q threshold). The V-shape preference function is a special case of the linear preference function where the Q indifference threshold is equal to 0. It is considered suited to quantitative criteria when even small deviations should be accounted for. The Level preference function is better suited to qualitative criteria when the decision-maker wants to modulate the preference degree according to the deviation between evaluation levels. The Linear preference is the best choice for quantitative criteria when a Q indifference threshold is preferred. The Gaussian preference function is an alternative to the linear preference. It is seldom used (Mareschal 2013).

### **5.5.4 Q, P and S thresholds**

Depending on the type of preference function that has been selected, up to two thresholds have to be assessed. These are Q (the indifference threshold), P (the preference threshold) and S (the Gaussian threshold). The Q indifference threshold is the largest deviation that is considered as negligible by the decision-maker. Preference



threshold is the smallest deviation that is considered as sufficient to generate a full preference. The S Gaussian threshold correspond to the inflection point of the Gaussian curve. It is thus, a deviation for which the preference degree is equal to 0.39 and it sits between a Q and a P value. It is also more difficult to assess (Mareschal 2013).

**Table 5.6** Preference functions for PROMETHEE analysis (Brans et al. 1986).

Preference function	Shape of the graph <sup>1</sup>
Linear	
V-shape	
Level	
U-shape	
Usual	
Gaussian	

### 5.5.5 PROMETHEE analysis

PROMETHEE was used in the study to rank the three biosorbents selected in order to identify the two biosorbents with the highest variation in physico-chemical properties. The three biosorbents (coconut shell biochar, tea factory waste and rice husk) were evaluated on the basis of 6 criteria; Specific surface area (SSA), pore size (PS), pore volume (PV), zeta potential (ZP), total acidic groups and total basic groups. PROMETHEE II Complete Ranking was employed. PROMETHEE analysis requires the assignment of three modelling parameters for each criterion: a ranking sense, a preference function and a weighting. A weight of 1 was selected for all criteria in order to ensure all variables were given the same importance in the analysis. The ranking sense and preference function assigned for each criterion are given in the Table 5.7. Table 5.8 gives the ranking results for the three materials. Tea factory waste and coconut shell biochar were selected for the rest of the study for the preparation of material mixtures given in Table 4.3 (Section 4.3) as the variability of physico-chemical parameters was highest between them.

**Table 5.7** Ranking sense and preference function assigned for each criterion

	<b>SSA</b>	<b>PV</b>	<b>PS</b>	<b>ZP</b>	<b>TAG</b>	<b>TBG</b>
Function	Linear	Linear	Linear	Linear	Linear	Linear
Min/Max	Max	Max	Max	Max	Max	Max
Weight	1	1	1	1	1	1
Unit	m <sup>3</sup> /g	cm <sup>3</sup> /g	A <sup>0</sup>	mV	mmol/g	mmol/g

**Table 5.8** PROMTHEE II complete ranking results for the three materials

<b>Material</b>	<b>Ø</b>	<b>Rank</b>
Coconut shell biochar	0.0389	1
Rice husk	0.0328	2
Tea factory waste	0.0275	3

## 5.6 SUMMARY

Samples taken from five industrial outlets were analysed for heavy metals. According to the results of the analysis,  $\text{Cu}^{2+}$ ,  $\text{Pb}^{2+}$  and  $\text{Cd}^{2+}$  were selected for the study as the concentration of these three metals in discharged wastewater exceeded the discharge limits specified in the country. Five biosorbents originating from agricultural waste were selected initially considering their availability and sorption capacity based on published literature. Three biosorbents (coconut shell biochar, rice husk and tea factory waste) were selected for the next screening process based on their sorption capacities. A MCDM method, PROMETHEE was used to identify the biosorbents with distinct physico-chemical properties based on the results of the analysis of quantitative parameters of the above three biosorbents. Accordingly, coconut shell biochar and tea factory waste were ranked 1 and 3, which indicated the highest difference among the three based on the physico-chemical properties considered. Thus, tea factory waste and coconut shell biochar were selected to prepare mixtures in order to generate sorbent samples for the study.

# CHAPTER 6: LABORATORY TEST METHODS AND CALIBRATIONS

---

## 6.1 BACKGROUND

The purpose of this chapter is to describe all the laboratory experiments conducted for the generation of data. These included instrumental analysis and titrimetric analysis that were conducted to quantify the physico-chemical properties of the selected biosorbents, batch experiment procedures and column experiments to generate sorption data. Furthermore, quality control and quality analysis procedures used are explained. Table 6.1 summarises the specific parameters measured during the study and the instruments/test methods applied for the measurements.

**Table 6.1** Specific parameters measured and the instruments/test methods used

Parameter	Test method or Instrument
Specific surface area, pore volume and pore size	Nitrogen gas adsorption isotherms using ASAP 2020 (Micrometrics Instrument Co.)
Zeta Potential	Malvern Zetasizer Nano ZS
Quantify surface functional groups; total acidic groups (carboxylic, hydroxyl and lactonic) and total basic groups	Boehm titration method
Surface morphology	Tescan mira3 FEG-SEM field emission scanning Electron Microscope
Surface functional groups	Thermo Scientific Nicolet S10 FTIR spectrometer
pH	TPS AQUA-pH-mV-Temperature meter
Metal Concentration	Atomic Absorption Spectrometry

## 6.2 MATERIAL SURFACE AREA

The specific surface area, pore volume and pore size of the samples were measured by the analysis of nitrogen gas adsorption isotherms at 77 K using ASAP 2020 instrument from Micrometrics Instrument Co., USA (Figure 6.1). ASAP stands for Accelerated Surface Area and Porosimetry System and the instrument uses multiple gas sorption techniques for the measurements.

Mixing of CSB and TFW was done after degassing the two biosorbents separately. Degassing was done at 200 °C and 60 °C, respectively, for 48 hours. These temperatures were selected by analysing differential scanning calorimetry (DSC) of CSB and TFW. DCS curves for CSB and TFW are given in Figure A1.1 in Appendix A1. According to the analysis, 208.3 °C and 63.7 °C were the maximum temperatures that can be applied without degrading the CSC and TFW samples, respectively. Mixtures were prepared using degassed TFW and CSB according to the weight percentages given in Table 3.2. The mixtures were then degassed again for 24 hours at 60 °C prior to the sorption studies. Total specific surface area (SSA) was assessed using multipoint Brunauer–Emmett–Teller method (Brunauer et al. 1938). Volume of pores was measured using ‘Barrett-Joyner-Halenda’ (BJH method) via desorption isotherm (Barrett et al. 1951). The relative pressure used was 0.99. Data processing was done using Microactive 2 software.

The ASAP 2020 uses two independent vacuum systems, one for sample analysis and one for sample preparation. This allows preparation and analysis to proceed concurrently. A two-station intelligent degas system is also incorporated into the instrument for fully automated degassing with controlled heating profiles. The degas systems are equipped with isothermal jackets. An analysis Dewar is available for condensing excess moisture in the centre. The glass sampling tube (Figure 6.1a) contained a seal frit (Figure 6.1c) and a glass rod (Figure 6.1b) in order to fill the excess void spaces when used for analysis. This instrument is capable of analysing surface area and porosity characteristics of powder or solids. The pore size range of the instrument is from 3.5 to 5000 Å. Having two independent systems avoids the possibility of cross-contamination between the degassing and analysis manifolds.

Accuracy of instruments was checked with standard reference materials in order to avoid/minimise instrumental error. For ASAP 2020, after analysing 10 samples,

carbon black was used as the reference material to check the accuracy of the results by comparing single point specific surface area values with multi point specific surface area values.

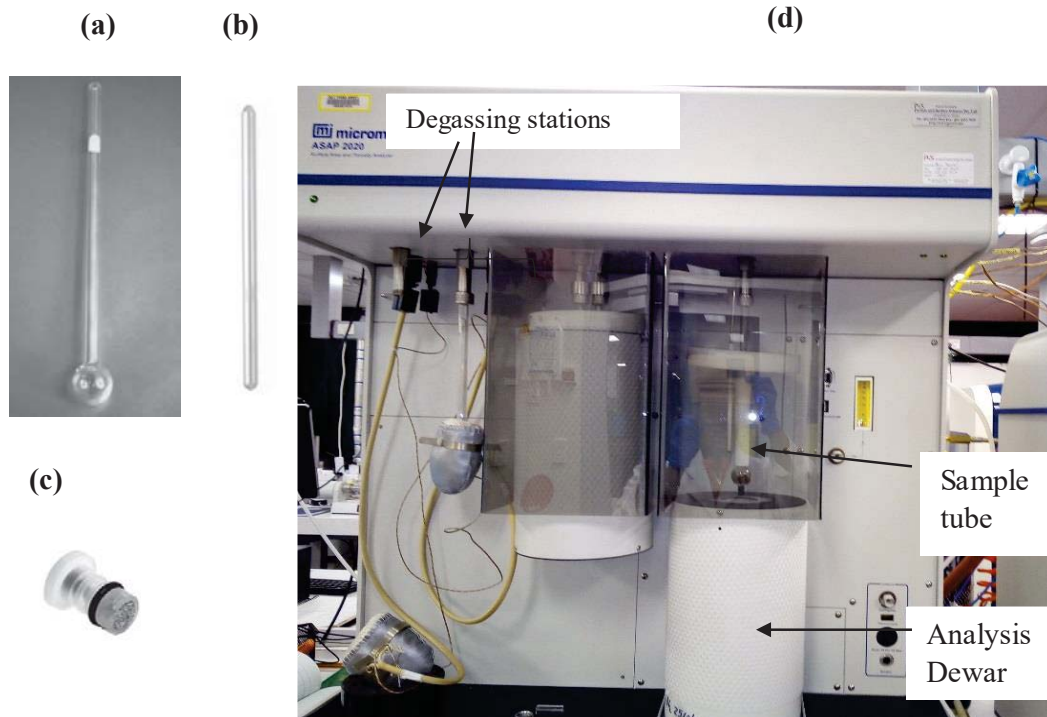


**Figure 6.1** BET specific surface area analysis (a) glass sampling tube (b) glass rod (c) seal frit (d) ASAP 2020 instrument

### 6.3 ZETA POTENTIAL

Zeta Potential (ZP) is the electric potential at the shear plane of a particle. It is the scientific term for electrokinetic potential in colloidal dispersions. Particles within a colloidal dispersion carry different charges that contribute to the net charge of a particle. As illustrated in Figure 6.2, each particle is surrounded by oppositely charged ions in a layer called a fixed or stern layer. Beyond the stern layer, there are both positive and negative ions gathered in a cloud of charges. This ‘diffuse’ layer together with the stern layer form the electrical double layer at the particle-liquid interface. The ions within the ‘diffuse’ layer move about freely becoming less and less further away from the particle and eventually reduces to zero. The boundary of the stern plane and

the diffuse region is known as the slipping plane or the shear plane. The electric potential at the shear plane is called Zeta Potential.

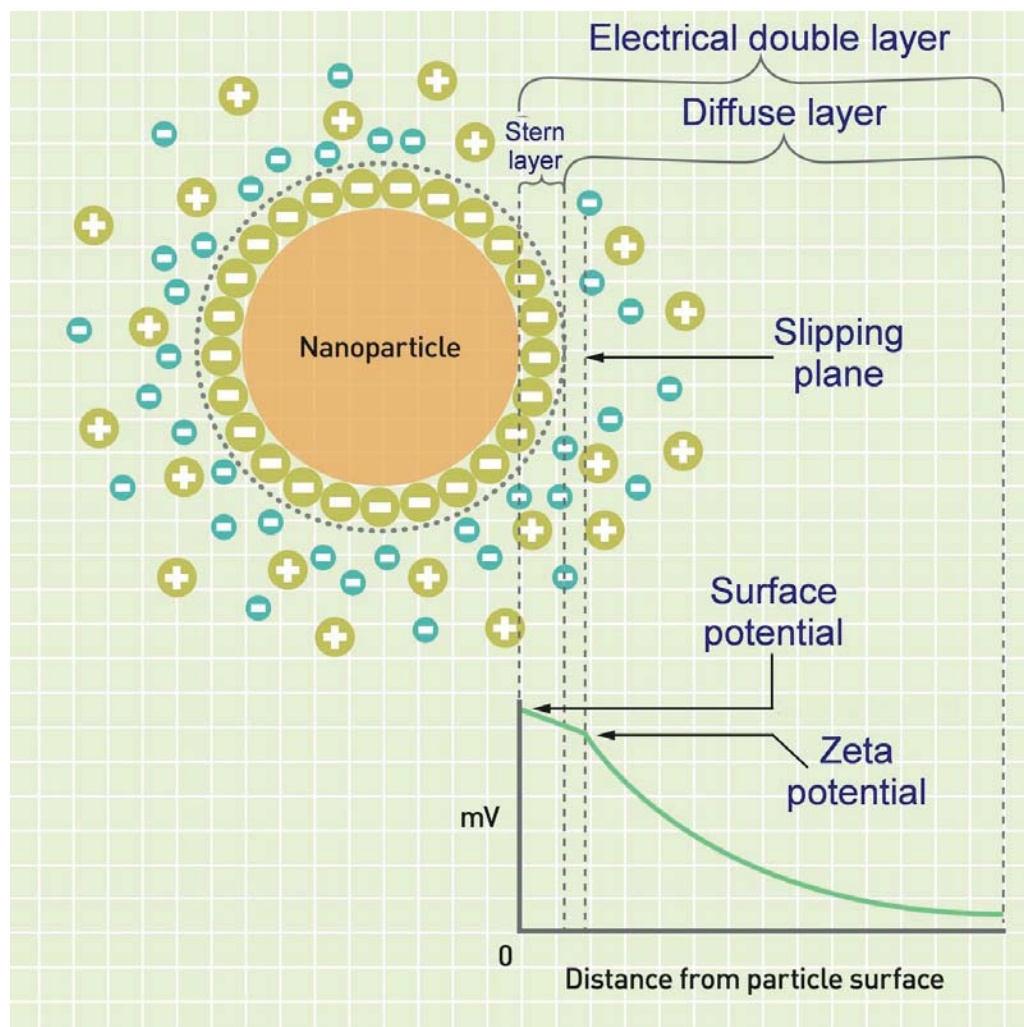


**Figure 6.2** Electrical double layer around a nanoparticle and the concept of Zeta potential (Marchese et al. 2008).

The ZP of particles is determined by measuring their velocities while they are moving due to electrophoresis. Particles and molecules that have a zeta potential will migrate towards an electrode if an adequate field is applied. The speed of the particles' movement is proportional to the field strength and its zeta potential. When the field strength is known, Laser Doppler electrophoresis is used to measure the speed of movement and established models are utilized to calculate the zeta potential.



As identified by the past researchers, zeta potential is an important chemical property of a particle that indicates the surface charge and explains stability of a particle in a solution. For the current study, Malvern Zetasizer Nano ZS was used for the analysis of ZP values. The instrument uses a technique called phase analysis light scattering (PALS) to improve the sensitivity and accuracy of the measurements. Since PALS only provides a mean zeta potential value, a patented technology called ‘M3-PALS multi-frequency measurement’ is used to determine the mean and distribution during the same measurement.

At first, a solution with a pH of 5 was prepared by mixing 0.01 M HNO<sub>3</sub> and 0.01 NaOH in deionised water. Samples were then dissolved in this solution and were kept for 30 minutes to settle. About 0.75 mL of the sample was then injected into a capillary cell (Figure 6.3 a) without trapping air bubbles inside. After injecting the sample, the capillary cell was kept inside the cell chamber of the instrument where a voltage was applied to the gold plated electrodes beside it. After three complete runs, the average zeta potential of the sample was displayed by the zetasizer software.

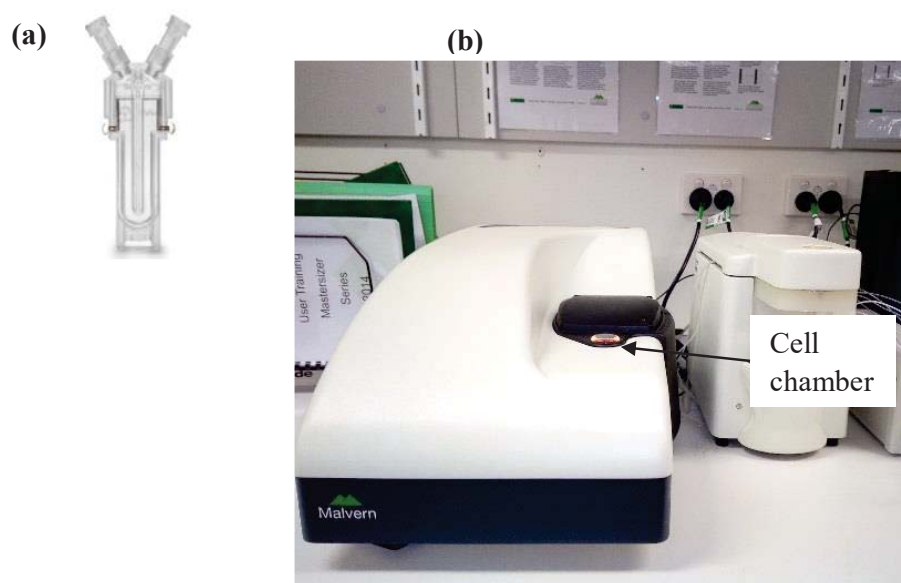


**Figure 6.3** Zeta potential analysis (a) capillary cell (b) Malvern Zetasizer Nano ZS

For quality control, each reusable capillary cell was renewed after being used for 10-15 times. Accuracy of the instrument was checked using standard reference materials in order to avoid/minimise instrumental error. Zeta potential transfer standard was run



whenever a new cell was used and always after 10 sample runs. Result of the instrument was checked with zeta potential value of the standard ( $42 \text{ mV} \pm 4.2 \text{ mV}$ ).

#### 6.4 SURFACE FUNCTIONAL GROUPS

Several types of functional groups are available in a sorbent material and they are commonly found in acidic form due to the complexation with  $\text{H}^+$  ion. For example, carboxylic functional groups are found as carboxylic acid. The negativity of the functional groups present in sorbents can attract metal cations and adsorb them via physisorption or chemisorption mechanisms. For example, a carboxylic functional group ( $\text{COO} \cdot \text{H}^+$ ) can attract a metal ion ( $\text{M}^{n+}$ ) via physisorption ( $\text{COO} \cdot \text{H}^+ \cdot \text{M}^{n+}$ ) or chemisorption ( $\text{COO} \cdot \text{M}^{n+}$ ), depending on the characteristics of the bonding. Spectroscopic techniques can be used to identify available functional groups. However, these techniques quantify all the functional groups available in the sorbent instead of considering only the ones that can participate in the sorption process. Hence, in this study, acid-base titration method was used to determine the types of negative sites in the structure of the sorbents and to quantify them.

The functional groups present in biosorbents can be broadly classified into carboxylic ( $-\text{COOH}$ ), hydroxyl ( $-\text{OH}$ ) and lactonic ( $-\text{COO}$ ) groups (Basso et al. 2002). These groups can be quantified using Boehm titration technique (Boehm 1994). The technique uses three bases, namely, sodium hydroxide ( $\text{NaOH}$ ), sodium carbonate ( $\text{Na}_2\text{CO}_3$ ) and sodium bicarbonate ( $\text{NaHCO}_3$ ) to quantify the acidic groups by means of back-titration.  $\text{NaHCO}_3$  can neutralise the acids having acid dissociation constant ( $\text{pK}_a$ ) values less than 6.37. Hence, it can only neutralise the carboxylic acidic group. In contrast, both carboxylic and lactonic groups can be neutralised by  $\text{Na}_2\text{CO}_3$  due to its ability to neutralise acids with  $\text{pK}_a$  values less than 10.25.  $\text{NaOH}$  can neutralise acids with  $\text{pK}_a$  values less than 15.74. Thus, it can neutralise the carboxylic, hydroxyl and lactonic groups (László et al. 2002). Accordingly, 0.5 g of sample was equilibrated with 50 mL of 0.1 M  $\text{NaOH}$ , 0.2 M  $\text{Na}_2\text{CO}_3$  and 0.1 M  $\text{NaHCO}_3$  separately at a constant temperature water bath for five days. Thereafter, 10 mL from the final solution was withdrawn and was titrated with 0.1 M of hydrochloric acid ( $\text{HCl}$ ) to quantify the

excess basic compounds in the solution. The quantities of carboxylic, hydroxyl and lactonic sites were estimated based on the titration (Figure 6.4) data.



**Figure 6.4** Quantification of active sites: titration setup

## 6.5 SCANNING ELECTRON MICROSCOPIC ANALYSIS

The Tescan mira3 FEG-SEM field emission scanning Electron Microscope (Figure 6.5) was used to study the surface morphology of TFW and CSB samples. This version of scanning electron microscope is suitable to study the surface characteristics of biomaterials at a micrometre or a nanometre scale. The SEM features a high-brightness Schottky emitter allowing the generation of high-resolution images with low noise and resolutions down to 1 nm. The utilization of Beam Deceleration Technology (BDT) allows enhanced resolutions at low beam voltages.

The samples were rigidly mounted on to carbon tapes pasted on stainless steel specimen stubs. In order to obtain good quality images, they were coated with thin layers of gold under vacuum conditions in an environment set with an argon ionization chamber (Figure 6.5 c). The SE detector operating under 2.5 kV together with a working distance of 8 mm was used for surface property investigations according to the methods given in literature (Nautiyal et al. 2016). The scan speed used was 8 together with line averaging 11, in order to obtain scanned images of good quality.

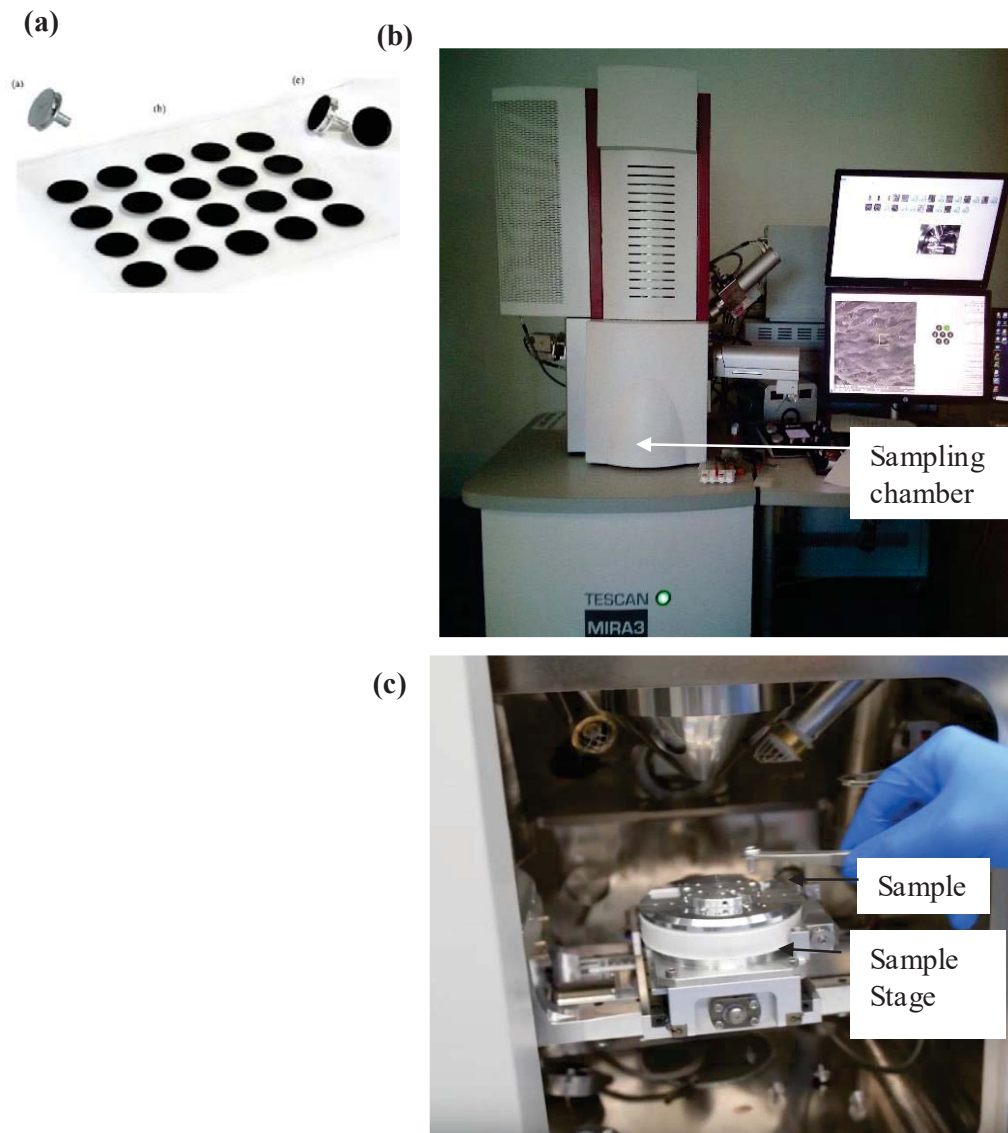


**Figure 6.5** Scanning electron microscopic analysis (a) SEM specimen mounts and carbon tabs (b) Tescan mira3 FEG-SEM (c) Inside of the sampling chamber

## 6.6 FOURIER TRANSFORM INFRARED SPECTROSCOPY (FTIR) ANALYSIS

Infrared spectroscopy is based on molecular vibrations caused by the oscillation of molecular dipoles. Bonds have characteristic vibrations depending on the atoms in the bond, the number of bonds and the orientation of those bonds with respect to the rest of the molecule. Thus, different molecules have specific spectra that can be captured

for distinguishing products or for identifying unknown substances. Analysis was carried out using Thermo Scientific Nicolet S10 FTIR spectrometer (Figure 6.6). This instrument is designed for spectroscopy elemental isotope analysis utilized for materials identification and verification. It uses a Potassium bromide (KBr) mid-infrared optimized beam splitter with Germanium (Ge) coating. Helium-Neon laser in which, a mixture of helium and neon gas is used as a gain medium is also employed.

In order to obtain homogenous samples, KBr pellets were prepared. Before the preparation of pellets, KBr was dried at 100 °C in an oven for 1 hour and was transferred into a mortar. Samples were added with a weight percentage of about 0.2 to 1 followed by mixing and grinding. These mixtures were then filled into stainless steel sample holders. Spectra were captured in the spectral range of 4000 - 525  $\text{cm}^{-1}$  using 64 scans at a resolution of 4  $\text{cm}^{-1}$  according to the method discussed in literature (Liu et al. 2010; Ruiz-Fuertes et al. 2010). This combination of operational conditions is suitable for biomaterials. The background spectra was set to correct the adsorption spectra of samples and was subtracted from the FTIR spectrum. Captured FTIR spectra were interpreted using Galactic 187 Industries Corporation GRAMS32 software package (Salem, NH, USA). The final FTIR spectra was normalised according to its distinct peaks. Surface functional groups present such as hydroxyl (-OH), carbonyl (-CO) and carboxylic (-COOH) on material surface were studied based on the normalized distinct peaks of the FTIR spectra.

The instrument comes with a powerful analytical program called OMNIC Spectra™ which gives unparalleled access to spectral interpretation tools. The OMNIC interface allows assigning functional groups, searching against libraries and to perform deeper analysis such as analysis of mixtures against a library of over 9000 compounds.



**Figure 6.6** Thermo Scientific Nicolet S10 FTIR spectrometer

## 6.7 pH

pH is a measure of acidic or alkaline nature of a solution and it is calculated based on the concentration of  $H^+$  ions according to the following equation:

$$pH = -\log_{10}[H^+] \quad \text{Equation 6.1}$$

where  $[H^+]$  denotes the concentration of  $H^+$  ions.

Metal removal mechanism is dependent on the pH of the solution (Section 3.5.1). Additionally, pH controls metal speciation, which has an influence on the interaction of metal ions with the active sites of a biosorbent as discussed in Section 3.5.1. Therefore, controlling the pH of the solution is crucial in sorption studies. A pH probe (Model: TPS IJ44) attached to a combined pH/EC meter (Model: TPS AQUA-pH-mV-Temperature meter) was used for pH measurements (Figure 6.7). This instrument is an economical waterproof pH meter with pH, mV and Temperature readouts with an accuracy of  $\pm 0.01$  for pH value. The calibrated pH/EC meter was immersed in the solution to record its pH.

The operation of the equipment involves two steps; calibration and verification. For calibration, two-point calibration technique was followed. Standard solutions of pH 6.8 and pH 4 were used for this purpose. The pH probe was thoroughly rinsed with deionised water and was blot dried before being immersed in the pH 6.8 solution for calibration. The second calibration of the probe was done with the pH 4 solution using

the same technique. For verification, the pH meter was checked with the pH 6.8 standard solution to ensure its performance after every ten measurements. The probe was re-calibrated if a significant variation ( $\pm 10\%$ ) in pH was detected.



**Figure 6.7** pH probe and pH/EC meter

## 6.8 ATOMIC ABSORPTION SPECTROMETRY

Atomic absorption spectrometry (AAS) is an analytical technique that measures the concentrations of elements. Atomic absorption is so sensitive that it can measure down to parts per billion of a gram in a sample. The technique makes use of the wavelengths of light specifically absorbed by an element. These wavelengths correspond to the energy needed to promote electrons from one energy level to a higher energy level. Background metal concentrations ( $\text{Pb}^{2+}$ ,  $\text{Cu}^{2+}$  and  $\text{Cd}^{2+}$ ) of biosorbents,  $\text{Pb}^{2+}$ ,  $\text{Cu}^{2+}$  and  $\text{Cd}^{2+}$  concentrations of samples obtained from batch and column experiments were determined using an Atomic absorption spectrometer (Thermo Scientific, iCE 3500) (Figure 6.8). This section describes the principles of the equipment, calibration of the instrument and analysis of the concentrations.

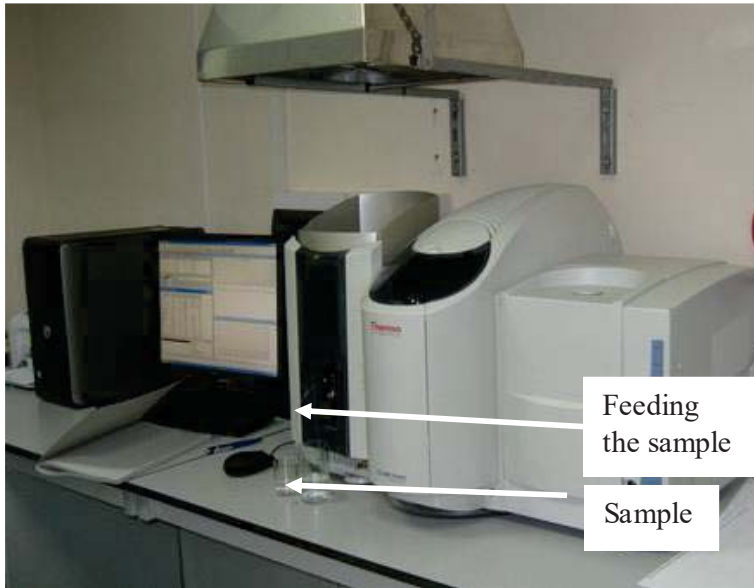


**Figure 6.8** Atomic absorption spectrometer

### 6.8.1 Principles of the instrument

Atoms of different elements absorb characteristic wavelengths of light. Analysing a sample to see if it contains a particular element involves using light from the same element. For example with lead, a lamp containing lead emits light from excited lead atoms that produce the right mix of wavelengths to be absorbed by any lead atoms from the sample. In AAS, the sample is atomized (converted to free atoms in the vapour state) and a beam of electromagnetic radiation emitted from excited lead atoms is passed through this vaporised sample. Some of the radiation is absorbed by the lead atoms in the sample. The greater the number of atoms there is in the vapour, the more radiation is absorbed. The amount of light absorbed is proportional to the number of lead atoms. A calibration curve is constructed by running several samples of known lead concentrations under the same conditions as the unknown sample. The amount the standard absorbs is compared with the calibration curve and this enables the calculation of the lead concentration in the unknown sample.

### 6.8.2 Calibration

Fitness of the standard curve was verified using standard solutions having known concentrations of  $\text{Pb}^{2+}$ ,  $\text{Cu}^{2+}$  and  $\text{Cd}^{2+}$ . These calibration curves (Figure 6.9a and 6.9b) were used to determine the unknown concentration of the metal in the samples.



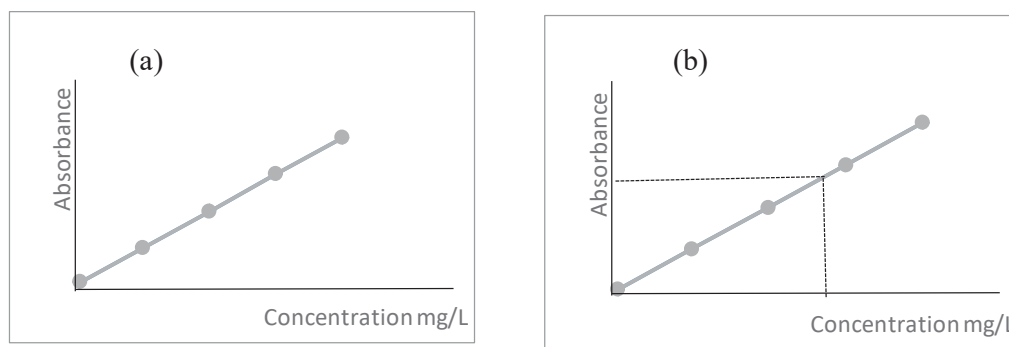


**Figure 6.9** (a) Calibration curve with known concentration (b) determine concentration of the sample using calibration curve

### 6.8.3 Analysis

The instrument was loaded with the element specific program and a suitable lamp was selected. Fitness of the standard curve was verified using a series of reference standards of the element. Samples were filtered and fed into the instrument. Absorbance of the samples were measured and recorded in the instrument. Concentrations of the samples were displayed on the computer attached to the instrument. This was done in triplicate and the average value was considered for the data analysis.

## 6.9 BATCH SORPTION EXPERIMENTS

Batch sorption experiments were conducted for the twenty one samples in order to obtain sorption capacities and equilibrium sorption times of the samples.

### 6.9.1 Determination of sorption capacity

Batch experiments were conducted to determine sorption capacities of the samples (biosorbent samples) for each metal ion by adding 3.0 g of biosorbent to 1000 mL of solution containing heavy metal ions at a pH range of  $5.5 \pm 0.5$  (adjusted by using 0.1M NaOH or HNO<sub>3</sub>). The concentrations of Pb<sup>2+</sup>, Cd<sup>2+</sup> and Cu<sup>2+</sup> were set at a range of 2–300 mg/L. The equilibrium time was 24 h and the experiments were conducted using a magnetic stirrer at 150 rpm (Figure 6.10). Samples of the solutions were taken out and analysed for the concentration of the heavy metal using Atomic absorption



spectrometer. Each experiment was performed in duplicate and the mean value was determined.

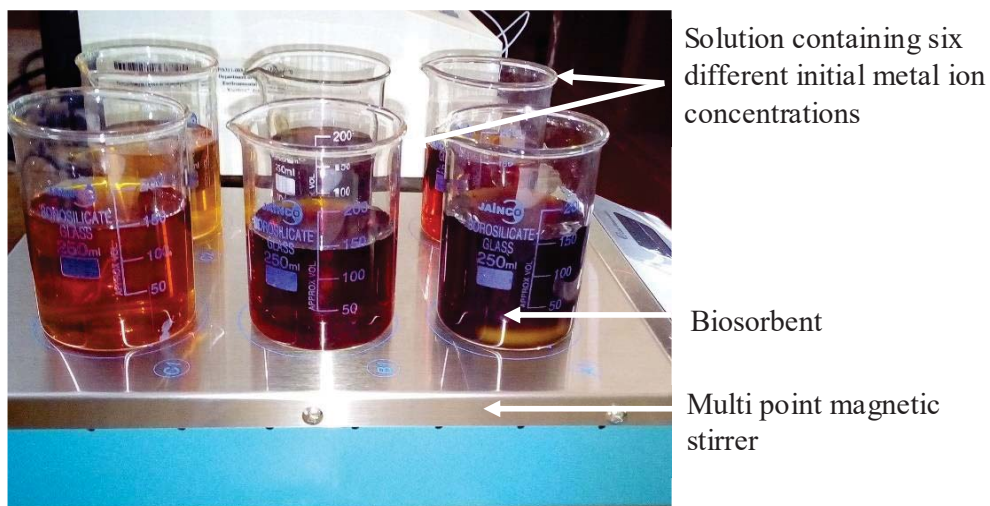


**Figure 6.10** Batch experimental set up (shaking samples at 150 rpm)

### 6.9.2 Kinetic studies

Volumetric flasks containing 1000 mL of metal solution and the biosorbent sample (3 g/L of dose) were agitated using a magnetic stirrer at 150 rpm at a constant room temperature ( $22 \pm 1$  °C). The experiment was conducted for 24 hours. 5 mL of the sample was withdrawn after 5, 10, 20, 40, 60, 120, 180, 270, 360 and 1500 minutes and was diluted to 25 mL. The samples were then filtered through 0.45  $\mu\text{m}$  glass fibre membrane filters and acidified with  $\text{HNO}_3$ . They were stored in plastic vials until AAS analysis. Additionally, pH of the solution was measured at the end of each experiment.

### 6.10 CONTINUOUS FIXED BED COLUMN EXPERIMENTS

Continuous fixed bed column experiments were conducted to determine the fixed bed breakthrough curves (BTCs) experimentally. Continuous fixed bed columns were used as they offer better simulation of real world application. These experiments were conducted for 21 samples for the three heavy metals ( $\text{Cu}^{2+}$ ,  $\text{Cd}^{2+}$ , and  $\text{Pb}^{2+}$ ) at 200 mg/L initial heavy metal ion concentration.

### 6.10.1 Preparation of the experimental set up

Fixed bed columns were fabricated using perspex to minimise wall effects which could interfere with the shape of the BTC (Worch 2012). The design of the single fixed column is given in Figure 6.11. Total length of the column was 35 cm and the internal diameters of the column was 5.6 cm. The column was filled up to 30 cm using the sample, maintaining porosity at 50%. A tightly packed column can cease the flow of the solution and a loosely packed columns can result in channelling within the column resulting in creating more accelerated pathways within the column (Worch 2012). At both ends of the column, two gravel layers of about 2.5 cm were provided. This helps to disperse the input solution across the column evenly and allows better migration through the column (Rodrigues et al. 2012). Between the sorbent layer and the gravel layer, a wire mesh was inserted. Wet packing was conducted in order to avoid air trapping and channelling within the column.

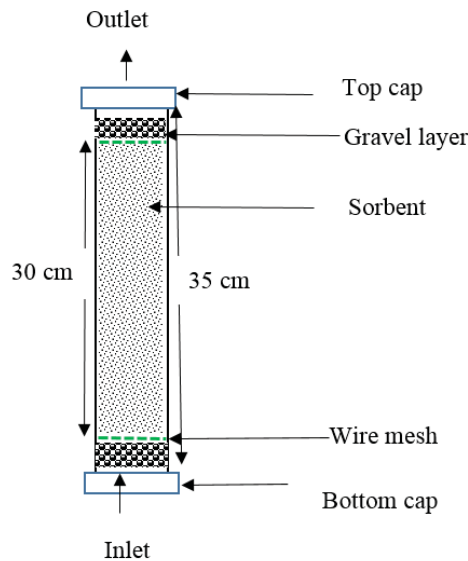


**Figure 6.11** Schematic of a column design

Columns were filled with deionised water (Patel and Vashi 2015; Chatterjee et al. 2018). Bulk density of the sample was determined using Equation 6.1. Particle density of the sample was measured using a pycnometer. Values obtained for particle density for the twenty one samples are given in Appendix A1.

$$\emptyset = 1 - \frac{\rho_b}{\rho_p} \quad \text{Equation 6.2}$$

Where  $\emptyset$  is porosity,  $\rho_b$  is bulk density and  $\rho_p$  is particle density.

$$\rho_b = \frac{W}{V} \quad \text{Equation 6.3}$$

Where  $W$  is the weight of the sample and  $V$  is the volume.

Using Equation 6.2, weight of the sample for a unit length ( $w$ ) was calculated. The column was graduated for 2 cm. After fitting the bottom cap, the gravel layer and the wire mesh, the column was filled with deionised water. Then, the first 2 cm length of the column was filled with 'W' amount of the sample as shown in Figure 6.12. This was continued up to the 32.5 cm of the column (total height of the column was 35 cm and the packing length of the sample was 30 cm). Excess deionised water on top of the packed (sample) column was removed. A wire mesh, layer of gravel and end cap was inserted.

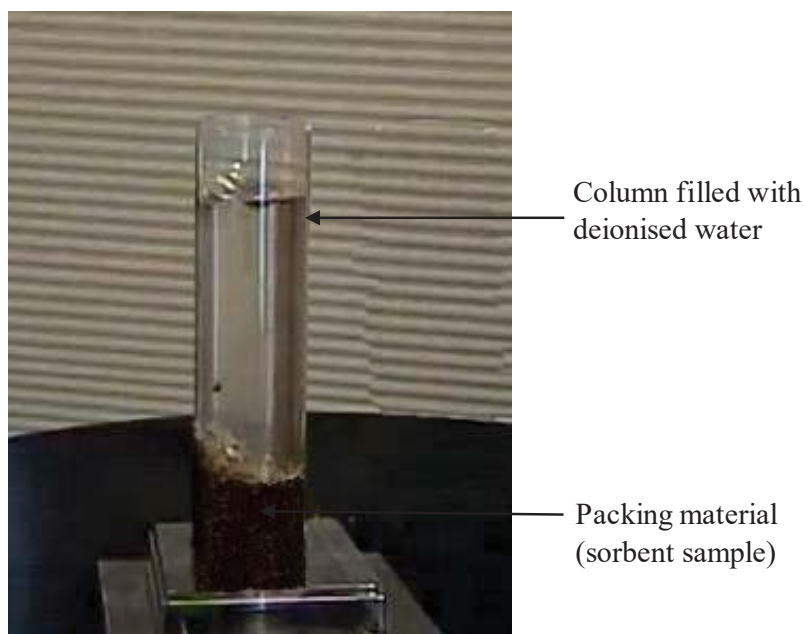


**Figure 6.12** Wet packing of a column

The experiential setup contained a Perspex sorption column, a solution reservoir for the continuous supply of the sample, a peristaltic pump to regulate the inflow and a sampling point as shown in Figure 6.13. The flow was directed from the bottom to the top of the column (up flow). This was done to avoid channelling and to ensure a uniform streaming (Rodrigues et al. 2012). Deionised water was first sent through the

column for about 1 hour for the column to settle as mentioned in past research studies (Mohan and Sreelakshmi 2008; Abdolali et al. 2017).

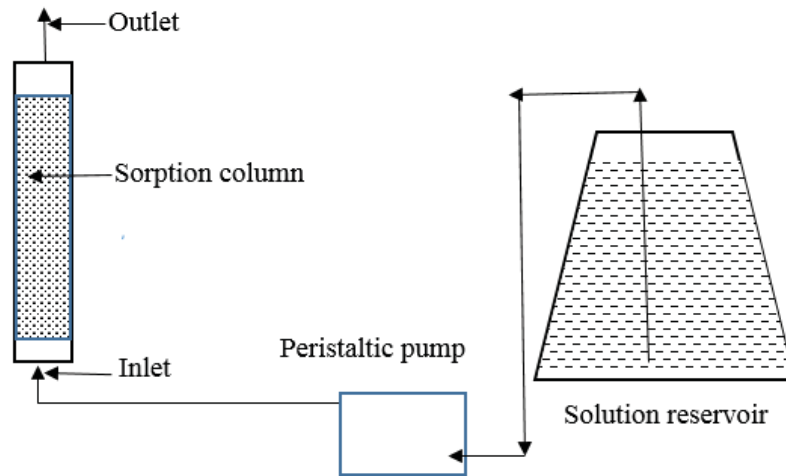


**Figure 6.13** Schematic of the column setup for breakthrough curve determination

### 6.10.2 Determining the breakthrough time

Metal solutions containing 200 mg/L of  $\text{Cu}^{2+}$ ,  $\text{Cd}^{2+}$ , and  $\text{Pb}^{2+}$  were fed to the columns (Figure 6.14) at a constant flow rate of 20 mL/min from the bottom. Solution leaving the system from the top was collected at frequent time intervals up to the column exhaust point (mentioned in Section 3.9) and these samples were analysed using AAS. According to theory (Worch 2012), the ideal column exhaustion occurs at the point where  $C/C_0$  is equal to 1.0. However, according to the observations from past studies, this point cannot be obtained practically (Miralles et al. 2010; Abdolali et al. 2017). Hence, the point where  $C/C_0$  is equal to 0.8 was considered as the exhaustion point for this study. Porosity of the column was measured once again after the experiment before unpacking the column.

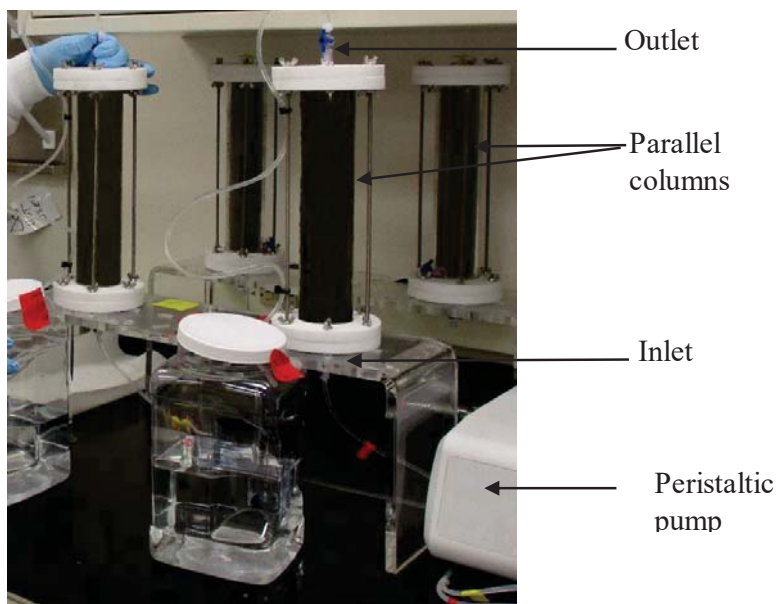


**Figure 6.14** Experimental setup for determination of breakthrough curve

## 6.11 QUALITY CONTROL AND QUALITY ASSURANCE

Standard quality control (QC) and quality assurance (QA) procedures were followed throughout the laboratory experiments to ensure the reliability and accuracy of the laboratory tests and the results obtained. Accordingly, certified reference materials, field blanks, laboratory reagent blanks, calibration standards, internal standards and analysis replications were used where appropriate. A comprehensive description of the QC/QA procedures adopted is given below.

As the first step, all laboratory glassware and plasticware, including polypropylene digestion tubes and centrifuge tubes were soaked in a  $\text{HNO}_3$  bath (10% v/v) overnight, followed by rinsing three times with deionised water. Furthermore, analytical grade quality chemicals and double-distilled deionised water were used to prepare all chemical solutions and for the dilutions. Each measurement in titrations and heavy metal analysis was undertaken in triplicate and the mean values were accepted if the error was within  $\pm 10\%$ . As explained in Sections 6.2 and 6.3, accuracy of instruments was checked with standard reference materials in order to avoid/minimise instrumental error.

## **6.12 SUMMARY**

Laboratory analysis was conducted to identify the physico-chemical properties of samples both, qualitatively and quantitatively. Batch sorption and column experiments were conducted to obtain sorption capacities of samples and to generate kinetic data. Standard QC/QA procedures were followed to ensure the reliability and accuracy of the laboratory tests and the results.

This page intentionally left blank.

# CHAPTER 7: INFLUENCE OF PHYSICO-CHEMICAL PROPERTIES ON SORPTION CAPACITY

---

## 7.1 INTRODUCTION

This chapter focuses on assessing the influence of physico-chemical properties of biosorbents on their capacity for the sorption of  $\text{Cu}^{2+}$ ,  $\text{Pb}^{2+}$  and  $\text{Cd}^{2+}$ . A number of studies have investigated heavy metal removal capacities of different biosorbents (Fu and Wang 2011; Cherdchoo et al. 2019) and suggested that material surface physico-chemical properties such as specific surface area (SSA), pore size (PS), pore volume (PV), zeta potential (ZP) and surface functional groups play a critical role in metal sorption capacity (Anastopoulos et al. 2013a; Han et al. 2013; Gupta and Sen 2017). However, the mathematical relationship between these parameters and the sorption capacity of a sorbent has not been investigated. Investigation of such relationships will provide guidance as to which of the parameters should be modified for improving sorption capacity, thereby optimising the sorption process. This knowledge will also serve to improve strategies for the design and development of heavy metal treatment systems based on sorption. Furthermore, such mathematical relationships will help in understanding the relative importance of each physico-chemical property in dictating the sorption capacity, thereby aiding the implementation of treatment methods targeting specific metal species. There are two terms frequently used to explain the sorption capacity for a given sorbent. The first one is the maximum sorption capacity ( $q_m$ ) when the sorbent has become saturated. This value is usually expressed as the sorption capacity of the sorbent. The second term, equilibrium sorption capacity ( $q_e$ ) corresponds to a specific experimental condition. Moreover, it tends to change with experimental conditions.

Firstly, variations of physico-chemical properties among the samples were assessed using the data obtained from the laboratory experiments (Section 3.1). Maximum sorption capacities for the three metal cations were obtained using relevant equilibrium curves. The raw data matrix was generated using the data as explained in Section 4.3 and a number of multivariate data analysis techniques were employed to analyse the data. Figure 7.1 outlines the statistical approach adopted for the analysis with the objectives of each step. The final step of the data analysis was aimed at generating



predictive models to calculate sorption capacities for the three divalent heavy metals using the physico-chemical properties of the selected biosorbents.

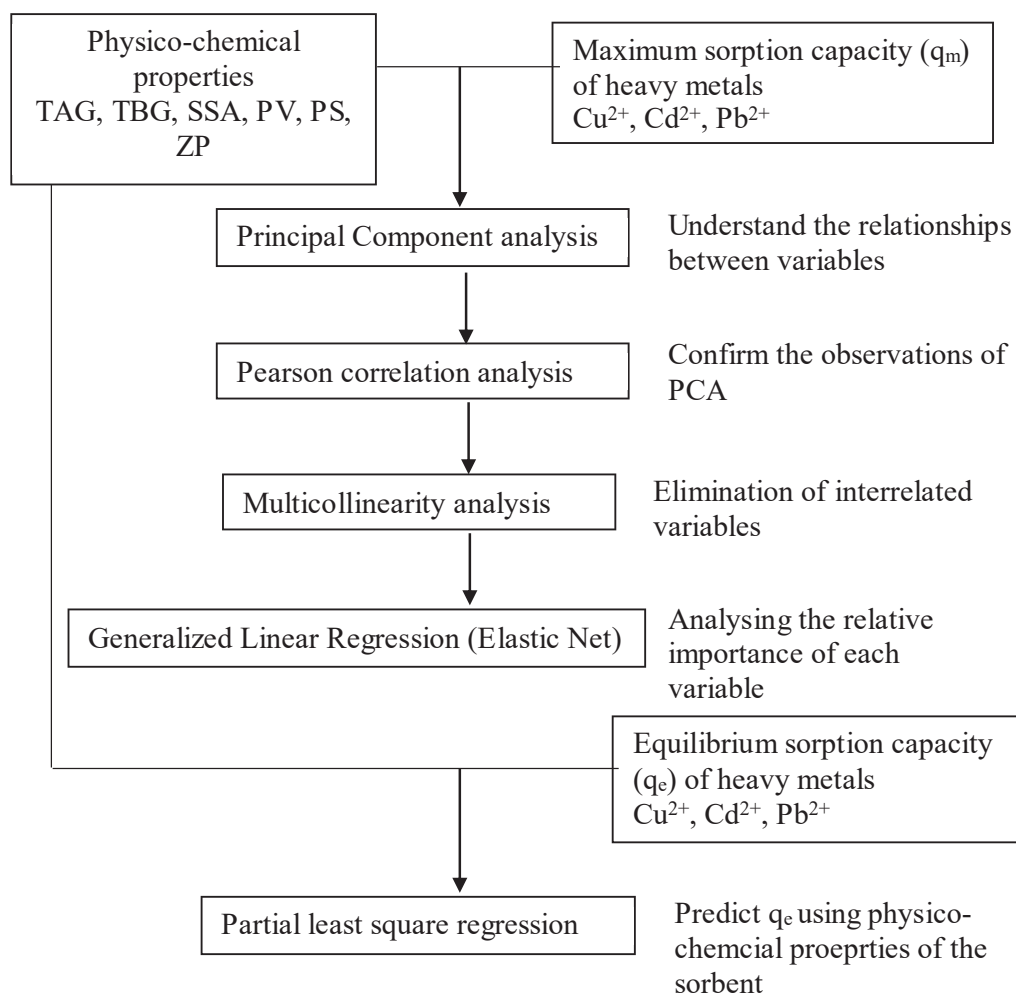


**Figure 7.1** Statistical approach adopted in the analysis

## 7.2 INVESTIGATION OF PHYSICO-CHEMICAL PROPERTIES

The physico-chemical properties quantified for the analysis were specific surface area (SSA), pore size (PS), pore volume (PV), zeta potential (ZP) and surface functional groups. Surface functional groups were measured as total acidic groups (TAG) and total basic groups (TBG). Further, TAG was divided into carboxylic, phenolic and lactonic group (Basso et al. 2002). SEM and FT-IR analysis were used for further investigation of the surface characteristics of the samples.

### 7.2.1 Specific surface area

Specific surface area (SSA) of solids is considered as a measurement of a particle's ability to retain pollutants on its surface (Jain and Ram 1997) and plays an important role in defining the sorption of pollutants and in describing surface dependent sorption behaviour. Brunauer–Emmett–Teller (BET) theory explains the physical sorption of gas molecules on a solid surface (Brunauer et al. 1938) and is widely employed as the basis for the measurement of specific surface area of biosorbents. This method, known as the BET N<sub>2</sub> gas sorption method, was employed for the present study.

Figure 7.2 illustrates the results of the analysis. BET specific surface area (hereafter referred to as SSA) of the twenty one samples (as mentioned in the Section 5.2) ranges between 0.2 and 200 m<sup>2</sup>/g. Sample 1 (100% CSB) shows the highest SSA and the readings gradually decrease to that of sample 21 (100% TFW) which is the lowest value for SSA. This is mainly due to the mix proportions. SSA is high when the proportion of CSB is high within the mixture.

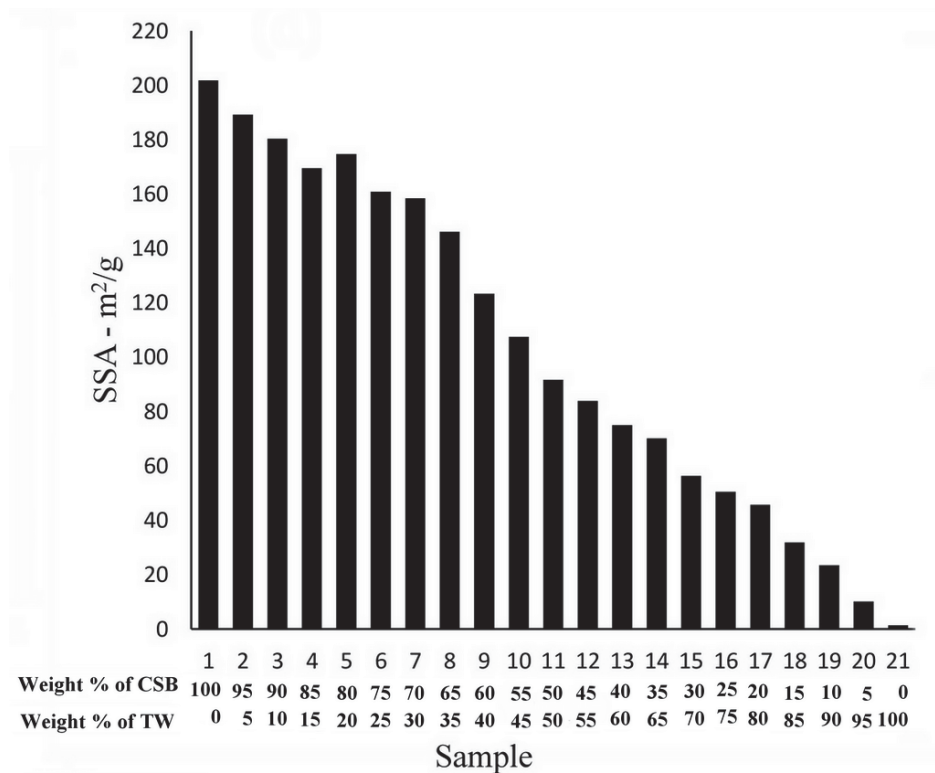


**Figure 7.2** Specific surface area variation of samples

### 7.2.2 Pore volume

For the present study, pore volume was calculated using the BJH method via desorption isotherm as described above. The results of the analysis (Figure 7.3) show that BJH pore volume (henceforth referred to as PV) of the twenty one samples (as mentioned in the Section 5.2) ranges between 0.0009 cm<sup>3</sup>/g and 0.0107 cm<sup>3</sup>/g. Sample 9 (60% CSB: 40% TFW) shows the highest PV while sample 21 (100% TFW) shows the lowest value. No clear pattern is visible as in the case of SSA.

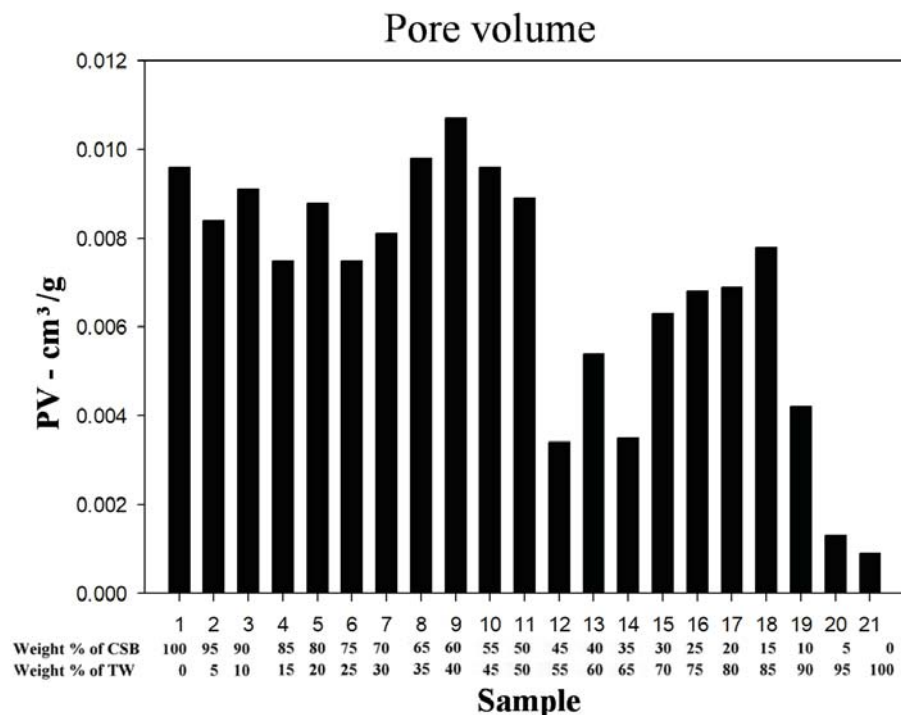


**Figure 7.3** Variation of pore volume

### 7.2.3 Pore size

For the present study, pore size calculation was done using the Barrett-Joyner-Halenda (BJH) method via desorption isotherm (Barrett et al. 1951). This technique was originally developed to deal with relatively coarse, porous adsorbents having a wide range of pore sizes capable of engaging molecules of many different sizes. However, the BJH method is considered to be applicable to porous solids of any nature. The method was developed based on the analysis of the relationship between nitrogen desorption isotherms at liquid nitrogen temperatures and the distribution of pore volume and area with respect to pore radius. Past researchers have made the assumption that equilibrium between the gas phase and the adsorbed phase during

desorption is determined by two mechanisms, namely, physical sorption on the pore walls and capillary condensation (Thommes et al. 2015).

Figure 7.4 depicts the results of the analysis. BJH pore size (henceforth referred to as PS) of the twenty one samples (as mentioned in the Section 5.2) ranges between 26.4 Å and 54.87 Å. Sample 14 (35% CSB:65% TFW) shows the highest PS while sample 9 (60% CSB:40% TFW) shows the lowest value. No clear pattern is visible as in the case of SSA. However, for most of the time the samples that have high PV have shown lower values for PS. PS was calculated using Equation 7.1 based on the assumption that all the pores presented are cylindrical.

$$PS = 4V/A \quad \text{Equation 7.1}$$

Where V is the volume of pores and A is cumulative surface area of pores. Accordingly, if the number of smaller pores are high within a unit mass of a sorbent, it gives a higher volume and area, but a lower value for PS.

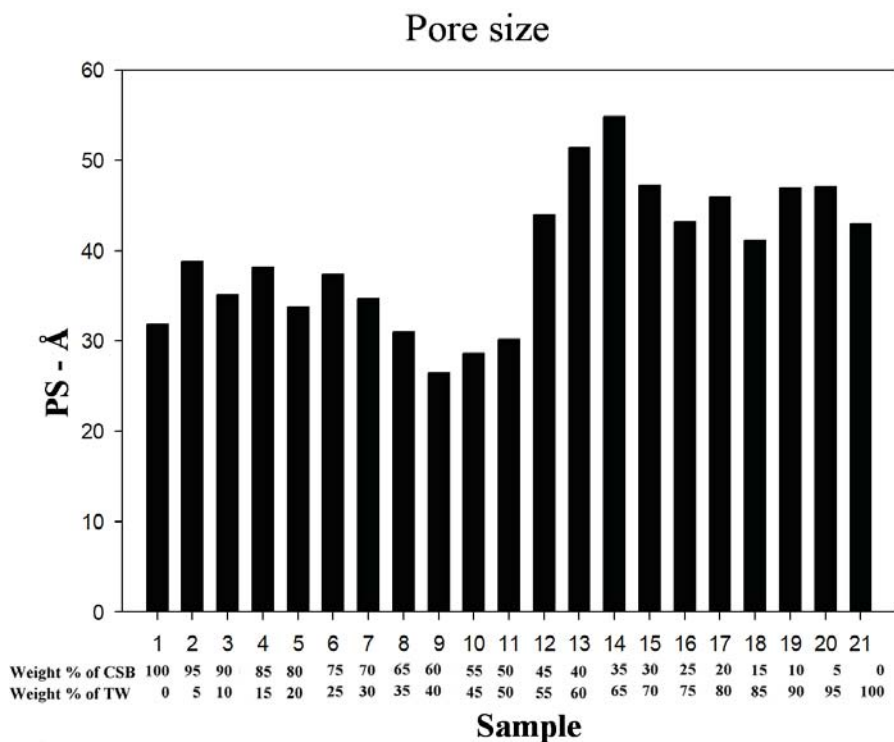


**Figure 7.4** Pore size variation of the samples.

### 7.2.4 Surface functional groups

Sorption behaviour of carbon materials is strongly influenced by surface oxides bound in the form of various functional groups. As discussed in Section 3.4.2, surface oxides

on a carbon surface can be acidic or basic. These functional groups can be quantified as total acidic and total basic groups using titration methods (Boehm et al. 1964). Carboxylic, phenolic and lactonic groups can be considered as the major acidic functional groups that affect the sorption of cations to the surface of materials (Basso et al. 2002). Concentration of these three can be quantified using titrations (Boehm et al. 1964). However, the acidity between each functional group should be sufficiently large to differentiate them by titration. FT-IR spectroscopy is another method used to identify the functional groups which assigns sorption bands based on molecular organic compounds (Sellitti et al. 1990; Fanning and Vannice 1993). This method can only be used for identification and not for quantification. Figure 7.5 depicts the variation of acidic surface functional groups observed among the 21 samples. Carboxylic group is the main contributor to TAG readings. The highest TAG reading was seen in sample 21 (100% TFW), whereas the lowest value belonged to sample 3 (90% CSB:10% TFW). Surface of TFW contains lignin, cellulose and hemicellulose which have carboxylic and lactonic groups (Wan 2014). According to Fahmi et al. (2018), biochar can also contain functional groups within their inner pores. However, functional groups on biochar surface is low according to published literature (Paranavithana et al. 2016).

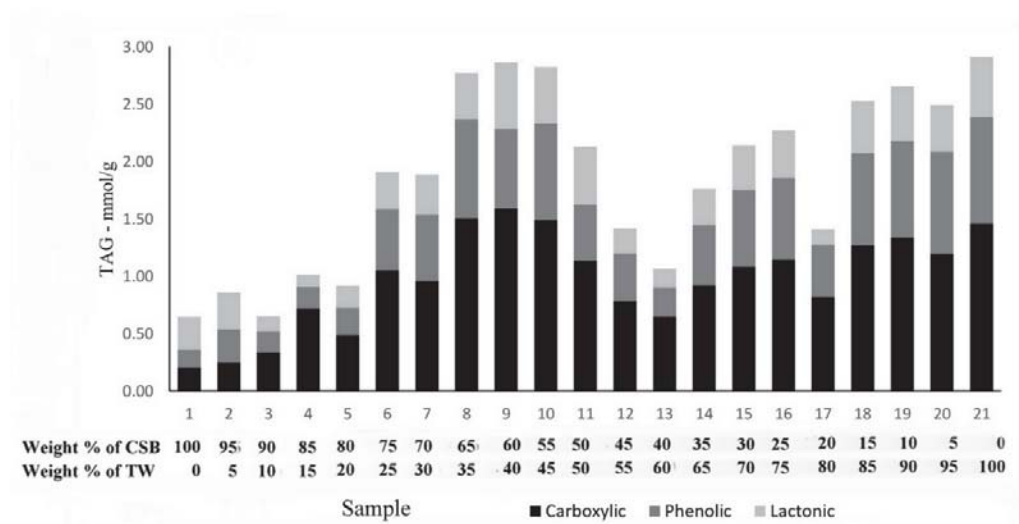


**Figure 7.5** Variation of acidic surface functional groups

Figure 7.6 shows the variation of basic surface functional groups seen among the twenty one samples. The highest TBG reading was seen in sample 7 (70% CSB:30% TFW), whereas the lowest value belonged to sample 11 (50% CSB: 50% TFW).

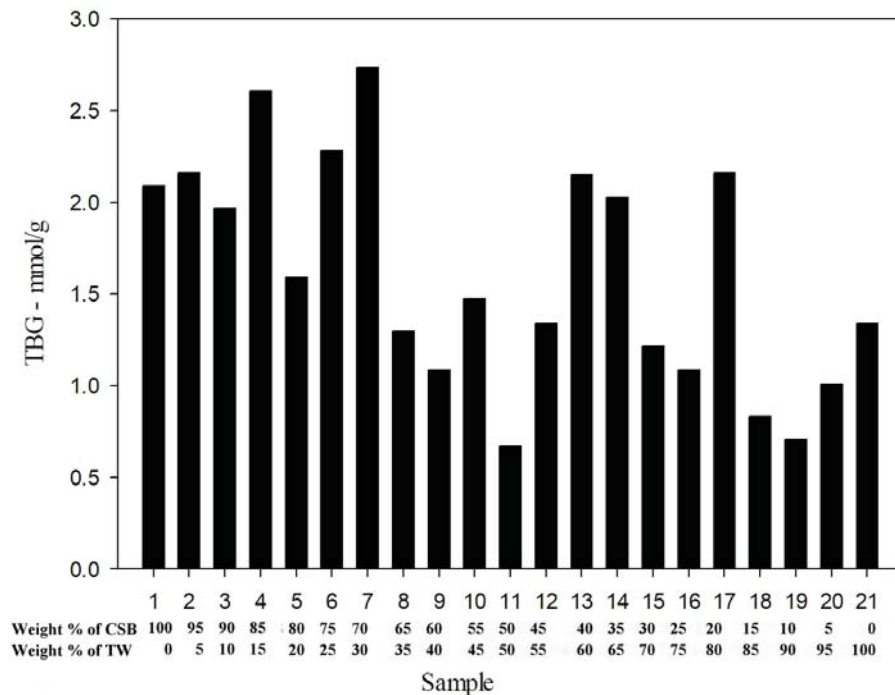


**Figure 7.6** Variation of basic surface functional groups

### 7.2.5 Zeta potential

Zeta Potential is the electric potential at the shear plane of a particle. In a colloidal dispersion where particles have different charges that contribute to the net charge of the sorbents. Each particle is surrounded by the stern layer having oppositely charged ions (Figure 6.7 in Section 6.5). Beyond this stern layer lies a diffuse (shear) layer with both positive and negative ions. These two layers form the electrical double layer at the particle-liquid interface and the potential at the boundary of the stern plane and the shear plane is known as the zeta potential. This value of surface charge is important for understanding and predicting interactions between particles in suspension. For this study, zeta potential was measured according to the principle of laser doppler electrophoresis, maintaining the solution pH at 5, using the Malvern zetasizer nano as described in Section 6.3.

Figure 7.7 depicts the values obtained from the analysis. The values range between 37.98 mV and 52.67 mV. Sample 9 (60% CSB:40% TFW) recorded the highest value, whilst sample 14 (35% CSB: 65% TFW) had the lowest. ZP of the two Sorbents used for the preparation of samples were 40 mV and 49.5 mV and the difference is very

narrow. Hence, the mixtures possibly cannot possess a wider range of ZP as in the case of SSA.

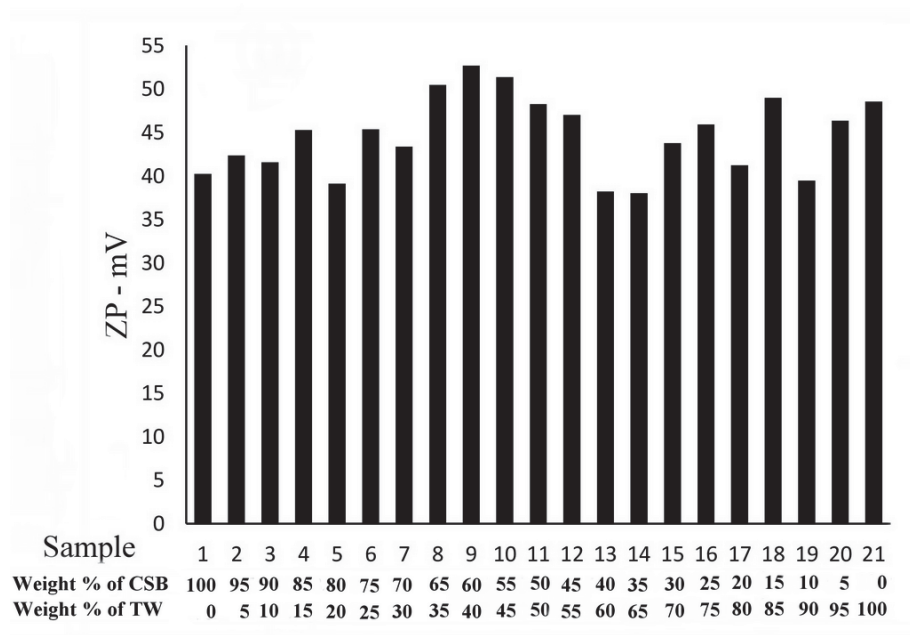


**Figure 7.7** Variation of zeta potential

### 7.2.6 SEM Analysis

SEM images are used for visualising the surface structure of materials. SEM image of sample 1 which contains 100% coconut shell biochar illustrated a porous structure. This explains the highest SSA obtained for sample 1 in BET analysis. SEM image of sample 21 which is 100% tea factory waste, did not show any porous structure and channels within the surface. According to the images, the surface is rough with indents and protrusions. Figure 7.8 gives selected SEM images of coconut shell biochar and tea waste. Pores of coconut shell biochar are displayed. According to Figure 7.8 (d), it is observed that TFW does not have a porous structure. This explains the lower SSA value observed for TFW in Figure 2.2.

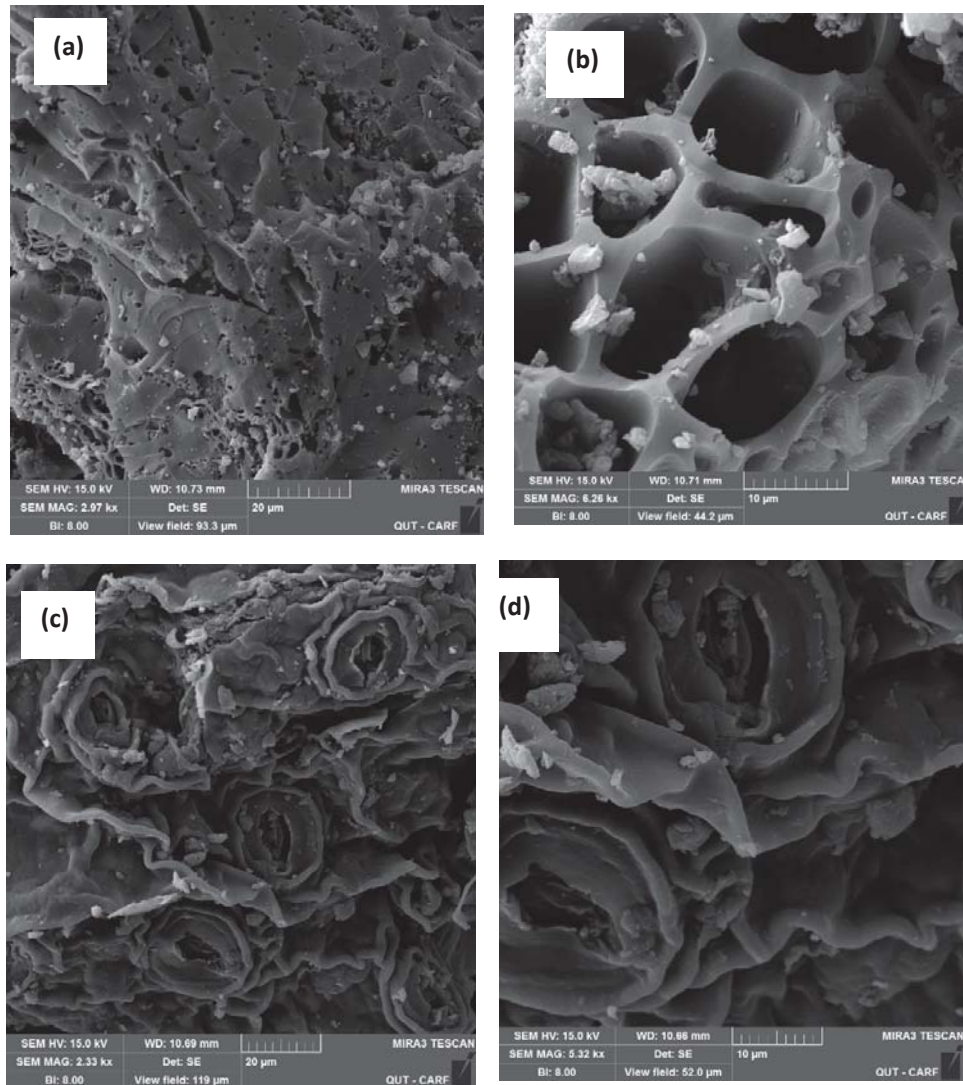


**Figure 7.8** SEM images of (a) CSB (b) Pores of CSB (c) TFW (d) Surface of TFW

### 7.2.7 FT-IR analysis

Sorption of a material is generally described by the morphology of the material and the chemical nature of its surface (Xu et al. 2017). Many heteroatoms exist as single atoms or as functional groups and among them and oxygen, is the dominant heteroatom. Carbon –oxygen (C-O) surface compounds are important in the surface reactions of materials (Gundogdu et al. 2013). FT-IR spectra were used to determine the functional groups present on the material surface and how material mixing affects the chemical nature of the mixtures. Figure 7.9 shows the FT-IR spectra for sample 1 (100% CSB), sample 21 (100% TFW), sample 6 (75% CSB:25% TFW), sample 11 (50% CSB:50% TFW) and sample 16 (25% CSB:75% TFW). FT-IR analysis of the



remainder are not presented as the discrimination among the spectra was not significant.

CSB (Figure 7.9(a)) has one broad peak at 1450-1500  $\text{cm}^{-1}$  due to C=C stretching. The broad adsorption peak around 3291  $\text{cm}^{-1}$  in Figure 7.9 (d) and (e) corresponds to the O-H stretching, due to inter molecular hydrogen bonding of polymeric compounds such as alcohols, phenols and carboxylic acid, and thus, shows the presence of free hydroxyl groups on the adsorbent surface (Gnanasambandam and Proctor 2000). The peak at 1700  $\text{cm}^{-1}$  in Figure (c), (d) and (e) corresponds to C=O stretching due to carboxylic acid. It is evident that the availability of the functional groups increases when the contribution of TFW is increased. According to Figure 7.5, samples having higher TFW percentages have higher amounts of acidic surface functional groups. However, samples 8, 9 and 10 which did not contain high amounts of TFW, also demonstrated higher amounts of acidic surface functional groups.

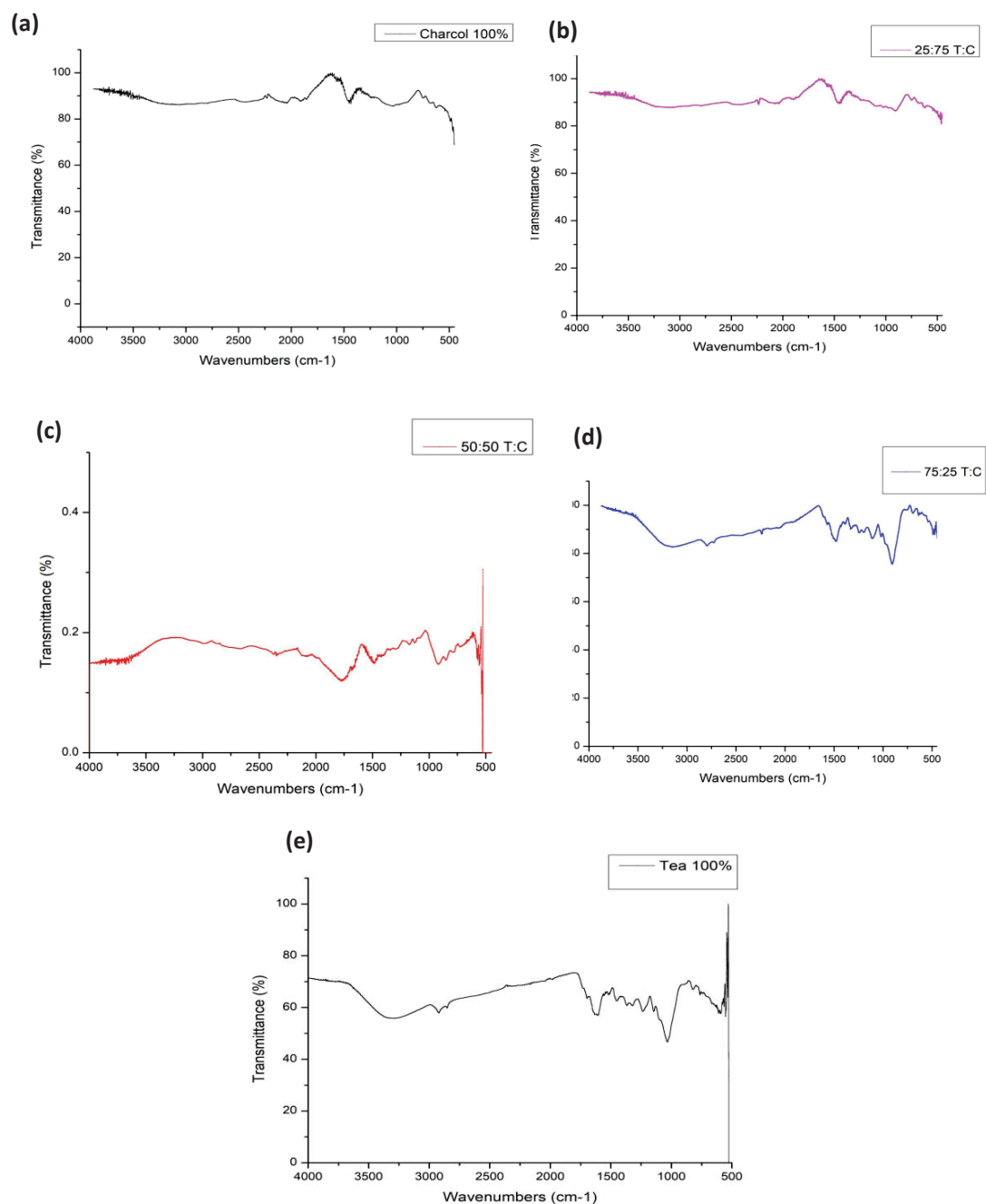


**Figure 7.9** FT-IR spectra for: (a) sample 1 (100% CSB); (b) sample 6 (25%TFW:75%CSB); (c) sample 11 (50%:TFW:50%:CSB); (d) sample 16 (75%:TFW :25%:CSB) and (e) sample 21 (100% TFW)

### 7.3 DETERMINATION OF MAXIMUM SORPTION CAPACITY

Maximum sorption capacity can be obtained through calculations/mathematical modelling using isotherms or by using equilibrium sorption capacities at different conditions. In most of the past studies, Langmuir isotherm (as given in Section 3.5.1) was employed to determine the  $q_m$  value (Xu et al. 2017; Cherdchoo et al. 2019; Gupta and Sen 2017). This method is suitable when the initial metal ion concentrations of the solutions used for the study remain low and cannot achieve saturation of the sorbent. Furthermore, Langmuir isotherm was developed for an ideal homogeneous sorption where all the sorption sites in the sorbents are considered identical and are equivalent. In the case of this study where sorbent samples were mixtures of two different biosorbents, it was not appropriate to consider all the sorbent sites as equal. Furthermore, in this study, solutions of both low and high concentration were used to determine sorption capacities. At high initial ion concentrations, sorbents become saturated and it was possible to determine  $q_m$  using equilibrium curves. Hence, Langmuir isotherm was not used in this study to determine  $q_m$ . For each of the twenty one biosorbent samples,  $q_m$  values for the three metal cations were determined using equilibrium curves. All the experimental conditions except the initial metal ion concentration of the solution, were kept unchanged as mentioned in Section 6.9.1. Sorption capacities for each metal ion at six different initial metal ion concentrations were calculated using Equation 3.1 given in Section 3.5.

Sorption capacity of biosorbents increases with increasing initial concentration of the metal solutions when other parameters of the system are kept constant. However, due to the limitation of available active sites of biosorbents, sorption capacity will plateau, where an increase in the initial concentration will not result in an increase in sorption capacity. The sorption capacity at plateau is considered as the maximum sorption capacity of a particular biosorbent and could be determined using the relevant equilibrium curve. A similar approach was used by Bo et al. (2016) for the determination of maximum sorption capacity.

Determination of maximum  $\text{Pb}^{2+}$  sorption capacity of biosorbent sample 1 using the equilibrium curve is described below. Figure 7.10 shows the variation of sorption capacity determined for  $\text{Pb}^{2+}$  at initial concentrations of 2 mg/L, 10 mg/L, 50 mg/L, 100 mg/L, 200 mg/L and 300 mg/L. The value gradually increased to 30.12 mg and levelled off. This value of 30.12 mg/g was taken as the maximum  $\text{Pb}^{2+}$  sorption capacity of biosorbent sample 1. The process was repeated for the rest of the 20 biosorbent samples (given in Section 4.3.2), for all three metal ions ( $\text{Cu}^{2+}$ ,  $\text{Pb}^{2+}$  and  $\text{Cd}^{2+}$ ). Sorption capacities for the 21 samples, at 6 different initial metal ion concentrations, for the three metal ions are given in Appendix A2.

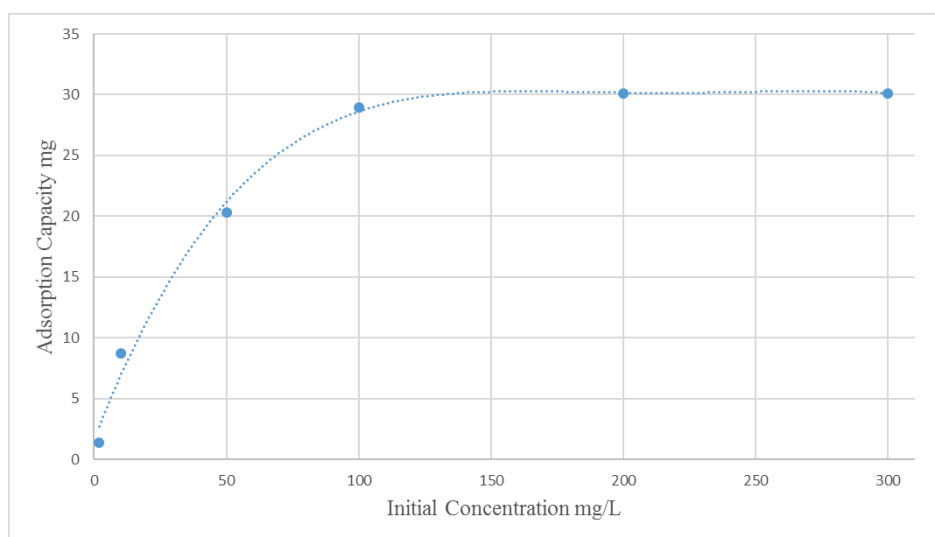


**Figure 7.10** Variation of sorption capacity determined for  $\text{Pb}^{2+}$  at six different initial concentrations: 2 mg/L, 10 mg/L, 50 mg/L, 100 mg/L, 200 mg/L and 300 mg/L

Figure 7.11 depicts the maximum sorption capacity values calculated for all the samples. For  $\text{Pb}^{2+}$  and  $\text{Cd}^{2+}$ , the highest values were recorded for sample 9 (60%TFW:40%CSB) whereas sample 8 (65%TFW:35%CSB) recorded the highest for  $\text{Cu}^{2+}$ . The lowest value for  $\text{Cd}^{2+}$  was for sample 14 (35%TFW:65%CSB). For  $\text{Pb}^{2+}$  and  $\text{Cu}^{2+}$ , the lowest values were recorded for samples 17 (20%TFW:80%CSB) and 1 (100%TFW), respectively. Table 7.1 gives the highest and lowest sorption capacities derived for  $\text{Cu}^{2+}$ ,  $\text{Pb}^{2+}$  and  $\text{Cd}^{2+}$  from the analysis.

**Table 7.1** Highest and lowest adoption capacities derived from the analysis

Metal Ion	Lowest Sorption capacity mg/g	Highest sorption capacity mg/g
Pb <sup>2+</sup>	30.12	47.73
Cd <sup>2+</sup>	9.26	19.32
Cu <sup>2+</sup>	19.12	33.8

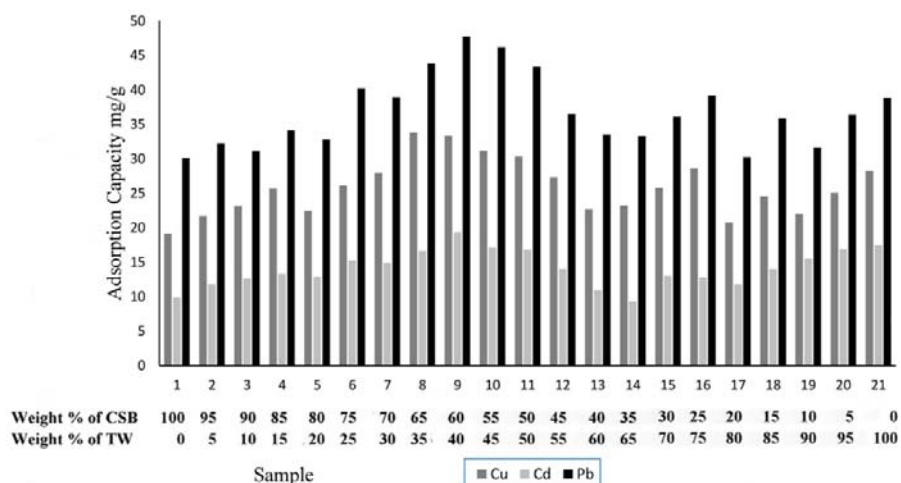


**Figure 7.11** Variation of maximum metal sorption capacities for the samples

#### 7.4 QUALITATIVE RELATIONSHIPS BETWEEN PHYSICO-CHEMICAL PROPERTIES OF BIOSORBENTS AND MAXIMUM SORPTION CAPACITY

The raw data matrix consisted of twelve variables and twenty-one objects (twenty-one biosorbent mixtures) (Section 5.2). The variables were the maximum sorption capacities for Pb<sup>2+</sup> ( $q_m(\text{pb})$ ), Cd<sup>2+</sup> ( $q_m(\text{Cd})$ ), and Cu<sup>2+</sup> ( $q_m(\text{Cu})$ ), SSA, PS, PV, ZP, TAG and TBG. Since TAG can be quantified as carboxylic, phenolic and lactonic groups (Basso et al. 2002), individual concentrations of the three acidic surface functional groups were also considered separately along with TAG, as variables.

Principal Component analysis (PCA) was undertaken as the first step for assessing and visualising the projection of variables. Data used for PCA was subjected to pre-

treatment (Einax et al. 1998). The variables in the data matrix were mean centred and standardised (auto scaled) in order to ensure these had equal weights in the analysis (Ku et al. 1995). The resulting biplots helped to visualize the interdependencies among the variables in the data matrix as described in Section 4.1. The first two PCs accounted for 83.7% of the total variability while PC3 represented only 5.7%. It was also noted that only the first two PCs had eigenvalues greater than one (6.976 and 3.068, respectively), whereas PC3 had a low eigenvalue (0.687). When the eigenvalue is less than one, the factor in question is considered to account for low variability than does a single variable (Abdi and Williams 2010a). For these reasons, only the first two PCs, in the biplot (Figure 7.12) were considered in the analysis.

Research literature recommends using a correlation matrix to confirm the correlations visually evident in a PCA biplot (Miguntanna, Egodawatta, et al. 2010). Pearson correlation analysis in the form of the correlation matrix (compiled using the raw data matrix) depicting Pearson product-moment correlation coefficient (PPMCC) values calculated for each pair of variables is given in Table 7.2. Each variable is correlated with the rest of the variables in the table providing an understanding of the highest correlation. PPMCC is a measure of the strength and direction of association that exists between two variables measured at an interval scale. PPMCC is defined as the covariance of the two variables divided by the product of their standard deviations. It has a value between +1 and -1. +1 implies total positive linear correlation while 0 implies nonlinear correlation and -1 refers to total negative linear correlation (Bruce and Bruce 2017). The assumptions involved in the analysis of PPMCC and other details are provided in Section 4.4. Statistical inference based on Pearson's correlation coefficient often involves running a permutation test (resampling test).

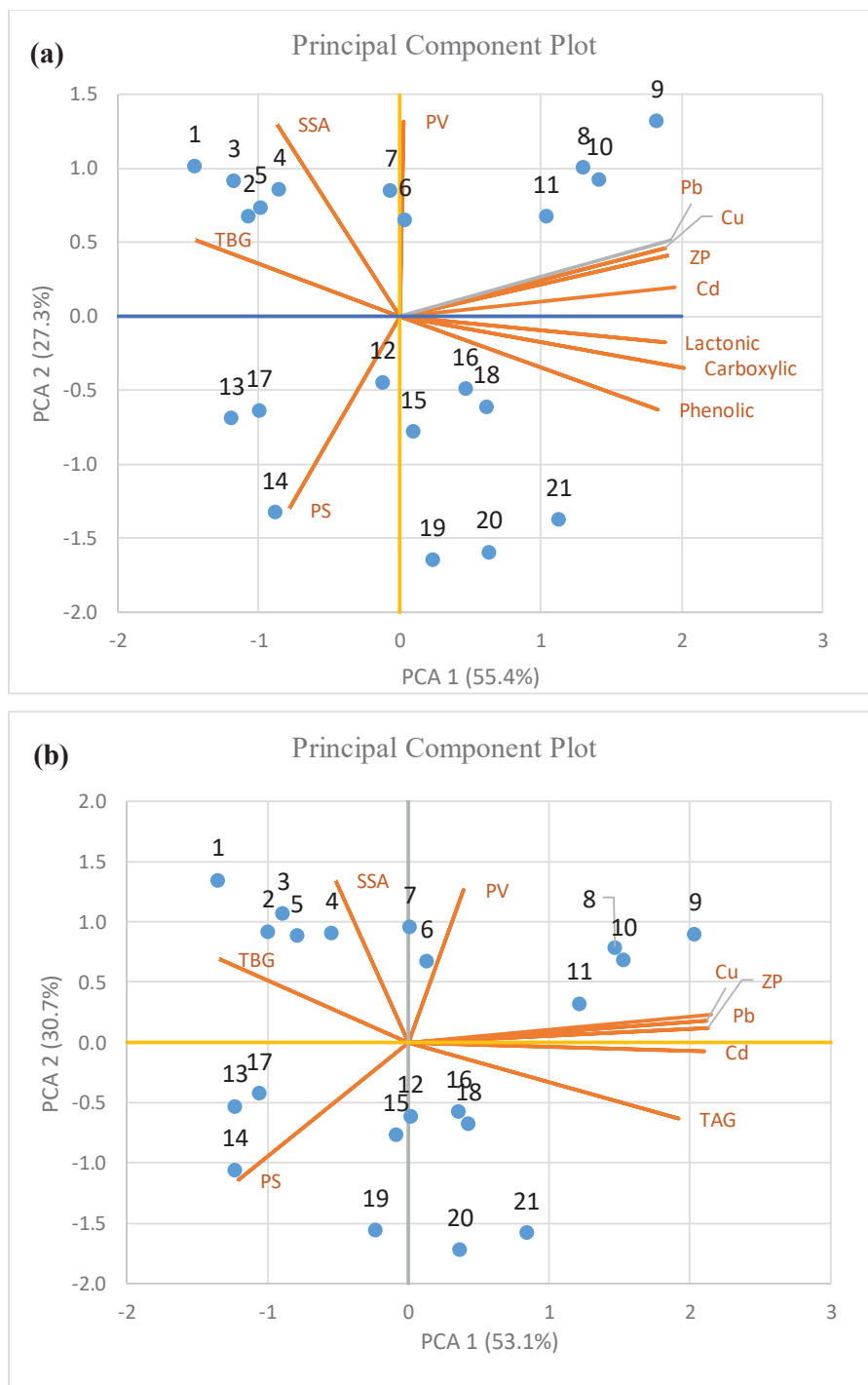


**Figure 7.12** PCA biplot consisting of physico-chemical properties and sorption capacities of biosorbent mixtures **(a)** three acidic functional groups together as TAG **(b)** Carboxilic, Lactonic and Phenolic separately

**Note:** SSA specific surface area, PV pore volume, PS pore size, ZP zeta potential, TAG total acidic group and TBG total basic group, Cu qm of  $\text{Cu}^{2+}$ , Cd qm of  $\text{Cd}^{2+}$ , Pb qm of  $\text{Pb}^{2+}$ )

The PCA biplot (Figure 7.12) illustrates that the angles between the vectors corresponding to carboxylic, phenolic, lactonic, TAG, Cd, Cu and Pb are acute suggesting a strong correlation between acidic surface functional groups and metal sorption capacity. This is confirmed by the significant positive correlation coefficient ( $p < 0.05$ ) as evident in Table 7.2. According to Wang et al. (2007a), functional groups could participate in sorption through electrostatic interaction or exchange of electrons to form complexes. Hence, a biosorbent with high total acidic surface functional groups is capable of cation sorption resulting in high sorption capacity (Fan et al. 2018). In contrast, TBG has a negative correlation with metal sorption capacity as indicated by the PCA biplot. This suggests that electrostatic repulsion caused by these basic functional groups weakens the sorption forces of positively charged metal ions (Jacobasch et al. 1998). Therefore, materials with high TBG could have lower sorption capacity for positively charged metals.

Vectors related to carboxylic, phenolic, lactonic concentrations, separately and cumulatively as TAG, show acute angles with ZP, indicating strong positive correlations among these parameters. This implies that these acidic functional groups can be ionised into negative ions, resulting in negative zeta potential (Wang et al. 2007). ZP shows a strong correlation with metal sorption capacity and this observation is confirmed by the correlation matrix (PPMCC values above 0.8 with  $p < 0.0005$ ). This could be attributed to the contribution of ZP to the process of physisorption. During physisorption, dipole interactions are developed when metal cations approach the negative sites of sorbents, allowing a relatively weak Van der Waals attractive force to develop between the outer sphere of metal cations and the sorbent framework (Inglezakis and Pouloupoulos 2006). Zeta potential provides an indication of surface negativity, which is favourable for cation sorption. High ZP value is favourable for attraction between the negatively charged biosorbent surface and cations. The strong attraction draws cations towards the biosorbent surface and increases the dispersion forces between the surface and cations. Jacobasch et al. (1998) noted that Van der Waals forces can be assessed by zeta potential measurements. This suggests that physisorption yields a higher contribution to the sorption process in materials with high zeta potential.



**Table 7.2** Pearson correlation matrix

	SSA	PS	PV	ZP	Carboxylic	Phenolic	Lactonic	TAG	Cu	Cd	Pb	TBG
SSA		**	***		*	**		**				**
PS	-0.620		***	*					*	*	*	
PV	0.717	-0.788										
ZP	-0.137	-0.538	0.197		***	*	**	**	***	***	***	*
Carboxylic	-0.579	-0.089	-0.156	0.702		***	***	***	***	***	***	**
Phenolic	-0.673	0.065	-0.326	0.582	0.910		***	***	*	**	*	**
Lactonic	-0.404	-0.254	-0.028	0.624	0.781	0.802		***	**	***	**	**
TAG	-0.606	-0.072	-0.197	0.682	0.978	0.964	0.865		**	***	***	**
Cu	-0.068	-0.493	0.214	0.853	0.743	0.553	0.592	0.688		***	***	**
Cd	-0.224	-0.484	0.025	0.809	0.777	0.672	0.693	0.764	0.775		***	*
Pb	-0.050	-0.548	0.276	0.852	0.750	0.560	0.685	0.711	0.950	0.791		
TBG	0.595	0.028	0.167	-0.452	-0.595	-0.628	-0.686	-0.651	-0.366	-0.512	-0.363	

**Note:** The lower triangular segment depicts correlation coefficient values while the upper triangular segment represents statistical significance levels; p<0.05 (\*), p<0.005 (\*\*), p<0.0005 (\*\*\*)

Amarasinghe and Williams (2007) found that metal sorption capacity increases with SSA when the SSA of a material is increased by reducing the particle size. This is because, the increase in SSA leads to an increase in the contact area between the biosorbent and metal cations. However, Han et al. (2013) and (Agrafioti et al. 2013) reported that materials with high surface functional group densities, i.e. the quantity of the functional groups per unit area, demonstrate high sorption capacity even when their SSA values are low. Further, Bradl (2004) also noted that the influence of SSA on sorption capacity should be understood in the context of the density of surface functional groups. Similarly, according to PCA (Figure 7.12) and the correlation matrix (Table 7.2), SSA does not have a significant correlation with the metal sorption capacity, whereas a strong correlation was observed between metal sorption capacity and the functional groups. This highlights the influence of surface functional group density on metal sorption capacity.

According to Table 7.2, PS has high negative correlation with PV (PPMCC= -0.788,  $p < 0.0005$ ) and SSA (PPMCC= 0.717,  $p < 0.0005$ ). For this study, PS assessment was done via BJH Desorption method (Barrett et al. 1951), which calculates PS as a function of PV and BJH Desorption cumulative surface area. While the surface area values obtained from BJH Desorption method is different from SSA values obtained for this study (using BET method (Brunauer et al. 1938)) for the same material, they are closely related. This explains the correlations detected in relation to PV, PS and SSA. However, the direction of the relationship between PS and PV for a particular surface mainly depends on its pore distribution (Bose et al. 2003). Pore size distribution provides the information on relative abundance of each pore size in a given volume. If the volume contains a large number of small pores, it gives a high value for PV.

Quality of representation of each variable on the two PCs was calculated via the squared cosine ( $\cos^2$ ) value (Krzanowski 1979), which indicates the contribution of a component to the squared distance of the observation to the origin. Calculation of  $\cos^2$  is a direct function of many statistical software packages. While it is possible to assess the quality of representation of each variable in a PCA biplot visually, such an analysis is highly subjective. Calculation of squared cosine values are useful as such calculations are objective and indicate numerical values that can be compared with others. Further details on the calculation of  $\cos^2$  including the R software code are

given in Appendix A3. Individual cos2 values are given in Table 7.3. Cos2 for PC1 was the highest in TAG followed by ZP, while cos2 for PC2 was the highest in SSA followed by PS and PV.

Cos2 values of variables together with factor scores of observations can be used to describe visual observations of the PCA biplot. Factor scores can be interpreted geometrically as the projections of the observations on the principal components. It was noted that PC1 discriminates the samples based on acidic functional groups since the 11 samples with the highest TAG also had positive factor scores on PC1 (Figure 7.5). On the other hand, PC2 demonstrates a clear discrimination based on SSA as samples 1 to 11 with the highest SSA values scored the lowest factor scores on PC2 (Figure 7.2).

**Table 7.3** cos2 values for PC1 and PC2.

<b>Variable</b>	<b>cos2 for PC1</b>	<b>Variable</b>	<b>cos2 for PC2</b>
TAG	0.9068	SSA	0.8150
ZP	0.7091	PS	0.7765
SSA	0.4609	PV	0.7116
PS	0.2076	ZP	0.1140
PV	0.0884	TBG	0.0882
TBG	0.0017	TAG	0.0515

The clustering seen with the first five samples having lower PC1 and PC2 factor scores can be explained by cos2 values of variables where TAG and SSA have the highest cos2 for PC1 and PC2, respectively. Figures 7.2 and 7.5 indicate that the first five samples have the lowest TAG values (resulting in low PC1 factor scores) coupled with the highest SSA values (resulting in low PC2 factor scores). Samples 8, 9, 10 and 11 with high PC1 factor scores and low PC2 scores are also clustered together. These four samples have a relatively higher capacity for metal sorption (Figure 7.11), suggesting that samples with high PC1 factor scores and low PC2 factor scores would have a relatively higher sorption capacity. According to the physico-chemical analysis in Section 7.2, samples 8, 9, 10 and 11 show relatively higher pore volume (Figure 7.3)

and lower pore size (Figure 7.4). Acidic functional groups present in these four samples are high according to Figure 7.5 and show lower values for total basic groups. Zeta potential of these four samples are also higher than most of the other samples. These observations imply that changes in physico-chemical properties have the ability to change the sorption capacity of the sorbent. An increase of some variables can increase the sorption capacity, whereas an increase of some parameters results in the decrease of the sorption capacity. Hence, it is important to understand the relative importance of each parameter in determining the sorption capacity of a sorbent. Furthermore, it is also necessary to understand the individual influence exerted quantitatively by each physico-chemical property on sorption capacity of a particular sorbent.

## **7.5 QUANTITATIVE ANALYSIS OF THE INFLUENCE OF PHYSICO-CHEMICAL PROPERTIES ON MAXIMUM SORPTION CAPACITY**

Generalized Linear Regression (GLR) was employed to model the relationship between the dependent variables and independent variables by fitting a linear equation to the observed data. As explained in Section 4.1, the choice of predictive variables for the modelling can be carried out by an automatic procedure depending on the method (algorithm) employed. The Elastic net (Enet) algorithm aims to shrink the coefficients of redundant variables exactly to zero (Zou and Hastie 2005a), thereby employing a selection of variables as an integral feature. Enet is therefore, considered as a ‘shrinkage method’ (Wang, Park and Carriere 2010) with the ability to overcome limitations of other popular methods such as ridge regression and Lasso regression (Ter Braak 2009).

Analysis of multicollinearity of the independent variables was done as the next step. Both, the correlation matrix and variance inflation factors (VIFs) calculation were employed for this purpose. VIF quantifies the severity of multicollinearity in an ordinary least squares regression analysis by estimating how much the variance of a regression coefficient is inflated due to multicollinearity in the model.

The correlation matrix illustrated high correlation between PV and SSA as well as between PV and PS. Since PS was also calculated using PV (Section 3.1), PV was excluded to reduce the multicollinearity for the subsequent statistical modelling. When all the independent variables were considered for the calculation of VIFs, R software

detected an error caused by ‘perfect multicollinearity’. This was caused by the fact that TAG is equal to the sum of carboxylic, phenolic and lactonic values. Therefore, the ‘perfect multicollinearity’ detected by the statistical software could be removed either by using TAG to represent carboxylic, phenolic and lactonic (Method 1) or by using them separately (Method 2). Calculation of VIFs was done using both these approaches and the results are given in Table 7.4.

VIFs were below 10 for the other variables, suggesting that variable selection could be done as per Method 1 or Method 2. Since TAG value can be obtained using a single titration, TAG was retained (Method 1) for the initial modelling, while the three surface acidic groups were excluded.

**Table 7.4** Variance inflation factors (VIFs) of the independent variables.

<b>Method 1:</b> TAG was used to represent acidic surface functional groups		<b>Method 2:</b> carboxylic, phenolic and lactonic groups were considered separately	
Variable	VIF	Variable	VIF
SSA	8.683927	SSA	7.074937
PS	7.697411	PS	8.018565
PV	3.525524	PV	3.849023
ZP	3.668455	ZP	3.990223
TAG	4.079687	carboxylic	8.190078
TBG	2.608812	phenolic	9.011234
		lactonic	4.660444
		TBG	3.156745

### 7.5.1 Relative importance of physico-chemical properties on sorption

Mathematical regression models were developed to define the influence of physico-chemical parameters on sorption capacity using generalised linear regression using the Enet method for the three metal ions. Repeated k-fold cross validation (k=10, repeated 10 times) was used as the resampling method and Enet algorithm was employed via R software for the regression. The codes used for the analysis are given in Appendix A3.

Table 7.5 provides a summary of the three regression models for Cu<sup>2+</sup>, Cd<sup>2+</sup> and Pb<sup>2+</sup> sorption. The Enet algorithm selects the optimal model using Root Mean Squared Error (RMSE) to determine the optimal values for the two parameters referred to as ‘lambda’ and ‘alpha’. Lambda is a penalization parameter while alpha sets the ratio between L1 and L2 regularizations. Further details of these parameters and the regression method is given in Section 4.1. RMSE value represents the square root of the variance of residuals and indicates how close the observed measurements are to the predicted values. Relevant RMSE values and regression coefficients for each model are given in Table 7.5 (p<0.001 for all regression coefficients).

**Table 7.5** Regression coefficients and model parameters

<b>Dependent variable</b>	<b>TAG</b>	<b>ZP</b>	<b>TBG</b>	<b>PS</b>	<b>SSA</b>	<b>RMSE</b>	<b>R squared</b>
q <sub>m</sub> (Pb)	98.824	72.609	4.4789	0	0.1092	2.7591	0.9906
q <sub>m</sub> (Cu)	103.127	98.858	7.5709	0	0.8308	2.2503	0.9842
q <sub>m</sub> (Cd)	79.683	34.720	1.4538	0.5371	0.2603	1.2081	0.9831

According to the model parameters (Table 7.5), the influence of different physico-chemical properties of the materials on sorption capacity is comparable for Pb<sup>2+</sup>, Cu<sup>2+</sup> and Cd<sup>2+</sup>. In all three cases, the influence of TAG is the highest followed by that of ZP, while the influence of TBG, PS and SSA is much smaller. The sorbates considered in this study are heavy metals and the ionic radius are 113 pm, 95 pm and 73 pm for Pb<sup>2+</sup>, Cu<sup>2+</sup> and Cd<sup>2+</sup>, respectively. These values are very low compared to the size of the pores as shown in Figure 7.4. Hence, the size of the pores does not have a clear impact on sorption. This suggests that ion exchange and chemisorption are the important mechanisms in metal sorption by biosorbents, where the acidic functional groups bind with metal cations via coordination and chelation (Lourie and Gjengedal 2011), with physisorption playing a lesser role. A relatively high influence of ZP despite the limited variation among samples (Section 5.2 and Figure 7.7) highlights the prominent role of ZP in metal sorption. Similar results were obtained by Li et al. (2003), for sorption of Cd<sup>2+</sup> and by Dai (1994), for the sorption of cationic dyes.

Physisorption of metal ions by sorbent materials depends on the charge densities of the metal ions (Erdem et al. 2004). Cations with high charge densities have a strong cationic field. Therefore, their interaction with an anionic field of sorbents is stronger compared to cations of low charge densities (Eisenman 1962). Consequently, the physisorption force is stronger for cations with high charge densities. Hence, the relatively higher influence of ZP on  $\text{Cu}^{2+}$  sorption compared to  $\text{Cd}^{2+}$  and  $\text{Pb}^{2+}$  could be attributed to the higher charge density of  $\text{Cu}^{2+}$ . Considering the sorption of  $\text{Pb}^{2+}$  and  $\text{Cu}^{2+}$ , the five parameters follow the same order of importance while the coefficient of PS was set to zero by the Enet algorithm. The same coefficient was low for  $\text{Cd}^{2+}$  as well, implying that the influence of PS on metal sorption is low. This study outcomes implies that increasing acidic functional groups and/or ZP of biosorbents will result in enhancing the sorption capacity for  $\text{Pb}^{2+}$ ,  $\text{Cu}^{2+}$  and  $\text{Cd}^{2+}$ . This knowledge is essential for undertaking modifications to existing biosorbents for enhancing their sorption capacity. Furthermore, available data in literature as well as future studies on key physico-chemical properties such as TAG and ZP of biosorbents, can be used to predict their sorption capacities when designing biosorbent based industrial wastewater treatment systems. Since the influence of different physico-chemical properties of the materials on sorption capacity is comparable for all three selected metal ions, it is possible that other metal ions would yield similar results. This could serve as a topic for future research.

### **7.5.2 Individual influence of acidic functional groups on sorption**

As an extension to the final step of the data analysis, mathematical models given in Table 7.5 were re-created after substituting individual values of carboxylic, phenolic and lactonic for TAG (Method 2 of variable selection in Section 7.4). This was done in order to investigate the influence of individual acidic functional group on metal sorption. Table 7.6 indicates the regression coefficients of acidic functional groups obtained from the analysis ( $p < 0.001$  for all regression coefficients). Based on the regression coefficients given in Table 7.6, carboxylic group had a higher influence on  $\text{Cu}^{2+}$  and  $\text{Pb}^{2+}$  sorption followed by phenolic and lactonic groups. This is compatible with the observation described by Neris et al. (2019) on the sorption of metal cations to modified water hyacinth fibres. For  $\text{Cd}^{2+}$ , lactonic group had a higher influence followed by carboxylic and phenolic groups. These observations can be explained by Lewis Hard Soft Acid Base (HSAB) theory (Pearson 1968). As  $\text{Cu}^{2+}$  and  $\text{Pb}^{2+}$  can be

considered as hard acids, they generally prefer to bind to hard bases such as carboxylic and phenolic groups.

**Table 7.6** Regression coefficients of acidic functional groups

<b>Dependent variable</b>	<b>Carboxylic</b>	<b>Phenolic</b>	<b>Lactonic</b>
$q_m(\text{Pb})$	28.3657	16.3951	11.2503
$q_m(\text{Cu})$	23.4117	15.4223	10.2314
$q_m(\text{Cd})$	14.2123	10.2378	19.2528

## 7.6 PREDICTING THE EQUILIBRIUM SORPTION CAPACITY

Maximum sorption capacity of a sorbent can be obtained using equilibrium curves as explained in Section 7.3. Maximum sorption capacity is the sorption capacity that can be recorded for a particular sorbent when it becomes saturated and serves as an initial indicator to understand the effectiveness and the performance of a sorbent under any experimental condition. Equilibrium sorption capacity ( $q_e$ ) is the amount sorbed at equilibrium, for a particular initial ion concentration. However, this value changes with the initial concentration of the solution (when all the other conditions are kept constant) and reaches a plateau, which is the maximum sorption capacity of the sorbent under investigation. Equilibrium sorption capacity is an important parameter that can be used to assess the sorption efficiency of a sorbent at given conditions (especially at a given initial solution concentration). As  $q_m$  is obtained at saturation, experimental conditions do not have an influence on  $q_m$ . It is dependent on sorbent physico-chemical properties and can be predicted using these physico-chemical properties (Pathirana et al. 2019). Even though  $q_e$  changes with the initial metal ion concentration, it is also important to assess the sorption efficiency of a sorbent at a given initial ion concentration. Hence, developing a mathematical model using physico-chemical properties and initial ion concentration to predict  $q_e$  is also important.



Partial least squares regression (PLS) was employed to formulate mathematical models to understand the relationships between the physico-chemical properties, metal concentrations and  $q_e$  of  $Pb^{2+}$ ,  $Cd^{2+}$  and  $Cu^{2+}$ . PLS is a popular multivariate data analytical technique with a combination of features from PCA and multiple linear regression. It aims to predict dependent variables (responses) from independent variables (predictors) by the extraction of a set of orthogonal factors called latent variables having the best predictive powers (Abdi and Williams 2010b). The efficiency and accuracy of the predictions obtained is commonly evaluated with cross-validation techniques such as bootstrapping and repeated k-fold cross validation. For the present study, repeated k-fold cross validation was utilized for extracting the optimal number of components to be retained in PLS models. For model development, the six data matrices (six initial metal ion concentrations) were combined to form a single data matrix (Appendix A2). The initial metal ion concentration was considered as a separate numerical variable and accordingly, seven independent variables were available for each of the metal cations.

It was decided to develop one model for each metal ion ( $Pb^{2+}$ ,  $Cd^{2+}$  and  $Cu^{2+}$ ). Repeated k-fold cross-validation was employed with  $k=5$  (100 repeats) for extracting the optimal number of components to be retained for each PLS model. Lowest root mean square error (RMSE) was the criteria used for the determination of the optimal number of components to be retained. Table 7.7 illustrates the model coefficients obtained for the three initial models. The R-squared values were above 0.6 for all the models with the highest being 0.646. This implies an acceptable level of fit for a mathematical model regarding a complex natural system. Therefore, the outcomes of PLS was considered reliable.

**Table 7.7** Regression parameters and coefficients for prediction of  $q_e$  using physico-chemical properties and initial metal ion concentration

	$q_e(\text{Pb})$	$q_e(\text{Cu})$	$q_e(\text{Cd})$
Intercept	-2.299	-1.612	1.738
SSA	0.0025	0.0027	-1.4383e-03
PS	-0.110	-0.079	-0.080
PV	156.2	78.9	-103.3
ZP	0.341	0.280	1.712e-01
TBG	-0.046	-0.046	-0.363
TAG	1.60	1.12	0.99
Concentration	0.103	0.066	0.032
R-squared	0.6460	0.6047	0.6278

**Note:** Units used for each of the variables are as follows SSA =  $\text{m}^2/\text{g}$ , TAG =  $\text{mmol}/\text{g}$ , TBG =  $\text{mmol}/\text{g}$ , PS =  $\text{\AA}$ , PV =  $\text{cm}^3/\text{g}$ , ZP =  $\text{mV}$ , concentration =  $\text{mg}/\text{L}$ ,  $q_e$  =  $\text{mg}/\text{g}$

## 7.7 SUMMARY OF KEY FINDINGS

The aim of this chapter was to mathematically quantify the influence of surface physico-chemical properties of biosorbents on heavy metal sorption and to identify the relative importance of each physico-chemical property on sorption capacity for  $\text{Cu}^{2+}$ ,  $\text{Cd}^{2+}$  and  $\text{Pb}^{2+}$ . Though various physico-chemical properties could influence  $\text{Cu}^{2+}$ ,  $\text{Cd}^{2+}$  and  $\text{Pb}^{2+}$  sorption, they do not equally contribute or are equally important for sorption. The main conclusions derived from the study were:

- Mixing sorbents can give higher performance compared to individual sorbents in terms of sorption capacity. Physical and chemical changes occurring with the sorbents during the mixing process changes the physico-chemical properties either by increasing or decreasing the values compared to the original sorbents used.

- The key physico-chemical property governing the sorption capacity of biosorbents for all the three metal cations are the acidic surface functional groups. Among these, carboxylic group play a relatively prominent role in the sorption of  $\text{Cu}^{2+}$  and  $\text{Pb}^{2+}$  which are hard acids, while lactonic groups are more important in providing binding sites to  $\text{Cd}^{2+}$ , which is a soft acid.
- Van der Waals forces can be assessed by zeta potential measurements. During physisorption, dipole interactions are developed when metal cations approach the negative sites of sorbents, allowing a relatively weak Van der Waals attractive force. Hence, zeta potential of biosorbents can be used for assessing the physisorption of these three metal cations.
- Though sorption is a surface phenomenon, specific surface area alone does not exert a prominent influence on the sorption of  $\text{Cu}^{2+}$ ,  $\text{Cd}^{2+}$  and  $\text{Pb}^{2+}$ , if materials with different functional group densities and same particle size are used.
- Importance of each physico-chemical property on sorption was assessed based on the regression coefficients. Identifying as to which of the physico-chemical properties should be manipulated to achieve higher sorption of these three metal ions would aid in planning treatment methods to modify locally available biosorbents.
- Equilibrium sorption capacity of a metal can be predicted using sorbent's physico-chemical properties and initial metal ion concentration of the solution.

# CHAPTER 8: INFLUENCE OF PHYSICO-CHEMICAL PROPERTIES ON SORPTION KINETICS

---

## 8.1 INTRODUCTION

Heavy metal sorption capacities of various biosorbents have been assessed based on their equilibrium capacity and reaction kinetics in past studies (Ho and McKay 1998). Equilibrium studies deal with the final state of a system, while kinetics characterises sorption uptake with respect to time. These two types of studies are imperative as they provide insights into the mechanisms and reaction pathways. In Chapter 7, the influence of physico-chemical properties of biosorbents on sorption capacity was described. This chapter describes the influence of physico-chemical properties of biosorbents on sorption rate.

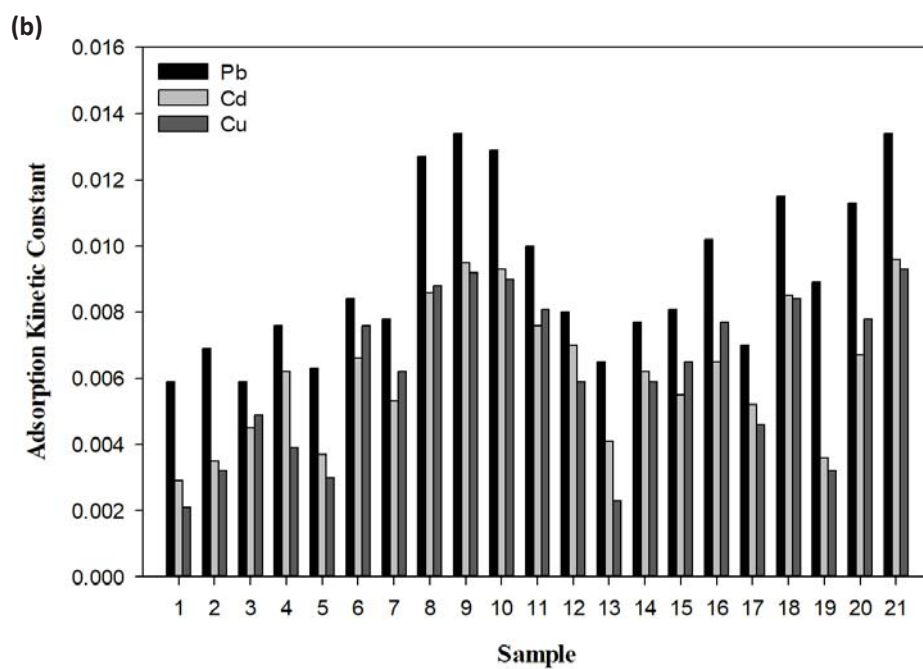
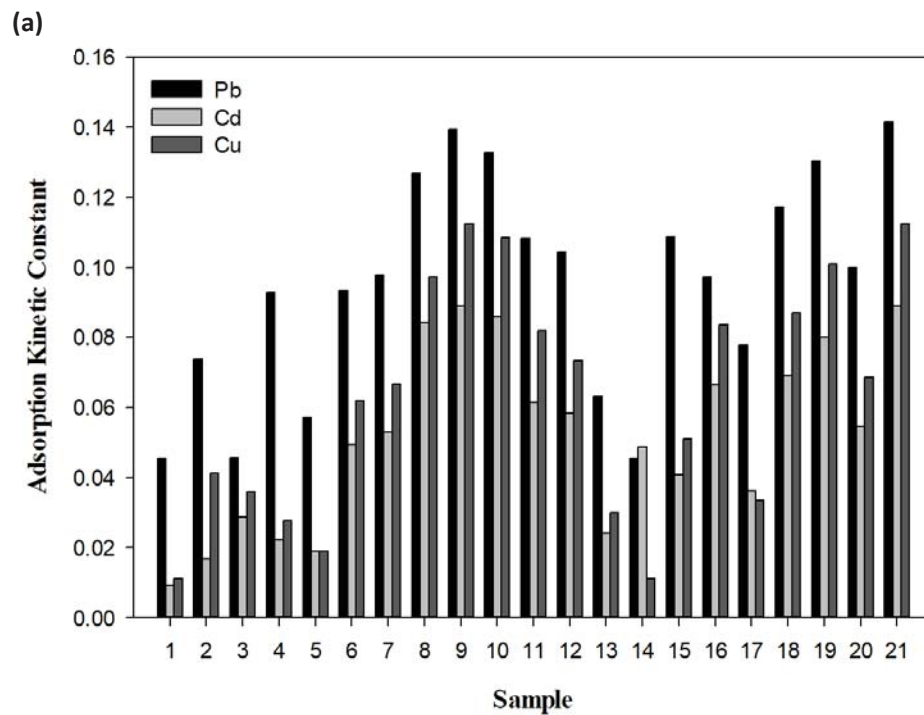
According to current knowledge on sorption kinetic modelling, these are generally classified as sorption reaction models and sorption diffusion models (Qiu et al. 2009). While both types of models are applied for the purpose of describing the sorption kinetics process, they are fundamentally different. A detailed description of these models was given in Section 3.4. The most commonly used models for simulating sorption kinetics data are the pseudo first order model proposed by Lagergren (1898) and the pseudo second order model proposed by Ho and McKay (1998), both of which are sorption reaction models (Simonin 2016). In some of these studies, kinetic models have been compared with regard to their ability in predicting the behaviour of experimental data (Dai et al. 2018; Iftekhar et al. 2018). More often, formulae such as pseudo first order and second order equations are applied to correlate kinetic data obtained for different biosorbents, followed by using equations of best fit to verify the mechanism (Cherdchoo et al. 2019). The two kinetic rate constants  $k_1$  and  $k_2$  in these two models are calculated and the rate constant of the best fitted model is generally used to determine initial sorption rate of biosorbents (Amarasinghe and Williams 2007). Furthermore, variation of the kinetic constants under different experimental conditions such as pH, temperature, adsorbent dose and concentration of the initial metal solution have been investigated and mathematical formulae have been developed to replicate such variations (Plazinski et al. 2009).

However, mathematical relationships have not been defined to describe how the variation of physico-chemical properties such as specific surface area, total acidic groups, total basic groups, zeta potential, pore volume and pore size (Section 7.1) could influence the kinetic rate constants. Such knowledge would facilitate the optimization of sorption mechanism pathways while guiding as to which of the parameters should be manipulated for exerting greater influence on the sorption rate, thereby improving the sorption process. Therefore, identifying mathematical relationships between material properties and kinetic rate constants is critical for the effective design and development of heavy metal removal systems based on sorption (Thompson et al. 2001).

The aim of this chapter is to present predictive models to determine the kinetic rate constants for the three selected divalent heavy metals using physico-chemical properties of the selected biosorbents. This would permit modifying physico-chemical properties of biosorbents for creating and optimizing biosorbent mixtures with enhanced sorption characteristics.

## 8.2 DETERMINING RATE CONSTANTS

According to the equations given in Section 4.3,  $k_1$  and  $k_2$  values for the 21 samples (Section 5.2) at initial metal concentrations of 200 mg/L, 100 mg/L, 50 mg/L and 25 mg/L were calculated. Both, pseudo first and second order models fit the experimental data well since the R-squared values are above 0.80 in almost all the cases. However, the pseudo second order model demonstrated better fit for all the four initial metal concentration as the  $R^2$  values were above 0.90 in all the cases. Furthermore, according to past research, metal binding processes of the majority of the biosorbents were well described by the pseudo second order kinetic model (Dudu et al. 2015; Cherdchoo et al. 2019). Ho et al. (1998) concluded that the pseudo second order model describes the metal binding process better than the pseudo first order model after testing both models using data available in research literature. Hence, pseudo second order kinetic constant ( $k_2$ ) was used for further analysis. Figures 8.1 illustrates the pseudo second order metal binding rate constant values ( $k_2$ ) obtained for the twenty one samples generated, for the four initial metal ion concentrations.  $k_2$  values for the samples are given in Table A2.5 in Appendix A2.



*Continued on next page.*

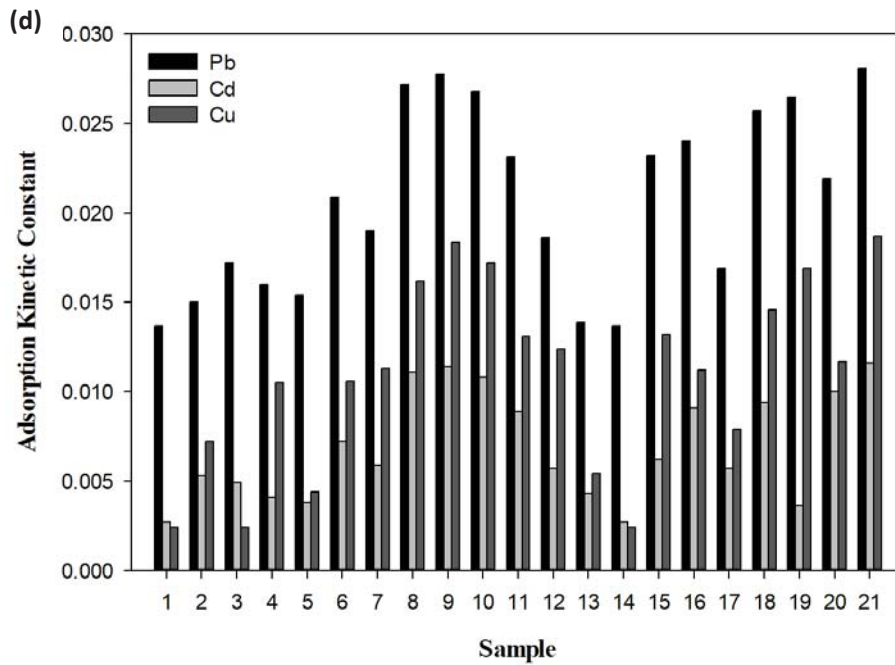
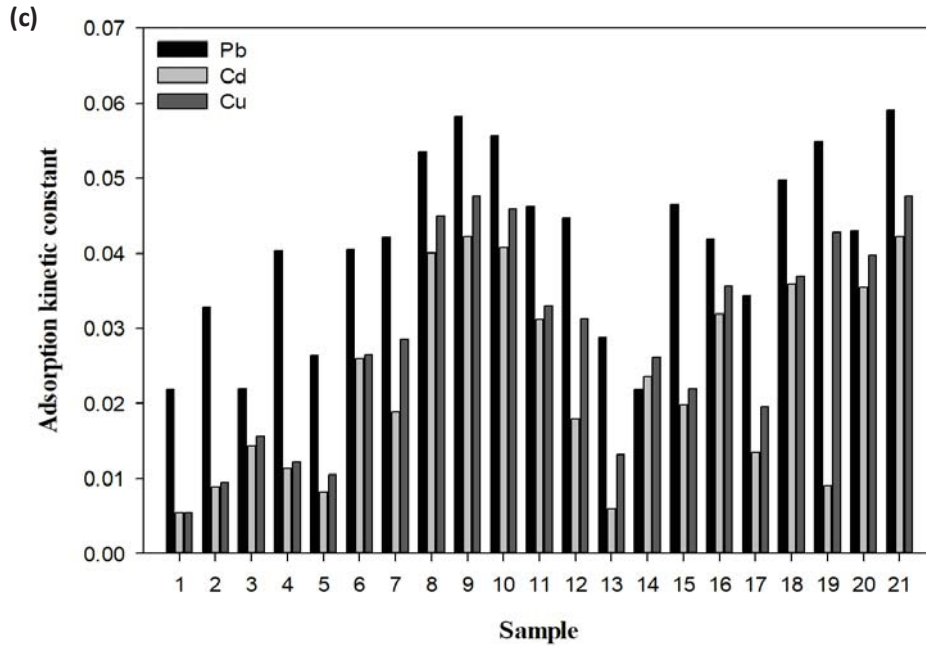


**Figure 8.1** Calculated  $k_2$  for the twenty one samples with initial metal ion concentration of: (a) 25 mg/L (b) 50 mg/L (c) 100 mg/L (d) 200 mg/L.

**Table 8.1** Comparison of  $k_2$  for  $Pb^{2+}$ ,  $Cu^{2+}$  and  $Cd^{2+}$  for different initial metal ion concentrations

Sample	Initial metal concentration			
	200 mg/L	100 mg/L	50 mg/L	25 mg/L
1	Pb > Cd > Cu	Pb > Cd > Cu	Pb > Cu > Cd	Pb > Cu > Cd
2	Pb > Cd > Cu	Pb > Cu > Cd	Pb > Cu > Cd	Pb > Cu > Cd
3	Pb > Cu > Cd	Pb > Cd > Cu	Pb > Cu > Cd	Pb > Cu > Cd
4	Pb > Cd > Cu	Pb > Cu > Cd	Pb > Cu > Cd	Pb > Cu > Cd
5	Pb > Cd > Cu	Pb > Cu > Cd	Pb > Cu > Cd	Pb > Cu > Cd
6	Pb > Cu > Cd	Pb > Cu > Cd	Pb > Cu > Cd	Pb > Cu > Cd
7	Pb > Cu > Cd	Pb > Cu > Cd	Pb > Cu > Cd	Pb > Cu > Cd
8	Pb > Cu > Cd	Pb > Cu > Cd	Pb > Cu > Cd	Pb > Cu > Cd
9	Pb > Cd > Cu	Pb > Cu > Cd	Pb > Cu > Cd	Pb > Cu > Cd
10	Pb > Cd > Cu	Pb > Cu > Cd	Pb > Cu > Cd	Pb > Cu > Cd
11	Pb > Cu > Cd	Pb > Cu > Cd	Pb > Cu > Cd	Pb > Cu > Cd
12	Pb > Cd > Cu	Pb > Cu > Cd	Pb > Cu > Cd	Pb > Cu > Cd
13	Pb > Cd > Cu	Pb > Cu > Cd	Pb > Cu > Cd	Pb > Cu > Cd
14	Pb > Cd > Cu	Pb > Cd > Cu	Cu > Cd > Pb	Pb > Cu > Cd
15	Pb > Cu > Cd	Pb > Cu > Cd	Pb > Cu > Cd	Pb > Cu > Cd
16	Pb > Cu > Cd	Pb > Cu > Cd	Pb > Cu > Cd	Pb > Cu > Cd
17	Pb > Cd > Cu	Pb > Cu > Cd	Pb > Cu > Cd	Pb > Cd > Cu
18	Pb > Cd > Cu	Pb > Cu > Cd	Pb > Cu > Cd	Pb > Cu > Cd
19	Pb > Cd > Cu	Pb > Cu > Cd	Pb > Cu > Cd	Pb > Cu > Cd
20	Pb > Cu > Cd	Pb > Cu > Cd	Pb > Cu > Cd	Pb > Cu > Cd
21	Pb > Cd > Cu	Pb > Cu > Cd	Pb > Cu > Cd	Pb > Cu > Cd



Rate series shown in Table 8.1 was derived for metal binding rate constants based on the  $k_2$  values. According to Figure 8.1 and Table 8.2, except for a few instances,  $k_2$  for  $Pb^{2+}$  remained the highest followed by the  $k_2$  values for  $Cu^{2+}$  and  $Cd^{2+}$ . Wan et al. (2014) had found similar observations for these metals using tea waste as the adsorbent suggesting that  $k_2$  for a given initial metal ion concentration in monometal systems follows the order of  $Pb^{2+} > Cu^{2+} > Cd^{2+}$ . It was noted that according to Section 7.3, sorption capacity also follows the same order ( $Pb^{2+} > Cu^{2+} > Cd^{2+}$ ). Figures 8.1 (a) and (b) for the two initial metal ion concentration ranges 25 mg/L and 50 mg/L, show that  $Pb^{2+}$  recorded the highest kinetic rate constant values for all the samples except for sample 14. From Figures 8.1 (c) and (d) for the initial metal ion concentration ranges 100 mg/L and 200 mg/L, respectively,  $Pb^{2+}$  recorded the highest kinetic rate constant values for all the samples. In this analysis, the rate for the metals were analysed in terms of their mass (mg/g/min). Considering the molar mass of these three metal ions, Pb has the highest molar mass of 207 g/mol. Molar mass of Cu and Cd is 63.5 mg/mol and 112 mg/mol, respectively. Accordingly, in the case of Pb, even if a smaller number of molecules are sorbed, the collective mass of Pb sorbed shows a relatively high value. Figure 8.2 shows the variation of  $k_2$  at different initial metal ion concentrations for  $Pb^{2+}$ ,  $Cu^{2+}$  and  $Cd^{2+}$ , separately. It can be observed that  $k_2$  values for  $Pb^{2+}$ ,  $Cu^{2+}$  and  $Cd^{2+}$  in most instances, decrease when the initial concentration of the solution is increased. Amarasinghe and Williams (2007) and Ebrahimian Pirbazari et al. (2014) reported similar observations in their analysis of  $k_2$  for different series of initial ion concentrations using biosorbents.

According to the pseudo second order model explained by Ho and McKay (1998) as illustrated in Equation 4.2 in Section 4.4, the initial sorption rate (h) of each biosorbent sample (expressed in  $mg\ g^{-1}\ min^{-1}$ ), is calculated when  $t$  approaches zero.

$$h = k_2 q_e^2 \quad \text{Equation 8.1}$$

Where  $k_2$  is pseudo second order kinetic constant and  $q_e$  is equilibrium sorption capacity.

Accordingly, it was observed that in all the instances, initial sorption rate (h) increased when the initial ion concentration was increased. At high concentrations, the difference between the metal ion concentration on the solid liquid interface and the metal ion concentration outside of the solution, which is the driving force for sorption, is high.

Thus, higher initial sorption rates are discernible at higher initial metal ion concentrations. According to past studies, a sorbent with higher initial sorption rate generally showed higher sorption affinity (Amarasinghe and Williams 2007). This is important in multi-metal systems in order to understand the affinities of different metal ions. Furthermore, higher the initial rate of sorption, higher the amount of metals that can be removed by sorption.

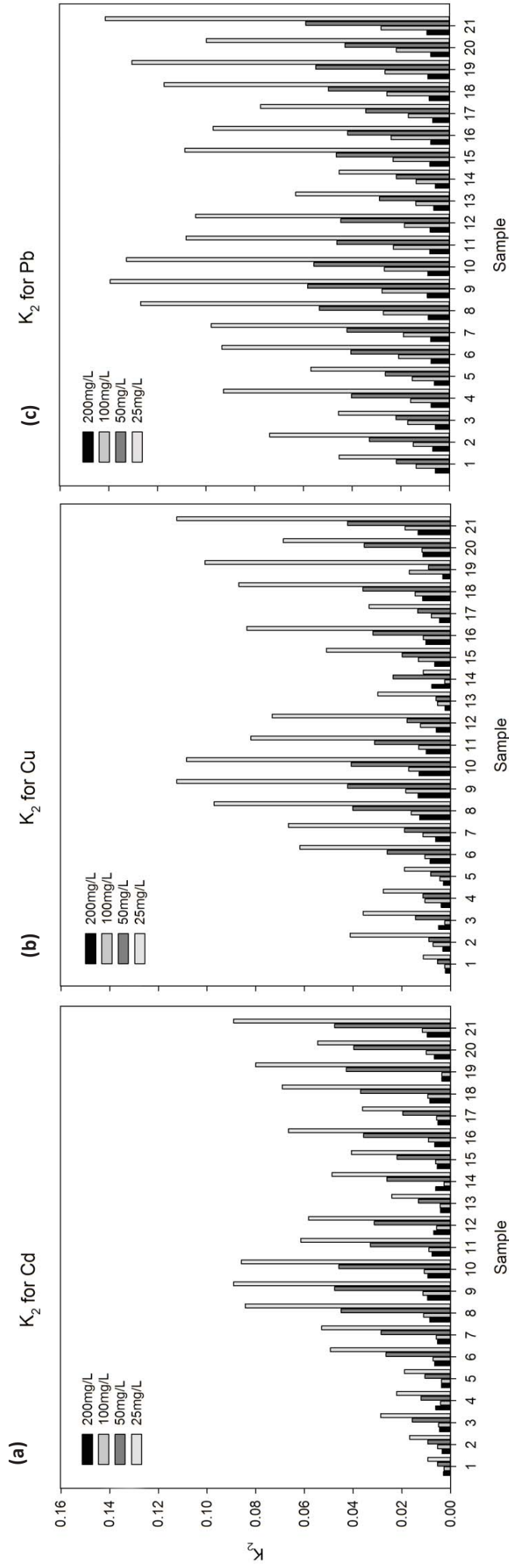
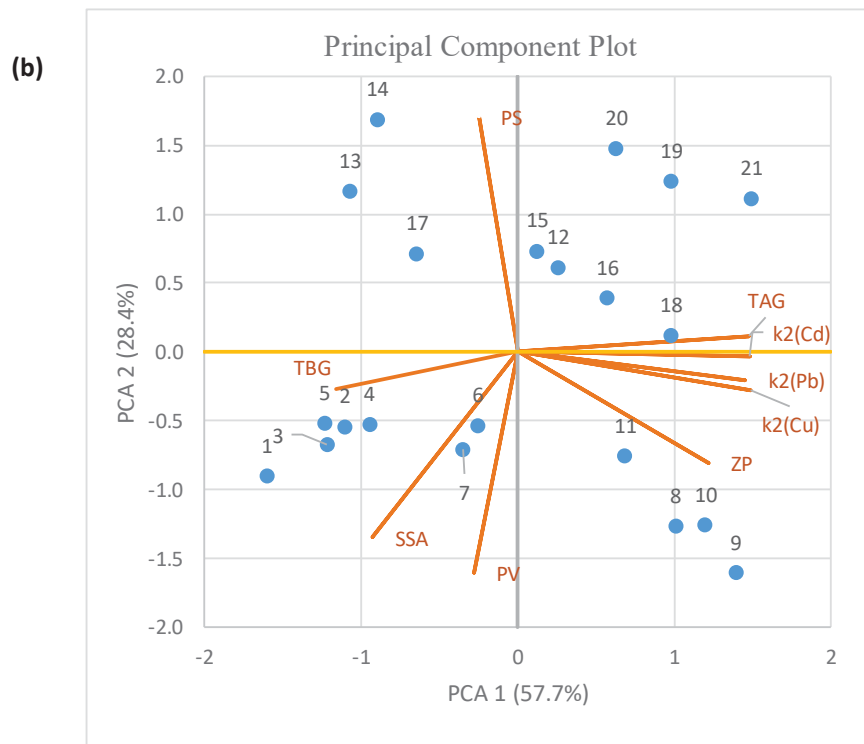
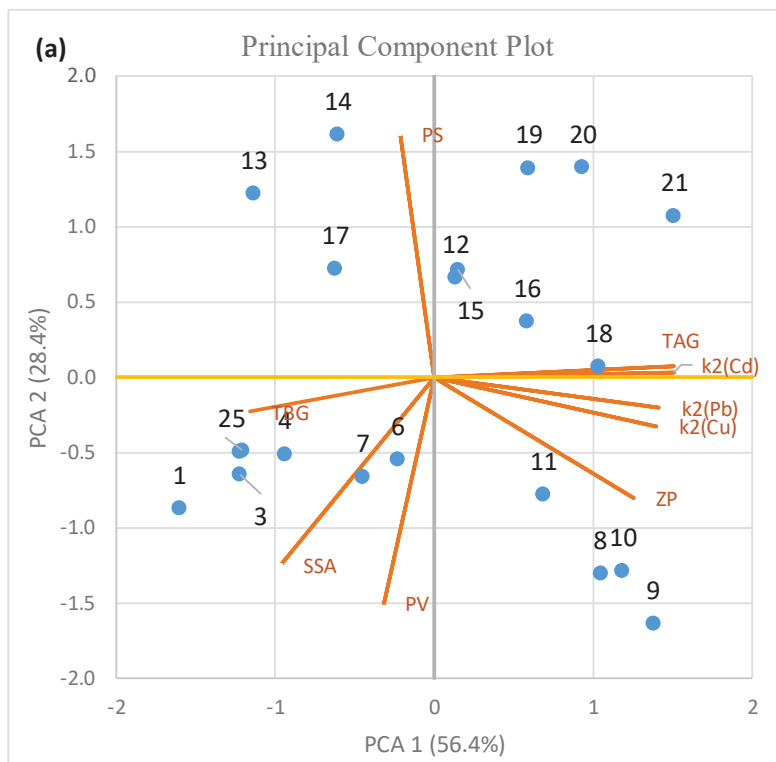


**Figure 8.2**  $k_2$  for the 21 samples with initial metal ion concentration of (a)  $Pb^{2+}$ , (b)  $Cu^{2+}$  and (c)  $Cd^{2+}$

### **8.3. QUALITATIVE RELATIONSHIPS BETWEEN PHYSICO-CHEMICAL PROPERTIES OF BIOSORBENTS AND PSEUDO SECOND ORDER KINETIC CONSTANTS ( $k_2$ )**

Four raw data matrices were generated for the statistical analysis. Each raw data matrix consisted of 21 biosorbent mixtures (objects) and 9 variables, i.e. pseudo second order rate constants ( $k_2$ ) for  $Pb^{2+}$ ,  $Cd^{2+}$  and  $Cu^{2+}$ , SSA, PS, PV, ZP, TAG and TBG. Since four different initial concentrations (200 mg/L, 100 mg/L, 50 mg/L and 25 mg/L) were used, four data matrices with a total of 84 objects were generated. The values of physico-chemical properties obtained for the 21 samples are given in Section 7.2.

Principal component analysis (PCA) was applied for each of the four solution concentrations separately. Data used for PCA was mean centered and standardised (auto scaled) in order to ensure that all the variables had equal weights in the analysis (Settle et al. 2007). Details of PCA is given in Section 4.3.3. The resulting biplots for each data matrix are given in Figures 8.3. The outcomes of the four biplots are comparable with similar relationships between vectors, suggesting that the initial concentration of metal ions do not exert a significant influence on the nature of the relationships between the variables.



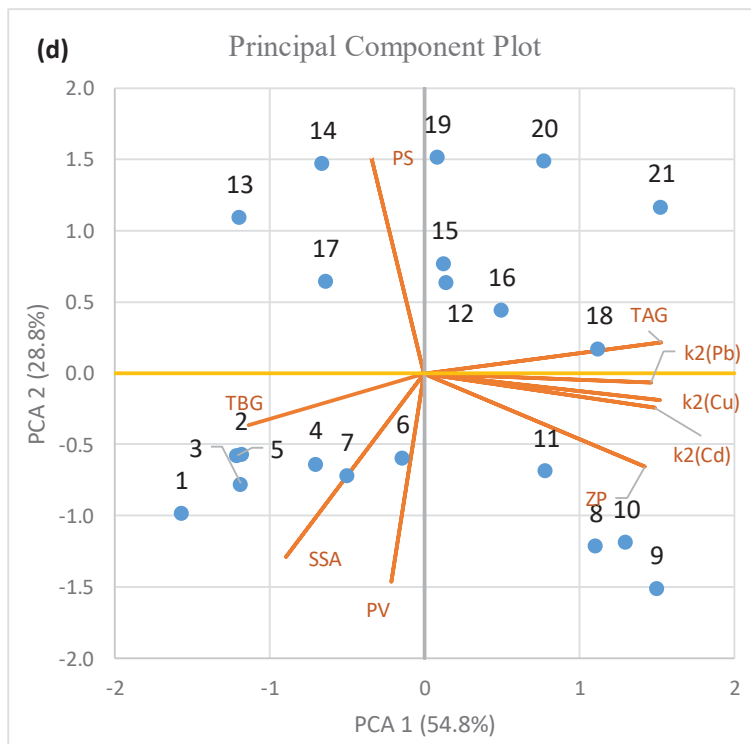
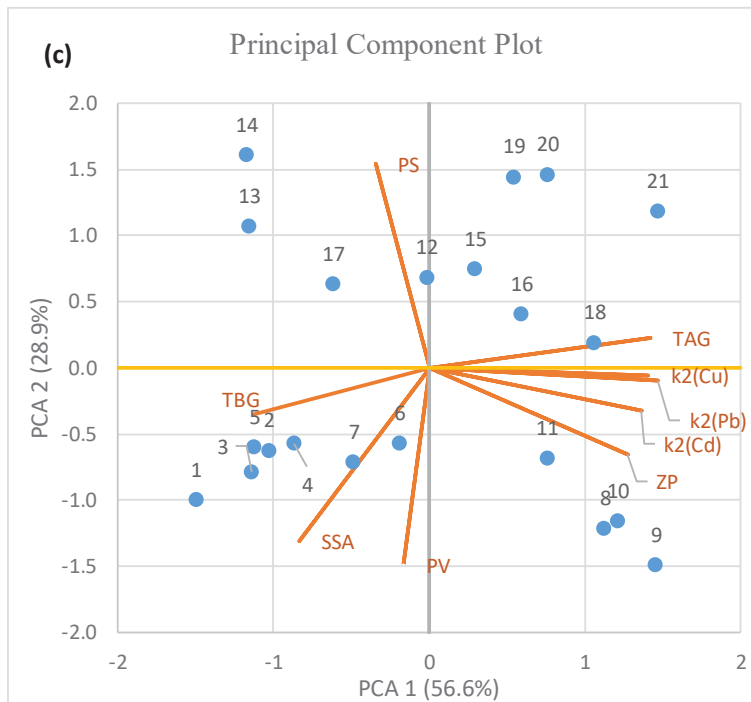


**Figure 8.3** PCA biplots for initial metal ion concentrations: **(a)** 25 mg/L **(b)** 50 mg/L **(c)** 100 mg/L and **(d)** 200 mg/L

**Note:** SSA specific surface area, PV pore volume, PS pore size, ZP zeta potential, TAG total acidic group and TBG total basic group)

The biplot depicted in Figure 8.3 (a) for 25 mg/L initial concentration shows that PC1 and PC2 collectively explain 86.1% of the total variance in the data matrix. The corresponding values for biplots for 50 mg/L, 100 mg/L and 200 mg/L are 84.8%, 85.5%, and 83.6%, respectively. Since these values were high, the outcomes from the biplots were considered reliable.

As illustrated in Figure 8.3 (a), vectors related to variables  $\text{Pb}^{2+}$ ,  $\text{Cd}^{2+}$  and  $\text{Cu}^{2+}$  are acute, implying the similarity of reaction mechanisms related to the three metals. The high correlation between the vectors corresponding to the variables  $\text{Pb}^{2+}$ ,  $\text{Cd}^{2+}$ ,  $\text{Cu}^{2+}$ , TAG and ZP implied by the acute angles suggests that the acidic functional groups acts as binding sites to immobilise these heavy metals either through electrostatic interactions or through exchange of electrons to form complexes (Wang et al. 2007). Therefore, it can be concluded that metal sorption reaction rates increase with increasing concentrations of acidic functional groups. When the concentration of acidic functional groups is high in a material, the competition between ions for active sites decreases and the rate of sorption increases. Zeta potential provides an indication of surface negativity, which is important for cation sorption. A high ZP value is favourable for the attraction between the negatively charged biosorbent surface and cations (Jacobasch et al. 1998).

TBG shows obtuse angles with vectors related to  $\text{Pb}^{2+}$ ,  $\text{Cd}^{2+}$  and  $\text{Cu}^{2+}$ , implying significant inverse correlations. This suggests that electrostatic repulsion caused by these basic functional groups weakens the sorption forces of positively charged metal ions and negatively affects the rate of the reaction. SSA also shows obtuse angles with vectors related to  $\text{Pb}^{2+}$ ,  $\text{Cd}^{2+}$  and  $\text{Cu}^{2+}$ , suggesting strong negative correlations. This indicates that high SSA could reduce sorption rates. Since high surface area is generally due to the micropore structure (Largitte and Pasquier 2016), the metals may take some time to diffuse inside the intraparticle structures and get adsorbed to the active sites, resulting in slower rates.

Vectors related to PS and PV do not have a significant correlation with reaction rates. PV demonstrates a high correlation with SSA as the angles between the corresponding vectors are acute. This could be due to the fact that surface area values can also be obtained from the method known as BJH Desorption cumulative surface area (Barrett et al. 1951). The surface area values obtained from this method are closely related to SSA values used in the study (via the BET method). However, BJH Desorption

cumulative surface area values can also be expressed as a function of PS and PV, causing the high correlation observed. An obtuse angle is seen between PS and PV, implying a negative relationship. The direction of the relationship between PS and PV is governed by the nature of pore distribution on the surface (Bose et al. 2003). No significant clustering of objects is evident in any of the biplots.

#### **8.4 MATHEMATICAL REPLICATION OF SORPTION KINETICS**

Mathematical replication of sorption kinetics was performed to facilitate the prediction of  $k_2$ . Such predictions are essential for estimating the rate of metal sorption in designing biosorbent treatment systems. Before this step, multicollinearity analysis of the independent variables was done using variance inflation factor (VIF) calculation with the objective of eliminating variables which are highly correlated with each other. VIF uses the variables for least squares regression analysis to quantify the severity of multicollinearity by estimating how much the variance of a regression coefficient is inflated. Including variables with VIF values above 10 in statistical modelling could have an adverse impact on the results (O'brien 2007). VIF values were found to be below 10 for all the independent variables.

As the next step, detection of outliers was carried out using a multivariate modelling approach with the calculation of Mahalanobis distance (Mahalanobis 1936), which measures the distance between a specific data point and the mean of a multidimensional data distribution in units of standard deviation. The distance approaches zero when the specific data point comes closer to the mean of the distribution in question and grows when the data point moves away from the mean of the distribution along each principal component axis. It is a unitless and scale-invariant measurement which takes into account the correlations of the data set and is frequently used to detect outliers in the development of linear regression models. 0.95 was considered as the threshold value for the present study. Objects scoring higher values were excluded from the subsequent modelling. Figure 8.4 indicates that objects 82 and 84 (sample number 19 and 21 for 200 mg/L initial concentration) was above the threshold value. These were excluded from the subsequent statistical modelling.



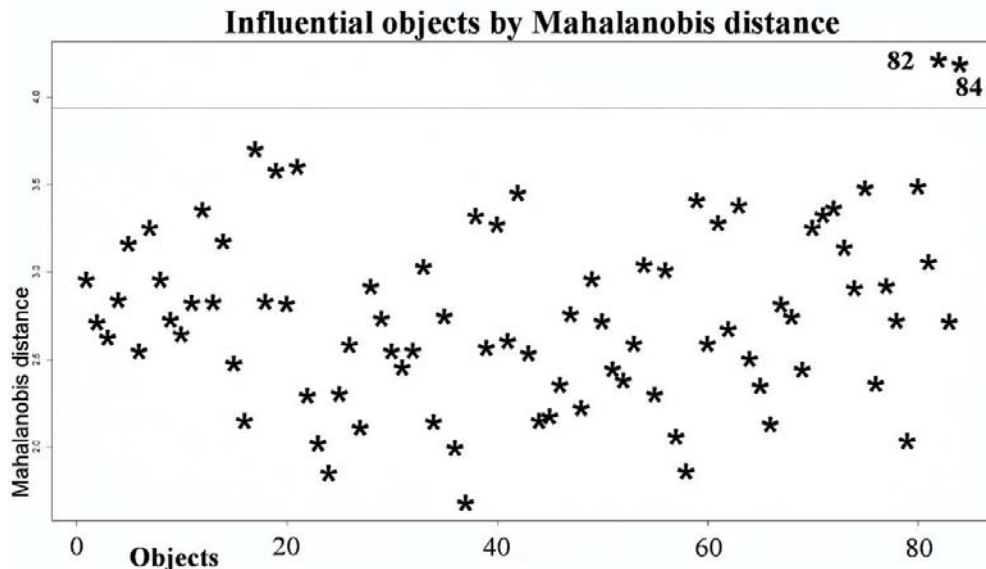


**Figure 8.4** Mahalanobis distance values scored by individual objects. Threshold value (straight horizontal line) at 0.95

#### 8.4.1. Initial and subsequent model development

Partial least squares regression (PLS) was employed to formulate mathematical models to understand the relationships between the independent variables and  $k_2$  of  $Pb^{2+}$ ,  $Cd^{2+}$  and  $Cu^{2+}$ . PLS is a popular multivariate data analytical technique with a combination of features from PCA and multiple linear regression. It aims to predict dependent variables (responses) from independent variables (predictors) by the extraction of a set of orthogonal factors called latent variables having the best predictive powers (Abdi and Williams 2010b). The efficiency and accuracy of the predictions obtained is commonly evaluated with cross-validation techniques such as bootstrapping and repeated k-fold cross validation. For the present study, repeated k-fold cross validation was utilized for extracting the optimal number of components to be retained in the PLS models.

Once the appropriate number of components to be retained was chosen, PLS models were developed. Assessment of statistical significance of the explanatory variables along with uncertainty quantification was carried out as the next step using non-parametric bootstrap resampling of the regression coefficients (Section 8.4.2). Variables with lower levels of statistical significance in terms of model contribution

were removed and subsequent PLS modelling was done with the remaining parameters. After that, quantification of uncertainty was repeated using the same bootstrap validation to detect any possible improvements. R software (Ver. 3.5.1) with RStudio was employed for the data analysis and the specific packages with codes are given in the Appendix A3. Figure 8.5 outlines the main steps of the statistical analysis employed.

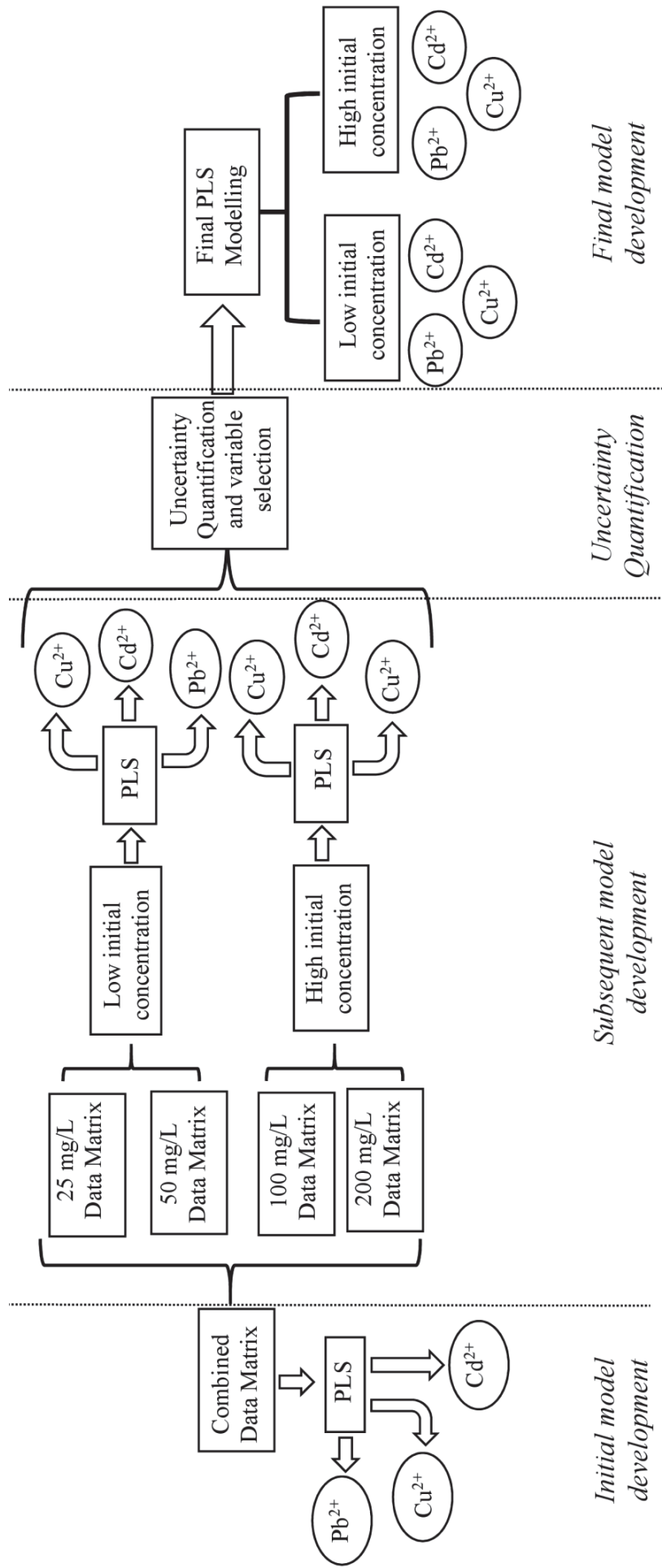


**Figure 8.5** Main steps of the statistical analysis

For the initial model development, the four data matrices were combined to form a single data matrix consisting of 82 (with two objects removed as discussed above) objects on which, PLS was performed. The initial metal ion concentration was considered as a separate numerical variable. Accordingly, seven independent variables were available for each of the metal cations.

It was decided to develop one model for each metal ion ( $\text{Pb}^{2+}$ ,  $\text{Cd}^{2+}$  and  $\text{Cu}^{2+}$ ). Repeated k-fold cross-validation was employed with  $k=5$  (100 repeats) for extracting the optimal number of components to be retained for each PLS model. Lowest root mean square error (RMSE) was the criteria used for the determination of the optimal number of components to be retained. Orthogonal scores algorithm (the NIPALS algorithm) was used for fitting the data. RMSE, R-squared ( $R^2$ ) and mean absolute error (MAE) were the parameters used for the comparison of the models. Table 8.2 illustrates the model factors obtained for the three initial models.

**Table 8.2** PLS regression parameters for the initial models to predict  $k_2$

<b>Rate constant</b>	<b>Number of Components</b>	<b>RMSE</b>	<b>R-squared</b>	<b>MAE</b>
$k_2(\text{Pb}^{2+})$	2	0.02369	0.615574	0.02016
$k_2(\text{Cd}^{2+})$	3	0.01568	0.595517	0.01238
$k_2(\text{Cu}^{2+})$	3	0.02046	0.522029	0.01642

The  $R^2$  values ranged between 0.522 and 0.616 and these were comparatively low values. One possible reason for this could be the influence of the initial metal ion concentration. To investigate this possibility further, it was decided to group the objects based on the initial concentration of metal ions and plot them on a single PCA scatterplot to see if there was a significant difference in object distribution in the multivariate space. The grouping of the objects was carried out based on the initial concentration of metal ions where objects with initial concentrations of 200 mg/L and 100 mg/L were grouped as ‘high concentration’, while those with 50 mg/L and 25 mg/L were grouped as ‘low concentration’. The resulting scatterplot is shown in Figure 8.6.

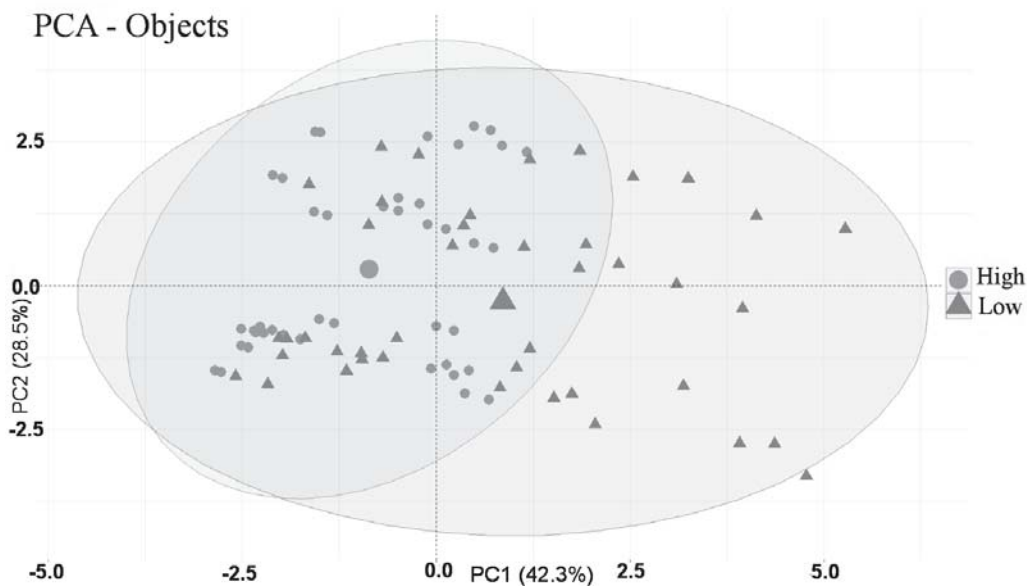


**Figure 8.6** Biplot of PCA with individual objects grouped into high (200 mg/L and 100 mg/L) and low (50 mg/L and 25 mg/L) initial concentrations.

Figure 8.6 shows that the variation of data is different for the two groups with higher scattering of objects visible in the lower initial concentrations group. This implies that the samples display different behaviour in terms of sorption kinetics when different initial concentrations are used. Rate constant is related to the rate of sorption according to Equation 4.3. Variation of equilibrium sorption capacity at higher concentrations is low as the sorbent is approaching saturation (Worch 2012). Hence, the rates of sorption at higher concentrations do not show much variation among the different concentrations. However, at lower concentrations, as the sorbent is not completely exhausted with active sites still available, the influence of concentration on sorption would be high. Therefore, developing two separate predictive models for these two groups of objects could yield better predictability and greater accuracy. Based on this assumption, subsequent model development was carried out by applying PLS separately for high and low initial concentrations of each metal ion. Accordingly, six new PLS models were developed using the same statistical principles as before and the model results are given in Table 8.3.

**Table 8.3** PLS regression parameters for the subsequent models of  $k_2$ 

Rate constant	Concentration	Number of Components	RMSE	R-squared	MAE
$k_2(\text{Pb}^{2+})$	Low	3	0.0147	0.8418	0.0122
	High	3	0.0025	0.8988	0.0022
$k_2(\text{Cd}^{2+})$	Low	4	0.0100	0.8477	0.0085
	High	4	0.0012	0.8105	0.0010
$k_2(\text{Cu}^{2+})$	Low	3	0.0157	0.7885	0.0130
	High	3	0.0022	0.8111	0.0016

$R^2$ , RMSE and MAE values were used to compare these six models with the previous three models given in Table 8.2.  $R^2$  values of all the six models were above 0.788 implying relatively high accuracy. Both, RMSE and MAE values showed significant improvements, which shows that the models are reliable. Since the scattering of data is lower for the high initial concentration group (Figure 8.6), the three models built for the high initial concentration group were seen to be having better RMSE and MAE values compared to those built for the low initial concentration group.

Although the initial objective was to develop a single predictive model for each of the metal ions, the improvement in model parameters evident in Table 8.3 justified developing two models for each metal ion based on the initial concentration; one for initial concentrations below 100 mg/L and the another for concentrations between 100 mg/L and 200 mg/L. As the next step, the statistical significance of the explanatory variables was assessed along with the uncertainty analysis.

#### **8.4.2. Uncertainty quantification and final model development**

Generally, two types of uncertainties can influence the outcomes of modelling any physical process. These are the uncertainty inherent to the processes in question and uncertainty in process modelling (Loucks and Van Beek 2017; Wijesiri et al. 2016; Zoppou 2001). Uncertainty arising from the intrinsic variability of the process is known as aleatory uncertainty (Der Kiureghian and Ditlevsen 2009) and cannot be reduced or eliminated due to its intrinsic nature (Ross et al. 2009). Modelling

uncertainty (epistemic uncertainty) arises from a variety of sources such as simplified or inaccurately conceptualised models, model structural deficiencies, input data and calibration data (Hofer et al. 2002). Modelling uncertainty is generally attributed to limited data and the knowledge regarding the process under investigation.

Modelling uncertainty can be expressed via confidence intervals, the width of which increases with increasing uncertainty. For the present study, only the modelling uncertainty was assessed via confidence interval estimation. The bootstrap resampling proposed by Efron (1979) was employed for this purpose where the distribution of a given statistic is inferred from the available data by generating many samples from the original sample using Monte Carlo simulations (Efron 1979). Among several bootstrap methods, non-parametric resampling was the method utilized for the present study. In non-parametric resampling, the bootstrap samples are constructed using resampling with replacement from the original sample (Efron and Tibshirani 1986). This method allows effective utilization of a limited number of samples to estimate the confidence interval of uncertainty without further sampling or the necessity of the assumption of normality (Carpenter and Bithell 2000).

After the bootstrap samples are obtained, a number of techniques exist for constructing confidence intervals from them. Among these are the percentile bootstrap, the bias-corrected bootstrap, the bias-corrected and accelerated (BCa) bootstrap and the standard (normal) bootstrap (Carpenter and Bithell 2000). In order to improve the coverage accuracy of the confidence intervals, BCa intervals, proposed in Efron and Tibshirani (1993) were used for the study. BCa confidence intervals are considered to be highly accurate as they automatically take into account the shape (in terms of skewness and kurtosis) and the bias of the distribution (Efron and Tibshirani 1993).

Accordingly, non-parametric bootstrapping was performed (1000 permutations) on standardised regression coefficients of the six models and 95% BCa confidence intervals were plotted. Figures 8.7, 8.8 and 8.9 illustrates the BCa confidence intervals in continuous lines for the high initial concentrations group. The figures for the low initial concentrations group are Figures 8.10, 8.11 and 8.12.

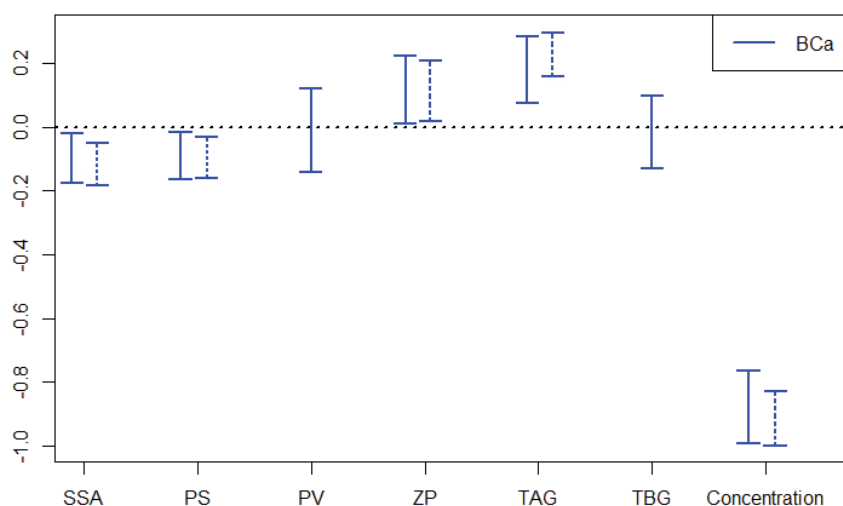


**Figure 8.7** 95% Confidence intervals for standardised regression coefficients of the models built for  $Pb^{2+}$  in high initial concentrations; when all variables were used for modelling (continuous line) and when PV and TBG were removed (dotted line)

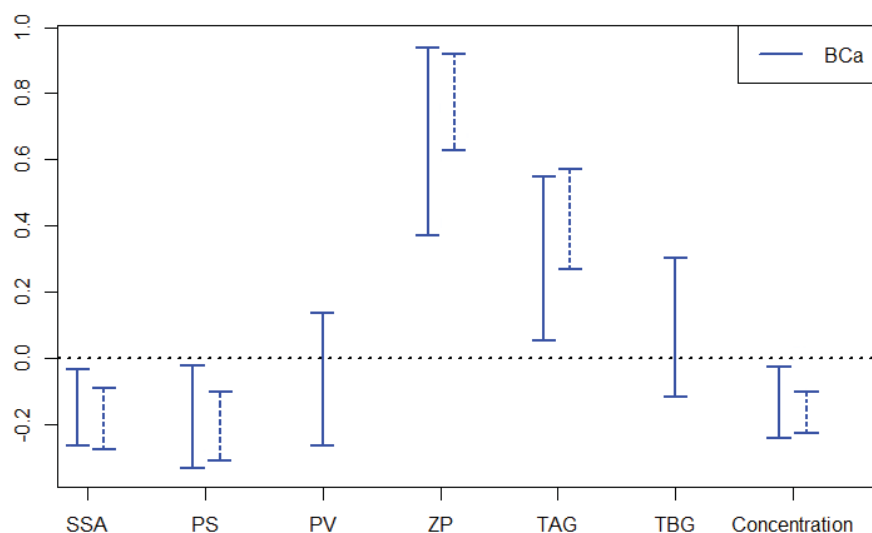


**Figure 8.8** 95% Confidence intervals for standardised regression coefficients of the models built for  $Cd^{2+}$  in high initial concentrations; when all variables were used for modelling (continuous line) and when PV and TBG were removed (dotted line)



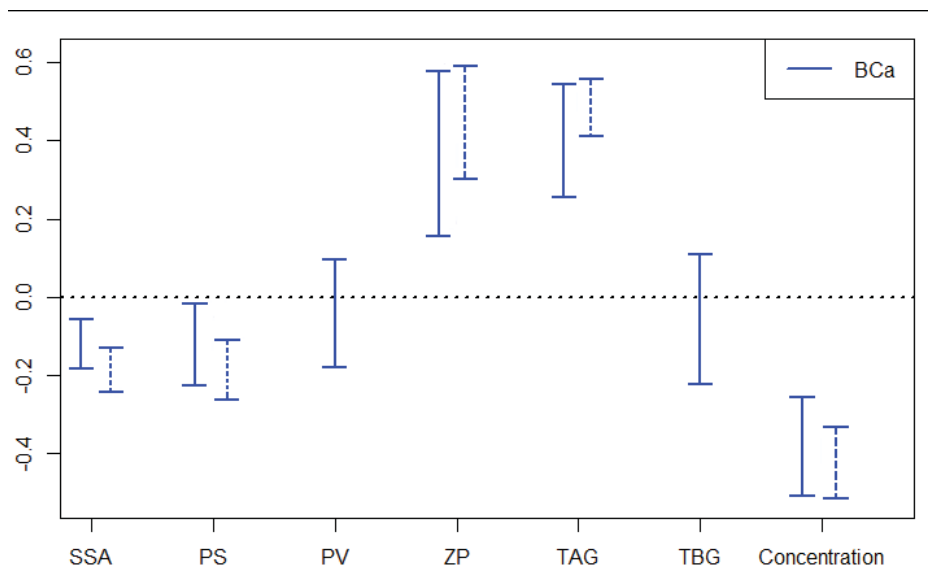


**Figure 8.9** 95% Confidence intervals for standardised regression coefficients of the models built for  $\text{Cu}^{2+}$  in high initial concentrations; when all variables were used for modelling (continuous line) and when PV and TBG were removed (dotted line)

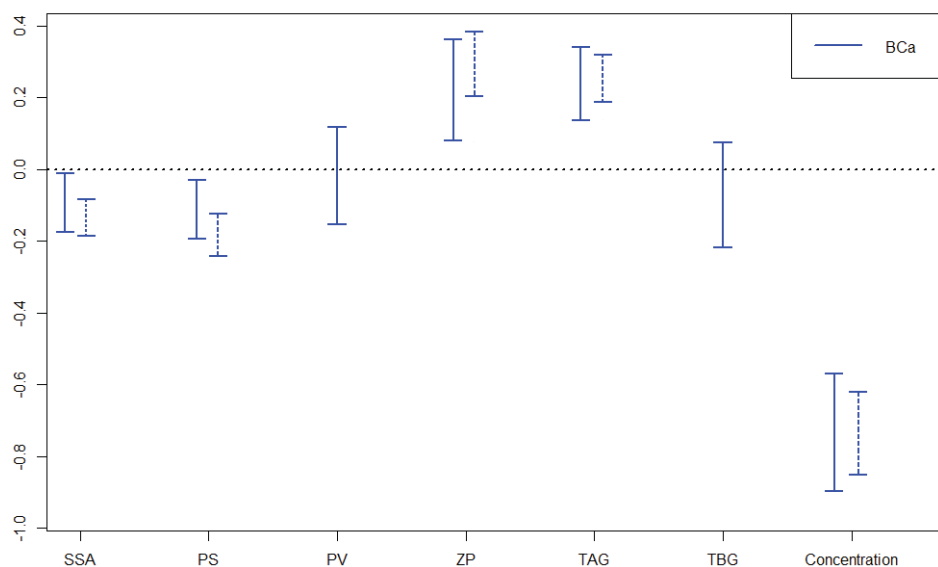


**Figure 8.10** 95% Confidence intervals for standardised regression coefficients of the models built for  $\text{Pb}^{2+}$  in low initial concentrations; when all variables were used for modelling (continuous line) and when PV and TBG were removed (dotted line)

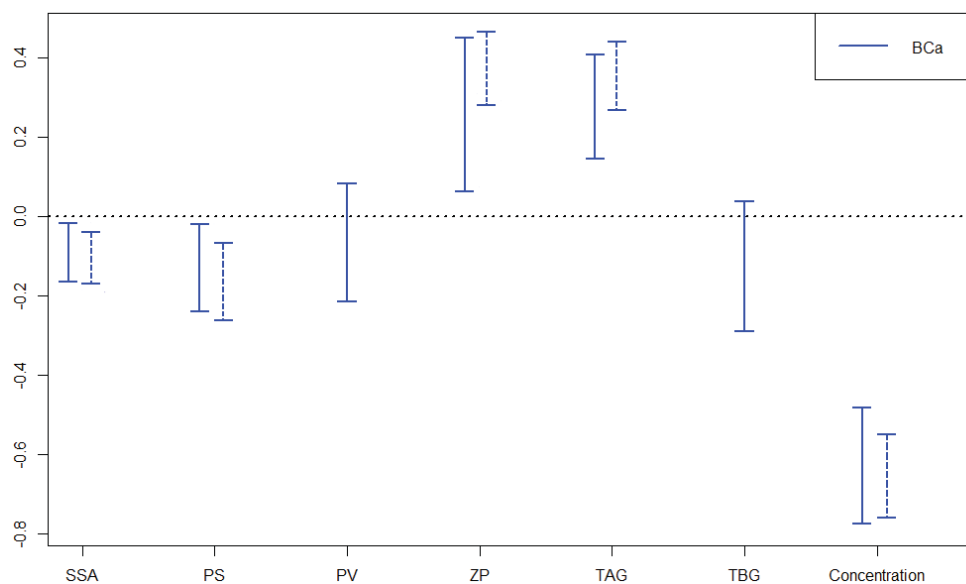


**Figure 8.11** 95% Confidence intervals for standardised regression coefficients of the models built for  $\text{Cd}^{2+}$  in low initial concentrations; when all variables were used for modelling (continuous line) and when PV and TBG were removed (dotted line)

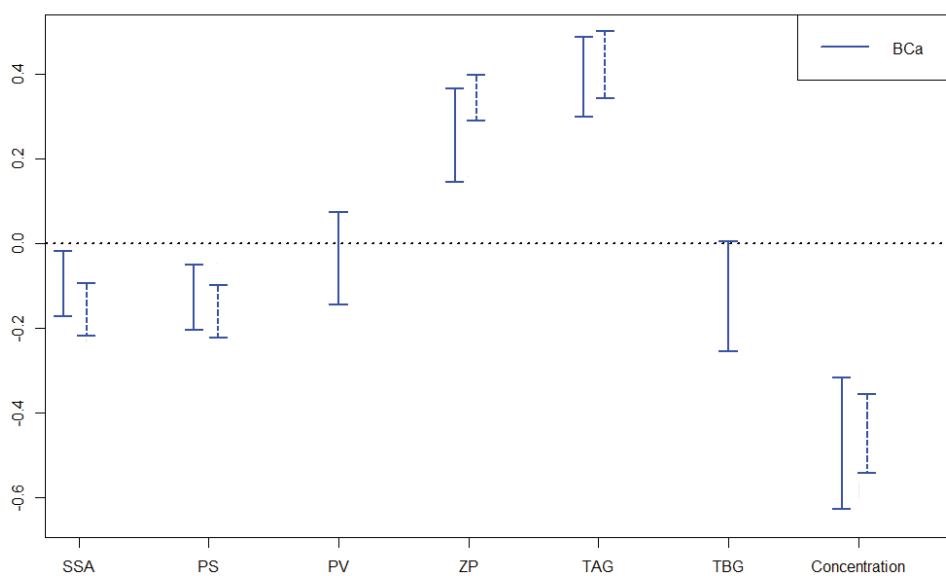


**Figure 8.12** 95% Confidence intervals for standardised regression coefficients of the models built for  $\text{Cu}^{2+}$  in low initial concentrations; when all variables were used for modelling (continuous line) and when PV and TBG were removed (dotted line)

The 95% BCa confidence intervals for all six models indicated that the significance of PV and TBG as independent variables was close to zero in influencing model outcomes. Therefore, the coefficients related to PV and TBG were not considered to be statistically significant and these two variables were removed from the final modelling.

The final six PLS models were constructed accordingly with the remaining five parameters using the same statistical principles as before. Their BCa confidence intervals were plotted again as explained above in order to investigate any improvement in modelling uncertainty. Figures 8.7, 8.8 and 8.9 illustrate the BCa confidence intervals of the high initial concentration group in dotted lines. Figures 8.10, 8.11 and 8.12 shows the BCa confidence intervals of the low initial concentration group in dotted lines. Table 8.4 gives the factors for the final models. Regression coefficients of the final models are provided in Table 8.5.

**Table 8.4** PLS regression parameters of the final models to predict  $k_2$

<b>Rate constant</b>	<b>Concentration</b>	<b>Number of Components</b>	<b>RMSE</b>	<b>R-squared</b>	<b>MAE</b>
$k_2(\text{Pb}^{2+})$	Low	2	0.0141	0.8546	0.0116
	High	2	0.0025	0.9038	0.0021
$k_2(\text{Cd}^{2+})$	Low	4	0.0096	0.8554	0.0082
	High	4	0.0013	0.8158	0.0009
$k_2(\text{Cu}^{2+})$	Low	2	0.0153	0.7987	0.0126
	High	2	0.0022	0.8220	0.0016

**Table 8.5** PLS regression coefficients for the predictor variable ( $k_2$ )

Rate constant	Initial concentration	Intercept	SSA	PS	ZP	TAG	Concentration
$k_2(\text{Pb}^{2+})$	Low	6.1968E-02	-6.8643E-05	-3.6496E-04	1.9109E-03	1.2578E-02	-2.1604E-03
	High	2.2806E-02	-1.0503E-05	-6.9026E-05	2.4838E-04	1.9745E-03	-1.3059E-04
$k_2(\text{Cd}^{2+})$	Low	5.5108E-03	-7.6191E-05	-2.1534E-04	1.3879E-03	1.3352E-02	-9.5914E-04
	High	-4.2419E-03	-7.1660E-06	-5.4914E-05	2.6388E-04	1.3015E-03	-3.3640E-06
$k_2(\text{Cu}^{2+})$	Low	5.5108E-03	-7.6190E-05	-2.1534E-04	1.3879E-03	1.3352E-02	-9.5914E-04
	High	-5.8252E-03	-1.3396E-05	-7.8559E-05	4.4071E-04	2.6130E-03	-3.3691E-05

**Note:** Units used for each of the variables are as follows; SSA= $\text{m}^2/\text{g}$ , TAG= $\text{mmol}/\text{g}$ , PS= $\text{\AA}$ , PV= $\text{cm}^3/\text{g}$ , ZP= $\text{mV}$ , concentration= $\text{mg}/\text{L}$ ,  $K_2= \text{g}\cdot\text{mg}^{-1}\cdot\text{min}^{-1}$

$R^2$ , RMSE and MAE values were used to compare the models in Tables 8.3 and 8.4. The final six models showed minor improvements in all the model parameters when compared with the previous six models. Since the improvements were slight, the Akaike's Information Criterion (AIC) was used as evidence in selecting the best models. AIC is an estimate of model parsimony which aims to resolve the trade-off between model fit and model complexity, to achieve the best predictive ability. The model with the lowest AIC is considered to be the most parsimonious while an improvement of greater than 2 is considered significant (Anderson et al. 1998; Burnham and Anderson 2004). Table 8.6 gives the AIC values for the 12 models and the models with PV and TBG removed.

**Table 8.6** Akaike's Information Criterion (AIC) of the models developed to predict  $k_2$  using physico-chemical properties and metal ion concentration

Rate constant	Concentration	AIC	
		With All independent variables	After removing PV and TBG
$k_2(\text{Pb}^{2+})$	Low	42.80	35.92
	High	26.14	19.12
$k_2(\text{Cd}^{2+})$	Low	49.19	38.60
	High	58.27	46.19
$k_2(\text{Cu}^{2+})$	Low	54.67	49.21
	High	65.37	50.21

A similar comparison was made between 95% BCa confidence intervals of the regression coefficients between the models. Figures 8.7 to 8.12 allow visual comparison between BCa confidence intervals of the regression coefficients for all the models. The removal of PV and TBG as independent variables had resulted in narrowing of the confidence intervals obtained for the new models implying a reduction in modelling uncertainty. Confidence intervals of some of the variables had shifted slightly further from zero implying an increase in statistical significance of the relevant coefficients.

Although the improvements in model factors (Tables 8.4 and 8.5) were too low to be considered statistically significant, it was possible to build the final six models with a

lesser number of variables with improved modelling uncertainty. Therefore, it was concluded that the final models with only five independent variables had higher precision and better predictability. It was also concluded that the inclusion of PV and TBG as variables was not necessary to build PLS prediction models for kinetic rate constants. Since the sample size was relatively small, only internal validation of the models was done. However, external validation of these models could assess their generalisability and this could serve as a topic for future research. Codes and packages used for the calculations are provided in Appendix A3.

## 8.5. SUMMARY OF KEY FINDINGS

The study was conducted to develop predictive models to estimate pseudo second order kinetic rate constants ( $k_2$ ) for three divalent heavy metals ( $\text{Pb}^{2+}$ ,  $\text{Cd}^{2+}$  and  $\text{Cu}^{2+}$ ) using surface physico-chemical properties of biosorbent mixtures of tea factory waste and coconut shell biochar. These mixtures contained sufficient variability of physico-chemical properties to consider them as different biosorbents. The study outcomes confirmed that:

- Reaction mechanisms explained by the kinetics related to  $\text{Pb}^{2+}$ ,  $\text{Cd}^{2+}$  and  $\text{Cu}^{2+}$  have similar relationships to physico-chemical properties of biosorbents. The nature of these relationships remained unchanged within the range of initial metal ion concentration analysed.
- The above observation suggests that the proposed equations can be used to design and optimise mixtures of biosorbents to remove the three metal cations.
- Acidic surface functional groups can increase reaction rates. Among other physico-chemical properties, its influence is prominent in relation to sorption mechanisms.
- High specific surface area with micropore structures can reduce the sorption rate as metals need to diffuse into intraparticle structures to meet active sites.
- Reliability and accuracy of the predictive models are significantly improved when separate models are developed for two ranges of initial metal ion concentrations; 0 mg/L - 100 mg/L and 100 mg/L - 200 mg/L.
- Pore volume and total basic groups as independent variables did not contribute significantly to the development of the predictive models.

This page intentionally left blank.

# CHAPTER 9: TRANSFERABILITY OF DATA BETWEEN BATCH AND COLUMN STUDIES

---

## 9.1 INTRODUCTION

Effectiveness of a sorbent for the removal of heavy metals is primarily assessed by sorption capacity and sorption kinetics, which mainly depend on the material physico-chemical properties. Hence, the investigation of the influence of sorbent physico-chemical properties on sorption capacity and kinetics is imperative to understand the effectiveness of a sorbent. Chapter 7 discussed the influence of sorbent physico-chemical properties on sorption capacity of biosorbents where the variation of physico-chemical properties was achieved using twenty one biosorbent samples. Chapter 8 investigated the influence of physico-chemical properties of biosorbents on sorption kinetics utilizing the pseudo second order kinetic model. Outcomes of Chapter 7 and 8 provided an improved understanding of the influence of sorbent physico-chemical properties on sorption capacity and sorption kinetics. The analysis undertaken in Chapters 7 and 8 was based on batch experiments which is commonly used to analyse the efficiency of sorbents in adsorbing a sorbate. However, it is noted that laboratory columns are widely used for investigating industrial applications of sorbents since industrial-scale sorption columns can be designed by scaling up the designed laboratory columns. As discussed in Section 3.7.1, continuous fixed bed columns were used in this study to replicate the practical application of an adsorption system (henceforth referred as column/s).

As discussed in Section 3.7.1, during the sorption process, the mass transfer zone (MTZ) is gradually displaced along the column. As long as MTZ does not reach the column outlet, the outlet concentration ( $C$ ) is maintained at Zero ( $C=0$ ). The adsorbate appears in the column outlet for the first time when the MTZ reaches the end of the sorbent bed. The time taken for this to happen is referred to as breakthrough time (BT). Determination of experimental breakthrough curve and identification of BT in a laboratory setting is necessary to verify the applicability of the chosen sorption system (Patel 2019). This approach requires a considerable amount of laboratory space and time. In order to calculate an accurate value for BT, running several trials based on the particular sorbate and sorbent system is essential. The batch approach, on the other



hand, does not require much laboratory space and can easily provide information on sorption equilibrium characteristics and sorption kinetics.

The aim of this chapter was to identify the batch sorption parameters that has the capacity to generate an acceptable relationship with BT in a column sorption setting and to present predictive models to calculate column BT for the three selected divalent heavy metals. These mathematical models can be used to predict laboratory BT values using parameters obtained via batch experiments. This exercise is useful as BT values, which are used for the design of industrial sorption columns, can be estimated using batch studies consuming fewer laboratory resources. This can be considered as a preliminary step for the design of industrial-scale columns.

## 9.2 DETERMINING BREAKTHROUGH TIME

Determination of the breakthrough time using breakthrough curve (time vs outlet concentration) for  $\text{Pb}^{2+}$  for sample 1 is shown in Figure 9.1. Time when the outlet concentration of  $\text{Pb}^{2+}$ ,  $\text{Cu}^{2+}$  and  $\text{Cd}^{2+}$  reached  $0.1 C_0$  ( $C_0$  is the initial metal ion concentration) was considered as the breakthrough time for the analysis (Bulgariu and Bulgariu 2013). BT values obtained for the twenty-one biosorbent samples generated for the column experimental setup explained in Section 4.3.3, for the sorption of  $\text{Pb}^{2+}$ ,  $\text{Cu}^{2+}$  and  $\text{Cd}^{2+}$  at 200 mg/L initial metal ion concentration are given in Table 9.1.

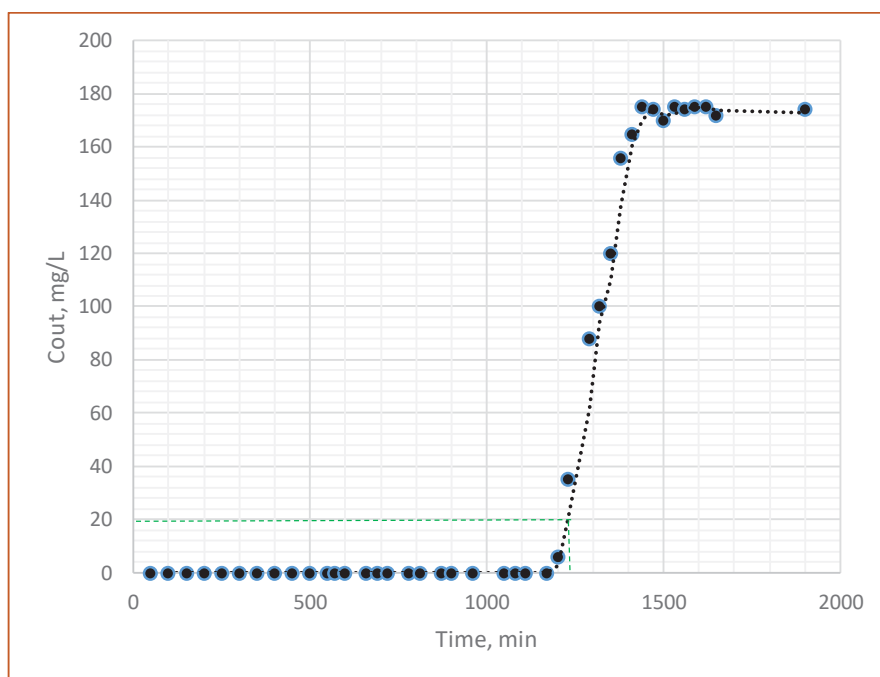


**Figure 9.1** Determination of breakthrough point for  $\text{Pb}^{2+}$  at 200 mg/L for sample 1

**Table 9.1** Breakthrough time obtained from column experiments for  $\text{Pb}^{2+}$ ,  $\text{Cu}^{2+}$  and  $\text{Cd}^{2+}$  at 200 mg/L initial metal ion concentration

Sample	Breakthrough time, min		
	BT( Pb)	BT (Cu)	BT (Cd)
1	1220	560	410
2	1290	620	420
3	1070	760	420
4	1510	1060	450
5	1350	660	420
6	1850	1180	430
7	1900	1280	420
8	1850	1600	450

<b>Breakthrough time, min</b>			
<b>Sample</b>	<b>BT( Pb)</b>	<b>BT (Cu)</b>	<b>BT (Cd)</b>
9	2540	1560	490
10	2170	1420	450
11	2110	1480	470
12	1750	1260	450
13	1650	700	400
14	1410	780	410
15	1630	1120	430
16	1950	1340	430
17	1520	580	420
18	1680	840	450
19	1870	600	430
20	1700	910	440
21	1820	1300	480

### **9.3 PREDICTING THE BREAKTHROUGH TIME USING BATCH PARAMETERS.**

In order to transfer experimental data from a batch system to a column sorption system, it is imperative to identify the batch system parameters that can be used to predict the experimental BT of a sorbent.

#### **9.3.1 Identifying relevant parameters generated through batch experiments**

Sorption capacity of a sorbent at a given concentration is assessed using the equilibrium sorption capacity ( $q_e$ ). This parameter is expressed by the amount of sorbate sorbed into a unit mass of a sorbent at a given initial ion concentration (Section 7.3). As explained in Section 3.4,  $q_e$  for a given sorbent varies with experimental

conditions such as pH, sorbent dose, agitation rate and initial metal ion concentration. Even though  $q_e$  increases with increasing initial metal ion concentration, it eventually reaches equilibrium where all the available binding sites on the surface are saturated. It is evident from past research that materials with high sorption capacity show longer BT when used in column systems (Amarasinghe and Williams 2007; Chatterjee et al. 2018).

In addition to the sorption capacity, another important parameter that can be obtained using batch sorption experiments which can be used to describe a sorbent, is the kinetic constant. As explained in research literature, pseudo second order kinetic constant ( $k_2$ ) calculated from the pseudo second order kinetic model (Ho and McKay 1998), best describes the kinetics of various biosorbents (Wan et al. 2014; Gautam et al. 2014). Hence,  $k_2$  was also considered as a potential parameter for the prediction of experimental BT. Extensive use of pseudo second order model has revealed that  $k_2$  depends on the experimental conditions of the system (Plazinski et al. 2009). Similar to  $q_e$ ,  $k_2$  also varies with the initial ion concentration. According to a significant number of research studies,  $k_2$  decreases with the increasing initial ion concentration (Sadhasivam et al. 2007; Nandi et al. 2009). At a higher initial ion concentration,  $q_e$  is observed to be high and it usually takes a longer time to reach equilibrium.

According to the pseudo second order model explained by Ho and McKay (1998) as illustrated in Equation 4.2 in Section 4.4, the initial sorption rate ( $h$ ) of biosorbent samples (expressed in  $\text{mg g}^{-1} \text{min}^{-1}$ ), was calculated at  $t = 0$ .

$$h = k_2 q_e^2 \quad \text{Equation 9.1}$$

Where  $k_2$  is pseudo second order kinetic constant and  $q_e$  is equilibrium sorption capacity.

Accordingly, it was observed that in all instances, the initial sorption rate ( $h$ ) increased when the initial ion concentration was increased (Amarasinghe and Williams 2007). As  $h$  is related to both,  $k_2$  and  $q_e$ ,  $h$  was also considered for the prediction of experimental BT.

### **9.3.2 Development of a mathematical model for the prediction of experimental BT**

Three data matrices were generated with each having the experimental BT as the dependent variable. The independent variables were  $q_e$ ,  $k_2$  and  $h$  for the three metal ions separately as given in Appendix A2. Therefore, three mathematical models, based on the three relationships under investigation (BT vs  $q_e$ , BT vs  $k_2$ , BT vs  $h$ ), were developed for each metal ion. Since only one independent variable was utilised for each model, simple linear regression was employed. Repeated k-fold cross validation was used as the validation method with  $k=10$  and 100 repeats. Table 9.2 summarises the parameters of the mathematical models created for the prediction of BT.

**Table 9.2** Parameters of the models developed for the prediction of BT

<b>Metal</b>	<b>Relationship</b>	<b>Multiple R-squared</b>	<b>Adjusted R-squared</b>	<b>F-statistic</b>	<b>p value (X 108)</b>
Pb <sup>2+</sup>	BT and q <sub>e</sub>	0.7608	0.7482	60.44	25.580
	BT and k <sub>2</sub>	0.6526	0.6344	35.7	947.300
	BT and h	0.8095	0.7994	80.71	2.871
Cd <sup>2+</sup>	BT and q <sub>e</sub>	0.7027	0.6871	44.91	209.100
	BT and k <sub>2</sub>	0.6905	0.6742	42.39	308.700
	BT and h	0.8161	0.8064	84.32	2.041
Cu <sup>2+</sup>	BT and q <sub>e</sub>	0.8795	0.8732	138.7	0.035
	BT and k <sub>2</sub>	0.8729	0.8662	130.5	0.059
	BT and h	0.9453	0.9424	328.2	0.000

For each metal ion, parameters were compared between the three models developed for the prediction of BT. When the model parameters were considered, the models developed for the prediction of BT of samples using h proved to be more effective according to the multiple and adjusted R-squared values shown in Table 9.2. The three models developed for Pb<sup>2+</sup>, Cu<sup>2+</sup> and Cd<sup>2+</sup> using h, yielded higher multiple R-squared and adjusted R-squared values indicating good fit. F-statistic was also used for the comparison of the models. The F-test of overall significance indicates if the linear regression model in question, can provide a better fit for the data than a model that contains no independent variables. If the p-value for the F-test is less than the significance level, the sample data provides sufficient evidence to conclude that the regression model fits the data better than a model with no independent variables. Table 9.2 indicates that F-statistic values were highest for the models built for the prediction of BT using h.

During the sorption process, sorption capacity remains unchanged when the equilibrium is reached. BT is the time taken for the bed to become saturated. If the

sorption rate is high, the bed will be saturated relatively faster (Worch 2012). Therefore,  $k_2$  is a factor which determines BT. If the equilibrium capacity is high, it takes longer to be saturated (Worch 2012; Patel 2019). Hence, the equilibrium capacity is also a factor which determines BT. Since,  $h$  is connected to both the parameters,  $h$  is able to describe BT well.

Regression plots were constructed for the models indicating their 95% prediction intervals and 95% confidence intervals. These plots were used for the visual comparison of the three models built for each of the metal ions. A prediction interval indicates a range of values that is likely to contain the value of a single new prediction for the model while confidence interval indicates a range of values containing the population mean. Figure 9.2 to 9.10 depict the 95% prediction intervals and 95% confidence intervals for the simple linear regression analysis. For each of the three metal ions, the model developed for BT using  $h$  shows narrower prediction intervals and narrower 95% confidence intervals when compared to the other two models. This indicates better prediction ability of the models developed using  $h$  as the independent variable.

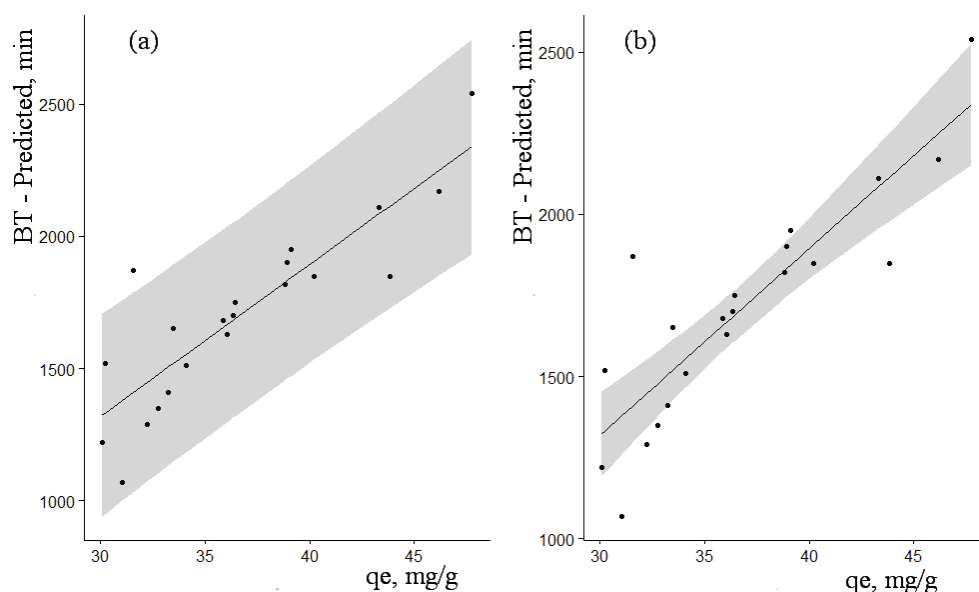


**Figure 9.2** (a) Prediction interval and (b) 95% confidence interval of the linear regression model developed for the relationship between BT and  $q_e$  for  $Pb^{2+}$  at 200 mg/L initial concentration

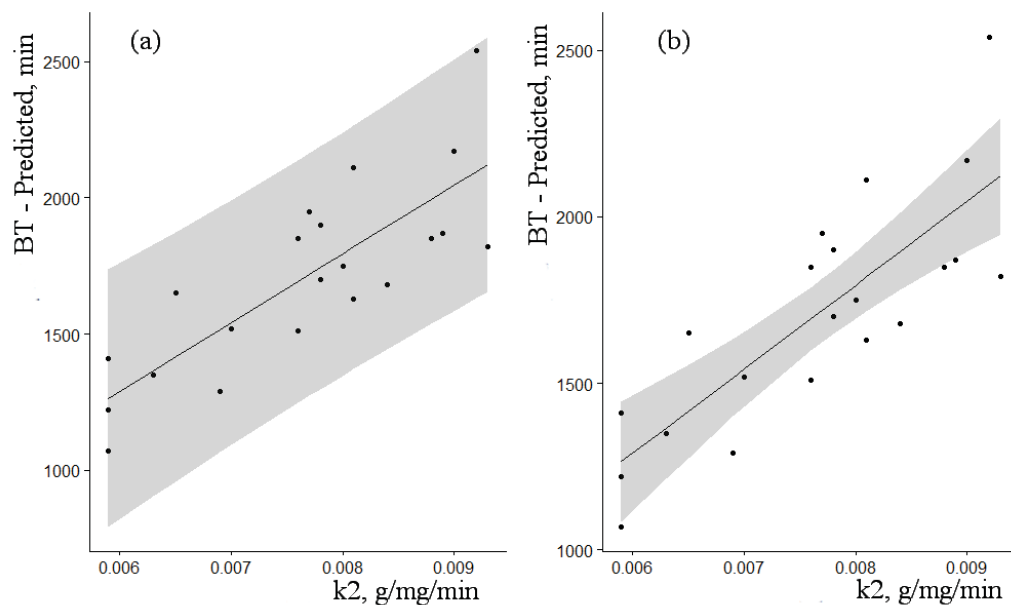


**Figure 9.3** (a) Prediction interval and (b) 95% confidence interval of the linear regression model developed for the relationship between BT and  $k_2$  for  $\text{Pb}^{2+}$

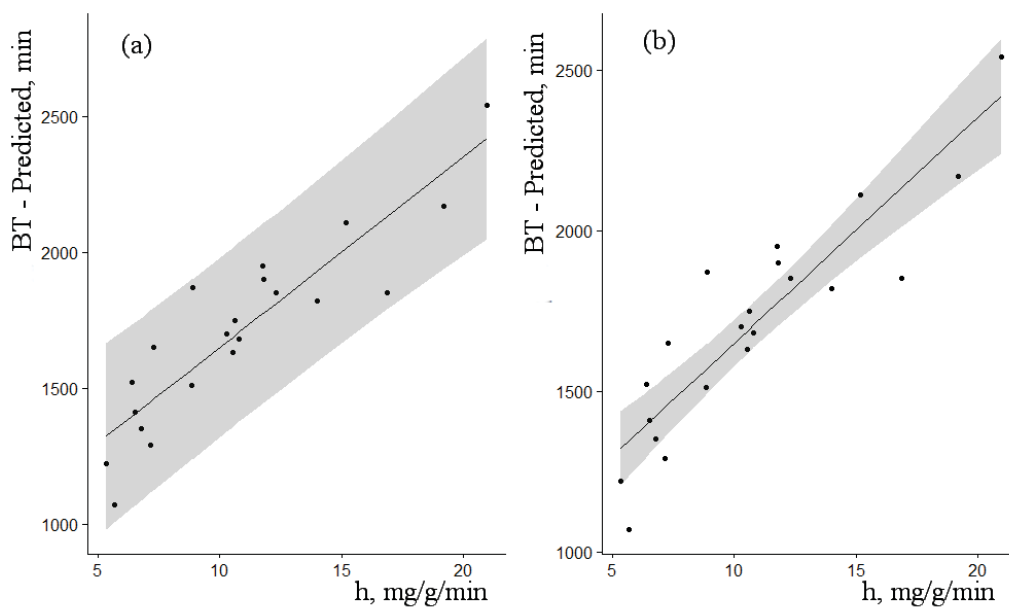


**Figure 9.4** (a) Prediction interval and (b) 95% confidence interval of the linear regression model developed for the relationship between BT and  $h$  for  $\text{Pb}^{2+}$



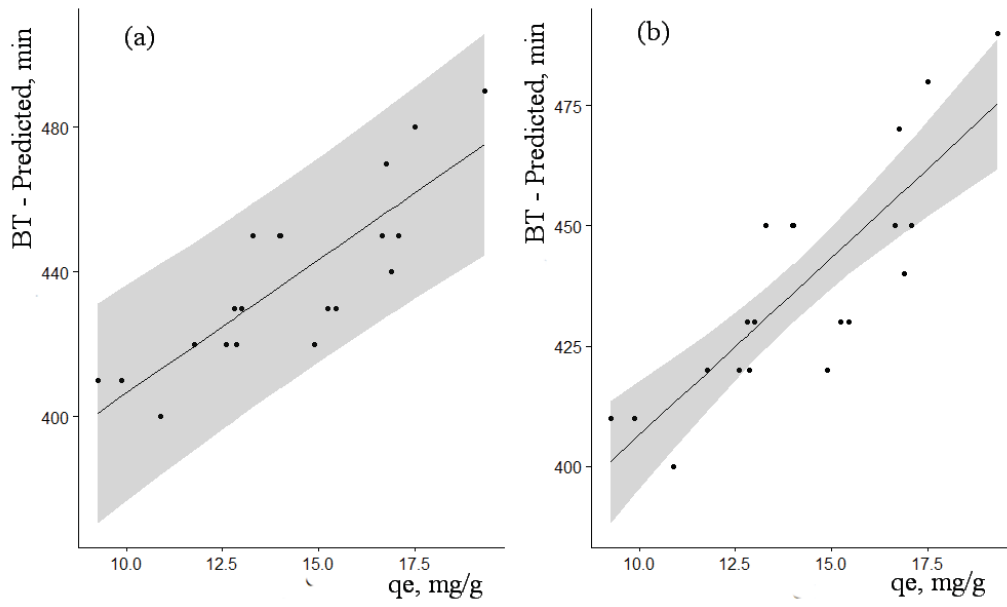


**Figure 9.5** (a) Prediction interval and (b) 95% confidence interval of the linear regression model developed for the relationship between BT and  $q_e$  for  $\text{Cd}^{2+}$  at 200 mg/L initial concentration

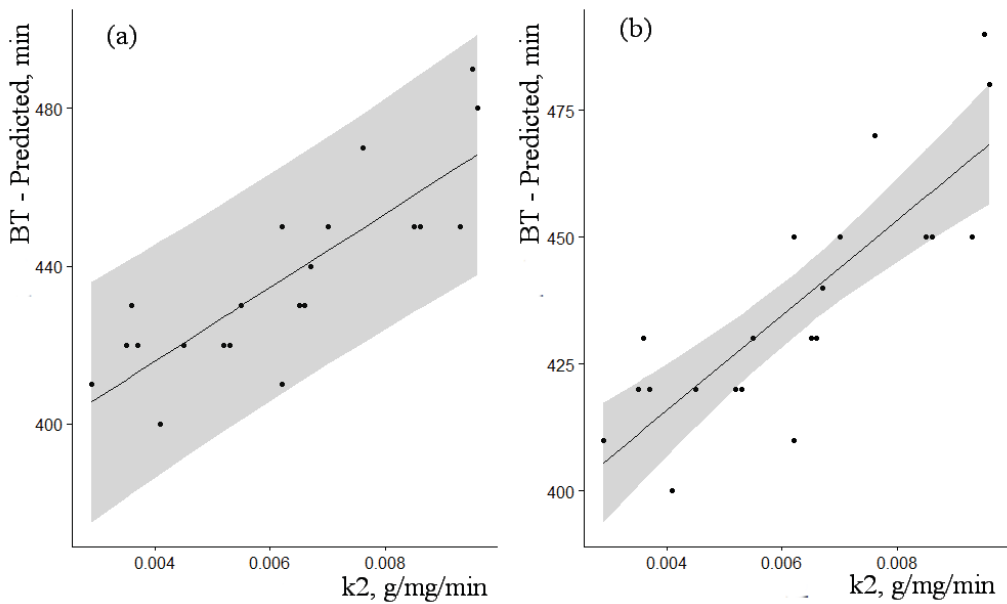


**Figure 9.6** (a) Prediction interval and (b) 95% confidence interval of the linear regression model developed for the relationship between BT and  $k_2$  for  $\text{Cd}^{2+}$

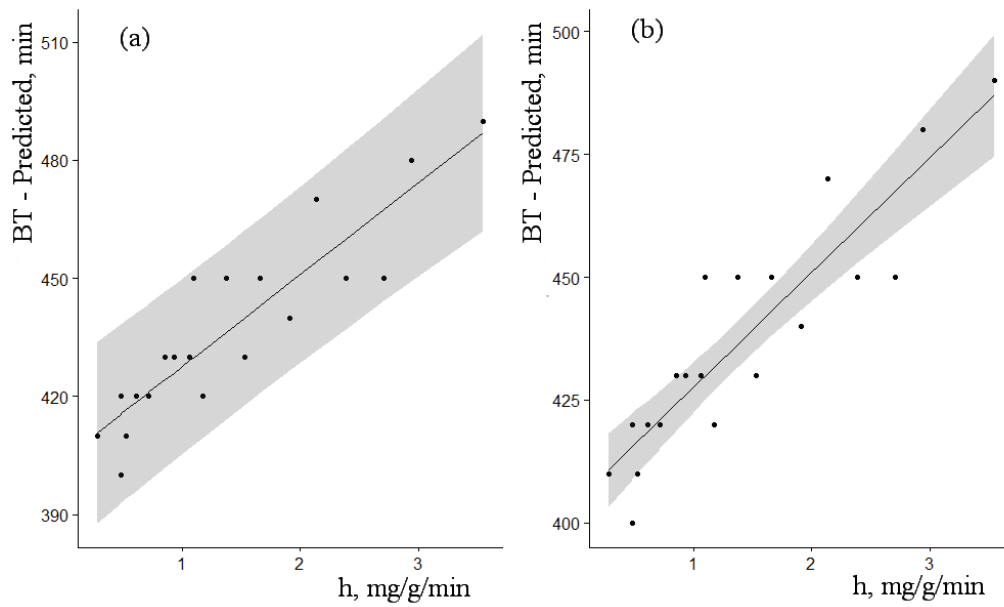


**Figure 9.7** (a) Prediction interval and (b) 95% confidence interval of the linear regression model developed for the relationship between BT and  $h$  for  $\text{Cd}^{2+}$

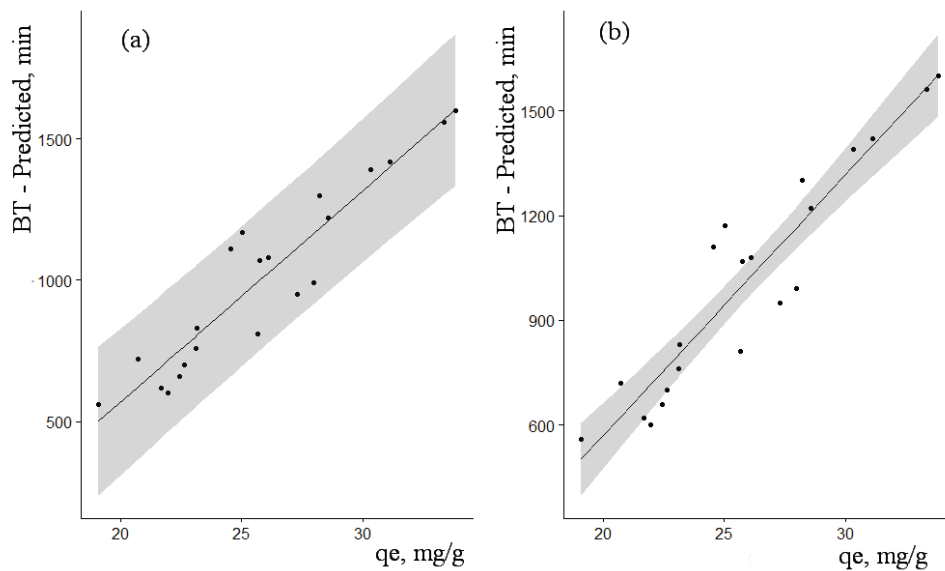


**Figure 9.8** (a) Prediction interval and (b) 95% confidence interval of the linear regression model developed for the relationship between BT and  $q_e$  for  $\text{Cu}^{2+}$  at 200 mg/L initial concentration

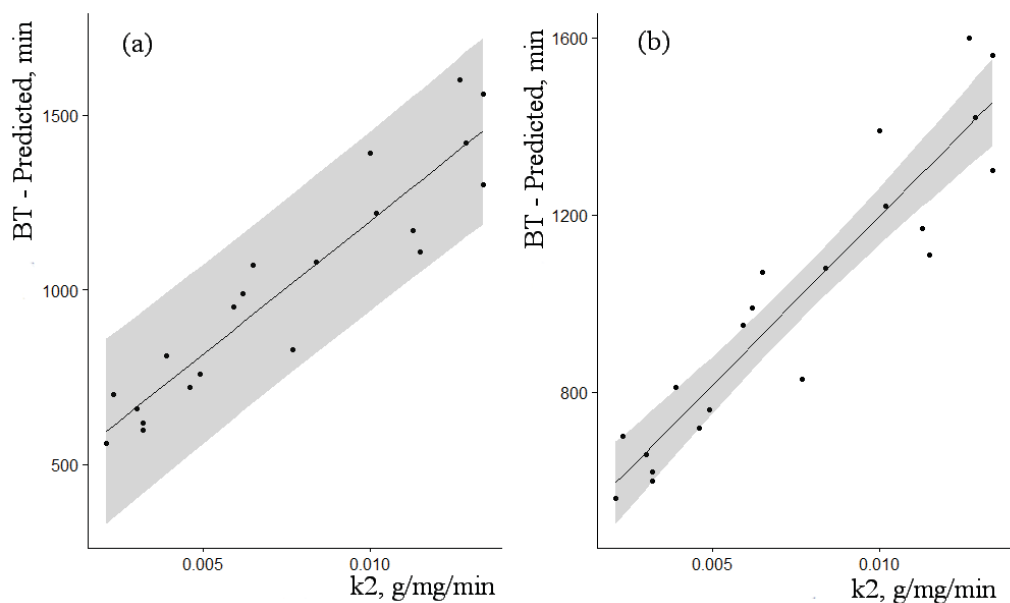


**Figure 9.9** (a) Prediction interval and (b) 95% confidence interval of the linear regression model developed for the relationship between BT and  $k_2$  for  $\text{Cu}^{2+}$

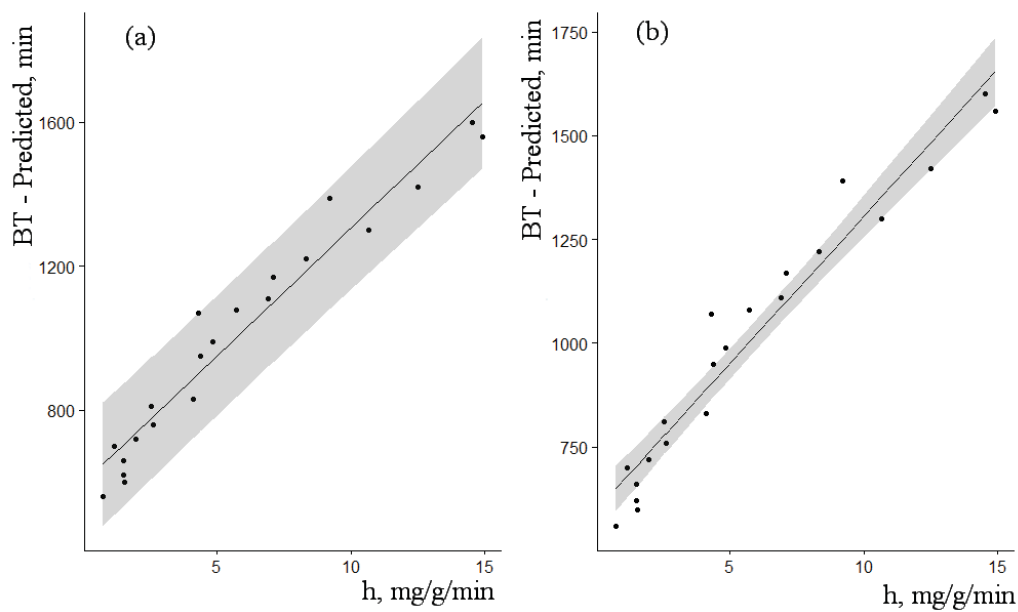


**Figure 9.10** (a) Prediction interval and (b) 95% confidence interval of the linear regression model developed for the relationship between BT and  $h$  for  $\text{Cu}^{2+}$

Improved model parameters as shown in Table 9.2 together with narrower prediction intervals and confidence intervals justify the selection of the three models which aim to predict BT using  $h$ . The models for the three metals are given below.

$$BT_{(Pb)} = 8.8362756 + 0.011520 h$$

$$BT_{(Cu)} = 7.5995997 + 0.013293 h$$

$$BT_{(Cd)} = 13.858733 + 0.034916 h$$

Accordingly,  $h$  calculated using  $k_2$  and  $q_e$ , generated from batch experiments, can be used to predict experimental BT values of a column system based on the same sorbent. Hence, a batch experiment conducted under similar solution conditions such as initial ion concentration and pH can be used to predict the experimental BT of a column system with the same initial solution concentration and pH. However, this prediction is only valid for the experimental conditions explained in Section 4.3.3 for batch and column experiments. This provides an initial approximation of the column breakthrough point using batch sorption and thus can be used for assessing the feasibility of a potential laboratory column.

## **9.4 SIMULATION OF SORPTION IN COLUMNS USING MODELS FROM BATCH EXPERIMENT**

As discussed in Chapters 8 and 9,  $q_e$  and  $k_2$  of a sorbent exerts a significant influence on column BT. In Chapter 7, models to estimate  $q_e$  with respect to a sorbents' physico-chemical properties and initial metal ion concentrations were presented. Chapter 8 introduces models to predict  $k_2$  using physico-chemical properties of sorbents and initial metal ion concentrations. These two types of models and existing equations in published literature (Ho and McKay 1999) can be used to predict sorption characteristics of sorbent mixtures. In this study, two types of models developed in Chapter 7 and Chapter 8 and other equations as presented in literature, were used to simulate metal ion sorption characteristics of experimental columns.

### **9.4.1 Design of the simulation**

For the simulation, material packed in an experimental column was considered as a series of 30 connected elements of sorbent materials as illustrated in Figure 9.11. In other words, a 30cm long column was treated as a collection of thirty material

elements, each having a height of 1cm. Inflow concentration of the metals to a particular element was denoted as ( $C_{in}$ ) while the outflow concentration was denoted as ( $C_{out}$ ).  $C_{in}$  for the first element is the concentration of the solution feeding the column. Each element has an input ( $C_{in}$ ) and output ( $C_{out}$ ). Outflow concentration from the element below was considered as the inflow concentration to the element above.  $C_{out}$  from the 30<sup>th</sup> element was considered as the outflow concentration from the column (Table 9.3).

For the convenience of simulation, a new variable ( $\delta q_{ad}$ ) was introduced to denote the amount sorbed during the given time interval ( $\delta t$ ) and was calculated using Equations 9.1 and 9.2. The Simulation was conducted in 5 min intervals.

According to the pseudo second order model presented by Ho et al. (1998), the rate of sorption at time ( $t$ ) can be expressed using Equation 9.1.

$$\frac{dq_t}{dt} = k_2(q_e - q_t)^2 \quad \text{Equation 9.1}$$

Where  $k_2$  ( $\text{min}^{-1}$ ) is the pseudo second order reaction rate.  $q_e$  and  $q_t$  ( $\text{mg/g}$ ) are the sorption capacities at equilibrium and time  $t$ , respectively.

$\delta q_{ad}$  was calculated using Equation 9.1 ,

$$\delta q_{ad} = k_2(q_e - q_t)^2 \delta t \quad \text{Equation 9.2}$$

At  $t=0$  ,  $q_t = 0$ ,  $q_t$  increases with increasing time and  $q_{t(n)} = q_{t(n-5)} + q_{ad(n-5)}$

$C_{out}$  was calculated using Equations 9.4- 9.6

$$q_t = V(C_t - C_o) / m \quad \text{Equation 9.3}$$

Equation 9.3 was re-arranged to express  $C_t$  as

$$C_t = C_o - (q_t * \frac{m}{V}) \quad \text{Equation 9.4}$$

Where  $q_t$  ( $\text{mg/g}$ ) is the quantity of metal ions adsorbed per unit mass of sorbent,  $C_o$  ( $\text{mg/L}$ ) is the initial metal ion concentration,  $C_t$  ( $\text{mg/L}$ ) is the metal ion concentration in the solution at time  $t$ ,  $V$  ( $\text{L}$ ) is the volume of solution used and  $m$  ( $\text{g}$ ) is the mass of the sorbent.

Accordingly,  $C_{out}$  was calculated using Equation 9.4

$$C_{out} = C_i - (q_{ad} * \frac{m}{V}) \quad \text{Equation 9.5}$$

$C_{out}$  at  $t=n$  of the first element is  $C_{in}$ . For the second element at  $t=n+5$ , the simulation model was developed using Microsoft XL software as illustrated in Figure 9.12.

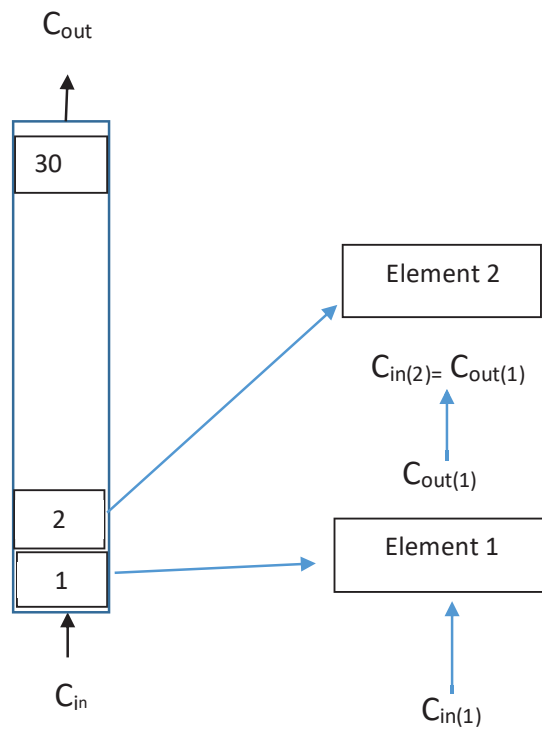


**Figure 9.11** Design of the column simulation using elements

Element 1

Element 2

Time, min	$C_{in}$ , mg/L	$q_t$ , mg/g	$q_{ad}$ , mg/g	$C_{out}$ , mg/L
0	200	$X_{0(1)}$	$Y_{0(1)}$	$Z_{0(1)}$
5	200	$X_{1(1)}=X_{0(1)}+Y_{0(1)}$	$Y_{1(1)}$	$Z_{1(1)}$
10	200	$X_{2(1)}=X_{1(1)}+Y_{1(1)}$		$Z_{2(1)}$
15				

Time, min	$C_{in}$ , mg/L
0	
5	$Z_{0(1)}$
10	$Z_{1(1)}$
15	$Z_{2(1)}$

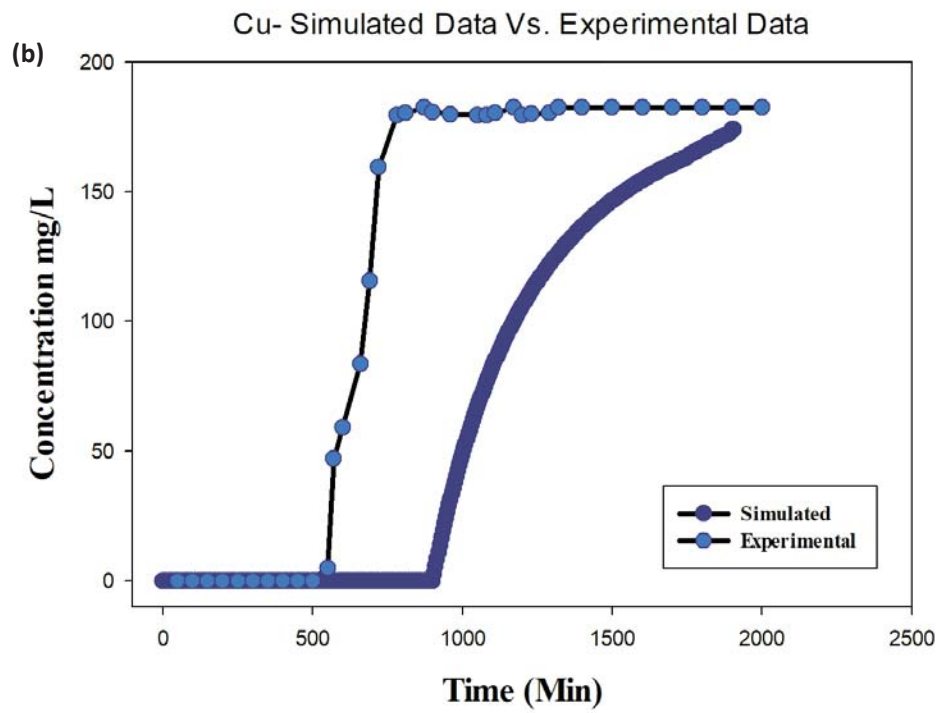
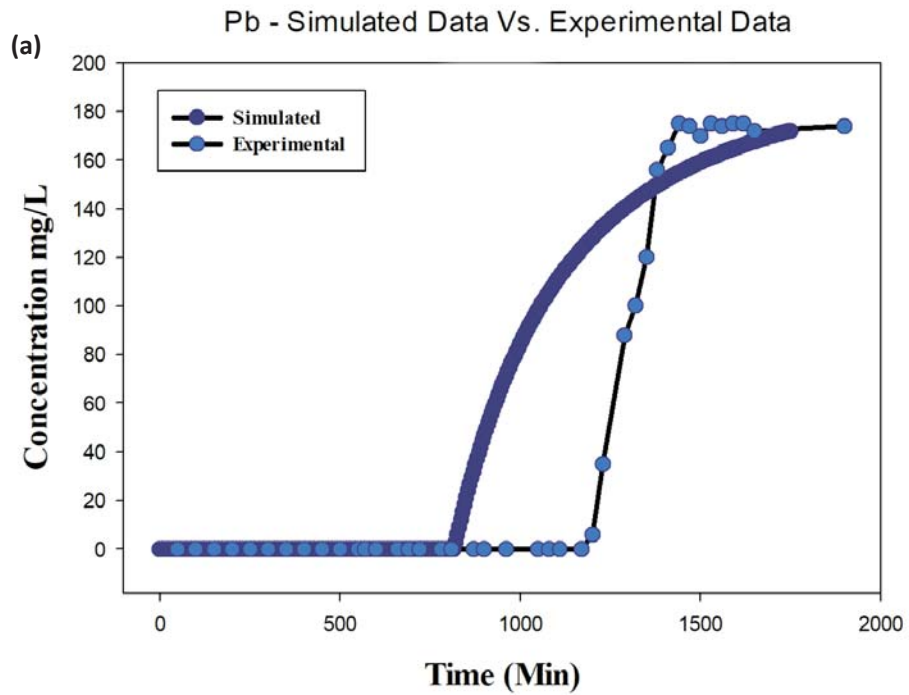
Section 2

Time, min	$C_{in}$ , mg/L	$q_t$ , mg/g	$q_{ad}$ , mg/g	$C_{out}$ , mg/L
0		$X_{0(2)}$	$Y_0$	$Z_{0(2)}$
5	$Z_{0(1)}$	$X_{1(2)}=X_{0(2)}+Y_{0(2)}$	$Y_1$	$Z_{1(2)}$
10	$Z_{1(1)}$	$X_{2(2)}=X_{1(2)}+Y_{1(2)}$		$Z_{2(2)}$
15	$Z_{2(1)}$			

**Figure 9.12** Simulation of sorption process

### 9.4.2 Comparison of outputs

The flow exiting the last element (element 30) was plotted with time and was compared with the breakthrough curve obtained from the laboratory experiments. The comparison for the three metal cations, for sample 1 (100% CSB) is given in Figure 9.13.



*Continued on next page.*



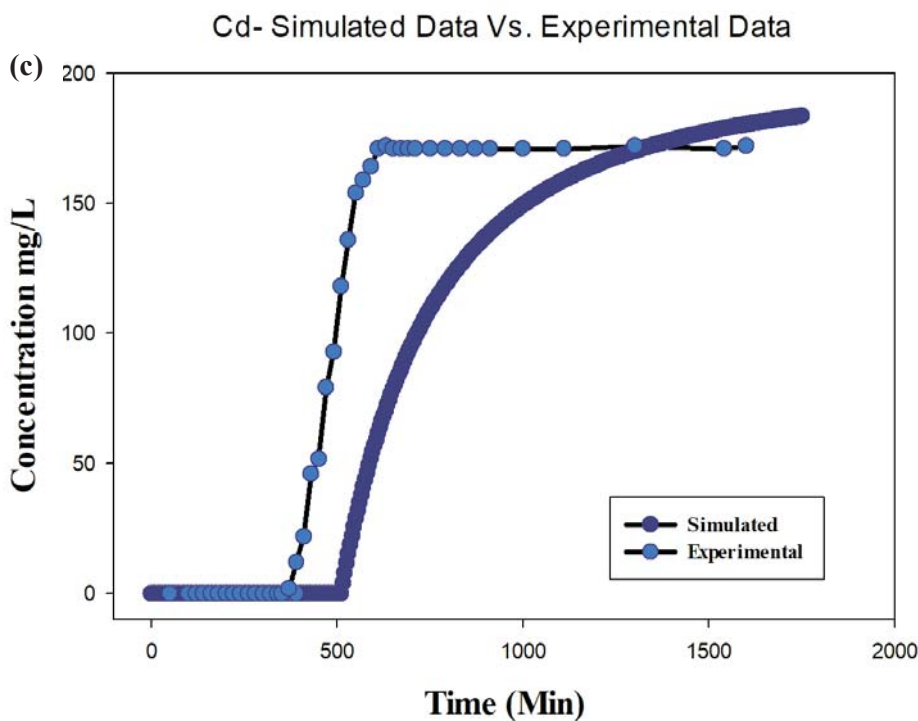


**Figure 9.13** Comparison of breakthrough curves obtained from the simulation and the laboratory experiment (a)  $\text{Pb}^{2+}$  (b)  $\text{Cu}^{2+}$  (c)  $\text{Cd}^{2+}$  for sample 1 (100% CSB)

According to Figure 9.13, experimental BT of Pb was achieved earlier than the calculated BT. In the case of Cu and Cd, calculated BT is greater than the experimental BT. It is evident that there are differences in the sorption behaviour of batch and column systems. Hence, bridging those two systems and to use batch relationships to predict column parameters is a challenge. Even though the simulation and experimental data did not exactly fit, the simulation explains the behaviour of the breakthrough curve. As explained above,  $q_e$  and  $k_2$  for the simulation were calculated using the predicative models developed using sorbent physico-chemical properties and metal ion concentrations. Goodness of fit of those developed models are between 60%-63% and 79%-90% for  $q_e$  and  $k_2$  respectively. Therefore, it is likely that the prediction errors of those two parameters were included in the simulation. Furthermore, as  $q_e$  and  $k_2$  depend on initial metal concentrations, variation in initial concentration within the column would have an influence on these two parameters. Hence, a calibration coefficient is needed to be introduced to relate the models developed using batch experiment data for simulating column behaviour. This is an issue that merits further investigations.

## 9.5 SUMMARY OF KEY FINDINGS

Determination of breakthrough curve and identification of breakthrough time in a laboratory setting is necessary to assess the industrial applicability of the chosen sorbate and sorbent system. Accordingly, predictive models were developed to understand the breakthrough time of a column using batch sorption parameters. For each metal ion, prediction models were generated using equilibrium sorption capacity, pseudo second order kinetic constant and initial sorption rate. Among these parameters, it was noted that the breakthrough time can be predicted using initial sorption rate, with a high predictability.

A column is operated in an entirely different scenario to a batch study. Breakthrough time of a column depends on several parameters such as bed depth, cross sectional area, porosity of the packing medium and flow rate. This limits the generation of a direct correlation between the two systems. However, breakthrough time is linked to the sorption efficiency of the sorbent. Hence, predicting the breakthrough value using initial sorption rate can be used as a preliminary estimation for the design of a laboratory column. However, this cannot be used as an absolute method to avoid column studies.

A simulation model was developed using Microsoft XL software to simulate sorption in a column using relationships developed from this study and published literature. Breakthrough curves obtained from experiment and simulation did not exactly fit. A calibration coefficient needs to be introduced to relate models developed using batch experimental data to simulate column behaviour. This is an important area for further research.

This page intentionally left blank.

# CHAPTER 10: CONCLUSIONS AND RECOMMENDATIONS FOR FUTURE RESEARCH

---

## 10.1 CONCLUSIONS

Utilising agricultural waste materials as sorbents to remove heavy metals from industrial wastewater has the capacity to mitigate disposal problems associated with these materials. However, the performance of these sorbents mainly depends on the material physico-chemical properties. Therefore, optimising sorbents to increase the sorption performance remains a challenge. Performance of a sorbent is determined by its sorption capacity and sorption kinetics. This research study investigated the influence of material physico-chemical properties such as specific surface area, acidic surface functional groups, basic surface functional groups, pore size, pore volume and zeta potential on sorption capacity (maximum and equilibrium) and sorption kinetics specifically in terms of the pseudo second order kinetic model which explains the kinetics of biosorbents in most instances. This in turn provides new knowledge on the relationship between material physico-chemical properties and its sorption performance.

Analysis of the performance of sorbents under investigation was undertaken using a series of batch sorption experiments to determine the sorption capacity at equilibrium and the kinetics. Continuous fixed bed column experiments, which reflect the real-world application of the sorbents, were used to understand the behaviour of potential industrial-scale sorbent columns utilising the sorbents in question. As these two types of experiments are used separately to describe a particular sorbent – sorbate system, it was important to develop a relationship which could aid in combining those two types of experiments for achieving an effective design for an industrial-scale continuous fixed bed column.

### 10.1.1 Influence of physico-chemical properties on sorption capacity

Physico-chemical properties of biosorbents influence the maximum sorption capacity and equilibrium sorption capacity of heavy metals. Though various physico-chemical properties could influence  $\text{Cu}^{2+}$ ,  $\text{Cd}^{2+}$  and  $\text{Pb}^{2+}$  sorption, they do not equally contribute or are equally important for the process of sorption. As identified in the current study:

- The key physico-chemical property governing the sorption capacity of the selected biosorbents for all the three metal cations is the acidic surface functional groups. Among different acidic surface functional groups, carboxylic groups play a relatively prominent role in the sorption of  $\text{Cu}^{2+}$  and  $\text{Pb}^{2+}$  which are hard acids, while laconic groups are more important in providing binding sites to  $\text{Cd}^{2+}$ , which is a soft acid.
- Though sorption is a surface phenomenon, specific surface area alone does not exert a prominent influence on the sorption of  $\text{Cu}^{2+}$ ,  $\text{Cd}^{2+}$  and  $\text{Pb}^{2+}$ . A strong correlation was observed between metal sorption capacity and the functional groups. This highlights the influence of surface functional group density on metal sorption capacity.

This study provided new knowledge on the influence of individual physico-chemical properties on both, maximum and equilibrium sorption capacity of the selected sorbents. Accordingly, a predictive model was developed to calculate the maximum and equilibrium sorption capacities of a biosorbent when the relevant physico-chemical properties are known. Similarly, the change in sorption capacity when an individual physico-chemical property is changed can also be determined.

### **10.1.2 Influence of physico-chemical properties on sorption kinetics**

Influence of physico-chemical properties of sorbents on sorption kinetics was assessed using the pseudo second order kinetic constant. This study developed predictive models to estimate the pseudo second order kinetic rate constant ( $k_2$ ) for three divalent heavy metals ( $\text{Pb}^{2+}$ ,  $\text{Cd}^{2+}$  and  $\text{Cu}^{2+}$ ), using surface physico-chemical properties of biosorbent mixtures made from tea factory waste and coconut shell biochar. These mixtures were found to demonstrate sufficient variability of physico-chemical properties in order to consider them as different biosorbents. According to the study outcomes:

- The relationship between material physico-chemical properties and the kinetic constants for  $\text{Pb}^{2+}$ ,  $\text{Cd}^{2+}$  and  $\text{Cu}^{2+}$  are comparable. The nature of these relationships remained unchanged within the ranges of initial metal ion concentrations under investigation.

- Acidic surface functional groups has the ability to increase reaction rates. Among the physico-chemical properties investigated, its influence is prominent on sorption mechanisms.
- High specific surface area with micropore structures can reduce the sorption rate as metals need to diffuse into the intraparticle structures for binding to active sites.
- Pore volume and total basic groups as independent variables did not contribute significantly to the development of predictive models.

The study generated new knowledge on how individual physico-chemical properties influence the rate of sorption of biosorbents. This in turn, provides new knowledge to guide how an individual or a suite of physico-chemical properties should be changed in order to enhance the speed of reaction.

The new knowledge created as discussed in this section and in Section 10.1.1, provides a quantitative approach to assess the sorption performance of a sorbent in terms of heavy metal removal. Furthermore, it allows comparisons among different sorbents in terms of their performance.

### **10.1.3 Transferability of research data between batch and column studies**

Batch experiments are used to determine the efficiency of sorbents by analysing their equilibrium and kinetics while columns are used to simulate the real world applications of using these sorbents in pollutant removal. Breakthrough time of a column system is an important parameter that expresses the life of the sorbent column. This parameter is important in designing industrial-scale sorbent columns. Breakthrough time of a column system varies with the sorbent used. Hence, sorption capacity and the rate of sorption of a particular sorbent has an influence on the breakthrough time determined for that sorbent in a column system. Hence, for each metal ion, predictive models were generated to estimate the column breakthrough time using parameters such as equilibrium sorption capacity, pseudo second order kinetic constant and initial sorption rate. Among these models, it was noted that breakthrough time of a sorbent in a column system can be predicted by the initial sorption rate of the same sorbent in a batch system, with higher predictability. A column is operated in an entirely different scenario to a batch study. Hence, predicting breakthrough value using initial sorption rate can be used as a preliminary estimation to design a laboratory column. However,

this cannot be used as an absolute method to avoid undertaking a column study. The present study is an initial attempt to understand the relationship between these two systems and to contribute to bridging the current knowledge gap.

## **10.2 PRACTICAL APPLICATION OF RESEARCH OUTCOMES**

Agricultural waste generation is a critical problem in developing countries. Use of these waste materials for alternative purposes will mitigate the accumulation of agricultural waste. Use of agricultural waste for the removal of pollutants in industrial wastewater is one such option. However, the use of agricultural waste as biosorbents for the removal of pollutants remains a challenge due to the high variability and the unpredictability of their sorption capacities.

The sorption capacity of a biosorbent primarily depends on physico-chemical properties of the sorbent. Furthermore, optimising the use of these biosorbents is not straightforward as the influence of sorbent physico-chemical properties on sorption capacity has not been scientifically investigated in-depth. Hence, a comprehensive analysis aimed at understanding the influence of physico-chemical properties on the removal of pollutants using biosorbents was considered to be important. Practical applications of the study outcomes are illustrated in Figure 10.1.

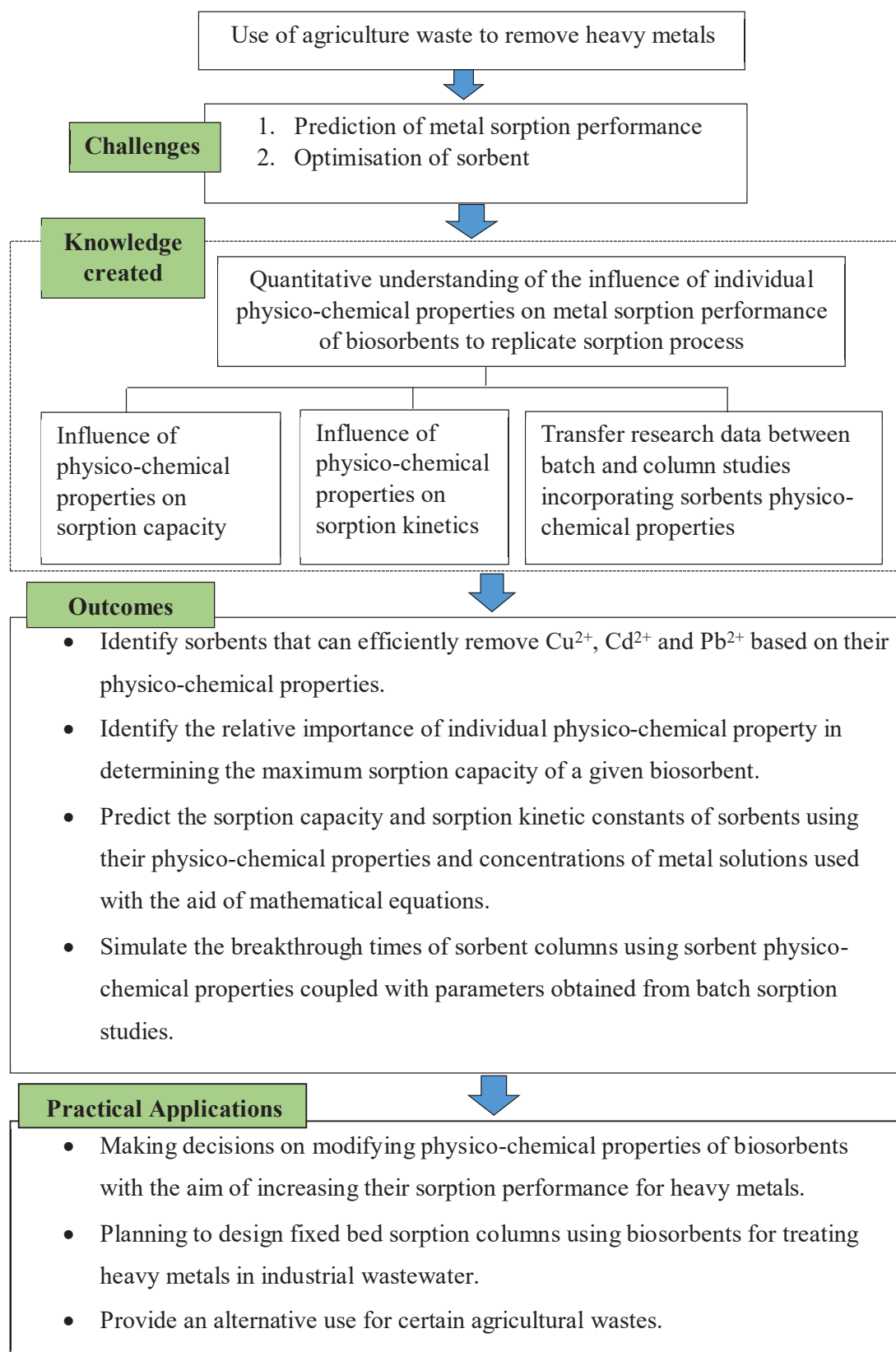


**Figure 10.1** Schematic representation of the potential application of research outcomes



### 10.3 RECOMMENDATIONS FOR FUTURE RESEARCH

This research study created new knowledge by investigating the influence of physico-chemical properties on sorption. The study outcomes can enhance the use of biosorbents for the removal of heavy metals in industrial wastewater. This study also identified specific areas to serve as topics for future research.

- The systems investigated in this study were well controlled single metal systems. As industrial wastewater comprises of a range of metal ions, it is necessary to incorporate the influence of other metals on sorption of a particular metal ion. Hence, investigations are necessary to understand the competition among different metal ions in controlled multi-metal systems. Furthermore, this study should be extended by using actual industrial wastewater to understand the applicability of the findings in a system where a range of pollutants are present.
- Since the influence of different physico-chemical properties of the materials on sorption capacity is comparable for all the three selected metal ions, it is possible that other metal ions would yield similar results. This could be investigated in future research as it is important to understand the influence of material physico-chemical properties of sorbents on common metals which are present in industrial wastewater. Such studies will aid in further understanding the nature of the influence exerted by physico-chemical properties on metal sorption.
- In this research, simpler forms of relationships were developed to predict column breakthrough time using initial sorption rate of the sorbent. This should serve as a preliminary estimation that could be useful for column design rather than an absolute method to avoid undertaking column studies. Hence, a proper simulation of actual column performance needs to be modelled using column parameters such as flow rate, porosity and bed volume along with the parameters obtained from batch experiments.
- Sorbent regeneration needs to be investigated in order to understand the potential for reusing sorbents and safe disposal of the sorbent. This should also go in hand with a recovery method in order to recover commercially valuable metals that have undergone sorption. Further, the environmental and techno- economic analysis of such a method has to be assessed for implementation.

## REFERENCES

---

- Abdi, H. and L.J. Williams. 2010a. "Principal component analysis 2 (4): 433-459. doi: doi:10.1002/wics.101.
- Abdi, H. and L.J.J.W. Williams. 2010b. "Principal component analysis 2 (4): 433-459.
- Abdolali, A., H.H. Ngo, W. Guo, J.L. Zhou, J. Zhang, S. Liang, S.W. Chang, D.D. Nguyen and Y. Liu. 2017. "Application of a breakthrough biosorbent for removing heavy metals from synthetic and real wastewaters in a lab-scale continuous fixed-bed column." *Bioresource Technology* 229: 78-87. doi: <https://doi.org/10.1016/j.biortech.2017.01.016>.
- Adriano, D.C. 2001. "Environmental Contamination and Regulation." In *Trace Elements in Terrestrial Environments*, 91-131: Springer.
- Agrafioti, E., G. Bouras, D. Kalderis and E. Diamadopoulou. 2013. "Biochar production by sewage sludge pyrolysis." *Journal of Analytical and Applied Pyrolysis* 101: 72-78. doi: <https://doi.org/10.1016/j.jaap.2013.02.010>.
- Ahluwalia, S. and D. Goyal. 2005. "Removal of heavy metals by waste tea leaves from aqueous solution." *Engineering in life Sciences* 5 (2): 158-162.
- Ahmadi, A., H. Najjaran, J. Holzman and M. Hoorfar. 2009. "Two-dimensional flow dynamics in digital microfluidic systems." *Journal of Micromechanics and Microengineering* 19 (6): 065003.
- Ahmed, M. and B. Hameed. 2018. "Removal of emerging pharmaceutical contaminants by adsorption in a fixed-bed column: a review." *Ecotoxicology and environmental safety* 149: 257-266.
- Ajmal, M., A. Mohammad, R. Yousuf and A. Ahmad. 1998. "Adsorption behavior of cadmium, zink, nickel, and lead from aqueous solution by mangifera india seed shell.
- Ajmal, M., R.A.K. Rao and M.A. Khan. 2005. "Adsorption of copper from aqueous solution on Brassica cumpestris (mustard oil cake)." *Journal of hazardous materials* 122 (1-2): 177-183.
- Albadarin, A.B., C. Mangwandi, H. Ala'a, G.M. Walker, S.J. Allen and M.N. Ahmad. 2012. "Modelling and fixed bed column adsorption of Cr (VI) onto orthophosphoric acid-activated lignin." *Chinese Journal of Chemical Engineering* 20 (3): 469-477.

- Albadarin, A.B., J. Mo, Y. Glocheux, S. Allen, G. Walker and C. Mangwandi. 2014. "Preliminary investigation of mixed adsorbents for the removal of copper and methylene blue from aqueous solutions." *Chemical Engineering Journal* 255: 525-534. doi: <https://doi.org/10.1016/j.cej.2014.06.029>.
- Ali, I. 2018. "Microwave assisted economic synthesis of multi walled carbon nanotubes for arsenic species removal in water: batch and column operations." *Journal of Molecular Liquids* 271: 677-685.
- Ali, I., M. Asim and T.A. Khan. 2012. "Low cost adsorbents for the removal of organic pollutants from wastewater." *Journal of environmental management* 113: 170-183.
- Aman, T., A.A. Kazi, M.U. Sabri and Q. Bano. 2008. "Potato peels as solid waste for the removal of heavy metal copper (II) from waste water/industrial effluent." *Colloids and Surfaces B: Biointerfaces* 63 (1): 116-121.
- Amarasinghe, B. and R. Williams. 2007. "Tea waste as a low cost adsorbent for the removal of Cu and Pb from wastewater." *Chemical Engineering Journal* 132 (1-3): 299-309.
- Amer, H., A. El-Gendy and S. El-Hagggar. 2017. "Removal of lead (II) from aqueous solutions using rice straw." *Water Science and Technology* 76 (5): 1011-1021.
- Amodio-Cocchieri, R. 1996. "Lead in human blood from children living in campania, italy." *Journal of Toxicology and Environmental Health* 47 (4): 311-320. doi: 10.1080/009841096161663.
- Amuda, O.S., I.A. Amoo and Y. Hung. 2011. "Radioactive element removal from contaminated groundwater by agricultural waste-based activated carbon." *Int. J. Water Resour. Arid Environ* 1 (1): 71-82.
- Anastopoulos, I., I. Massas and C. Ehaliotis. 2013a. "Composting improves biosorption of Pb<sup>2+</sup> and Ni<sup>2+</sup> by renewable lignocellulosic materials. Characteristics and mechanisms involved." *Chemical Engineering Journal* 231: 245-254. doi: <https://doi.org/10.1016/j.cej.2013.07.028>.
- Anastopoulos, I., I. Massas and C. Ehaliotis. 2013b. *Composting improves biosorption of Pb<sup>2+</sup> and Ni<sup>2+</sup> by renewable lignocellulosic materials. Characteristics and mechanisms involved*. Vol. 231. doi: 10.1016/j.cej.2013.07.028.
- Anderson, D., K. Burnham and G. White. 1998. "Comparison of Akaike information criterion and consistent Akaike information criterion for model selection and

statistical inference from capture-recapture studies." *Journal of Applied Statistics* 25 (2): 263-282.

- Anwar, J., U. Shafique, M. Salman, A. Dar and S. Anwar. 2010. "Removal of Pb (II) and Cd (II) from water by adsorption on peels of banana." *Bioresource technology* 101 (6): 1752-1755.
- Apiratikul, R. and P. Pavasant. 2008. "Batch and column studies of biosorption of heavy metals by *Caulerpa lentillifera*." *Bioresource technology* 99 (8): 2766-2777.
- Apostoli, P., P. Kiss, S. Porru, J.P. Bonde and M. Vanhoorne. 1998. "Male reproductive toxicity of lead in animals and humans. ASCLEPIOS Study Group." *Occupational and Environmental Medicine* 55 (6): 364. <http://oem.bmj.com/content/55/6/364.abstract>.
- Ararem, A., O. Bouras and A. Bouzidi. 2013. "Batch and continuous fixed-bed column adsorption of Cs<sup>+</sup> and Sr<sup>2+</sup> onto montmorillonite-iron oxide composite: comparative and competitive study." *Journal of Radioanalytical and Nuclear Chemistry* 298 (1): 537-545.
- Atar, N., A. Olgun and S. Wang. 2012. "Adsorption of cadmium (II) and zinc (II) on boron enrichment process waste in aqueous solutions: Batch and fixed-bed system studies." *Chemical Engineering Journal* 192: 1-7. doi: <https://doi.org/10.1016/j.cej.2012.03.067>.
- Atia, A.A., A.M. Donia and K.Z. Elwakeel. 2005. "Selective separation of mercury (II) using a synthetic resin containing amine and mercaptan as chelating groups." *Reactive and Functional Polymers* 65 (3): 267-275.
- Aydın, H., Y. Bulut and Ç. Yerlikaya. 2008. "Removal of copper (II) from aqueous solution by adsorption onto low-cost adsorbents." *Journal of Environmental Management* 87 (1): 37-45.
- Ayoub, G., L. Semerjian, A. Acra, M.E. Fadel and B. Koopman. 2001. "Heavy metal removal by coagulation with seawater liquid bittern." *Journal of Environmental Engineering* 127 (3): 196-207.
- Aziz, A.S.A., L.A. Manaf, H.C. Man and N.S. Kumar. 2014. "Column dynamic studies and breakthrough curve analysis for Cd(II) and Cu(II) ions adsorption onto palm oil boiler mill fly ash (POFA)." *Environmental Science and Pollution Research* 21 (13): 7996-8005. doi: 10.1007/s11356-014-2739-5.

- Babel, S. and T.A. Kurniawan. 2003. "Low-cost adsorbents for heavy metals uptake from contaminated water: a review." *Journal of hazardous materials* 97 (1-3): 219-243.
- Babel, S. and T.A. Kurniawan. 2004. "Cr(VI) removal from synthetic wastewater using coconut shell charcoal and commercial activated carbon modified with oxidizing agents and/or chitosan." *Chemosphere* 54 (7): 951-967. doi: <https://doi.org/10.1016/j.chemosphere.2003.10.001>.
- Bailey, S.E., T.J. Olin, R.M. Bricka and D.D. Adrian. 1999. "A review of potentially low-cost sorbents for heavy metals." *Water research* 33 (11): 2469-2479.
- Banerjee, M., N. Bar, R.K. Basu and S.K. Das. 2018. "Removal of Cr (VI) from its aqueous solution using green adsorbent pistachio shell: a fixed bed column study and GA-ANN modeling." *Water Conservation Science and Engineering* 3 (1): 19-31.
- Banerjee, S. and M. Chattopadhyaya. 2017. "Adsorption characteristics for the removal of a toxic dye, tartrazine from aqueous solutions by a low cost agricultural by-product." *Arabian Journal of Chemistry* 10: S1629-S1638.
- Barakat, M., Y. Chen and C. Huang. 2004. "Removal of toxic cyanide and Cu (II) Ions from water by illuminated TiO<sub>2</sub> catalyst." *Applied Catalysis B: Environmental* 53 (1): 13-20.
- Barakat, M. and R. Kumar. 2015. "Synthesis and characterization of porous magnetic silica composite for the removal of heavy metals from aqueous solution." *Journal of Industrial and Engineering Chemistry* 23: 93-99.
- Baran, A., E. Bıçak, Ş.H. Baysal and S. Önal. 2007. "Comparative studies on the adsorption of Cr (VI) ions on to various sorbents." *Bioresource technology* 98 (3): 661-665.
- Barquilha, C., E. Cossich, C. Tavares and E. Silva. 2017. "Biosorption of nickel (II) and copper (II) ions in batch and fixed-bed columns by free and immobilized marine algae *Sargassum* sp." *Journal of Cleaner Production* 150: 58-64.
- Barrett, E.P., L.G. Joyner and P.P. Halenda. 1951. "The Determination of Pore Volume and Area Distributions in Porous Substances. I. Computations from Nitrogen Isotherms." *Journal of the American Chemical Society* 73 (1): 373-380. doi: 10.1021/ja01145a126.
- Basci, N., E. Kocadagistan and B. Kocadagistan. 2004. "Biosorption of copper (II) from aqueous solutions by wheat shell." *Desalination* 164 (2): 135-140.

- Basso, M.C., E.G. Cerrella and A.L. Cukierman. 2002. "Lignocellulosic Materials as Potential Biosorbents of Trace Toxic Metals from Wastewater." *Industrial & Engineering Chemistry Research* 41 (15): 3580-3585. doi: 10.1021/ie020023h.
- Behzadian, M., R.B. Kazemzadeh, A. Albadvi and M. Aghdasi. 2010. "PROMETHEE: A comprehensive literature review on methodologies and applications." *European journal of Operational research* 200 (1): 198-215.
- Belkacem, M., M. Khodir and S. Abdelkrim. 2008. "Treatment characteristics of textile wastewater and removal of heavy metals using the electroflotation technique." *Desalination* 228 (1-3): 245-254.
- Bentahar, Y., C. Hurel, K. Draoui, S. Khairoun and N. Marmier. 2016. "Adsorptive properties of Moroccan clays for the removal of arsenic (V) from aqueous solution." *Applied Clay Science* 119: 385-392.
- Bernardin Jr, F. 1985. "Experimental design and testing of adsorption and adsorbates." *Adsorption technology: a step-by-step approach to process evaluation and application*. New York: 37-90.
- Beyersmann, D. and A. Hartwig. 2008. "Carcinogenic metal compounds: recent insight into molecular and cellular mechanisms." *Archives of toxicology* 82 (8): 493.
- Bhaumik, M., K. Setshedi, A. Maity and M.S. Onyango. 2013. "Chromium (VI) removal from water using fixed bed column of polypyrrole/Fe<sub>3</sub>O<sub>4</sub> nanocomposite." *Separation and Purification Technology* 110: 11-19.
- Birch, G. and A. Scollen. 2003. "Heavy metals in road dust, gully pots and parkland soils in a highly urbanised sub-catchment of Port Jackson, Australia." *Soil Research* 41 (7): 1329-1342.
- Biswas, S. and U. Mishra. 2015. "Continuous fixed-bed column study and adsorption modeling: removal of lead ion from aqueous solution by charcoal originated from chemical carbonization of rubber wood sawdust." *Journal of Chemistry* 2015.
- Bo, A., S. Sarina, H. Liu, Z. Zheng, Q. Xiao, Y. Gu, G.A. Ayoko and H. Zhu. 2016. "Efficient Removal of Cationic and Anionic Radioactive Pollutants from Water Using Hydrotalcite-Based Getters." *ACS Applied Materials & Interfaces* 8 (25): 16503-16510. doi: 10.1021/acsami.6b04632.

- Boehm, H.-P., E. Diehl, W. Heck and R. Sappok. 1964. "Surface Oxides of Carbon 3 (10): 669-677. doi: doi:10.1002/anie.196406691.
- Boehm, H. 1994. "Some aspects of the surface chemistry of carbon blacks and other carbons." *Carbon* 32 (5): 759-769.
- Bose, S., J. Darsell, M. Kintner, H. Hosick and A. Bandyopadhyay. 2003. "Pore size and pore volume effects on alumina and TCP ceramic scaffolds." *Materials Science and Engineering: C* 23 (4): 479-486. doi: [https://doi.org/10.1016/S0928-4931\(02\)00129-7](https://doi.org/10.1016/S0928-4931(02)00129-7).
- Bosma, J. and J. Wesselingh. 1998. "pH dependence of ion-exchange equilibrium of proteins." *AIChE journal* 44 (11): 2399-2409.
- Bradl, H. 2002. "Adsorption of heavy metal ions on clays": Marcel Dekker, Inc., New York.
- Bradl, H.B. 2004. "Adsorption of heavy metal ions on soils and soils constituents." *Journal of Colloid and Interface Science* 277 (1): 1-18. doi: <https://doi.org/10.1016/j.jcis.2004.04.005>.
- Brahmaiah, T., L. Spurthi, K. Chandrika, S. Ramanaiah and K. Prasad. 2015. "Kinetics of Heavy Metal (Cr & Ni) Removal from the Wastewater by Useing Low Cost Adsorbent." *World Journal of Pharmacy and Pharmaceutical Sciences* 4 (11): 1600-1610.
- Brans, J.-P., P. Vincke and B. Mareschal. 1986. "How to select and how to rank projects: The PROMETHEE method." *European journal of operational research* 24 (2): 228-238.
- Bro, R. and A.K. Smilde. 2003. "Centering and scaling in component analysis." *Journal of Chemometrics* 17 (1): 16-33.
- Bruce, P. and A. Bruce. 2017. *Practical Statistics for Data Scientists: 50 Essential Concepts*: " O'Reilly Media, Inc."
- Brunauer, S., P.H. Emmett and E. Teller. 1938. "Adsorption of Gases in Multimolecular Layers." *Journal of the American Chemical Society* 60 (2): 309-319. doi: 10.1021/ja01269a023.
- Bulgariu, D. and L. Bulgariu. 2013. "Sorption of Pb(II) onto a mixture of algae waste biomass and anion exchanger resin in a packed-bed column." *Bioresource Technology* 129: 374-380. doi: <https://doi.org/10.1016/j.biortech.2012.10.142>.



- Burnham, K.P. and D.R. Anderson. 2004. "Multimodel inference: understanding AIC and BIC in model selection." *Sociological methods & research* 33 (2): 261-304.
- Carmody, O., R. Frost, Y. Xi and S. Kokot. 2007. "Adsorption of hydrocarbons on organo-clays—implications for oil spill remediation." *Journal of Colloid and Interface Science* 305 (1): 17-24.
- Carpenter, J. and J. Bithell. 2000. "Bootstrap confidence intervals: when, which, what? A practical guide for medical statisticians." *Statistics in medicine* 19 (9): 1141-1164.
- Cavalcante Jr, C. 2000. "Industrial adsorption separation processes: Fundamentals, modeling and applications." *Latin American Applied Research* 30 (4): 357-364.
- CEA. 2015. "Central Environmental Authority, Sri Lanka, A report submitted by Environment protection License division.
- Centeno, J.A., F.G. Mullick, L. Martinez, N.P. Page, H. Gibb, D. Longfellow, C. Thompson and E.R. Ladich. 2002. "Pathology related to chronic arsenic exposure." *Environmental health perspectives* 110 (suppl 5): 883-886.
- Cerato, A.B. and A.J. Luttenegger. 2002. "Determination of surface area of fine-grained soils by the ethylene glycol monoethyl ether (EGME) method." *Geotechnical Testing Journal* 25 (3): 315-321.
- Chatterjee, S., S. Mondal and S. De. 2018. "Design and scaling up of fixed bed adsorption columns for lead removal by treated laterite." *Journal of Cleaner Production* 177: 760-774. doi: <https://doi.org/10.1016/j.jclepro.2017.12.249>.
- Chen, C.-Y., C.-L. Chiang and C.-R. Chen. 2007. "Removal of heavy metal ions by a chelating resin containing glycine as chelating groups." *Separation and Purification Technology* 54 (3): 396-403.
- Chen, J.-d., J.-x. Yu, F. Wang, J.-q. Tang, Y.-f. Zhang, Y.-l. Xu and R.-a. Chi. 2017. "Selective adsorption and recycle of Cu<sup>2+</sup> from aqueous solution by modified sugarcane bagasse under dynamic condition." *Environmental Science and Pollution Research* 24 (10): 9202-9209.
- Chen, S., Q. Yue, B. Gao, Q. Li, X. Xu and K. Fu. 2012. "Adsorption of hexavalent chromium from aqueous solution by modified corn stalk: A fixed-bed column



- study." *Bioresource Technology* 113: 114-120. doi: <https://doi.org/10.1016/j.biortech.2011.11.110>.
- Cheraghi, E., E. Ameri and A. Moheb. 2015. "Adsorption of cadmium ions from aqueous solutions using sesame as a low-cost biosorbent: kinetics and equilibrium studies." *International journal of environmental science and technology* 12 (8): 2579-2592.
- Cherdchoo, W., S. Nithettham and J. Charoenpanich. 2019. "Removal of Cr(VI) from synthetic wastewater by adsorption onto coffee ground and mixed waste tea." *Chemosphere* 221: 758-767. doi: <https://doi.org/10.1016/j.chemosphere.2019.01.100>.
- Chorover, J. and M.L. Brusseau. 2008. "Kinetics of sorption—desorption." In *Kinetics of water-rock interaction*, 109-149: Springer.
- Chowdhury, Z., S. Zain, A. Rashid, R. Rafique and K. Khalid. 2012. "Breakthrough curve analysis for column dynamics sorption of Mn (II) ions from wastewater by using Mangostana garcinia peel-based granular-activated carbon." *Journal of chemistry* 2013.
- Chuah, T.G., A. Jumariah, I. Azni, S. Katayon and S.Y. Thomas Choong. 2005. "Rice husk as a potentially low-cost biosorbent for heavy metal and dye removal: an overview." *Desalination* 175 (3): 305-316. doi: <https://doi.org/10.1016/j.desal.2004.10.014>.
- Churchman, G., W. Gates, B. Theng and G. Yuan. 2006. ".1 clays and clay minerals for pollution control." *Developments in clay science* 1: 625-675.
- Dąbrowski, A., Z. Hubicki, P. Podkościelny and E. Robens. 2004. "Selective removal of the heavy metal ions from waters and industrial wastewaters by ion-exchange method." *Chemosphere* 56 (2): 91-106.
- Dai, M. 1994. "The Effect of Zeta Potential of Activated Carbon on the Adsorption of Dyes from Aqueous Solution: I. The Adsorption of Cationic Dyes: Methyl Green and Methyl Violet." *Journal of Colloid and Interface Science* 164 (1): 223-228. doi: <https://doi.org/10.1006/jcis.1994.1160>.
- Dai, Y., Q. Sun, W. Wang, L. Lu, M. Liu, J. Li, S. Yang, et al. 2018. "Utilizations of agricultural waste as adsorbent for the removal of contaminants: A review." *Chemosphere* 211: 235-253. doi: <https://doi.org/10.1016/j.chemosphere.2018.06.179>.

- Dakova, I., I. Karadjova, I. Ivanov, V. Georgieva, B. Evtimova and G. Georgiev. 2007. "Solid phase selective separation and preconcentration of Cu (II) by Cu (II)-imprinted polymethacrylic microbeads." *Analytica chimica acta* 584 (1): 196-203.
- Das, B.M. and K. Sobhan. 2013. *Principles of geotechnical engineering*: Cengage learning.
- Davis, T.A., B. Volesky and A. Mucci. 2003. "A review of the biochemistry of heavy metal biosorption by brown algae." *Water research* 37 (18): 4311-4330.
- De Gisi, S., G. Lofrano, M. Grassi and M. Notarnicola. 2016. "Characteristics and adsorption capacities of low-cost sorbents for wastewater treatment: a review." *Sustainable Materials and Technologies* 9: 10-40.
- De Villiers, P.G.R., J. Van Deventer and L. Lorenzen. 1997. "The use of ion-exchange resins for the recovery of valuable species from slurries of sparingly soluble solids." *Minerals engineering* 10 (9): 929-945.
- Debnath, S., K. Biswas and U.C. Ghosh. 2010. "Removal of Ni (II) and Cr (VI) with Titanium (IV) Oxide Nanoparticle Agglomerates in Fixed-Bed Columns." *Ind. Eng. Chem. Res.* 49: 2031.
- Deepatana, A. and M. Valix. 2006. "Recovery of nickel and cobalt from organic acid complexes: Adsorption mechanisms of metal-organic complexes onto aminophosphonate chelating resin." *Journal of hazardous materials* 137 (2): 925-933.
- Del Campillo, M., S. Van der Zee and J. Torrent. 1999. "Modelling long-term phosphorus leaching and changes in phosphorus fertility in excessively fertilized acid sandy soils." *European Journal of Soil Science* 50 (3): 391-399.
- Deletic, A. and D.W. Orr. 2005. "Pollution buildup on road surfaces." *Journal of Environmental Engineering* 131 (1): 49-59.
- Demirbas, A. 2008. "Heavy metal adsorption onto agro-based waste materials: a review." *Journal of hazardous materials* 157 (2-3): 220-229.
- Der Kiureghian, A. and O. Ditlevsen. 2009. "Aleatory or epistemic? Does it matter?" *Structural Safety* 31 (2): 105-112.
- Dermont, G., M. Bergeron, G. Mercier and M. Richer-Lafleche. 2008. "Soil washing for metal removal: a review of physical/chemical technologies and field applications." *Journal of hazardous materials* 152 (1): 1-31.

- Dimitriu, D., M. Aflori, L. Ivan, C. Ionita and R. Schrittwieser. 2007. "Common physical mechanism for concentric and non-concentric multiple double layers in plasma." *Plasma Physics and Controlled Fusion* 49 (3): 237.
- Ding, Y., D. Jing, H. Gong, L. Zhou and X. Yang. 2012. "Biosorption of aquatic cadmium (II) by unmodified rice straw." *Bioresource technology* 114: 20-25.
- Dizge, N., E. Demirbas and M. Kobya. 2009. "Removal of thiocyanate from aqueous solutions by ion exchange." *Journal of hazardous materials* 166 (2-3): 1367-1376.
- Dong, R., D. Goldfarb, M. Moseley, Z. Luz and H. Zimmermann. 1984. "Translational diffusion in discotic mesophases studied by the nuclear magnetic resonance pulsed field gradient method." *The Journal of Physical Chemistry* 88 (14): 3148-3152.
- Dong, Z. and L. Zhao. 2018. "Covalently bonded ionic liquid onto cellulose for fast adsorption and efficient separation of Cr (VI): Batch, column and mechanism investigation." *Carbohydrate polymers* 189: 190-197.
- Donia, A.M., A.A. Atia, H. El-Boraey and D.H. Mabrouk. 2006. "Uptake studies of copper (II) on glycidyl methacrylate chelating resin containing Fe<sub>2</sub>O<sub>3</sub> particles." *Separation and purification technology* 49 (1): 64-70.
- Dorado, A.D., X. Gamisans, C. Valderrama, M. Solé and C. Lao. 2014. "Cr (III) removal from aqueous solutions: a straightforward model approaching of the adsorption in a fixed-bed column." *Journal of Environmental Science and Health, Part A* 49 (2): 179-186.
- Du, Z.H., M.C. Jia and J.F. Men. 2014. "Removal of cesium from aqueous solution using PAN-based ferrocyanide composite spheres: Adsorption on a fixed-bed column." In *Applied Mechanics and Materials*, edited, 259-263: Trans Tech Publ.
- Dubey, A. and S. Shiwani. 2012. "Adsorption of lead using a new green material obtained from Portulaca plant." *International Journal of Environmental Science and Technology* 9 (1): 15-20. doi: 10.1007/s13762-011-0012-8.
- Dudu, T.E., M. Sahiner, D. Alpaslan, S. Demirci and N. Aktas. 2015. "Removal of As (V), Cr (III) and Cr (VI) from aqueous environments by poly (acrylonitril-co-acrylamidopropyl-trimethyl ammonium chloride)-based hydrogels." *Journal of environmental management* 161: 243-251.

- Ebrahimian Pirbazari, A., E. Saberikhah, M. Badrouh and M.S. Emami. 2014. "Alkali treated Foumanat tea waste as an efficient adsorbent for methylene blue adsorption from aqueous solution." *Water Resources and Industry* 6: 64-80. doi: <https://doi.org/10.1016/j.wri.2014.07.003>.
- Efron, B. 1979. "Bootstrap Methods: Another Look at the Jackknife." *The Annals of Statistics*: 1-26.
- Efron, B. and R. Tibshirani. 1986. "Bootstrap methods for standard errors, confidence intervals, and other measures of statistical accuracy." *Statistical science*: 54-75.
- Efron, B. and R.J. Tibshirani. 1993. "Permutation tests." In *An introduction to the bootstrap*, 202-219: Springer.
- Einax, J.W., D. Truckenbrodt and O. Kampe. 1998. "River Pollution Data Interpreted by Means of Chemometric Methods." *Microchemical Journal* 58 (3): 315-324. doi: <https://doi.org/10.1006/mchj.1997.1560>.
- Eisenbud, M., Y. Mochizuki, A.S. Goldin and G.R. Laurer. 1962. "Iodine-131 Dose from Soviet Nuclear Tests." *Science* 136: 370.
- Eisenman, G. 1962. "Cation selective glass electrodes and their mode of operation." *Biophysical journal* 2 (2): 259-323.
- EPA, U. 1983. "Methods for chemical analysis of water and wastes." *Environmental Monitoring and Support Laboratory*.
- Erdem, E., N. Karapinar and R. Donat. 2004. "The removal of heavy metal cations by natural zeolites." *Journal of Colloid and Interface Science* 280 (2): 309-314. doi: <https://doi.org/10.1016/j.jcis.2004.08.028>.
- Factor-Litvak, P., V. Slavkovich, X. Liu, D. Popovac, E. Preteni, S. Capuni-Paracka, S. Hadzialjevic, et al. 1998. "Hyperproduction of erythropoietin in nonanemic lead-exposed children." *Environmental Health Perspectives* 106 (6): 361-364. <http://www.ncbi.nlm.nih.gov/pmc/articles/PMC1532998/>.
- Fahmi, A.H., A.W. Samsuri, H. Jol and D. Singh. 2018. "Bioavailability and leaching of Cd and Pb from contaminated soil amended with different sizes of biochar." *Royal Society open science* 5 (11): 181328.
- Fan, Q., J. Sun, L. Chu, L. Cui, G. Quan, J. Yan, Q. Hussain and M. Iqbal. 2018. "Effects of chemical oxidation on surface oxygen-containing functional groups

- and adsorption behavior of biochar." *Chemosphere* 207: 33-40. doi: <https://doi.org/10.1016/j.chemosphere.2018.05.044>.
- Fanning, P.E. and M.A. Vannice. 1993. "A DRIFTS study of the formation of surface groups on carbon by oxidation." *Carbon* 31 (5): 721-730. doi: [https://doi.org/10.1016/0008-6223\(93\)90009-Y](https://doi.org/10.1016/0008-6223(93)90009-Y).
- Farquhar, M.L., D.J. Vaughan, C.R. Hughes, J.M. Charnock and K.E. England. 1997. "Experimental studies of the interaction of aqueous metal cations with mineral substrates: Lead, cadmium, and copper with perthitic feldspar, muscovite, and biotite." *Geochimica et Cosmochimica Acta* 61 (15): 3051-3064.
- Fat'hi, M.R., A. Asfaram, A. Hadipour and M. Roosta. 2014. "Kinetics and thermodynamic studies for removal of acid blue 129 from aqueous solution by almond shell." *Journal of Environmental Health Science and Engineering* 12 (1): 62.
- Feng, N., X. Guo and S. Liang. 2009. "Adsorption study of copper (II) by chemically modified orange peel." *Journal of Hazardous Materials* 164 (2-3): 1286-1292.
- Filep, G. 1999. *Soil chemistry: Processes and constituents*.
- Fiol, N., I. Villaescusa, M. Martínez, N. Miralles, J. Poch and J. Serarols. 2006. "Sorption of Pb (II), Ni (II), Cu (II) and Cd (II) from aqueous solution by olive stone waste." *Separation and Purification technology* 50 (1): 132-140.
- Foo, K.Y. and B.H. Hameed. 2010. "Insights into the modeling of adsorption isotherm systems." *Chemical engineering journal* 156 (1): 2-10.
- Freundlich, H. 1906. "Over the adsorption in solution." *J. Phys. Chem* 57 (385471): 1100-1107.
- Fu, F. and Q. Wang. 2011. "Removal of heavy metal ions from wastewaters: A review." *Journal of Environmental Management* 92 (3): 407-418. doi: <https://doi.org/10.1016/j.jenvman.2010.11.011>.
- Gardea-Torresdey, J., M. Hejazi, K. Tiemann, J. Parsons, M. Duarte-Gardea and J. Henning. 2002. "Use of hop (*Humulus lupulus*) agricultural by-products for the reduction of aqueous lead (II) environmental health hazards." *Journal of hazardous materials* 91 (1-3): 95-112.
- Garg, U., M. Kaur, G. Jawa, D. Sud and V. Garg. 2008. "Removal of cadmium (II) from aqueous solutions by adsorption on agricultural waste biomass." *Journal of hazardous materials* 154 (1-3): 1149-1157.

- Gautam, R.K., A. Mudhoo, G. Lofrano and M.C. Chattopadhyaya. 2014. "Biomass-derived biosorbents for metal ions sequestration: Adsorbent modification and activation methods and adsorbent regeneration." *Journal of Environmental Chemical Engineering* 2 (1): 239-259. doi: <https://doi.org/10.1016/j.jece.2013.12.019>.
- Genç-Fuhrman, H., P.S. Mikkelsen and A. Ledin. 2007. "Simultaneous removal of As, Cd, Cr, Cu, Ni and Zn from stormwater: Experimental comparison of 11 different sorbents." *Water research* 41 (3): 591-602.
- Ghaedi, M., A. Ghaedi, F. Abdi, M. Roosta, A. Vafaei and A. Asghari. 2013. "Principal component analysis-adaptive neuro-fuzzy inference system modeling and genetic algorithm optimization of adsorption of methylene blue by activated carbon derived from Pistacia khinjuk." *Ecotoxicology and environmental safety* 96: 110-117.
- Girish, C. and V. Ramachandra Murty. 2014. "Adsorption of phenol from aqueous solution using Lantana camara, forest waste: kinetics, isotherm, and thermodynamic studies." *International scholarly research notices* 2014.
- Gnanasambandam, R. and A. Proctor. 2000. "Determination of pectin degree of esterification by diffuse reflectance Fourier transform infrared spectroscopy." *Food Chemistry* 68 (3): 327-332. doi: [https://doi.org/10.1016/S0308-8146\(99\)00191-0](https://doi.org/10.1016/S0308-8146(99)00191-0).
- Grim, R.E. 1962. "Applied Clay Mineralogy McGraw-Hill Book Company." *New York, USA*.
- Guechi, E.-K. and O. Hamdaoui. 2016. "Biosorption of methylene blue from aqueous solution by potato (*Solanum tuberosum*) peel: equilibrium modelling, kinetic, and thermodynamic studies." *Desalination and Water Treatment* 57 (22): 10270-10285.
- Gunawardana, C., A. Goonetilleke, P. Egodawatta and L.A. Dawes. 2011. "Influence of organic matter in road deposited particulates in heavy metal accumulation and transport.
- Gundogdu, A., C. Duran, H.B. Senturk, M. Soylak, M. Imamoglu and Y. Onal. 2013. "Physicochemical characteristics of a novel activated carbon produced from tea industry waste." *Journal of Analytical and Applied Pyrolysis* 104: 249-259. doi: <https://doi.org/10.1016/j.jaap.2013.07.008>.
- Gupta, N. and R. Sen. 2017. "Kinetic and equilibrium modelling of Cu (II) adsorption from aqueous solution by chemically modified Groundnut husk (*Arachis*

- hypogaea)." *Journal of Environmental Chemical Engineering* 5 (5): 4274-4281. doi: <https://doi.org/10.1016/j.jece.2017.07.048>.
- Gupta, V., A. Shrivastava and N. Jain. 2001. "Biosorption of chromium (VI) from aqueous solutions by green algae *Spirogyra* species." *Water Research* 35 (17): 4079-4085.
- Gupta, V.K., P. Carrott, M. Ribeiro Carrott and Suhas. 2009. "Low-cost adsorbents: growing approach to wastewater treatment—a review." *Critical reviews in environmental science and technology* 39 (10): 783-842.
- Hamdaoui, O. 2009. "Removal of copper (II) from aqueous phase by Purolite C100-MB cation exchange resin in fixed bed columns: Modeling." *Journal of hazardous materials* 161 (2-3): 737-746.
- Han, Y., A. Boateng, P. Qi, I. Lima and J. Chang. 2013. *Heavy Metal and Phenol Adsorptive Properties of Biochars from Pyrolyzed Switchgrass and Woody Biomass in Correlation with Surface Properties*. Vol. 118C. doi: 10.1016/j.jenvman.2013.01.001.
- Hancock, R.D. and F. Marsicano. 1978. "Parametric correlation of formation constants in aqueous solution. 1. Ligands with small donor atoms." *Inorganic Chemistry* 17 (3): 560-564.
- Hancock, R.D. and A.E. Martell. 1996. "Hard and soft acid-base behavior in aqueous solution: steric effects make some metal ions hard: a quantitative scale of hardness-softness for acids and bases." *Journal of chemical education* 73 (7): 654.
- Hansen, H.K., F. Arancibia and C. Gutiérrez. 2010. "Adsorption of copper onto agriculture waste materials." *Journal of Hazardous Materials* 180 (1): 442-448. doi: <https://doi.org/10.1016/j.jhazmat.2010.04.050>.
- Haque, R. and R. Sexton. 1968. "Kinetic and equilibrium study of the adsorption of 2, 4-dichlorophenoxy acetic acid on some surfaces." *Journal of colloid and interface science* 27 (4): 818-827.
- Hasfalina, C., R. Maryam, C. Luqman and M. Rashid. 2012. "Adsorption of copper (II) from aqueous medium in fixed-bed column by kenaf fibres." *APCBEE procedia* 3: 255-263.
- He, J., A. Cui, F. Ni, S. Deng, F. Shen and G. Yang. 2018. "A novel 3D yttrium based-graphene oxide-sodium alginate hydrogel for remarkable adsorption of fluoride from water." *Journal of colloid and interface science* 531: 37-46.



- Hegazi, H.A. 2013. "Removal of heavy metals from wastewater using agricultural and industrial wastes as adsorbents." *HBRC Journal* 9 (3): 276-282. doi: <https://doi.org/10.1016/j.hbrcj.2013.08.004>.
- Herngren, L., A. Goonetilleke and G.A. Ayoko. 2006. "Analysis of heavy metals in road-deposited sediments." *Analytica Chimica Acta* 571 (2): 270-278.
- Herrmann, J.-M. 1999. "Heterogeneous photocatalysis: fundamentals and applications to the removal of various types of aqueous pollutants." *Catalysis today* 53 (1): 115-129.
- Hertz-Picciotto, I. 2000. "The evidence that lead increases the risk for spontaneous abortion." *American Journal of Industrial Medicine* 38 (3): 300-309. Accessed 2018/09/27. doi: 10.1002/1097-0274(200009)38:3<300::AID-AJIM9>3.0.CO;2-C.
- Ho, Y.-S. and G. McKay. 1998. "Sorption of dye from aqueous solution by peat." *Chemical engineering journal* 70 (2): 115-124.
- Ho, Y.-S. and G. McKay. 2002. "Application of kinetic models to the sorption of copper (II) on to peat." *Adsorption Science & Technology* 20 (8): 797-815.
- Ho, Y.S. and G. McKay. 1999. "Pseudo-second order model for sorption processes." *Process Biochemistry* 34 (5): 451-465. doi: [https://doi.org/10.1016/S0032-9592\(98\)00112-5](https://doi.org/10.1016/S0032-9592(98)00112-5).
- Hofer, E., M. Kloos, B. Krzykacz-Hausmann, J. Peschke and M. Wolterreck. 2002. "An approximate epistemic uncertainty analysis approach in the presence of epistemic and aleatory uncertainties." *Reliability Engineering & System Safety* 77 (3): 229-238.
- Holan, Z.n. and B.n. Volesky. 1995. "Accumulation of cadmium, lead, and nickel by fungal and wood biosorbents." *Applied Biochemistry and Biotechnology* 53 (2): 133-146.
- Hossain, M., H. Ngo, W. Guo and T. Setiadi. 2012. "Adsorption and desorption of copper (II) ions onto garden grass." *Bioresource technology* 121: 386-395.
- Huang, C.-C., C.-H. Chen and S.-M. Chu. 2006. "Effect of moisture on H<sub>2</sub>S adsorption by copper impregnated activated carbon." *Journal of hazardous materials* 136 (3): 866-873.



- Hui, K., C.Y.H. Chao and S. Kot. 2005. "Removal of mixed heavy metal ions in wastewater by zeolite 4A and residual products from recycled coal fly ash." *Journal of Hazardous Materials* 127 (1-3): 89-101.
- Ibrahim, H.S., T.S. Jamil and E.Z. Hegazy. 2010. "Application of zeolite prepared from Egyptian kaolin for the removal of heavy metals: II. Isotherm models." *Journal of Hazardous materials* 182 (1-3): 842-847.
- Iftekhhar, S., D.L. Ramasamy, V. Srivastava, M.B. Asif and M. Sillanpää. 2018. "Understanding the factors affecting the adsorption of Lanthanum using different adsorbents: A critical review." *Chemosphere* 204: 413-430. doi: <https://doi.org/10.1016/j.chemosphere.2018.04.053>.
- Inglezakis, V.J. and S.G. Pouloupoulos. 2006. "2 - Adsorption, Ion Exchange, and Catalysis." In *Adsorption, Ion Exchange and Catalysis*, edited by Vassilis J. Inglezakis and Stavros G. Pouloupoulos, 31-56. Amsterdam: Elsevier. doi: <https://doi.org/10.1016/B978-044452783-7/50002-1>.
- Iqbal, M. and R.G.J. Edyvean. 2005. "Loofa sponge immobilized fungal biosorbent: A robust system for cadmium and other dissolved metal removal from aqueous solution." *Chemosphere* 61 (4): 510-518. doi: <https://doi.org/10.1016/j.chemosphere.2005.02.060>.
- Iqbal, M., A. Saeed and N. Akhtar. 2002. "Petiolar felt-sheath of palm: a new biosorbent for the removal of heavy metals from contaminated water." *Bioresource Technology* 81 (2): 151-153.
- Iqbal, M., A. Saeed and I. Kalim. 2009. "Characterization of adsorptive capacity and investigation of mechanism of Cu<sup>2+</sup>, Ni<sup>2+</sup> and Zn<sup>2+</sup> adsorption on mango peel waste from constituted metal solution and genuine electroplating effluent." *Separation Science and Technology* 44 (15): 3770-3791.
- Ismail, A.A., R. Mohamed, I. Ibrahim, G. Kini and B. Koopman. 2010. "Synthesis, optimization and characterization of zeolite A and its ion-exchange properties." *Colloids and Surfaces A: Physicochemical and Engineering Aspects* 366 (1-3): 80-87.
- Jacobasch, H.-J., F. Simon and P. Weidenhammer. 1998. "Adsorption of ions onto polymer surfaces and its influence on zeta potential and adhesion phenomena." *Colloid and polymer science* 276 (5): 434-442.
- Jain, C.K. and D. Ram. 1997. "Adsorption of lead and zinc on bed sediments of the river Kali." *Water Research* 31 (1): 154-162. doi: [https://doi.org/10.1016/S0043-1354\(96\)00232-1](https://doi.org/10.1016/S0043-1354(96)00232-1).

- Jamil, T.S., H.S. Ibrahim, I.A. El-Maksoud and S. El-Wakeel. 2010. "Application of zeolite prepared from Egyptian kaolin for removal of heavy metals: I. Optimum conditions." *Desalination* 258 (1-3): 34-40.
- Jiang, J.-Q., C. Cooper and S. Ouki. 2002. "Comparison of modified montmorillonite adsorbents: part I: preparation, characterization and phenol adsorption." *Chemosphere* 47 (7): 711-716.
- Jiang, J., R.-k. Xu, T.-y. Jiang and Z. Li. 2012. "Immobilization of Cu (II), Pb (II) and Cd (II) by the addition of rice straw derived biochar to a simulated polluted Ultisol." *Journal of hazardous materials* 229: 145-150.
- Johnston, A.W. and A.F. Johnston. 1996. "Multi-stage microbiological water filter": Google Patents.
- Jolliffe, I. 2011. *Principal component analysis*: Springer.
- Joseph, L., B.-M. Jun, J.R.V. Flora, C.M. Park and Y. Yoon. 2019. "Removal of heavy metals from water sources in the developing world using low-cost materials: A review." *Chemosphere* 229: 142-159. doi: <https://doi.org/10.1016/j.chemosphere.2019.04.198>.
- Kadirvelu, K., K. Thamaraiselvi and C. Namasivayam. 2001. "Removal of heavy metals from industrial wastewaters by adsorption onto activated carbon prepared from an agricultural solid waste." *Bioresource technology* 76 (1): 63-65.
- Kafshgari, M.H., M. Mansouri, M. Khorram and S.R. Kashani. 2013. "Kinetic modeling: a predictive tool for the adsorption of zinc ions onto calcium alginate beads." *International Journal of Industrial Chemistry* 4 (1): 5.
- Kajitvichyanukul, P., J. Ananpattarachai and S. Pongpom. 2005. "Sol-gel preparation and properties study of TiO<sub>2</sub> thin film for photocatalytic reduction of chromium (VI) in photocatalysis process." *Science and Technology of Advanced Materials* 6 (3-4): 352.
- Kammerer, J., D.R. Kammerer, U. Jensen and R. Carle. 2010. "Interaction of apple polyphenols in a multi-compound system upon adsorption onto a food-grade resin." *Journal of food engineering* 96 (4): 544-554.
- Kannan, N. and G. Rengasamy. 2005. "Comparison of cadmium ion adsorption on various activated carbons." *Water, air, and soil pollution* 163 (1-4): 185-201.

- Kapur, M. and M.K. Mondal. 2016. "Design and model parameters estimation for fixed-bed column adsorption of Cu (II) and Ni (II) ions using magnetized saw dust." *Desalination and Water Treatment* 57 (26): 12192-12203.
- Karnitz Jr, O., L.V.A. Gurgel, J.C.P. De Melo, V.R. Botaro, T.M.S. Melo, R.P. de Freitas Gil and L.F. Gil. 2007. "Adsorption of heavy metal ion from aqueous single metal solution by chemically modified sugarcane bagasse." *Bioresource technology* 98 (6): 1291-1297.
- Kaul, B., R.S. Sandhu, C. Depratt and F. Reyes. 1999. "Follow-up screening of lead-poisoned children near an auto battery recycling plant, Haina, Dominican Republic." *Environmental Health Perspectives* 107 (11): 917-920. <http://www.ncbi.nlm.nih.gov/pmc/articles/PMC1566703/>.
- Keller, H., D. Massart and J. Brans. 1991. "Multicriteria decision making: a case study." *Chemometrics and Intelligent laboratory systems* 11 (2): 175-189.
- Kennedy, B.A. 1990. "Society for Mining, Metallurgy and Exploration." *Inc., Littleton, Colorado*.
- Kesraoui-Ouki, S., C.R. Cheeseman and R. Perry. 1994. "Natural zeolite utilisation in pollution control: A review of applications to metals' effluents." *Journal of Chemical Technology & Biotechnology: International Research in Process, Environmental AND Clean Technology* 59 (2): 121-126.
- Khalil, W.A.-S., A. Goonetilleke, S. Kokot and S. Carroll. 2004. "Use of chemometrics methods and multicriteria decision-making for site selection for sustainable on-site sewage effluent disposal." *Analytica Chimica Acta* 506 (1): 41-56.
- Khamizov, R.K., D.A. Sveshnikova, A.E. Kucherova and L.A. Sinyaeva. 2018. "Kinetic Models of Batch Sorption in a Limited Volume." *Russian Journal of Physical Chemistry A* 92 (9): 1782-1789. doi: 10.1134/S0036024418090121.
- Khan, T.A. and V.V. Singh. 2010. "Removal of cadmium (II), lead (II), and chromium (VI) ions from aqueous solution using clay." *Toxicological and Environmental Chemistry* 92 (8): 1435-1446.
- Khan, U. and R.A.K. Rao. 2017. "A high activity adsorbent of chemically modified *Cucurbita moschata* (a novel adsorbent) for the removal of Cu (II) and Ni (II) from aqueous solution: Synthesis, characterization and metal removal efficiency." *Process Safety and Environmental Protection* 107: 238-258.

- Klopman, G. 1968. "Chemical reactivity and the concept of charge-and frontier-controlled reactions." *Journal of the American Chemical Society* 90 (2): 223-234.
- Kocaoba, S., Y. Orhan and T. Akyüz. 2007. "Kinetics and equilibrium studies of heavy metal ions removal by use of natural zeolite." *Desalination* 214 (1-3): 1-10.
- Kokot, S., G. King, H. Keller and D. Massart. 1992. "Microwave digestion: an analysis of procedures." *Analytica Chimica Acta* 259 (2): 267-279.
- Krishnan, K.A. and T. Anirudhan. 2003. "Removal of cadmium (II) from aqueous solutions by steam-activated sulphurised carbon prepared from sugar-cane bagasse pith: Kinetics and equilibrium studies." *Water Sa* 29 (2): 147-156.
- Krzanowski. 1979. "Between-Groups Comparison of Principal Components AU - Krzanowski, W. J." *Journal of the American Statistical Association* 74 (367): 703-707. doi: 10.1080/01621459.1979.10481674.
- Ku, W., R.H. Storer and C. Georgakis. 1995. "Disturbance detection and isolation by dynamic principal component analysis." *Chemometrics and Intelligent Laboratory Systems* 30 (1): 179-196. doi: [https://doi.org/10.1016/0169-7439\(95\)00076-3](https://doi.org/10.1016/0169-7439(95)00076-3).
- Ku, Y. and I.-L. Jung. 2001. "Photocatalytic reduction of Cr (VI) in aqueous solutions by UV irradiation with the presence of titanium dioxide." *Water research* 35 (1): 135-142.
- Kulkarni, S. and J. Kaware. 2014. "Isotherm and kinetics of phenol removal by adsorption-A Review." *International Journal of Research (IJR) Vol 1*: 287-293.
- Kumar, P.S., A.S. Deepthi, R. Bharani and G. Rakkesh. 2015. "Study of adsorption of Cu (II) ions from aqueous solution by surface-modified Eucalyptus globulus seeds in a fixed-bed column: experimental optimization and mathematical modeling." *Research on Chemical Intermediates* 41 (11): 8681-8698.
- Kundu, S. and A. Gupta. 2006. "Arsenic adsorption onto iron oxide-coated cement (IOCC): regression analysis of equilibrium data with several isotherm models and their optimization." *Chemical Engineering Journal* 122 (1-2): 93-106.
- Kurniawan, T.A., G.Y. Chan, W.-H. Lo and S. Babel. 2006. "Physico-chemical treatment techniques for wastewater laden with heavy metals." *Chemical engineering journal* 118 (1-2): 83-98.

- Kwak, J.-H., M.S. Islam, S. Wang, S.A. Messele, M.A. Naeth, M.G. El-Din and S.X. Chang. 2019. "Biochar properties and lead(II) adsorption capacity depend on feedstock type, pyrolysis temperature, and steam activation." *Chemosphere*. doi: <https://doi.org/10.1016/j.chemosphere.2019.05.128>.
- Lagergren, S. 1898. "Zur theorie der sogenannten adsorption geloster stoffe." *Kunliga svenska vetenskapsakademiens. Handlingar* 24: 1-39.
- Langmuir, I. 1916. "The constitution and fundamental properties of solids and liquids. Part I. Solids." *Journal of the American chemical society* 38 (11): 2221-2295.
- Largitte, L. and R. Pasquier. 2016. "A review of the kinetics adsorption models and their application to the adsorption of lead by an activated carbon." *Chemical Engineering Research and Design* 109: 495-504.
- Larous, S., A.-H. Meniai and M.B. Lehocine. 2005. "Experimental study of the removal of copper from aqueous solutions by adsorption using sawdust." *Desalination* 185 (1-3): 483-490.
- László, K., K. JOSEPOVITS and E. TOMBÁ CZ. 2002. "Analysis of active sites on synthetic carbon surfaces by various methods." In *Analytical Sciences/Supplements Proceedings of IUPAC International Congress on Analytical Sciences 2001 (ICAS 2001)*, edited, i1741-i1744: The Japan Society for Analytical Chemistry.
- Lazaridis, N. and D. Asouhidou. 2003. "Kinetics of sorptive removal of chromium (VI) from aqueous solutions by calcined Mg–Al–CO<sub>3</sub> hydrotalcite." *Water research* 37 (12): 2875-2882.
- Lee, C.-G., J.-H. Kim, J.-K. Kang, S.-B. Kim, S.-J. Park, S.-H. Lee and J.-W. Choi. 2015. "Comparative analysis of fixed-bed sorption models using phosphate breakthrough curves in slag filter media." *Desalination and Water Treatment* 55 (7): 1795-1805.
- Leung, W.C., M.-F. Wong, H. Chua, W. Lo, P. Yu and C. Leung. 2000. "Removal and recovery of heavy metals by bacteria isolated from activated sludge treating industrial effluents and municipal wastewater." *Water science and technology* 41 (12): 233-240.
- Li, W., H. Zhao, P. Teasdale, R. John and S. Zhang. 2002. "Synthesis and characterisation of a polyacrylamide–polyacrylic acid copolymer hydrogel for environmental analysis of Cu and Cd." *Reactive and Functional Polymers* 52 (1): 31-41.

- Li, Y.-H., S. Wang, Z. Luan, J. Ding, C. Xu and D. Wu. 2003. "Adsorption of cadmium(II) from aqueous solution by surface oxidized carbon nanotubes." *Carbon* 41 (5): 1057-1062. doi: [https://doi.org/10.1016/S0008-6223\(02\)00440-2](https://doi.org/10.1016/S0008-6223(02)00440-2).
- Li, Y., S.-L. Lau, M. Kayhanian and M.K. Stenstrom. 2006. "Dynamic characteristics of particle size distribution in highway runoff: Implications for settling tank design." *Journal of Environmental Engineering* 132 (8): 852-861.
- Liang, S., X. Guo and Q. Tian. 2011. "Adsorption of Pb<sup>2+</sup> and Zn<sup>2+</sup> from aqueous solutions by sulfured orange peel." *Desalination* 275 (1-3): 212-216.
- Lim, A.P. and A.Z. Aris. 2014. "Continuous fixed-bed column study and adsorption modeling: Removal of cadmium (II) and lead (II) ions in aqueous solution by dead calcareous skeletons." *Biochemical Engineering Journal* 87: 50-61.
- Liu, D. and D. Sun. 2012. "Modeling adsorption of Cu (II) using polyaniline-coated sawdust in a fixed-bed column." *Environmental Engineering Science* 29 (6): 461-465.
- Liu, H., Z. Zheng, D. Yang, X. Ke, E. Jaatinen, J.C. Zhao and H.Y. Zhu. 2010. "Coherent Interfaces between Crystals in Nanocrystal Composites." *ACS Nano* 4: 6219.
- Liu, Y., X. Chang, D. Yang, Y. Guo and S. Meng. 2005. "Highly selective determination of inorganic mercury (II) after preconcentration with Hg (II)-imprinted diazoaminobenzene–vinylpyridine copolymers." *Analytica Chimica Acta* 538 (1-2): 85-91.
- López-Cervantes, J., D.I. Sánchez-Machado, R.G. Sánchez-Duarte and M.A. Correa-Murrieta. 2018. "Study of a fixed-bed column in the adsorption of an azo dye from an aqueous medium using a chitosan–glutaraldehyde biosorbent." *Adsorption Science & Technology* 36 (1-2): 215-232.
- Loucks, D.P. and E. Van Beek. 2017. *Water resource systems planning and management: An introduction to methods, models, and applications*: Springer.
- Lourie, E. and E. Gjengedal. 2011. "Metal sorption by peat and algae treated peat: Kinetics and factors affecting the process." *Chemosphere* 85 (5): 759-764. doi: <https://doi.org/10.1016/j.chemosphere.2011.06.055>.
- Macharis, C., J. Springael, K. De Brucker and A. Verbeke. 2004. "PROMETHEE and AHP: The design of operational synergies in multicriteria analysis.:

- Strengthening PROMETHEE with ideas of AHP." *European Journal of Operational Research* 153 (2): 307-317.
- Mahalanobis, P.C. 1936. "On the generalized distance in statistics, edited: National Institute of Science of India.
- Maheshwari, U. and S. Gupta. 2016. "Removal of Cr (VI) from wastewater using activated neem bark in a fixed-bed column: interference of other ions and kinetic modelling studies." *Desalination and Water Treatment* 57 (18): 8514-8525.
- Malkoc, E. and Y. Nuhoglu. 2005. "Investigations of nickel (II) removal from aqueous solutions using tea factory waste." *Journal of hazardous materials* 127 (1-3): 120-128.
- Marchese, D., G. Bello, M. Greco, V. Lapenna, E. Rizzo and V. Telesca. 2008. "Self Potential Tomographic Technique to Detect Soil Water Movements in the Vadose Zone: Laboratory Measurements." *Environmental Semeiotics* 1: 137-153. doi: 10.3383/es.1.1.10.
- Marcus, Y. 1988. "Ionic radii in aqueous solutions." *Chemical Reviews* 88 (8): 1475-1498.
- Marcus, Y. 1991. "Thermodynamics of solvation of ions. Part 5.—Gibbs free energy of hydration at 298.15 K." *Journal of the Chemical Society, Faraday Transactions* 87 (18): 2995-2999.
- Mareschal, B. 2013. "Visual PROMETHEE 1.4 manual." *Visual PROMETHEE* 1.
- Marsh, H. and F. Rodríguez-Reinoso. 2006. "CHAPTER 4 - Characterization of Activated Carbon." In *Activated Carbon*, edited by Harry Marsh and Francisco Rodríguez-Reinoso, 143-242. Oxford: Elsevier Science Ltd. doi: <https://doi.org/10.1016/B978-008044463-5/50018-2>.
- Mavrov, V., T. Erwe, C. Blöcher and H. Chmiel. 2003. "Study of new integrated processes combining adsorption, membrane separation and flotation for heavy metal removal from wastewater." *Desalination* 157 (1-3): 97-104.
- McBride, M.B. 1994. "ENVIRONMENTAL CHEMISTRY OF SOILS.
- McConnell, R.L., D.C. Abel and D.C. Abel. 2013. *Environmental geology today*: Jones & Bartlett Publishers.



- Miessler, G., P. Fischer and D. Tarr. 2013. "Inorganic Chemistry, 5th": Pearson: London, England.
- Miguntanna, N.P., A. Goonetilleke, P. Egodawatta and S. Kokot. 2010. "Understanding nutrient build-up on urban road surfaces." *Journal of Environmental Sciences* 22 (6): 806-812.
- Miguntanna, N.S., P. Egodawatta, S. Kokot and A. Goonetilleke. 2010. "Determination of a set of surrogate parameters to assess urban stormwater quality." *Science of The Total Environment* 408 (24): 6251-6259. doi: <https://doi.org/10.1016/j.scitotenv.2010.09.015>.
- Milojković, J., L. Pezo, M. Stojanović, M. Mihajlović, Z. Lopičić, J. Petrović, M. Stanojević and M. Kragović. 2016. "Selected heavy metal biosorption by compost of *Myriophyllum spicatum*—a chemometric approach." *Ecological engineering* 93: 112-119.
- Min, S., J. Han, E. Shin and J. Park. 2004. "Improvement of cadmium ion removal by base treatment of juniper fiber." *Water Research* 38 (5): 1289-1295.
- Minceva, M., R. Fajgar, L. Markovska and V. Meshko. 2008. "Comparative study of Zn<sup>2+</sup>, Cd<sup>2+</sup>, and Pb<sup>2+</sup> removal from water solution using natural clinoptilolitic zeolite and commercial granulated activated carbon. Equilibrium of adsorption." *Separation Science and Technology* 43 (8): 2117-2143.
- Minceva, M., J. Taparcevska, L. Markovska, B. Koumanova and V. Meshko. 2008. "Adsorption kinetics of Pb<sup>2+</sup> onto natural zeolite." *Journal of the University of Chemical Technology and Metallurgy* 43 (1): 93-100.
- Miralles, N., C. Valderrama, I. Casas, M. Martínez and A. Florido. 2010. "Cadmium and Lead Removal from Aqueous Solution by Grape Stalk Wastes: Modeling of a Fixed-Bed Column." *Journal of Chemical & Engineering Data* 55 (9): 3548-3554. doi: 10.1021/jc100200w.
- Mohan, D. and K.P. Singh. 2002. "Single-and multi-component adsorption of cadmium and zinc using activated carbon derived from bagasse—an agricultural waste." *Water research* 36 (9): 2304-2318.
- Mohan, S. and G. Sreelakshmi. 2008. "Fixed bed column study for heavy metal removal using phosphate treated rice husk." *Journal of Hazardous Materials* 153 (1): 75-82. doi: <https://doi.org/10.1016/j.jhazmat.2007.08.021>.



- Mollah, M.Y.A., R. Schennach, J.R. Parga and D.L. Cocke. 2001. "Electrocoagulation (EC)—science and applications." *Journal of hazardous materials* 84 (1): 29-41.
- Monash, P. and G. Pugazhenti. 2010. "Investigation of equilibrium and kinetic parameters of methylene blue adsorption onto MCM-41." *Korean Journal of Chemical Engineering* 27 (4): 1184-1191.
- Moscatello, N., G. Swayambhu, C.H. Jones, J. Xu, N. Dai and B.A. Pfeifer. 2018. "Continuous removal of copper, magnesium, and nickel from industrial wastewater utilizing the natural product yersiniabactin immobilized within a packed-bed column." *Chemical Engineering Journal* 343: 173-179.
- Moyo, M., V.E. Pakade and S.J. Modise. 2017. "Biosorption of lead (II) by chemically modified *Mangifera indica* seed shells: adsorbent preparation, characterization and performance assessment." *Process Safety and Environmental Protection* 111: 40-51.
- Mozgawa, W. and T. Bajda. 2005. "Spectroscopic study of heavy metals sorption on clinoptilolite." *Physics and Chemistry of Minerals* 31 (10): 706-713.
- Murray, H.H. 2006. *Applied clay mineralogy: occurrences, processing and applications of kaolins, bentonites, palygorskitesepiolite, and common clays*. Vol. 2: Elsevier.
- Murzin, D.Y. and T. Salmi. 2005. *Catalytic kinetics*: Elsevier.
- Nagao, M. 1971. "Physisorption of water on zinc oxide surface." *The Journal of Physical Chemistry* 75 (25): 3822-3828.
- Naja, G., M. Vanessa and B. Volesky. 2010. "Biosorption, metal, encyclopedia of industrial biotechnology: bioprocess, bioseparation, and cell technology": New York: Wiley.
- Najam, R. and S.M.A. Andrabi. 2016. "Removal of Cu (II), Zn (II) and Cd (II) ions from aqueous solutions by adsorption on walnut shell-Equilibrium and thermodynamic studies: treatment of effluents from electroplating industry." *Desalination and Water Treatment* 57 (56): 27363-27373.
- Nandi, B.K., A. Goswami and M.K. Purkait. 2009. "Adsorption characteristics of brilliant green dye on kaolin." *Journal of Hazardous Materials* 161 (1): 387-395. doi: <https://doi.org/10.1016/j.jhazmat.2008.03.110>.

- Nautiyal, P., K. Subramanian and M. Dastidar. 2016. "Adsorptive removal of dye using biochar derived from residual algae after in-situ transesterification: alternate use of waste of biodiesel industry." *Journal of environmental management* 182: 187-197.
- Navarro, R.R., K. Tatsumi, K. Sumi and M. Matsumura. 2001. "Role of anions on heavy metal sorption of a cellulose modified with poly (glycidyl methacrylate) and polyethyleneimine." *Water research* 35 (11): 2724-2730.
- Neris, J.B., F.H.M. Luzardo, P.F. Santos, O.N. de Almeida and F.G. Velasco. 2019. "Evaluation of single and tri-element adsorption of Pb<sup>2+</sup>, Ni<sup>2+</sup> and Zn<sup>2+</sup> ions in aqueous solution on modified water hyacinth (*Eichhornia crassipes*) fibers." *Journal of Environmental Chemical Engineering* 7 (1): 102885. doi: <https://doi.org/10.1016/j.jece.2019.102885>.
- Nestorov, I., M. Rowland, S. Hadjitodorov and I. Petrov. 1999. "Empirical versus mechanistic modelling: comparison of an artificial neural network to a mechanistically based model for quantitative structure pharmacokinetic relationships of a homologous series of barbiturates." *AAPS PharmSci* 1 (4): 5-13.
- Ngah, W.W. and M. Hanafiah. 2008. "Removal of heavy metal ions from wastewater by chemically modified plant wastes as adsorbents: a review." *Bioresource technology* 99 (10): 3935-3948.
- Ngah, W.W., L. Teong, R. Toh and M. Hanafiah. 2012. "Utilization of chitosan-zeolite composite in the removal of Cu (II) from aqueous solution: adsorption, desorption and fixed bed column studies." *Chemical Engineering Journal* 209: 46-53.
- Norkus, E., I. Stalnionienė and D.C. Crans. 2003. "Interaction of pyridine-and 4-hydroxypyridine-2, 6-dicarboxylic acids with heavy metal ions in aqueous solutions." *Heteroatom Chemistry: An International Journal of Main Group Elements* 14 (7): 625-632.
- O'Brien, R.M. 2007. "A caution regarding rules of thumb for variance inflation factors." *Quality & quantity* 41 (5): 673-690.
- Ofomaja, A.E. 2010. "Intraparticle diffusion process for lead (II) biosorption onto mansonia wood sawdust." *Bioresource technology* 101 (15): 5868-5876.
- Önder, H., M. Şahin, S. Çankaya, Y. Tahtalı and Z. Cebeci. 2003. "Use of t-Statistics with Permutation Test: For Small Sample Size." In *International Congress on Information Technology in Agriculture, Food and Environment, Izmir-Turkey*, edited, 7-10.

- Ören, A.H. and A. Kaya. 2006. "Factors affecting adsorption characteristics of Zn<sup>2+</sup> on two natural zeolites." *Journal of Hazardous Materials* 131 (1-3): 59-65.
- Pagnanelli, F., A. Esposito and F. Vegliò. 2002. "Multi-metallic modelling for biosorption of binary systems." *Water research* 36 (16): 4095-4105.
- Palma, G., J. Freer and J. Baeza. 2003. "Removal of metal ions by modified *Pinus radiata* bark and tannins from water solutions." *Water Research* 37 (20): 4974-4980.
- Panayotova, M. 2001. "Kinetics and thermodynamics of copper ions removal from wastewater by use of zeolite." *Waste Management* 21 (7): 671-676.
- Paranavithana, G.N., K. Kawamoto, Y. Inoue, T. Saito, M. Vithanage, C.S. Kalpage and G.B.B. Herath. 2016. "Adsorption of Cd<sup>2+</sup> and Pb<sup>2+</sup> onto coconut shell biochar and biochar-mixed soil." *Environmental Earth Sciences* 75 (6): 484. doi: 10.1007/s12665-015-5167-z.
- Parr, R.G. and R.G. Pearson. 1983. "Absolute hardness: companion parameter to absolute electronegativity." *Journal of the American Chemical Society* 105 (26): 7512-7516.
- Patel, H. 2019. "Fixed-bed column adsorption study: a comprehensive review." *Applied Water Science* 9 (3): 45. doi: 10.1007/s13201-019-0927-7.
- Patel, H. and R.T. Vashi. 2015. "Chapter 5 - Fixed-Bed Column Studies of Dyeing Mill Wastewater Treatment Using Naturally Prepared Adsorbents." In *Characterization and Treatment of Textile Wastewater*, edited by Himanshu Patel and R. T. Vashi, 127-145. Boston: Elsevier. doi: <https://doi.org/10.1016/B978-0-12-802326-6.00005-8>.
- Pathirana, C., Ziyath A.M., Jinadasa, K.B.S.N., Egodawatta, P., Sarina, S. and Goonetilleke, A. 2019. "Quantifying the influence of surface physico-chemical properties of biosorbents on heavy metal adsorption." *Chemosphere* 234: 488-495. doi: <https://doi.org/10.1016/j.chemosphere.2019.06.074>.
- Pearson, R.G. 1968. "Hard and soft acids and bases, HSAB, part 1: Fundamental principles." *Journal of Chemical Education* 45 (9): 581.
- Pehlivan, E., Altun, T. and Parlayici, Ş. 2012. "Modified barley straw as a potential biosorbent for removal of copper ions from aqueous solution." *Food chemistry* 135 (4): 2229-2234.

- Pereira, M., M.C. Bartolomé and S. Sánchez-Fortún. 2013. "Bioadsorption and bioaccumulation of chromium trivalent in Cr(III)-tolerant microalgae: A mechanisms for chromium resistance." *Chemosphere* 93 (6): 1057-1063. doi: <https://doi.org/10.1016/j.chemosphere.2013.05.078>.
- Perić, J., M. Trgo and N.V. Medvidović. 2004. "Removal of zinc, copper and lead by natural zeolite—a comparison of adsorption isotherms." *Water research* 38 (7): 1893-1899.
- Petrov, S. and V. Nenov. 2004. "Removal and recovery of copper from wastewater by a complexation-ultrafiltration process." *Desalination* 162: 201-209.
- Plazinski, W., W. Rudzinski and A. Plazinska. 2009. "Theoretical models of sorption kinetics including a surface reaction mechanism: A review." *Advances in Colloid and Interface Science* 152 (1): 2-13. doi: <https://doi.org/10.1016/j.cis.2009.07.009>.
- Polcaro, A., A. Vacca, S. Palmas and M. Mascia. 2003. "Electrochemical treatment of wastewater containing phenolic compounds: oxidation at boron-doped diamond electrodes." *Journal of Applied Electrochemistry* 33 (10): 885-892.
- Pramanik, S., P.K. Dhara and P. Chattopadhyay. 2004. "A chelating resin containing bis (2-benzimidazolylmethyl) amine: synthesis and metal-ion uptake properties suitable for analytical application." *Talanta* 63 (2): 485-490.
- Puth, M.-T., M. Neuhäuser and G.D. Ruxton. 2014. "Effective use of Pearson's product–moment correlation coefficient." *Animal behaviour* 93: 183-189.
- Qiu, H., L. Lv, B.-c. Pan, Q.-j. Zhang, W.-m. Zhang and Q.-x. Zhang. 2009. "Critical review in adsorption kinetic models." *Journal of Zhejiang University-Science A* 10 (5): 716-724.
- Raji, C., G. Manju and T. Anirudhan. 1997. "Removal of heavy metal ions from water using sawdust-based activated carbon.
- Rao, K., S. Anand and P. Venkateswarlu. 2011. "Modeling the kinetics of Cd (II) adsorption on *Syzygium cumini* L leaf powder in a fixed bed mini column." *Journal of industrial and engineering chemistry* 17 (2): 174-181.
- Rao, R.A.K. and M. Kashifuddin. 2016. "Adsorption studies of Cd (II) on ball clay: Comparison with other natural clays." *Arabian Journal of Chemistry* 9: S1233-S1241.

- Raychaudhuri, S., J.M. Stuart and R.B. Altman. 1999. "Principal components analysis to summarize microarray experiments: application to sporulation time series." In *Biocomputing 2000*, 455-466: World Scientific.
- Recepoğlu, Y.K., N. Kabay, I.Y. Ipek, M. Arda, M. Yüksel, K. Yoshizuka and S. Nishihama. 2018. "Packed bed column dynamic study for boron removal from geothermal brine by a chelating fiber and breakthrough curve analysis by using mathematical models." *Desalination* 437: 1-6.
- Rengaraj, S., C.K. Joo, Y. Kim and J. Yi. 2003. "Kinetics of removal of chromium from water and electronic process wastewater by ion exchange resins: 1200H, 1500H and IRN97H." *Journal of hazardous materials* 102 (2-3): 257-275.
- Rengaraj, S., K.-H. Yeon and S.-H. Moon. 2001. "Removal of chromium from water and wastewater by ion exchange resins." *Journal of hazardous materials* 87 (1-3): 273-287.
- Ribé, V., E. Nehrenheim, M. Odlare, L. Gustavsson, R. Berglind and Å. Forsberg. 2012. "Ecotoxicological assessment and evaluation of a pine bark biosorbent treatment of five landfill leachates." *Waste management* 32 (10): 1886-1894.
- Rocha, C.G., D.A.M. Zaia, R.V. da Silva Alfaya and A.A. da Silva Alfaya. 2009. "Use of rice straw as biosorbent for removal of Cu (II), Zn (II), Cd (II) and Hg (II) ions in industrial effluents." *Journal of hazardous materials* 166 (1): 383-388.
- Rodrigues, A.E., M.D. LeVan and D. Tondeur. 2012. *Adsorption: Science and Technology*: Springer Netherlands.  
<https://books.google.lk/books?id=a4TpCAAQBAJ>.
- Ross, J.L., M.M. Ozbek and G.F. Pinder. 2009. "Aleatoric and epistemic uncertainty in groundwater flow and transport simulation." *Water Resources Research* 45 (12).
- Ruiz-Fuertes, J., M. Sanz-Ortiz, J. González, F. Rodríguez, A. Segura and D. Errandonea. 2010. "Optical absorption and Raman spectroscopy of CuWO<sub>4</sub>." In *Journal of Physics: Conference Series*, edited, 012048: IOP Publishing.
- Ruthven, D.M. 1984. *Principles of adsorption and adsorption processes*: John Wiley & Sons.
- Sadhasivam, S., S. Savitha and K. Swaminathan. 2007. "Exploitation of *Trichoderma harzianum* mycelial waste for the removal of rhodamine 6G from aqueous solution." *Journal of Environmental Management* 85 (1): 155-161. doi: <https://doi.org/10.1016/j.jenvman.2006.08.010>.

- Sahmoune, M.N. and A.R. Yeddou. 2016. "Potential of sawdust materials for the removal of dyes and heavy metals: examination of isotherms and kinetics." *Desalination and Water Treatment* 57 (50): 24019-24034.
- Sapari, N., A. Idris and N.H.A. Hamid. 1996. "Total removal of heavy metal from mixed plating rinse wastewater." *Desalination* 106 (1-3): 419-422.
- Saravanan, A., P.S. Kumar and M. Yaswanthraj. 2018. "Modeling and analysis of a packed-bed column for the effective removal of zinc from aqueous solution using dual surface-modified biomass." *Particulate Science and Technology* 36 (8): 934-944.
- Satarug, S. and M.R. Moore. 2004. "Adverse Health Effects of Chronic Exposure to Low-Level Cadmium in Foodstuffs and Cigarette Smoke." *Environmental Health Perspectives* 112 (10): 1099-1103. doi: 10.1289/ehp.6751.
- Schiewer, S. and B. Volesky. 1996. "Modeling Multi-Metal Ion Exchange in Biosorption." *Environmental Science & Technology* 30 (10): 2921-2927. doi: 10.1021/es950800n.
- Sellitti, C., J.L. Koenig and H. Ishida. 1990. "Surface characterization of graphitized carbon fibers by attenuated total reflection fourier transform infrared spectroscopy." *Carbon* 28 (1): 221-228. doi: [https://doi.org/10.1016/0008-6223\(90\)90116-G](https://doi.org/10.1016/0008-6223(90)90116-G).
- Semerjian, L. and G. Ayoub. 2003. "High-pH–magnesium coagulation–flocculation in wastewater treatment." *Advances in Environmental Research* 7 (2): 389-403.
- Serencam, H., A. Gundogdu, Y. Uygur, B. Kemer, V.N. Bulut, C. Duran, M. Soylak and M. Tufekci. 2008. "Removal of cadmium from aqueous solution by Nordmann fir (*Abies nordmanniana* (Stev.) Spach. Subsp. *nordmanniana*) leaves." *Bioresource Technology* 99 (6): 1992-2000. doi: <https://doi.org/10.1016/j.biortech.2007.03.021>.
- Settle, S., A. Goonetilleke and G.A. Ayoko. 2007. "Determination of surrogate indicators for phosphorus and solids in urban stormwater: application of multivariate data analysis techniques." *Water, air, and soil pollution* 182 (1-4): 149-161.
- Shahbazi, A., H. Younesi and A. Badii. 2013. "Batch and fixed-bed column adsorption of Cu (II), Pb (II) and Cd (II) from aqueous solution onto functionalised SBA-15 mesoporous silica." *The Canadian Journal of Chemical Engineering* 91 (4): 739-750.

- Sheng, L., Y. Zhang, F. Tang and S. Liu. 2018. "Mesoporous/microporous silica materials: preparation from natural sands and highly efficient fixed-bed adsorption of methylene blue in wastewater." *Microporous and Mesoporous Materials* 257: 9-18.
- Shim, H.Y., K.S. Lee, D.S. Lee, D.S. Jeon, M.S. Park, J.S. Shin, Y.K. Lee, J.W. Goo, S.B. Kim and D.Y. Chung. 2014. "Application of electrocoagulation and electrolysis on the precipitation of heavy metals and particulate solids in washwater from the soil washing." *Journal of Agricultural Chemistry and Environment* 3 (04): 130.
- Shon, H., S. Vigneswaran, I.S. Kim, J. Cho and H. Ngo. 2004. "The effect of pretreatment to ultrafiltration of biologically treated sewage effluent: a detailed effluent organic matter (EfOM) characterization." *Water Research* 38 (7): 1933-1939.
- Shukla, S., R.S. Pai and A.D. Shendarkar. 2006. "Adsorption of Ni (II), Zn (II) and Fe (II) on modified coir fibres." *Separation and Purification Technology* 47 (3): 141-147.
- Simonin, J.-P. 2016. "On the comparison of pseudo-first order and pseudo-second order rate laws in the modeling of adsorption kinetics." *Chemical Engineering Journal* 300: 254-263.
- Sing, K.S.W. 1985. "Reporting physisorption data for gas/solid systems with special reference to the determination of surface area and porosity (Recommendations 1984)". In *Pure and Applied Chemistry*.
- Sobhanardakani, S., H. Parvizmosaed and E. Olyaie. 2013. "Heavy metals removal from wastewaters using organic solid waste—rice husk." *Environmental Science and Pollution Research* 20 (8): 5265-5271.
- Sörme, L. and R. Lagerkvist. 2002. "Sources of heavy metals in urban wastewater in Stockholm." *Science of the Total Environment* 298 (1-3): 131-145.
- Sparks, D.L. 2003. *Environmental Soil Chemistry*: Elsevier Science. [https://books.google.com.au/books?id=qY\\_1pJHHI-IC](https://books.google.com.au/books?id=qY_1pJHHI-IC).
- Stevenson, F. 1976. "Binding of metal ions by humic acids." *Environmental biogeochemistry* 2: 519-540.



- Stoica, L., C. Constantin and C. Calin. 2012. "Fluoride removal from aqueous solutions by sorbtion-flotation." *Univ Politeh Buchar Sci Bull Ser B Chem Mater Sci* 74 (4): 87-102.
- Sukumar, C., V. Janaki, K. Vijayaraghavan, S. Kamala-Kannan and K. Shanthi. 2017. "Removal of Cr (VI) using co-immobilized activated carbon and *Bacillus subtilis*: fixed-bed column study." *Clean Technologies and Environmental Policy* 19 (1): 251-258.
- Tan, G. and D. Xiao. 2009. "Adsorption of cadmium ion from aqueous solution by ground wheat stems." *Journal of hazardous materials* 164 (2-3): 1359-1363.
- Taty-Costodes, V.C., H. Fauduet, C. Porte and A. Delacroix. 2003. "Removal of Cd (II) and Pb (II) ions, from aqueous solutions, by adsorption onto sawdust of *Pinus sylvestris*." *Journal of hazardous materials* 105 (1-3): 121-142.
- Tchounwou, P.B., J.A. Centeno and A.K. Patlolla. 2004. "Arsenic toxicity, mutagenesis, and carcinogenesis—a health risk assessment and management approach." *Molecular and cellular biochemistry* 255 (1-2): 47-55.
- Ter Braak, C.J. 2009. "Regression by L1 regularization of smart contrasts and sums (ROSCAS) beats PLS and elastic net in latent variable model." *Journal of Chemometrics: A Journal of the Chemometrics Society* 23 (5): 217-228.
- Terry, P.A. and W. Stone. 2002. "Biosorption of cadmium and copper contaminated water by *Scenedesmus abundans*." *Chemosphere* 47 (3): 249-255. doi: [https://doi.org/10.1016/S0045-6535\(01\)00303-4](https://doi.org/10.1016/S0045-6535(01)00303-4).
- Teutscherova, N., J. Houška, M. Navas, A. Masaguer, M. Benito and E. Vazquez. 2018. "Leaching of ammonium and nitrate from Acrisol and Calcisol amended with holm oak biochar: a column study." *Geoderma* 323: 136-145.
- Thommes, M., K. Kaneko, V. Neimark Alexander, P. Olivier James, F. Rodriguez-Reinoso, J. Rouquerol and S.W. Sing Kenneth. 2015. "Physisorption of gases, with special reference to the evaluation of surface area and pore size distribution (IUPAC Technical Report)". In *Pure and Applied Chemistry*.
- Thompson, G., J. Swain, M. Kay and C. Forster. 2001. "The treatment of pulp and paper mill effluent: a review." *Bioresource technology* 77 (3): 275-286.
- Tran, R., Z. Xu, B. Radhakrishnan, D. Winston, W. Sun, K.A. Persson and S.P. Ong. 2016. "Surface energies of elemental crystals." *Scientific data* 3: 160080.



- Trivunac, K., Z. Sekulić and S. Stevanović. 2012. "Zinc removal from wastewater by complexation-microfiltration process." *Journal of the Serbian Chemical Society* 77 (11): 1661-1670.
- Tunell, I. and C. Lim. 2006. "Factors governing the metal coordination number in isolated group IA and IIA metal hydrates." *Inorganic chemistry* 45 (12): 4811-4819.
- Uluozlu, O.D., A. Sari, M. Tuzen and M. Soylak. 2008. "Biosorption of Pb (II) and Cr (III) from aqueous solution by lichen (*Parmelina tiliaceae*) biomass." *Bioresource Technology* 99 (8): 2972-2980.
- Unger, K.K., R. Skudas and M.M. Schulte. 2008. "Particle packed columns and monolithic columns in high-performance liquid chromatography-comparison and critical appraisal." *Journal of chromatography A* 1184 (1-2): 393-415.
- van der Linden, A.M.A., A. Tiktak, J.J.T.I. Boesten and A. Leijnse. 2009. "Influence of pH-dependent sorption and transformation on simulated pesticide leaching." *Science of The Total Environment* 407 (10): 3415-3420. doi: <https://doi.org/10.1016/j.scitotenv.2009.01.059>.
- Velazquez-Jimenez, L.H., A. Pavlick and J.R. Rangel-Mendez. 2013. "Chemical characterization of raw and treated agave bagasse and its potential as adsorbent of metal cations from water." *Industrial Crops and Products* 43: 200-206.
- Vijayaraghavan, K., T. Padmesh, K. Palanivelu and M. Velan. 2006. "Biosorption of nickel (II) ions onto *Sargassum wightii*: application of two-parameter and three-parameter isotherm models." *Journal of hazardous materials* 133 (1-3): 304-308.
- Vilvanathan, S. and S. Shanthakumar. 2018. "Ni<sup>2+</sup> and Co<sup>2+</sup> adsorption using *Tectona grandis* biochar: kinetics, equilibrium and desorption studies." *Environmental technology* 39 (4): 464-478.
- Volesky, B. 2003. *Sorption and biosorption*. Vol. 549: BV Sorbex Montreal.
- Wan, S., Z. Ma, Y. Xue, M. Ma, S. Xu, L. Qian and Q. Zhang. 2014. "Sorption of Lead(II), Cadmium(II), and Copper(II) Ions from Aqueous Solutions Using Tea Waste." *Industrial & Engineering Chemistry Research* 53 (9): 3629-3635. doi: 10.1021/ie402510s.
- Wang, F., J. Yu, Z. Zhang, Y. Xu and R.-a. Chi. 2018. "An amino-functionalized ramie stalk-based adsorbent for highly effective Cu<sup>2+</sup> removal from water:

Adsorption performance and mechanism." *Process Safety and Environmental Protection* 117: 511-522.

- Wang, H., A. Zhou, F. Peng, H. Yu and J. Yang. 2007. "Mechanism study on adsorption of acidified multiwalled carbon nanotubes to Pb (II)." *Journal of Colloid and Interface Science* 316 (2): 277-283.
- Wang, J. and C. Chen. 2009. "Biosorbents for heavy metals removal and their future." *Biotechnology Advances* 27 (2): 195-226. doi: <https://doi.org/10.1016/j.biotechadv.2008.11.002>.
- Wang, S., M. Soudi, L. Li and Z. Zhu. 2006. "Coal ash conversion into effective adsorbents for removal of heavy metals and dyes from wastewater." *Journal of Hazardous Materials* 133 (1-3): 243-251.
- Wang, W., M. Li and Q. Zeng. 2015. "Adsorption of chromium (VI) by strong alkaline anion exchange fiber in a fixed-bed column: experiments and models fitting and evaluating." *Separation and Purification Technology* 149: 16-23.
- Wang, X., T. Park and K.C. Carriere. 2010. "Variable selection via combined penalization for high-dimensional data analysis." *Computational Statistics & Data Analysis* 54 (10): 2230-2243. doi: <https://doi.org/10.1016/j.csda.2010.03.026>.
- Wang, X., T. Park, K.J.C.S. Carriere and D. Analysis. 2010. "Variable selection via combined penalization for high-dimensional data analysis 54 (10): 2230-2243.
- Wang, Y., S.-H. Ho, C.-L. Cheng, W.-Q. Guo, D. Nagarajan, N.-Q. Ren, D.-J. Lee and J.-S. Chang. 2016. "Perspectives on the feasibility of using microalgae for industrial wastewater treatment." *Bioresource technology* 222: 485-497.
- Wasewar, K.L., M. Atif, B. Prasad and I.M. Mishra. 2008. "Adsorption of zinc using tea factory waste: kinetics, equilibrium and thermodynamics." *CLEAN–Soil, Air, Water* 36 (3): 320-329.
- Weber, G. 1963. "Study and evaluation of regulation of enzyme activity and synthesis in mammalian liver." *Advances in Enzyme Regulation* 1: 1-35.
- White, K. 2006. "Bioavailability of polycyclic aromatic hydrocarbons in the aquatic environment.
- Wijesiri, B., P. Egodawatta, J. McGree and A. Goonetilleke. 2016. "Assessing uncertainty in stormwater quality modelling." *Water Research* 103: 10-20. doi: <https://doi.org/10.1016/j.watres.2016.07.011>.

- Witek-Krowiak, A. 2012. "Analysis of temperature-dependent biosorption of Cu<sup>2+</sup> ions on sunflower hulls: Kinetics, equilibrium and mechanism of the process." *Chemical Engineering Journal* 192: 13-20.
- Worch, E. 2012. *Adsorption Technology in Water Treatment, Fundamentals, Processes, and Modeling*. Accessed 2019-09-18t07:49:38.335+02:00. doi: 10.1515/9783110240238.
- Wu, F.-C., R.-L. Tseng and R.-S. Juang. 2009. "Initial behavior of intraparticle diffusion model used in the description of adsorption kinetics." *Chemical Engineering Journal* 153 (1): 1-8. doi: <https://doi.org/10.1016/j.cej.2009.04.042>.
- Xavier, A.L.P., O.F.H. Adarme, L.M. Furtado, G.M.D. Ferreira, L.H.M. da Silva, L.F. Gil and L.V.A. Gurgel. 2018. "Modeling adsorption of copper (II), cobalt (II) and nickel (II) metal ions from aqueous solution onto a new carboxylated sugarcane bagasse. Part II: Optimization of monocomponent fixed-bed column adsorption." *Journal of colloid and interface science* 516: 431-445.
- Xu, C., S. He, Y. Liu, W. Zhang and D. Lu. 2017. "Bioadsorption and biostabilization of cadmium by *Enterobacter cloacae* TU." *Chemosphere* 173: 622-629. doi: <https://doi.org/10.1016/j.chemosphere.2017.01.005>.
- Xue, Y., B. Gao, Y. Yao, M. Inyang, M. Zhang, A.R. Zimmerman and K.S. Ro. 2012. "Hydrogen peroxide modification enhances the ability of biochar (hydrochar) produced from hydrothermal carbonization of peanut hull to remove aqueous heavy metals: batch and column tests." *Chemical Engineering Journal* 200: 673-680.
- Ye, Y., J. Yang, W. Jiang, J. Kang, Y. Hu, H.H. Ngo, W. Guo and Y. Liu. 2018. "Fluoride removal from water using a magnesia-pullulan composite in a continuous fixed-bed column." *Journal of environmental management* 206: 929-937.
- Year, F. 2013. "Agency for Toxic Substances and Disease Registry.
- Yu, Y., Y.-Y. Zhuang and Z.-H. Wang. 2001. "Adsorption of water-soluble dye onto functionalized resin." *Journal of colloid and interface science* 242 (2): 288-293.
- Zacaroni, L.M., Z.M. Magriotis, M. das Graças Cardoso, W.D. Santiago, J.G. Mendonça, S.S. Vieira and D.L. Nelson. 2015. "Natural clay and commercial activated charcoal: properties and application for the removal of copper from cachaça." *Food control* 47: 536-544.

- Zaini, H., S. Abubakar, T. Rihayat and S. Suryani. 2018. "Adsorption and kinetics study of manganese (II) in waste water using vertical column method by sugar cane bagasse." In *IOP Conference Series: Materials Science and Engineering*, edited, 012025: IOP Publishing.
- Zendehdel, M. and H. Mohammadi. 2018. "The Fixed-bed Column Study for Heavy Metals Removal from the Wastewater by Poly Acrylamide-co-acrylic Acid/Clinoptilolite Nanocomposite." *Nanoscience & Nanotechnology-Asia* 8 (1): 67-74.
- Zhang, F.-S. and H. Itoh. 2006. "Photocatalytic oxidation and removal of arsenite from water using slag-iron oxide-TiO<sub>2</sub> adsorbent." *Chemosphere* 65 (1): 125-131.
- Zhu, M. and A. Ghodsi. 2006. "Automatic dimensionality selection from the scree plot via the use of profile likelihood." *Computational Statistics & Data Analysis* 51 (2): 918-930.
- Ziyath, A.M., P. Mahbub, A. Goonetilleke, M.O. Adebajo, S. Kokot and A. Oloyede. 2011. "Influence of physical and chemical parameters on the treatment of heavy metals in polluted stormwater using zeolite: A review." *Journal of Water Resource and protection* 3: 758-767.
- Zoppou, C. 2001. "Review of urban storm water models." *Environmental Modelling & Software* 16 (3): 195-231.
- Zou, H. and T. Hastie. 2005a. "Regularization and Variable Selection via the Elastic Net." *Journal of the Royal Statistical Society. Series B (Statistical Methodology)* 67 (2): 301-320. <http://www.jstor.org/stable/3647580>.
- Zou, H. and T.J.J.o.t.R.S.S.B. Hastie. 2005b. "Regularization and variable selection via the elastic net 67 (2): 301-320.
- Zou, W., L. Zhao and L. Zhu. 2013. "Adsorption of uranium (VI) by grapefruit peel in a fixed-bed column: experiments and prediction of breakthrough curves." *Journal of Radioanalytical and Nuclear Chemistry* 295 (1): 717-727.



# APPENDIX A1

---

## Background data analysis

**Table A1.1** Particle density of biosorbent samples calculated using Picnometer

Sample No.	Particle density, g/cm <sup>3</sup>
1	1.97
2	1.93
3	1.77
4	1.69
5	1.62
6	1.57
7	1.53
8	1.51
9	1.45
10	1.42
11	1.38
12	1.31
13	1.22
14	1.19
15	1.16
16	1.10
17	1.04
18	1.01
19	0.91
20	0.88
21	0.86

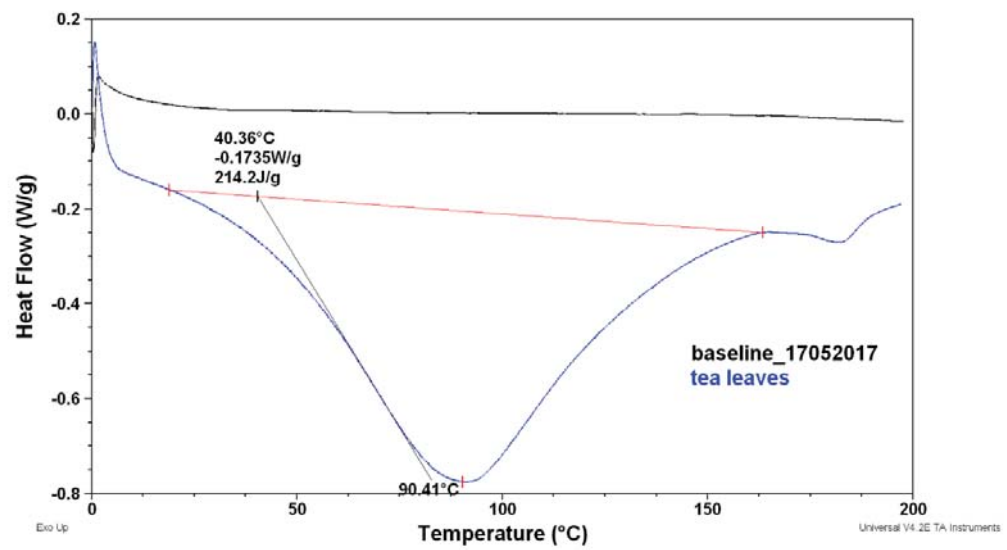
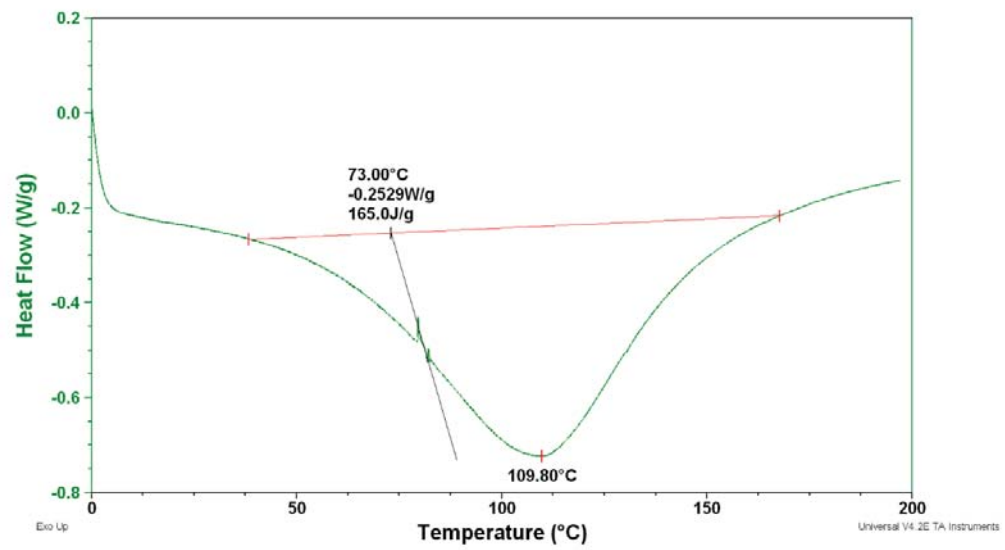


Figure A1.1 DSC curves for (a) Coconut shell biochar (b) tea factory waste



This page intentionally left blank.

## APPENDIX A2

---

**Data generated from laboratory analysis of the twenty one biosorbent samples used in the batch and column studies**

**Table A2.1** Laboratory analysis of physico-chemical properties

Sample No	SSA, m <sup>2</sup> /g	PV, cm <sup>3</sup> /g	PS, mV	ZP, mV	Surface Functional groups, mmol/g				
					Carboxylic	Phenolic	Lactonic	TAG	TBG
1	202	0.0096	31.80	40.21	0.21	0.16	0.28	0.65	2.09
2	189	0.0084	38.76	42.34	0.25	0.29	0.32	0.86	2.16
3	180	0.0091	35.11	41.56	0.34	0.18	0.13	0.65	1.97
4	169	0.0075	38.21	45.25	0.72	0.19	0.11	1.01	2.61
5	175	0.0088	33.76	39.10	0.49	0.24	0.19	0.92	1.59
6	161	0.0075	37.39	45.34	1.05	0.54	0.32	1.91	2.28
7	158	0.0081	34.67	43.34	0.96	0.58	0.35	1.88	2.73
8	146	0.0098	31.00	50.45	1.50	0.86	0.41	2.77	1.30
9	123	0.0107	26.40	52.67	1.59	0.69	0.58	2.86	1.08
10	107	0.0096	28.64	51.34	1.49	0.84	0.49	2.82	1.47
11	92	0.0089	30.21	48.26	1.13	0.49	0.50	2.13	0.67
12	84	0.0034	43.96	47.00	0.78	0.42	0.22	1.42	1.34
13	75	0.0054	51.45	38.21	0.65	0.25	0.16	1.07	2.15
14	70	0.0035	54.87	37.98	0.92	0.52	0.32	1.76	2.03
15	56	0.0063	47.23	43.76	1.08	0.67	0.39	2.14	1.21
16	50	0.0068	43.21	45.89	1.15	0.71	0.41	2.27	1.09
17	46	0.0069	45.93	41.21	0.82	0.46	0.13	1.41	2.16
18	32	0.0078	41.11	48.98	1.27	0.80	0.45	2.53	0.83
19	23	0.0042	46.98	39.45	1.33	0.84	0.48	2.65	0.71
20	10	0.0013	47.11	46.32	1.20	0.89	0.41	2.49	1.01
21	1	0.0009	42.98	48.54	1.46	0.93	0.52	2.91	1.34

**Table A2.2** Sorption capacities obtained from batch experiments for Pb<sup>2+</sup> for the different biosorbents samples

Sample No	Sorption Capacity mg/L					
	2 mg/L	10 mg/L	50 mg/L	100 mg/L	200 mg/L	300 mg/L
1	1.34	8.73	20.34	28.96	30.12	30.12
2	1.53	9.18	21.16	29.88	32.24	32.24
3	1.67	8.00	19.98	28.70	31.06	31.06
4	2.00	10.00	23.03	32.75	34.11	34.11
5	1.98	9.70	21.68	30.54	32.76	32.76
6	2.00	10.00	29.13	36.85	40.21	40.21
7	2.00	10.00	27.84	36.56	38.92	38.92
8	2.00	10.00	32.73	41.45	43.81	43.81
9	2.00	10.00	36.65	45.37	47.73	47.73
10	2.00	10.00	34.91	43.63	46.19	46.19
11	2.00	10.00	32.24	40.96	43.32	43.32
12	2.00	10.00	25.34	34.06	36.42	36.42
13	2.00	10.00	22.43	31.15	33.51	33.51
14	2.00	10.00	21.89	30.91	33.27	33.27
15	2.00	10.00	24.96	33.68	36.04	36.04
16	2.00	10.00	29.83	37.75	39.11	39.11
17	2.00	7.97	19.15	27.87	30.23	30.23
18	2.00	10.00	25.09	33.51	35.87	35.87
19	1.48	8.92	20.50	29.22	31.58	31.58
20	2.00	10.00	25.26	33.98	36.34	36.34
21	2.00	10.00	26.74	36.46	38.82	38.82

**Table A2.3** Sorption capacities obtained from batch experiments for Cu<sup>2+</sup> for the different biosorbents samples

Sample No	Sorption capacity , mg/g					
	2 mg/L	10 mg/L	50 mg/L	100 mg/L	200 mg/L	300 mg/L
1	1.76	8.02	14.33	19.07	19.12	19.12
2	1.62	9.40	15.78	20.45	21.67	21.67
3	2.00	10.00	17.69	22.56	23.10	23.10
4	2.00	10.00	18.98	23.65	25.67	25.67
5	2.00	9.82	16.20	20.87	22.43	22.43
6	2.00	10.00	19.88	24.55	26.11	26.11
7	2.00	10.00	21.74	26.39	27.95	27.95
8	2.00	10.00	27.57	32.24	33.80	33.80
9	2.00	10.00	27.11	31.78	33.34	33.34
10	2.00	10.00	25.18	29.55	31.11	31.11
11	2.00	10.00	24.09	28.76	30.32	30.32
12	2.00	10.00	21.07	25.74	27.30	27.30
13	2.00	10.00	16.42	21.09	22.65	22.65
14	2.00	10.00	16.93	21.60	23.16	23.16
15	2.00	10.00	19.53	24.20	25.76	25.76
16	2.00	10.00	22.33	27.00	28.56	28.56
17	2.00	8.11	14.49	19.16	20.72	20.72
18	2.00	10.00	17.91	22.98	24.54	24.54
19	2.00	9.37	14.75	20.42	21.98	21.98
20	2.00	10.00	18.81	23.48	25.04	25.04
21	2.00	10.00	21.98	26.65	28.21	28.21

**Table A2.4** Sorption capacities obtained from batch experiments for Cd<sup>2+</sup> for the different biosorbents samples

Sample No	Sorption capacity , mg/g					
	2 mg/L	10 mg/L	50 mg/L	100 mg/L	200 mg/L	300 mg/L
1	1.56	3.90	5.39	9.02	9.89	9.89
2	1.22	5.57	7.26	9.89	11.76	11.76
3	1.96	6.61	8.80	11.73	12.60	12.60
4	2.00	7.38	9.50	12.43	13.30	13.30
5	2.00	6.88	9.07	12.33	12.87	12.87
6	2.00	9.24	10.13	14.36	15.23	15.23
7	2.00	8.90	11.09	13.02	14.89	14.89
8	2.00	10.00	12.85	15.78	16.65	16.65
9	2.00	10.00	14.99	18.45	19.32	19.32
10	2.00	10.00	13.26	16.19	17.06	17.06
11	2.00	10.00	12.96	15.69	16.76	16.76
12	2.00	8.01	10.20	13.13	14.00	14.00
13	2.00	4.91	7.10	10.03	10.90	10.90
14	2.00	3.57	5.46	8.39	9.26	9.26
15	2.00	7.01	9.20	12.13	13.00	13.00
16	2.00	6.81	9.00	11.43	12.80	12.80
17	2.00	5.77	7.96	10.89	11.76	11.76
18	2.00	7.69	10.18	13.11	13.98	13.98
19	2.00	9.46	11.65	14.58	15.45	15.45
20	2.00	10.00	13.09	16.02	16.89	16.89
21	2.00	10.00	13.67	16.12	17.50	17.50

**Table A2.5** Pseudo second order kinetic constants ( $k_2$ ) obtained from batch experiments for  $\text{Pd}^{2+}$ ,  $\text{Cu}^{2+}$  and  $\text{Cd}^{2+}$

Pseudo second order kinetic constant g/mg/min									
Sample	Metal ion	200 mg/L		100 mg/L		50 mg/L		25 mg/L	
		$^1K_2$	$R^2$	$K_2$	$R^2$	$K_2$	$R^2$	$K_2$	$R^2$
1	Pb	0.0059	0.9960	0.0137	0.9980	0.0219	0.9930	0.0454	0.9940
	Cu	0.0021	0.9520	0.0024	0.9880	0.0054	0.9460	0.0112	0.9690
	Cd	0.0029	0.9940	0.0027	0.9710	0.0052	0.9510	0.0093	0.9470
2	Pb	0.0069	0.9900	0.0150	0.9750	0.0329	0.9810	0.0739	0.9900
	Cu	0.0032	0.9700	0.0072	0.9720	0.0089	0.9910	0.0412	0.9580
	Cd	0.0035	0.9580	0.0053	0.9690	0.0094	0.9880	0.0168	0.9630
3	Pb	0.0057	0.9630	0.0172	0.9740	0.0220	0.9890	0.0456	0.9830
	Cu	0.0049	0.9700	0.0024	0.9790	0.0144	0.9830	0.0359	0.9790
	Cd	0.0045	0.9980	0.0049	0.9800	0.0157	0.9790	0.0287	0.9930
4	Pb	0.0076	0.9810	0.0160	0.9960	0.0403	0.9740	0.0929	0.9920
	Cu	0.0039	0.9960	0.0105	0.9870	0.0114	0.9850	0.0276	0.9840
	Cd	0.0062	0.9880	0.0041	0.9830	0.0122	0.9930	0.0222	0.9750
5	Pb	0.0063	0.9520	0.0154	0.9860	0.0264	0.9800	0.0570	0.9840
	Cu	0.0030	0.9940	0.0044	0.9930	0.0082	0.9880	0.0189	0.9560
	Cd	0.0037	0.9930	0.0038	0.9890	0.0105	0.9750	0.0186	0.9080
6	Pb	0.0076	0.9990	0.0209	0.9810	0.0405	0.9920	0.0935	0.9790
	Cu	0.0084	0.9550	0.0106	0.9700	0.0260	0.9930	0.0619	0.9820
	Cd	0.0066	0.9810	0.0072	0.9900	0.0265	0.9790	0.0493	0.9900
7	Pb	0.0078	0.9950	0.0190	0.9670	0.0422	0.9900	0.0979	0.9890
	Cu	0.0062	0.9940	0.0113	0.9910	0.0189	0.9820	0.0666	0.9860
	Cd	0.0053	0.9860	0.0059	0.9820	0.0285	0.9920	0.0529	0.9830
8	Pb	0.0088	0.9780	0.0272	0.9890	0.0535	0.9870	0.1269	0.9790
	Cu	0.0127	0.9730	0.0162	0.9860	0.0401	0.9960	0.0971	0.9930
	Cd	0.0086	0.9530	0.0111	0.9870	0.0450	0.9690	0.0843	0.9920
9	Pb	0.0092	0.9980	0.0278	0.9840	0.0583	0.9540	0.1394	0.9840
	Cu	0.0134	0.9950	0.0184	0.9930	0.0423	0.9230	0.1124	0.9750
	Cd	0.0095	0.9880	0.0114	0.9830	0.0476	0.9740	0.0891	0.9320
10	Pb	0.0090	0.9710	0.0268	0.9740	0.0557	0.9650	0.1327	0.9690
	Cu	0.0129	0.9910	0.0172	0.9790	0.0408	0.9500	0.1084	0.9850
	Cd	0.0093	0.9940	0.0108	0.9800	0.0459	0.9490	0.0859	0.9930
11	Pb	0.0081	0.9400	0.0231	0.9720	0.0463	0.9820	0.1082	0.9800
	Cu	0.0100	0.9700	0.0131	0.9920	0.0312	0.9860	0.0820	0.9860
	Cd	0.0076	0.9620	0.0089	0.9690	0.0330	0.9230	0.0615	0.9750
12	Pb	0.0080	0.9350	0.0186	0.9850	0.0447	0.9470	0.1043	0.9810

Pseudo second order kinetic constant g/mg/min									
Sample	Metal ion	200 mg/L		100 mg/L		50 mg/L		25 mg/L	
		<sup>1</sup> K <sub>2</sub>	R <sup>2</sup>	K <sub>2</sub>	R <sup>2</sup>	K <sub>2</sub>	R <sup>2</sup>	K <sub>2</sub>	R <sup>2</sup>
	Cu	0.0059	0.9810	0.0124	0.9860	0.0179	0.9800	0.0733	0.9720
	Cd	0.0070	0.9900	0.0057	0.9700	0.0313	0.9740	0.0583	0.9740
13	Pb	0.0065	0.9730	0.0139	0.9750	0.0288	0.9640	0.0632	0.9790
	Cu	0.0023	0.9430	0.0054	0.9960	0.0060	0.9820	0.0299	0.9830
	Cd	0.0041	0.9830	0.0043	0.9810	0.0132	0.9860	0.0241	0.9810
14	Pb	0.0059	0.9940	0.0137	0.9670	0.0219	0.9840	0.0454	0.9860
	Cu	0.0077	0.8990	0.0024	0.9910	0.0236	0.9830	0.0112	0.9840
	Cd	0.0062	0.9690	0.0027	0.9860	0.0262	0.9810	0.0487	0.9790
15	Pb	0.0081	0.9470	0.0232	0.9930	0.0465	0.9860	0.1088	0.9810
	Cu	0.0065	0.9850	0.0132	0.9830	0.0199	0.9840	0.0510	0.9830
	Cd	0.0055	0.9640	0.0062	0.9850	0.0220	0.9790	0.0407	0.9930
16	Pb	0.0077	0.9880	0.0240	0.9750	0.0419	0.9810	0.0971	0.9630
	Cu	0.0102	0.9890	0.0112	0.9930	0.0319	0.9830	0.0837	0.9960
	Cd	0.0065	0.9340	0.0091	0.9740	0.0357	0.9930	0.0665	0.9930
17	Pb	0.0070	0.9940	0.0169	0.9960	0.0344	0.9630	0.0777	0.9860
	Cu	0.0046	0.8940	0.0079	0.9800	0.0135	0.9920	0.0335	0.9920
	Cd	0.0052	0.9650	0.0057	0.9840	0.0196	0.9870	0.0362	0.9870
18	Pb	0.0084	0.9120	0.0257	0.9920	0.0498	0.9810	0.1173	0.9810
	Cu	0.0115	0.9490	0.0146	0.9810	0.0360	0.9930	0.0870	0.9930
	Cd	0.0085	0.9960	0.0094	0.9870	0.0370	0.9910	0.0691	0.9750
19	Pb	0.0089	0.8690	0.0265	0.9790	0.0549	0.9860	0.1305	0.9860
	Cu	0.0032	0.9650	0.0169	0.9820	0.0091	0.9930	0.1009	0.9790
	Cd	0.0036	0.9570	0.0036	0.9900	0.0428	0.9830	0.0801	0.9850
20	Pb	0.0078	0.9900	0.0219	0.9890	0.0430	0.9850	0.0999	0.9920
	Cu	0.0113	0.9710	0.0117	0.9860	0.0355	0.9750	0.0687	0.9900
	Cd	0.0067	0.9600	0.0100	0.9720	0.0398	0.9930	0.0546	0.9860
21	Pb	0.0093	0.9400	0.0281	0.9690	0.0591	0.9740	0.1414	0.9880
	Cu	0.0134	0.9710	0.0187	0.9690	0.0423	0.9960	0.1124	0.9910
	Cd	0.0096	0.9930	0.0116	0.9840	0.0476	0.9850	0.0891	0.9750



This page intentionally left blank.

## APPENDIX A3

---

### **Packages, libraries and R studio codes used for the data analysis**

## 1. Packages and Libraries used for statistical analysis using R studio.

The following packages and Libraries were loaded.

```
library(devtools)
library(caret)
library(factoextra)
library(elasticnet)
library(glmnet)
library(VIF)
library(fmsb)
library(tidyverse)
library(plyr)
library(scales)
library(grid)
library(RVAideMemoire)
```

## 2. Codes used for statistical analysis using R studio.

```
# Loading Libraries for analysis
```

```
library(devtools)
library(caret)
library(factoextra)
library(elasticnet)
library(glmnet)
library(VIF)
library(fmsb)
library(tidyverse)
```

```
# datamatrix is the original data matrix.
```

```
# DataPbAll is a data matrix created by removing Cu and Cd adsorption data from the
original data matrix.
```

```
# DataCuAll is a data matrix created by removing Pb and Cd adsorption data from the original data matrix.
```

```
# DataCdAll is a data matrix created by removing Pb and Cu adsorption data from the original data matrix.
```

```
# Prepare the correlation matrix
```

```
correlationmatrix <- cor(datamatrix)
```

```
# summarize the correlation matrix
```

```
print(correlationMatrix)
```

```
# Permutation test for PPMCC. Example:- PPMCC between PV and SSA is tested with 10000
```

```
# Resamples.
```

```
x<-datamatrix$PV
```

```
y<-datamatrix$SSA
```

```
perm.cor.test(x, y, nperm = 10000, progress = TRUE)
```

```
# Prepare PCA analysis
```

```
pcatest1 <- prcomp(datamatrix,
```

```
center = TRUE,
```

```
scale. = TRUE)
```

```
# Print and summarize output
```

```
print(pcatest1)
```

```
summary(pcatest1)
```

```
# Attributes of PCA test
```

```
res.var <-get_pca_var(pcatest1)
```

```
res.var$coord
```

```
res.var$contrib
```

```
# Obtain cos2 values for the variables
```

```
res.var$cos2
```

```

# Print the biplot for PCA
fviz_pca_biplot(pc1,
  pointsize = 2,
  col.var="dark blue",
  repel = TRUE)

# Assessing VIF of variables was done using the following codes. Model 1 is a linear
model where Pb is the dependent variable. Cu or Cd can also be used as the dependent
variable and the VIF values will be the same.

model1 <- lm(Pb~., data=DataPbAll)
car::vif(model1)

#Checking for aliased coefficients
alias(model1)

# Building models with Enet using glmnet package.
# DataCuSel = A data matrix created by removing following from the original data
matrix; Pb, Cd, Carboxylic, Phenolic, Lactonic, PV.
# DataPbSel = A data matrix created by removing following from the original data
matrix; Cu, Cd, Carboxylic, Phenolic, Lactonic, PV.
# DataCdSel = A data matrix created by removing following from the original data
matrix; Pb, Cu, Carboxylic, Phenolic, Lactonic, PV.

# Defining repeated k-fold cross validation (k=10, repeats=10).
fitControl <- trainControl(method = 'repeatedcv',
  number = 10,
  repeats=10,
  search = "grid")

# Building model for Cu.
model.Cu <- caret::train(Cu~ .,
  data = DataCuSel,

```

```

        method="glmnet",
        trControl = fitControl,
        tuneLength = 20)

# Printing the model.
summary(model.Cu)
print(model.Cu)

# Attributes for final model
model.Cu$finalModel
model.Cu$bestTune
model.Cu$coefnames

# Coefficients when lambda is set to the optimal value
FinModCu <- model.Cu$finalModel
coef(FinModCu, s=model.Cu$finalModel$lambdaOpt)
model.Cu$finalModel$lambdaOpt

# Defining and summarize importance of variables
impCu <- varImp(model.Cu, scale=FALSE)
print(impCu)

# Building model for Cd.
model.Cd <- caret::train(Cd~ .,
        data = DataCdSel,
        method="glmnet",
        trControl = fitControl,
        tuneLength = 20)

# Printing the model.
summary(model.Cd)
print(model.Cd)

# Attributes for final model

```

```

model.Cd$finalModel
model.Cd$bestTune
model.Cd$coefnames

# Coefficients when lambda is set to the optimal value
FinModCd <- model.Cd$finalModel
coef(FinModCd, s=model.Cd$finalModel$lambdaOpt)
model.Cd$finalModel$lambdaOpt

# Defining and summarize importance of variables
impCd <- varImp(model.Cd, scale=FALSE)
print(impCd)

# Building model for Pb.

model.Pb <- caret::train(Pb~ .,
                        data = DataPbSel,
                        method="glmnet",
                        trControl = fitControl,
                        tuneLength = 20)

# Printing the model.
summary(model.Pb)
print(model.Pb)

# Attributes for final model
model.Pb$finalModel
model.Pb$bestTune
model.Pb$coefnames

# Coefficients when lambda is set to the optimal value
FinModPb <- model.Pb$finalModel
coef(FinModPb, s=model.Pb$finalModel$lambdaOpt)
model.Pb$finalModel$lambdaOpt

```

```
# Defining and summarize importance of variables
impPb <- varImp(model.Pb, scale=FALSE)
print(impPb)
```

### **PLS to develop models for sorption capacity and kinetic constants**

```
# Building PLS Models

# Database = ModPb1

library(caret)

library(plsRglm)

# Calculate optimal number of components

set.seed(123)

modelplsPbA<-cv.plsRglm(Pb~.,data=ModPb1,nt=5,K=5,NK=100,random=TRUE,
                        verbose = FALSE)

res.modelplsPbA=cvtable(summary(modelplsPbA))

plot(res.modelplsPbA)

summary(modelplsPbA)

# Apply the optimal number of components to build PLS model

modelplsPbA1<-plsRglm(Pb~.,data=ModPb1,nt=2,pvals.expli=TRUE)

modelplsPbA1

# Plot confidence intervals

set.seed(123)

modelplsPbA1.bootYX1=bootpls(modelplsPbA1,R=1000,verbose=FALSE)

boxplots.bootpls(modelplsPbA1.bootYX1,indice=2:8)

temp.ci=confints.bootpls(modelplsPbA1.bootYX1,indice=2:8)
```



```
plots.confints.bootpls(temp.ci,typeIC="BCa",
                        colIC=c("blue","blue","blue","blue"),
                        legendpos="topright")
```

### **Develop relation with column breakthrough time with kinetic constant, sorption capacity and initial sorption rate**

Building simple linear regression models

```
# database = Pb200
```

```
library(caret)
```

```
control <- trainControl(method = "repeatedcv",
                        number = 5,
                        repeats = 5)
```

```
model_lm <- train(K2 ~ BT, data = Pb200, method='lm',
                  trControl = control, tuneLength = 10)
```

```
summary(model_lm$finalModel)
```

```
# Plotting Confidence intervals and Prediction intervals side bay side
```

```
pred <- predict(model_lm, Pb200)
```

```
pred <- data.frame(pred = pred, BT = Pb200$BT)
```

```
library(ggplot2)
```

```
ggplot(data = pred)+
```

```
  geom_line(aes(x = BT, y = pred))+
```

```
  geom_point(data = Pb200, aes(x=BT, y = K2))
```

```
pred <- predict(model_lm$finalModel, Pb200, se.fit = TRUE, interval =
"prediction")
```

```
pred <- data.frame(pred = pred$fit[,1], BT = Pb200$BT, lwr = pred$fit[,2], upr =  
pred$fit[,3])
```

```
pred_int <- ggplot(data = pred)+  
  geom_line(aes(x = BT, y = pred))+  
  geom_point(data = Pb200, aes(x = BT, y = K2)) +  
  geom_ribbon(aes(ymin = lwr, ymax = upr, x = BT), alpha = 0.2)
```

```
pred <- predict(model_lm$finalModel, Pb200, se.fit = TRUE, interval =  
"confidence")
```

```
pred <- data.frame(pred = pred$fit[,1], BT = Pb200$BT, lwr = pred$fit[,2], upr =  
pred$fit[,3])
```

```
pred_conf <- ggplot(data = pred)+  
  geom_line(aes(x = BT, y = pred))+  
  geom_point(data = Pb200, aes(x = BT, y = K2)) +  
  geom_ribbon(aes(ymin = lwr, ymax = upr, x = BT), alpha = 0.2)
```

```
library(cowplot)
```

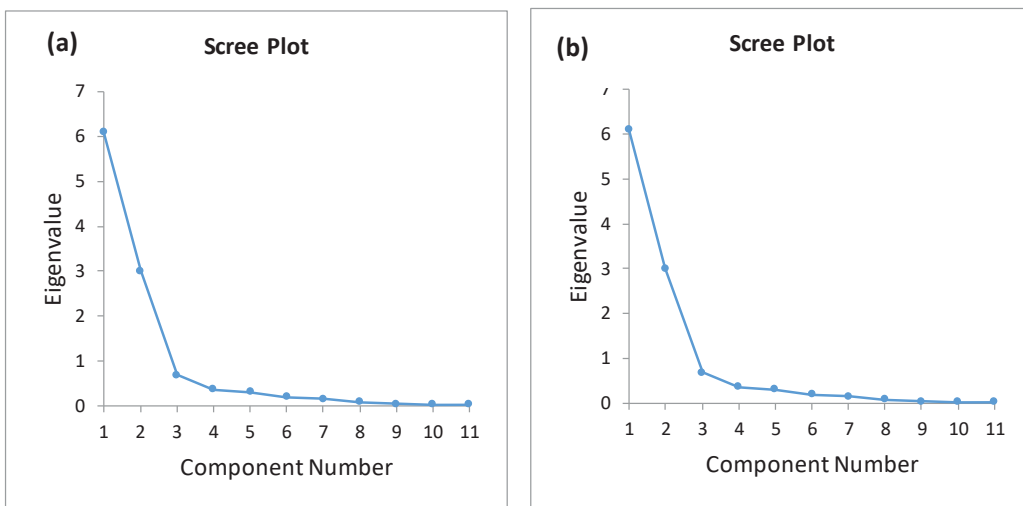
```
plot_grid(pred_int, pred_conf)
```

This page intentionally left blank.

## APPENDIX A4

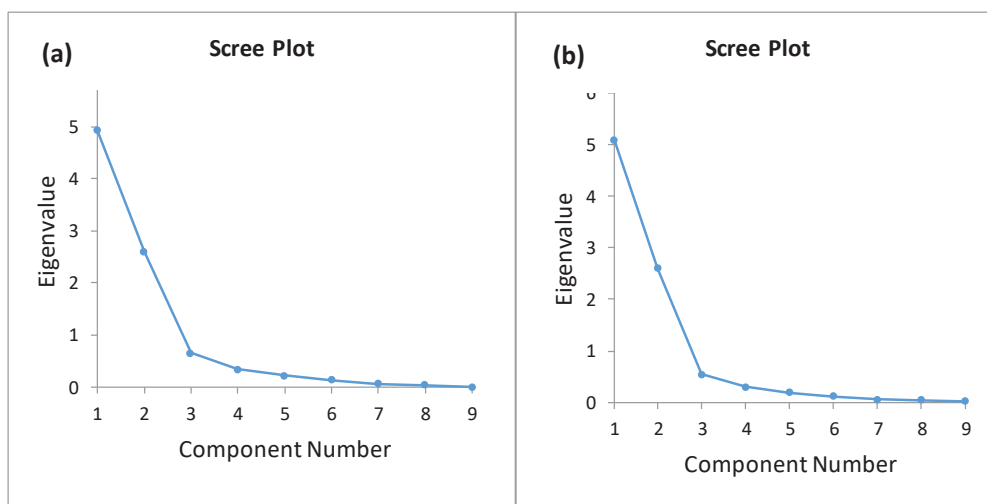
---

### Statistical analysis outputs



**Figure A4. 1** PCA Scree plots for physico-chemical properties and maximum sorption capacity. **(a)** Total acidic group as single variable **(b)** Carboxylic, Lactonic and phenolic separately.

**Note:** These figures correspond to 7.12 in Section 7.4 of Chapter 7



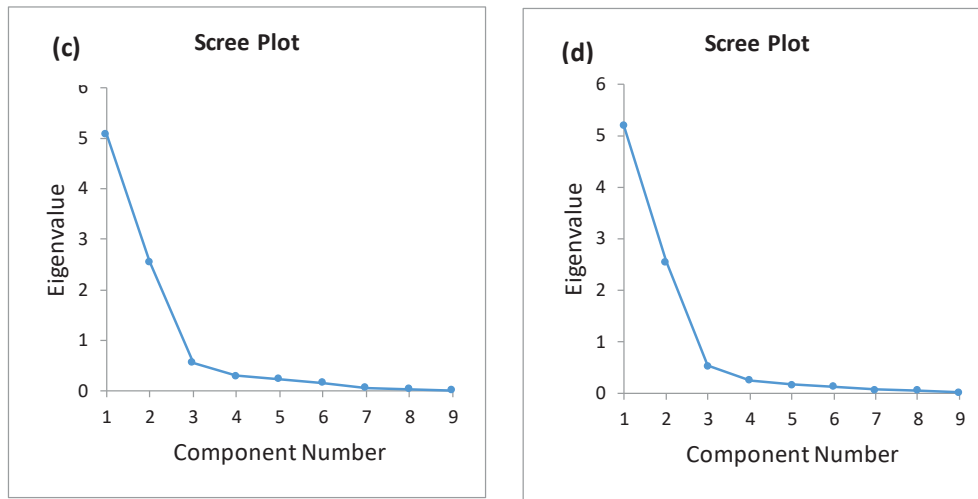


**Figure A4.2** PCA Scree plots for physico-chemical properties and  $k_2$  (a) 200 mg/L (b) 100 mg/L (c) 50 mg/L (d) 25 mg/L

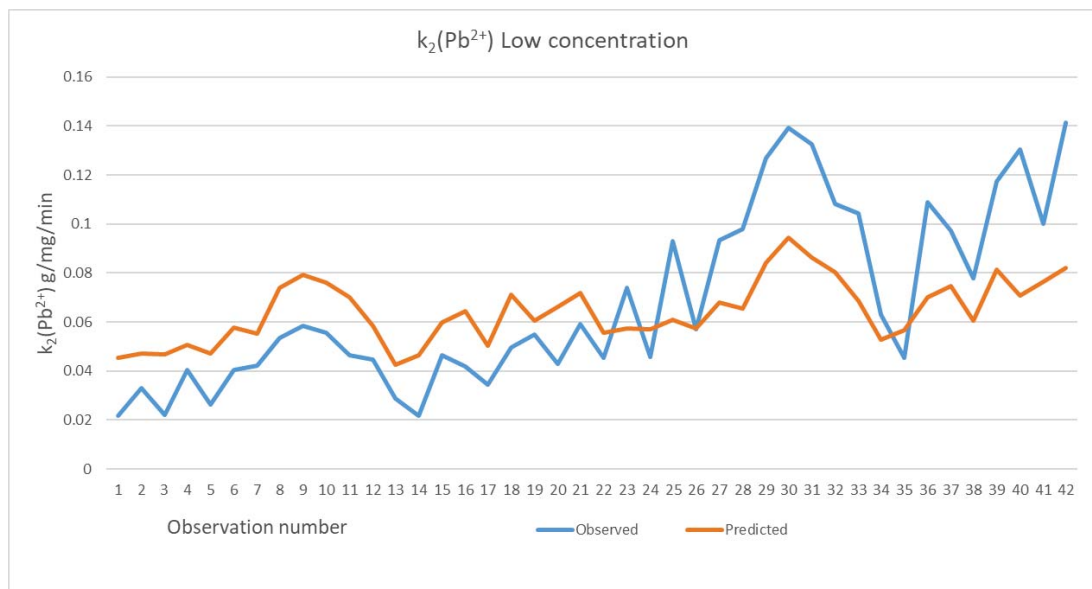


**Figure A4.3** Final predictive model for  $k_2 - \text{Pb}^{2+}$  (low concentration). Observation numbers 1-21 represent samples with a concentration of 50mg/L and observation numbers 22-42 represent samples with a concentration of 25mg/L

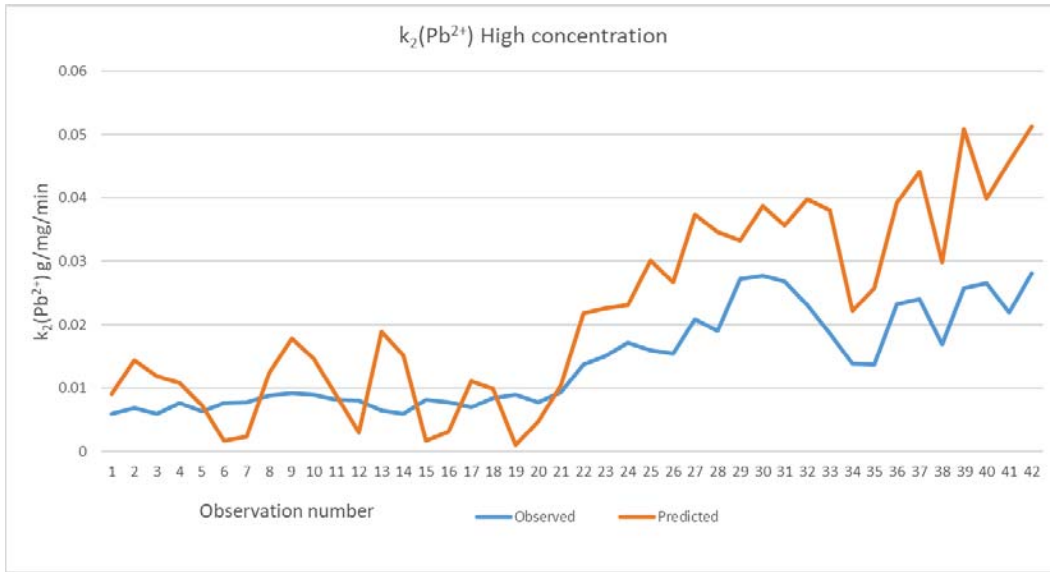


**Figure A4.4** Final predictive model for  $k_2 - \text{Pb}^{2+}$  (high concentration). Observation numbers 1-21 represent samples with a concentration of 200mg/L and observation numbers 22-42 represent samples with a concentration of 100mg/L

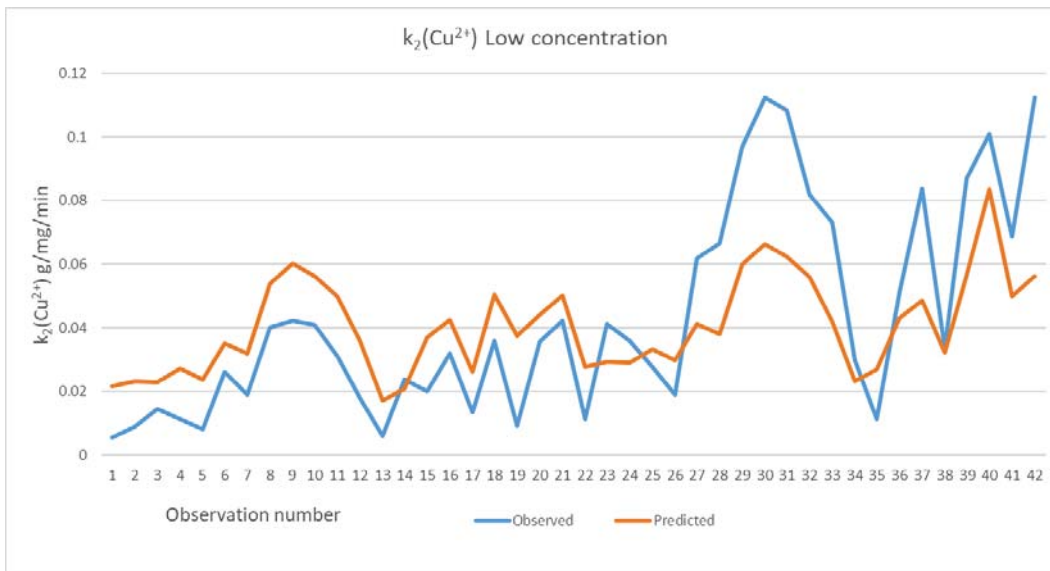


**Figure A4.5** Final predictive model for  $k_2 - \text{Cu}^{2+}$  (low concentration). Observation numbers 1-21 represent samples with a concentration of 50mg/L and observation numbers 22-42 represent samples with a concentration of 25mg/L

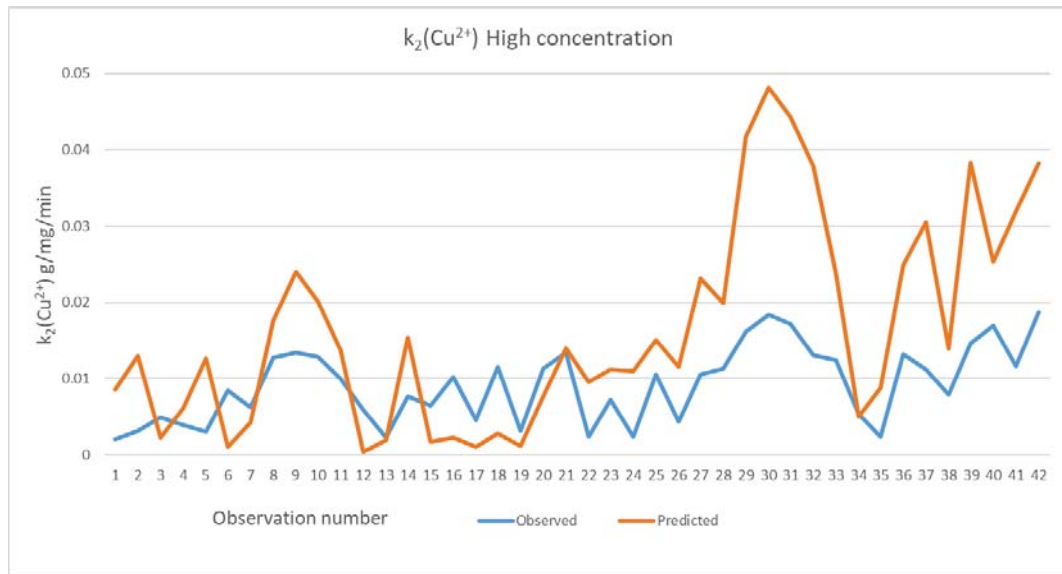


**Figure A4.6** Final predictive model for  $k_2 - \text{Cu}^{2+}$  (high concentration). Observation numbers 1-21 represent samples with a concentration of 200mg/L and observation numbers 22-42 represent samples with a concentration of 100mg/L

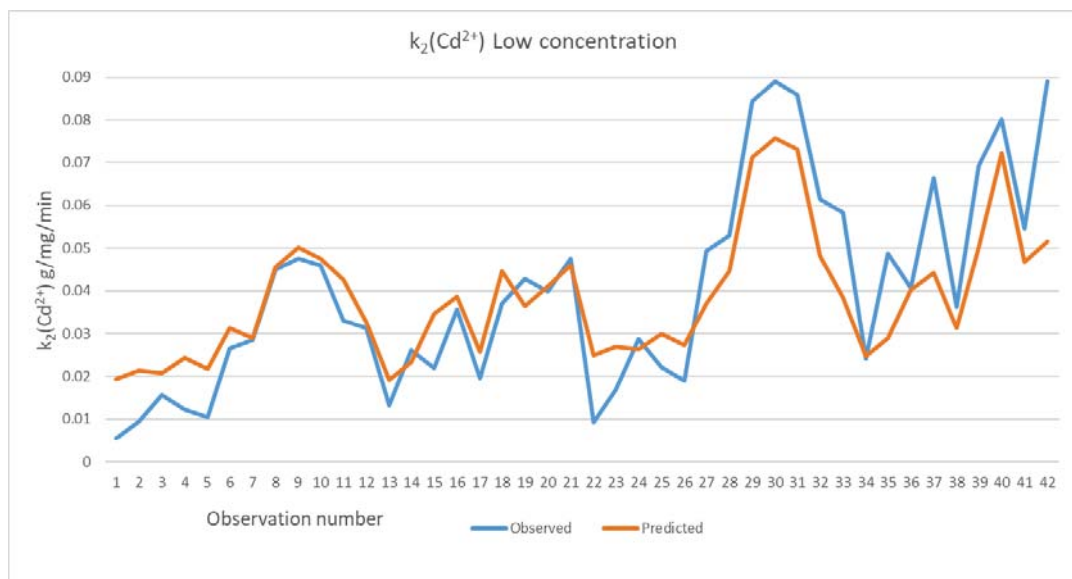


**Figure A4.7** Final predictive model for  $k_2 - \text{Cd}^{2+}$  (low concentration). Observation numbers 1-21 represent samples with a concentration of 50mg/L and observation numbers 22-42 represent samples with a concentration of 25mg/L



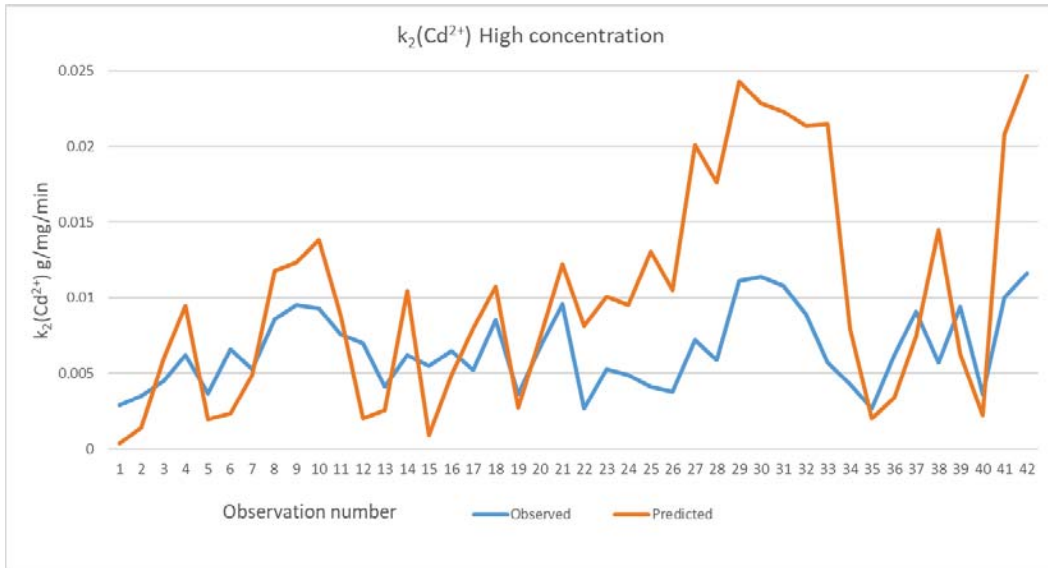


**Figure A4.8** Final predictive model for  $k_2 - \text{Cd}^{2+}$  (high concentration). Observation numbers 1-21 represent samples with a concentration of 200mg/L and observation numbers 22-42 represent samples with a concentration of 100mg/L